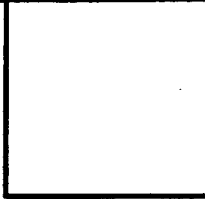


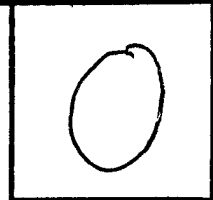
LOAN DOCUMENT

PHOTOGRAPH THIS SHEET

DTIC ACCESSION NUMBER



LEVEL



INVENTORY

AFRL-ML-TY-TR-1999-4527

DOCUMENT IDENTIFICATION

18 JAN 99

DISTRIBUTION STATEMENT A
Approved for Public Release
Distribution Unlimited

DISTRIBUTION STATEMENT

ACCESSION BY	
NTIS	GRAM <input checked="" type="checkbox"/>
DTIC	TRAC <input type="checkbox"/>
UNANNOUNCED JUSTIFICATION	
BY	
DISTRIBUTION/	
AVAILABILITY CODES	
DISTRIBUTION	AVAILABILITY AND/OR SPECIAL
<i>A-1</i>	

DISTRIBUTION STAMP

--

DATE ACCESSIONED

--

DATE RETURNED

--

REGISTERED OR CERTIFIED NUMBER

<i>19990611 077</i>

DATE RECEIVED IN DTIC

PHOTOGRAPH THIS SHEET AND RETURN TO DTIC-FDAC

H
A
N
D
L
E

W
I
T
H

C
A
R
E

AFRL-ML-TY-TR-1999-4527



SOLID SORBENT CONTROL OF NITROGEN OXIDES (NO_x)

MAXWELL RICHARDSON MENTZER LEE

**UNIVERSITY OF FLORIDA
COLLEGE OF ENGINEERING
PO BOX 116450
GAINESVILLE FL 32611-6450**

Approved for Public Release; Distribution Unlimited

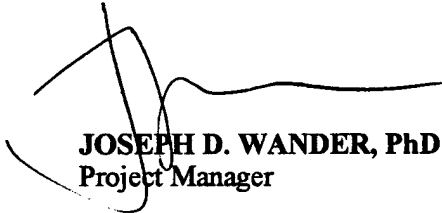
**AIR FORCE RESEARCH LABORATORY
MATERIALS & MANUFACTURING DIRECTORATE
AIRBASE & ENVIRONMENTAL TECHNOLOGY DIVISION
TYNDALL AFB FL 32403-5323**

NOTICES

WHEN GOVERNMENT DRAWINGS, SPECIFICATIONS, OR OTHER DATA INCLUDED IN THIS DOCUMENT FOR ANY PURPOSE OTHER THAN GOVERNMENT PROCUREMENT DOES NOT IN ANY WAY OBLIGATE THE US GOVERNMENT. THE FACT THAT THE GOVERNMENT FORMULATED OR SUPPLIED THE DRAWINGS, SPECIFICATIONS, OR OTHER DATA DOES NOT LICENSE THE HOLDER OR ANY OTHER PERSON OR CORPORATION, OR CONVEY ANY RIGHTS OR PERMISSION TO MANUFACTURE, USE, OR SELL ANY PATENTED INVENTION THAT MAY RELATE TO THEM.

THIS REPORT IS RELEASABLE TO THE NATIONAL TECHNICAL INFORMATION SERVICE (NTIS). AT NTIS, IT WILL BE AVAILABLE TO THE GENERAL PUBLIC, INCLUDING FOREIGN NATIONS.

THIS TECHNICAL REPORT HAS BEEN REVIEWED AND IS APPROVED FOR PUBLICATION.



JOSEPH D. WANDER, PhD
Project Manager



CHRISTINE WAGENER-HULME, Lt Col, USAF, BSC
Chief, Environmental Technology Development Branch



ANDREW D. POULIS
Scientific & Technical
Information Program Manager



RANDY L. GROSS, Lt Col, USAF, BSC
Chief, Airbase & Environmental
Technology Division

IF YOUR ADDRESS HAS CHANGED, IF YOU WISH TO BE REMOVED FROM OUR MAILING LIST, OR IF THE ADDRESSEE IS NO LONGER EMPLOYED BY YOUR ORGANIZATION, PLEASE NOTIFY AFRL/MLQP, TYNDALL AFB, FLORIDA 32403-5323, TO HELP MAINTAIN A CURRENT MAILING LIST.

Do not return copies of this report unless contractual obligations or notice on a specific document requires its return.

REPORT DOCUMENTATION PAGE			Form Approved OMB No. 0704-0188	
Public reporting burden for this collection of information is estimated to average 1 hour per response, including the time for reviewing instructions, searching existing data sources, gathering and maintaining the data needed, and completing and reviewing the collection of information. Send comments regarding this burden estimate or any other aspect of this collection of information, including suggestions for reducing this burden, to Washington Headquarters Services, Directorate for Information Operations and Reports, 1215 Jefferson Davis Highway, Suite 1204, Arlington, VA 22202-4302, and to the Office of Management and Budget, Paperwork Reduction Project (0704-0188), Washington, DC 20503.				
1. AGENCY USE ONLY (Leave blank)	2. REPORT DATE 18 Jan 1999	3. REPORT TYPE AND DATES COVERED Final (Sept 96 - Jan 99)		
4. TITLE AND SUBTITLE Solid Sorbent Control of Nitrogen Oxides (NOx)			5. FUNDING NUMBERS F08637-C-6015	
6. AUTHOR(S) Lee, Maxwell Richardson Mentzer				
7. PERFORMING ORGANIZATION NAME(S) AND ADDRESS(ES) University of Florida College of Engineering PO Box 116450 Gainesville FL 32611-6450			8. PERFORMING ORGANIZATION REPORT NUMBER	
9. SPONSORING/MONITORING AGENCY NAME(S) AND ADDRESS(ES) Joseph Wander, PhD AFRL/MLQE 139 Barnes Drive, Ste 2 Tyndall AFB FL 32403-5323			10. SPONSORING/MONITORING AGENCY REPORT NUMBER AFRL-ML-TY-TR-1999-4527	
11. SUPPLEMENTARY NOTES Technical Monitor: Dr. Joseph Wander, AFRL/MLQE, (850) 283-6240				
12a. DISTRIBUTION AVAILABILITY STATEMENT Approved for Public Release; Distribution Unlimited ASC-99-1226			12b. DISTRIBUTION CODE A	
13. ABSTRACT (Maximum 200 words) Solid materials have demonstrated applicable control of combustion-source NOx. A support material of (gamma)-alumina can provide improved NOx sorption in comparison to a previously applied sorbent, magnesia-coated vermiculite. NOx sorption of treated (gamma)-alumina correlates with the ionization potential of the group-1 element. General mechanisms of NOx sorption have been developed for untreated, K2CO3-treated and KOH-treated (gamma)-alumina. Sorption of NO appears to increase formation of nitrite. Untreated (gamma)-alumina formed little nitrite. For the treated (gamma)-alumina, the ratio of nitrite-to-nitrate formed relates to the ratio of NO-to-NO2 sorbed. Additional NO2 exposure converts nitrite into nitrate and NO. This nitrite-to-nitrate conversion correlates with the thermal stability of subsurface species. In addition, thermal-decomposition tests indicated similarities of NOx-exposed sorbents to nitrite and nitrate salts. The proposed mechanisms suggest that formed nitrite stability is crucial to improving NOx sorption. Effects of additional gases (O2, SO2, CO2, or water vapor) to NO and NO2 sorption at 25 and 250 oC by untreated, K2CO3-treated and KOH-treated (gamma)-alumina were evaluated. Only SO2 and water vapor were observed to affect NOx sorption.				
14. SUBJECT TERMS NOX sorption, alumina, combustion-source gases			15. NUMBER OF PAGES	
			16. PRICE CODE	
17. SECURITY CLASSIFICATION OF REPORT Unclassified	18. SECURITY CLASSIFICATION OF THIS PAGE Unclassified	19. SECURITY CLASSIFICATION OF ABSTRACT Unclassified	20. LIMITATION OF ABSTRACT UL	

UNCLASSIFIED

SECURITY CLASSIFICATION OF THIS PAGE

CLASSIFIED BY:

DECLASSIFY ON:

PREFACE

This report was prepared by the University of Florida, Environmental Engineering Science, Air Pollution Group, under contract No. F08637-C-6015 for the Air Force Research Laboratory, Armstrong Laboratories, Airbase and Environics Directorate, Tyndall AFB, Florida, 32403.

This final report describes background information and experimental methods with presentation of results and conclusions of improved solid sorbents of nitrogen oxides. The work was performed from September 1996 to January 1999. The project officer was Joseph D. Wander, Ph.D.

Graduate research members include Maxwell Lee and David Pocengal. Expert guidance and assistance to this project was provided by the project officer and professors at the University of Florida including the principal investigator, Eric R. Allen, Dale Lundgren, Emmett Bolch, and Gar Hoflund. Laboratory experiments were conducted in laboratories throughout the University of Florida facilities with a majority of work performed in the Department of Environmental Engineering Sciences. This dissertation is reproduced exactly as it was submitted to the University of Florida, and does not conform to the usual style standards for AFRL reports.

EXECUTIVE SUMMARY

A. OBJECTIVE

The objective of this research effort was to determine and evaluate improved solid sorbent materials of nitrogen oxides (NO_x) under typical exhaust-gas conditions. Materials were to be determined that improved NO_x sorption under combustion-source exhaust conditions in a laboratory environment in comparison to previous materials with proposed sorption mechanisms explaining tests observations.

B. BACKGROUND

Evolving government regulations have increased the need for alternative methods of NO_x control to improve the applicable range of conditions and efficiencies of conventional methods. Previous USAF-funded work established a solid sorbent (magnesia-coated vermiculite (MgO/v)) that is applicable to control of NO_x from various USAF point sources that are not well suited for conventional NO_x controls. Given the promising results of these studies additional work was recommended to further develop this applicable simple method of NO_x control.

C. SCOPE

This report describes laboratory tests that evaluated solid sorbents using primarily a fixed-bed dynamic reactor system. This system was specifically built for this project. In addition to this system, analytical systems including ion-specific electrode, x-ray photoelectron spectroscopy, surface measures (BET), and infrared spectroscopy (FTIR) were employed to provide a broader scope of data that enforced the proposed NO_x-sorption mechanism for the improved sorbents.

D. METHODOLOGY

A laboratory-scale flow-through tubular reactor system was used to expose sorbent materials to NO_x under isothermal constant gas flow conditions. The data collected from these tests and data from supporting analyses were used to evaluate characteristics controlling the sorption process. Also, the data supported the proposed sorption mechanisms.

E. TEST DESCRIPTION

Samples were exposed to NO_x in the fixed-bed reactor system with NO_x measures obtained at the bed outlet using a chemiluminescent NO_x analyzer. Following exposure samples were tested using various analytical techniques that include ion-specific electrode (ISE), x-ray photoelectron spectroscopy (XPS), surface area analysis (BET), and Fourier

transform infrared spectroscopy (FTIR). Also, certain samples were thermally decomposed within the system after NO_x exposure.

F. RESULTS

In comparison to MgO/v that was tested by other researchers, γ -alumina showed increased activity for sorption of NO_x. Both MgO/v and alumina did not sorb NO alone and NO₂ sorption resulted in the formation of NO. The amount of NO formed was proportional to NO₂ sorbed in a 1:3 molar ratio. γ -Alumina treated with group-I carbonate and hydroxide compounds significantly improved NO₂ sorption as well as sorbing NO. NO_x sorption improved in relation to the ionization potential of the group-I element. Using supporting analysis techniques, proposed sorption mechanisms were developed for the untreated and treated alumina sorbents. Also, the stability of formed nitrite species shows a relation to the observed sorption of NO resulting in nitrite formation. Additional gases of O₂, H₂O, SO₂, and CO₂ were evaluated in the fixed-bed reactor system that indicated only SO₂ and H₂O significantly affected NO_x sorption.

G. CONCLUSIONS

The proposed mechanisms of NO sorption are supported by the findings from laboratory results. Based on these mechanisms sorption of NO₂ results in nitrite and nitrate formation on the sorbent surface. Sorption of NO and NO₂ results in formation of nitrite. After additional NO₂ exposure, formed nitrite species convert to nitrate and NO. The sorption of NO by treated alumina sorbents relates to the stability of formed nitrite species.

H. RECOMMENDATIONS

Additional research is needed to improve the treated alumina sorbents by increasing the stability of formed nitrite or altering it such that further NO_x exposure does not convert nitrite to nitrate and NO. The sorbent materials should be evaluated for various surface characteristics (surface area, porosity, etc.) to improve sorption under applicable exposure conditions. Regeneration of sorbent is critical to its application. One possible regeneration method that should be investigated is thermal desorption in the presence of a reducing gas.

This work is dedicated to my father, John Augustus Lee,
for his firm belief in the value of education
that laid the foundation of this achievement.

ACKNOWLEDGMENTS

My sincere gratitude is given to Professor Eric R. Allen for his support and guidance in this academic endeavor. His knowledge and patience expressing such knowledge have proven the meaning of an advisor. During our meetings and conversations his advice has been demonstrative of issues much more than only this research. To Professor Dale Lundgren, I have appreciated his quick wit and pragmatism to real-world issues of air pollution. I offer my sincere appreciation to Professor Gar Hoflund for his continual interest in this research and support of new ideas. To Professor Emmett Bolch, I offer my gratitude for serving as a committee member and as the professor whom I initially met in the Environmental Engineering Department. That initial conversation helped persuade me to pursue a career in this field. As well, I give thanks to the numerous graduate students of the Air Pollution Program, present and past. I especially thank Larry Kimm for his encouragement to continue on with his research.

The advice of Joseph Wander through email and conference meetings has given me an additional point of view one can only have as an experienced manager and scientist. His friendship and advice have covered sage-like knowledge to the whimsical note.

XPS analysis and laboratory assistance of John Wolan and other members of Professor Hoflund's research group, and the added value of the work and experience that they have provided to this research are sincerely appreciated. Regarding technical

assistance, I wish to thank Professor B. Moudgil, UF Materials Science Engineering Department, for the use of the BET analyzer, including instrument training by his graduate student, Josh Adler. As well, the use of an FTIR from Professor K. Williams, which included the assistance of Mr. Russ Pierce, is appreciated.

I wish to thank the numerous undergraduate assistants I have had the opportunity to work with: John Lindsay, Tyler Crone, Michael Diehl, Tiffany Burns, Paul Dehart, and Jacob Mauldin. I give special thanks to undergraduate assistant Jacob Mauldin, who has worked with me during a major portion of this research. His talents in construction and design as well as computer skills have proven invaluable. The computer work of Dr. George Harder to create a successful data-acquisition program is appreciated.

Regarding the persons outside of the academic arena, I wish to thank Nancy Szabo for support of this endeavor and commitment to me. I also give thanks to my family including my nine brothers and sisters, who have taught me many things including the valuable lessons of working with others.

I would like to thank the United States Air Force, Armstrong Laboratory, Tyndall AFB, Florida, for the financial support to perform this research project. Also, financial support received from the National Science Foundation is appreciated.

TABLE OF CONTENTS

	<u>page</u>
ACKNOWLEDGMENTS.....	viii
LIST OF TABLES.....	xiii
LIST OF FIGURES.....	xiv
INtroduction	1
Chemical and Physical Properties of NO _x	3
NO _x Related Atmospheric Chemistry.....	4
Formation of Combustion NO _x	4
Thermal NO _x Formation.....	4
Fuel NO _x Formation	9
Prompt NO _x	11
Detrimental Effects of NO and NO ₂	11
Biological Effects.....	11
Material Effects	13
Government Regulations Related to NO _x Control.....	13
NO _x Control Technologies	17
Combustion Modification	17
Flue-Gas Treatment	18
Reduction Methods	19
Sorption Methods	21
Wet Sorption	21
Dry Sorption	22
Applied methods of dry sorption.....	24
Hybrid Systems	27
Related SO ₂ -Control Methods.....	29
Other NO _x -Control Methods	29
Research Justification.....	30
Research Objectives	30
Experimental	32
Fixed-Bed Reactor System	32
Initial Fixed-Bed Reactor System.....	32
Redesigned System: Single and Triple Bed	35

Triple bed	37
Water injection	38
System automation	38
Fixed-bed reactor system: experimental error	39
Redesigned system	40
General Fixed-Bed Reactor Experimental Procedure	43
Experimental Conditions	43
Sample Preparation	47
Magnesium-Oxide Coated Vermiculite (MgO/v)	47
γ -Alumina: Untreated and Treated	49
Ion-Specific Electrode (ISE) Measurements	50
X-ray Photoelectron Spectroscopy	56
BET Analyses	58
Fourier Transform Infrared (FTIR) Analyses	61
REsults and discussion	63
Initial MgO/v Laboratory Experiments	65
NO _x Sorption: MgO/v	66
MgO/v: Internal Diffusion of NO ₂	67
MgO/v: External Diffusion	70
MgO/v: Sorption of NO	70
MgO/v: Effect of Water on NO _x Sorption	71
Comparison of MgO/v and Alumina Sorbents	79
MgO/v vs. Alumina: NO _x Sorption	79
Formation of NO	82
Initial Studies of Untreated and KOH-Treated γ -Alumina	84
Different Sources of γ -Alumina	84
Alumina: Removal of Gaseous NO	89
X-ray Photoelectron Spectroscopy (XPS) Analysis of Untreated γ -Alumina	89
KOH-Treated γ -Alumina: Initial Testing	90
KOH Treatment Parameters: NO _x -Sorption Effects	99
Studies of Group-I Treated γ -Alumina	101
NO _x Sorption: Temperature Effects	108
NO _x Sorption: Concentration Effects	108
NO _x Sorption: Saturation	116
Comparison of Alkali Compounds: NO _x Sorption	116
Alkali-Hydroxide Treatments	117
Alkali-Carbonate Treatments	117
Cesium Treatments	118
Alkali-Treated Alumina: Surface Area Measurements	124
Relation of Alkali Element Ionization Potential to NO _x Sorption	128
Sorption Studies of the Effect of Varying NO and NO ₂ Concentrations	129
Initial Tests on Sorption of Gaseous NO	130
Interaction of NO with Sorbents following NO ₂ Sorption	131
Effect of Varying the Inlet NO Concentration	136

Effect of Varying Inlet NO ₂ Concentrations.....	138
Gas and Surface Profile for the Sorption Process	139
Molar Ratio of Nitrite to Nitrate.....	147
Trends in ΔNO_2 sorbed/ ΔNO formed: Untreated and Treated Alumina.....	149
Proposed Reaction Mechanisms of NO _x with Alkali-Treated or Untreated	
Alumina.....	149
Untreated γ -Alumina	153
KOH-Treated γ -Alumina.....	154
K ₂ CO ₃ -Treated γ -Alumina	155
Confirmation of NO Production from Nitrite-NO ₂ Interaction	155
Fourier Transform Infrared (FTIR) Spectroscopy Confirmation of ISE	
Measurements.....	156
Thermal Decomposition Studies	169
Decomposition of NO ₂ -Exposed Sorbents: Varied Exposure Time	171
Decomposition of Pure Compounds Treated onto γ -Alumina	172
Decomposition of Pure Salts	173
Effect of Additional Gases on NO _x Sorption.....	181
Added H ₂ O vapor	181
Added O ₂ gas.....	182
Added CO ₂ gas	182
Added SO ₂ gas.....	183
Conclusions and recommendations	184
REFERENCES.....	193
NO _x sorption: constant NO ₂ (500 ppm), varied NO concentration	201
NO _x sorption: constant NO (500 ppm), varied NO ₂ concentration	217
Added gases, so ₂ AND H ₂ O	233
BIOGRAPHICAL SKETCH.....	249

LIST OF TABLES

Table	page
Table 1-1. General properties of nitrogen oxide (N_xO_y) species (US EPA, 1993).....	5
Table 1-2. Theoretical estimates of equilibrium concentrations for NO and NO_2 in air (21% O_2) and 50% relative humidity (US EPA, 1993).	8
Table 2-1. Physical properties of sorbent materials studied.	50
Table 2-2. ISE measurement error of NO_x -exposed untreated, K_2CO_3 -treated and KOH-treated alumina samples.	55
Table 2-3. Cumulative measurement error of fixed-bed reactor testing and subsequent ISE measurement of three samples of NO_x -exposed untreated, K_2CO_3 -treated and KOH-treated alumina.	57
Table 3-1. NO_x saturation capacity of untreated and KOH-treated γ -alumina (Lee et al., 1998b).....	98
Table 3-2. Saturation capacity of treated alumina samples.	118
Table 3-3. BET surface area measurement of treated γ -alumina sorbents.	125
Table 3-4. Fractional NO_2 removal of group-I treated compound alumina and element ionization potential.	130
Table 3-5. Fractional recovery of surface nitrogen species (NO_2^- and NO_3^-) to sorbed NO_x gas.	148

LIST OF FIGURES

Figure	page
Figure 1-1. Schematic diagram of the combined reactions of nitrogen, oxygen, and hydrogen (Carmichael and Peters, 1984).....	6
Figure 1-2. Production of hydrocarbons, carbon monoxide, and nitrogen oxides as a function of A/F ratio (Heywood, 1988).....	10
Figure 2-1. Experimental system developed by Kimm (1995) to study NO _x removal by magnesium oxide coated vermiculite (MgO/v) sorbent.	33
Figure 2-2. Redesigned experimental arrangement for fixed-bed reactor system.	36
Figure 2-3. Sorbent tube temperature profile of triple fixed-bed reactor system.	42
Figure 2-4. Experimental reproducibility tests: a) simultaneously run samples of untreated alumina, b) consecutively run samples of untreated alumina.	45
Figure 2-5. Reproducibility of decomposed samples separately sorption tested.....	48
Figure 2-6. Samples prepared by different coating methods with similar mass amounts of coating showing similar NO _x sorption characteristics.....	52
Figure 2-7. XPS survey spectra obtained from (a) untreated γ -alumina, NO _x saturated (b) untreated γ -alumina after KOH-coating and NO _x -saturated (c) untreated γ -alumina, NO _x saturated (d) untreated γ -alumina after KOH coating and NO _x saturated.	59
Figure 2-8. FTIR reproducibility of Cs ₂ CO ₃ -treated alumina a) initial survey, b) second survey after mixing sample.....	62
Figure 3-1. NO _x -sorption test for MgO/v compared with Kimm's (1995) data.	68
Figure 3-2. NO _x -sorption tests for sieved MgO/v samples.....	69
Figure 3-3. External mass transfer test for NO _x sorption on MgO/v.	72
Figure 3-4. Variation of NO _x sorption at 0, 5 and 25% water additions to MgO/v at 1-second residence time at 50 °C.....	74

Figure 3-5. Variation of NO _x sorption at 0, 5 and 25% water additions to MgO/v at 2-second residence time at 50 °C.....	75
Figure 3-6. Variation of NO _x sorption at 0, 5 and 25% water additions to MgO/v at 1-second residence time at 200 °C.....	76
Figure 3-7. Variation of NO _x sorption at 0, 5 and 25% water additions to MgO/v at 2-second residence time at 200 °C.....	77
Figure 3-8. NO _x -saturation study of MgO/v and added water at 200 °C.....	78
Figure 3-9. NO _x sorption by MgO/v and untreated γ -alumina (Al ₂ O ₃) on equal volume beds (Lee et al., 1998b).	81
Figure 3-10. Sorption of NO _x to Fisher Scientific [®] , acid, basic and neutral “pH” forms of alumina.	87
Figure 3-11. γ -Alumina from different sources exposed to NO ₂	88
Figure 3-12. XPS survey spectra obtained from (a) fresh and (b) NO _x -saturated γ -alumina pressed powder samples (Lee et al., 1998b). Assignments made pertain to both spectra.....	91
Figure 3-13. Bed outlet NO and NO ₂ concentrations as a function of time for untreated and KOH-treated γ -alumina (Lee et al., 1998b).	93
Figure 3-14. XPS survey spectra obtained from (a) KOH-impregnated and (b) NO _x -saturated KOH alumina pressed powder samples (Lee et al., 1998b). Assignments made pertain to both spectra.....	94
Figure 3-15. Unexposed (a) and NO _x -saturated (b) KOH-precipitated γ -Al ₂ O ₃ pressed powder samples (Lee et al., 1998b). Assignments made pertain to both spectra.	95
Figure 3-16. XPS (A) N 1s and (B) K 2p spectra obtained from (a) KOH-precipitated and (b) NO _x -saturated KOH-precipitated alumina pressed powder samples (Lee et al., 1998b).....	96
Figure 3-17. NO _x sorption by KOH-treated and untreated alumina samples at 200 °C.	103
Figure 3-18. NO _x sorption by NaOH-treated alumina samples at 200 °C.	104
Figure 3-19. NO _x sorption by K ₂ CO ₃ -treated alumina samples at 200 °C.	105
Figure 3-20. NO _x sorption by Na ₂ CO ₃ -treated alumina samples at 200 °C.....	106
Figure 3-21. Effect of temperature on NO _x sorption by KOH-treated alumina.....	109

Figure 3-22. Effect of temperature on NO _x sorption by NaOH-treated alumina.	110
Figure 3-23. Effect of temperature on NO _x sorption by K ₂ CO ₃ -treated alumina.	111
Figure 3-24. Effect of temperature on NO _x sorption by Na ₂ CO ₃ -treated alumina.	112
Figure 3-25. Effect of varied NO concentration on the sorption of NO _x by KOH-treated alumina.	113
Figure 3-26. Effect of varied NO concentration on the sorption of NO _x by K ₂ CO ₃ -treated alumina.	114
Figure 3-27. Group-I hydroxide equimolar-treated γ -alumina sorption of NO _x	119
Figure 3-28. Group-I carbonate equimolar-treated γ -alumina sorption of NO _x	120
Figure 3-29. Sorption of NO (balance N ₂) by untreated and CsOH-treated and Cs ₂ CO ₃ -treated alumina.	121
Figure 3-30. Effect of varied amount of cesium carbonate treated onto γ -alumina on the sorption of NO _x	122
Figure 3-31. Pore size distribution of a) untreated γ -alumina, b) Cs ₂ CO ₃ -treated alumina, and c) NO _x -saturated Cs ₂ CO ₃ -treated alumina.	126
Figure 3-32. Incremental molar ratio of NO ₂ /NO for Cs ₂ CO ₃ -treated alumina sorption of NO ₂	129
Figure 3-33. Effect of presence of NO ₂ on sorption of NO for KOH-treated and K ₂ CO ₃ -treated alumina.	132
Figure 3-34. Surface interaction of NO following exposure of K ₂ CO ₃ -treated alumina to NO ₂ at 25 °C.	134
Figure 3-35. Nitrite and nitrate measured on incremental layers of a sorbent bed of untreated alumina.	141
Figure 3-36. Nitrite and nitrate measured on incremental layers of a sorbent bed of K ₂ CO ₃ -treated alumina.	142
Figure 3-37. Nitrite and nitrate measured on incremental layers of a sorbent bed of KOH-treated alumina.	143
Figure 3-38. Change of NO and NO ₂ gas concentrations throughout a bed of untreated γ -alumina.	144

Figure 3-39. Change of NO and NO ₂ gas concentration throughout a bed of K ₂ CO ₃ - treated γ -alumina.	145
Figure 3-40. Change of NO and NO ₂ gas concentrations throughout a bed of KOH- treated γ -alumina.	146
Figure 3-41. Incremental ratio of NO ₂ sorbed/ NO formed for successive bed layers of untreated alumina.	150
Figure 3-42. Incremental ratio of NO ₂ sorbed/ NO formed for successive bed layers of layers of K ₂ CO ₃ -treated alumina.	151
Figure 3-43. Incremental ratio of NO ₂ sorbed/ NO formed for successive bed layers of layers of KOH-treated alumina.	152
Figure 3-44. NO ₂ sorption activity of KNO ₂ -treated and untreated alumina.	157
Figure 3-45. Sorption of NO ₂ to KNO ₂ -treated alumina with subsequent ISE analysis.	159
Figure 3-46. FTIR spectrum of reagent-grade KNO ₂	162
Figure 3-47. FTIR spectrum of reagent-grade KNO ₃	163
Figure 3-48. FTIR spectrum of reagent-grade K ₂ CO ₃	164
Figure 3-49. FTIR spectrum of untreated alumina.	165
Figure 3-50. FTIR spectrum of K ₂ CO ₃ -treated alumina.	166
Figure 3-51. FTIR spectrum of K ₂ CO ₃ -treated alumina after exposure to NO _x (1st layer)	167
Figure 3-52. FTIR spectrum of K ₂ CO ₃ -treated alumina after exposure to NO _x (4th layer)	168
Figure 3-53. Representative NO _x -exposure test for samples decomposed after varied NO _x -exposure times.	174
Figure 3-54. Thermal decomposition of untreated alumina after 10-min exposure to NO _x	175
Figure 3-55. Thermal decomposition of untreated alumina after 30-min exposure to NO _x	175
Figure 3-56. Thermal decomposition of untreated alumina after 120-min exposure to NO _x	176
Figure 3-57. Thermal decomposition of K ₂ CO ₃ -treated alumina after 10-min exposure to NO _x	176

Figure 3-58. Thermal decomposition of K_2CO_3 -treated alumina after 30-min exposure to NO_x .	177
Figure 3-59. Thermal decomposition of K_2CO_3 -treated alumina after 120-min exposure to NO_x .	177
Figure 3-60. Thermal decomposition of KOH-treated alumina after 10-min exposure to NO_x .	178
Figure 3-61. Thermal decomposition of KOH-treated alumina after 30-min exposure to NO_x .	178
Figure 3-62. Thermal decomposition of KOH-treated alumina after 120-min exposure to NO_x .	179
Figure 3-63. Thermal decomposition of KNO_3 -treated alumina.	179
Figure 3-64. Thermal decomposition of KNO_2 -treated alumina.	180
Figure 3-65. Thermal decomposition of aluminum nitrate-treated alumina.	180

CHAPTER 1 INTRODUCTION

Nitrogen oxides (N_xO_y) are gaseous compounds that can be produced in combustion processes. Seven oxides of nitrogen species-- N_2O , NO , N_2O_3 , NO_2 , N_2O_4 , N_2O_5 , and NO_3 --exist and may be present in ambient air, but the main species of concern in the lower troposphere are NO and NO_2 . These two species, collectively designated as NO_x , are key in atmospheric chemical processes producing photochemical smog and acid rain. Within the United States in 1990, 90 percent of man-made NO_x emissions originated from combustion sources (US EPA, 1993). Although the majority of nitrogen oxides in the atmosphere originate from natural sources, localized elevated concentrations of NO_x originating from man-made sources can occur at concentrations several orders of magnitude greater than ambient background levels. The United States Environmental Protection Agency (US EPA) has established primary and secondary National Ambient Air Quality Standards (NAAQS) for nitrogen dioxide (NO_2) at $100 \mu g NO_2/m^3$ - annual arithmetic mean, due to its proven detrimental health effects. In addition, more recently the US EPA has mandated emission reductions of NO_x from point sources to reduce ambient ozone concentrations on a regional scale.

Man-made NO_x sources include transportation, stationary-source combustion, various industrial processes, solid waste disposal, and others, such as forest fires (prescribed burning). Sources other than transportation contribute over 60% of the total man-made NO_x of which industrial and utility combustion-generated power sources

account for over 95% (US EPA, 1993). Typical combustion processes result in emissions of NO and NO₂ in a molar ratio near 20/1 depending on the combustion parameters (Cooper and Alley, 1986). Despite the relatively small proportion of NO₂ in combustion exhaust, NO is an atmospheric precursor to other pollutants including NO₂ and ozone. Given the cumulative detrimental effects of NO_x, emissions control from combustion sources is a necessary factor in the overall health and welfare of society.

Various control technologies for NO_x emissions have been developed and are discussed later in this chapter. Conventional control technologies have limitations related to certain combustion conditions. As deadlines approach for the various government regulators' pollution control requirements, more cost-efficient abatement methods will be sought.

This research provides an in-depth analysis and development of NO_x control using solid sorbent materials. Initial research investigated magnesium-oxide-coated on vermiculite in this application; improved sorbents consisting of treated γ -alumina were subsequently investigated. Based on previous research these materials had been found to provide for removal of NO_x in pilot and full-scale systems. Large-scale application studies do not allow for a detailed analysis of the NO_x -sorption process. Laboratory experiments were used to determine the overall chemical mechanisms for three sorbents, untreated γ -alumina, K₂CO₃-treated alumina, and KOH-treated alumina. Based on these studies, an in-depth evaluation was conducted of the effects of significant parameters that determined the limiting conditions of operation. Controlling mechanisms of adsorption were used to determine conditions under which mass-transfer or chemical-controlling conditions are dominant.

Chapter one provides a general background on the formation, interactions and general properties of NO_x, as well as applied methods of control. Chapter two provides a detailed description of the applied experimental methods and relevant limits of the experimental systems applied. Chapter three is a chronological discussion of experimental results. Chapter four draws conclusions concerning the findings from this research and presents ideas for potential future research.

Chemical and Physical Properties of NO_x

Nitric oxide is an odorless and colorless gas. Generally, it is a more stable compound than NO₂. It is only slightly soluble in water (0.006 g/100 g of water at 25 °C and 1 atm). The covalent bonds in NO results in an uneven number of electrons causing the nitrogen atom to become slightly electropositive. Nitric oxide is a by-product of combustion through the oxidation of molecular nitrogen and fuel-bound nitrogen. Thermal production of NO can be explained by the extended Zeldovitch mechanism (Zeldovitch, 1946).

Nitrogen dioxide has a smell similar to that of chlorine and in high concentrations produces a brown-yellowish haze. Combustion NO₂ is created in secondary reactions that follow NO formation. In the troposphere NO₂ absorbs UV light (430-290 nm) and photodissociates to form NO and O. It reacts with water to form nitrous (HONO) and nitric (HONO₂) acids and is highly corrosive and oxidative as an acid or in anhydrous form. It will dimerize to N₂O₄ at higher concentrations and pressures and lower temperatures, but the dimer is not significant at ambient concentrations and temperatures. General properties of N_xO_y species are provided in Table 1-1.

NOx Related Atmospheric Chemistry

Nitrogen oxides help to regulate the amount of free radicals in the troposphere and therefore help regulate the oxidizing potential of the atmosphere. Figure 1-1 provides a flow diagram of significant tropospheric reactions of NOx. From this diagram the concentration of NOx can be observed to affect tropospheric ozone and organic chemistry as well as acidification of the atmosphere.

Formation of Combustion NOx

Oxides of nitrogen (NOx) created by combustion processes are formed through chemical reaction between oxygen in combustion air and nitrogen compounds, which are present in both the combustion air and fuel. Formation of NO₂ in combustion processes is secondary to NO formation, NO and molecular oxygen combining to form NO₂. Typically exhaust gases contain a ratio of NO/NO₂ near 20/1. However, this ratio can vary significantly depending on combustion conditions. Three major mechanisms of combustion contribute to the formation of NOx during fossil fuel combustion.

Thermal NOx Formation

Thermal NOx results from formation of NOx due to the reaction of molecular nitrogen with atomic oxygen as described by the Zeldovitch mechanism. The rate-limiting step in the production of thermally-produced NO is described by



Table 1-1. General properties of nitrogen oxide (N_xO_y) species (US EPA, 1993).

Oxide type	Mol. weight	Melting point (°C)	Boiling point (°C)	Henry's Law coeff. at 25 °C (M/atm)	Solubility in water (cm ³ /100 g) at 0 °C, 1 atm	Thermodynamic Functions (Ideal Gas, 25 °C, 1 atm) Enthalpy of formation (kcal/mol) Entropy of form. (cal/mol-deg)	Theoretical conc. at equilibrium with N ₂ , O ₂ and water in air (25 °C, 1 atm, 50% rel. hum.) (ppm)	Equilibrium	Sunlight-irradiated polluted atm.
NO	30.01	-163.6	-151.8	1.93×10^{-3}	7.34	21.58 50.35	2.69×10^{10}	10^{-1}	
NO ₂	46.01	-11.2	21.2	1.2×10^{-2}	forms HONO and HONO ₂	7.91 57.34	1.91×10^{-4}	10^{-1}	
N ₂ O	44.01	-90.8	-88.5	2.47×10^{-2}	130.52	19.61 52.55			
N ₂ O ₃	76.01	-102	47 (decomp)	0.6 ± 0.2	forms HONO	19.80 73.91	2.96×10^{20}	$10^{-9} - 10^{-8}$	
N ₂ O ₄	92.02	-11.3	21.2	1.4 ± 0.8	forms HONO and HONO ₂	2.17 72.72	2.48×10^{13}	$10^{-8} - 10^{-7}$	
N ₂ O ₅	108.01	30	3.24 (decomp)		forms HONO ₂	2.7 82.8	3.16×10^{17}	$10^{-5} - 10^{-3}$	

The high activation energy (75 kcal/mol) necessary to break the triple-bond of molecular nitrogen is extremely temperature sensitive (Bowman, 1973). The concentration of atomic oxygen is also highly temperature sensitive and dependent on the air-to-fuel ratio (A/F). Thermally-formed NO_x is dependent not on reaction equilibrium but on gas kinetics. Table 1-2 shows estimates of the equilibrium concentrations of NO and NO₂ that would be expected at various temperatures.

When comparing the data in Table 2 with real situations, it appears that the concentration of NO_x in actual combustion systems does not reach equilibrium. The rate of reaction (1-1) is not fast enough to reach equilibrium in the high-temperature flame zone. However, the removal mechanisms for NO are even slower to reach equilibrium. If the available heat produced from combustion is not used to produce useful work then the NO_x species formed would result in lower concentrations. Thus, rapid cooling of the combustion flame zone “freezes” the NO_x formed at concentrations characteristic of the high-temperature combustion zone. As a result, control of thermal NO_x is a function of combustion time as well as temperature.

The air-to-fuel (A/F) ratio defines the stoichiometric weight ratio of the combustion reactants in the influent mixture. A high or “lean” A/F ratio provides excess air that can increase power output and also the concentration of oxygen available to react and form NO_x. However, high A/F ratios provide excess air conditions that act to cool the combustion zone, thus controlling peak temperatures and reducing thermal NO_x production. A low or “rich” A/F ratio reduces the concentration of oxygen available and thus reduces NO_x. However, in this case the combustion efficiency is reduced due to a

Table 1-2. Theoretical estimates of equilibrium concentrations for NO and NO₂ in air (21% O₂) and 50% relative humidity (US EPA, 1993).

Temperature (K)	Concentration (ppm)	
	Nitric Oxide (NO)	Nitrogen Dioxide (NO ₂)
298	2.63×10^{-10}	1.88×10^{-4}
500	6.54×10^{-4}	3.86×10^{-2}
1000	34.4	1.80
1500	1,296	6.57
2000	7,957	12.7

lack of available oxygen. Figure 1-2 shows the effect of varying the A/F ratio on the concentrations of pollutants in the exhaust gas.

Also, in Figure 1-2 it can be seen that by modifying the A/F ratio some pollutants can be reduced while others are increased. Several NO_x control strategies utilize the A/F ratio to control NO_x formation and are discussed later in the section NO_x Control Methods. To minimize thermal NO_x formation, it is necessary to reduce combustion zone temperatures and residence time, minimizing atomic oxygen concentrations in the combustion process.

Thermal NO_x formation from combustion of heavy fuel oil represents approximately 40-20% of the total NO_x produced. For coal, thermal NO_x can comprise approximately 50-20% of the total NO_x generated from conventional pulverized coal boilers. This contribution can vary significantly depending on boiler design and fuel

properties. For fuels that contain no inherent nitrogen (e.g., natural gas), essentially 100% of NO_x is thermal NO_x.

Fuel NO_x Formation

Fuel NO_x pertains to NO_x emissions resulting from the conversion of nitrogen organically bound in the fuel. Reaction mechanisms have been developed for the numerous fuel-bound nitrogen (FBN) species (US EPA, 1993). Considering only FBN compounds, a 'lean' A/F ratio results in high NO formation, while fuel 'rich' conditions tend to produce N₂. This mechanism represents 80-50% of the NO_x produced from heavy fuel oil combustion, and approximately 80-60% of the NO_x produced from pulverized coal combustion. Formation of fuel NO_x is also affected by burner design, and type of boiler employed.

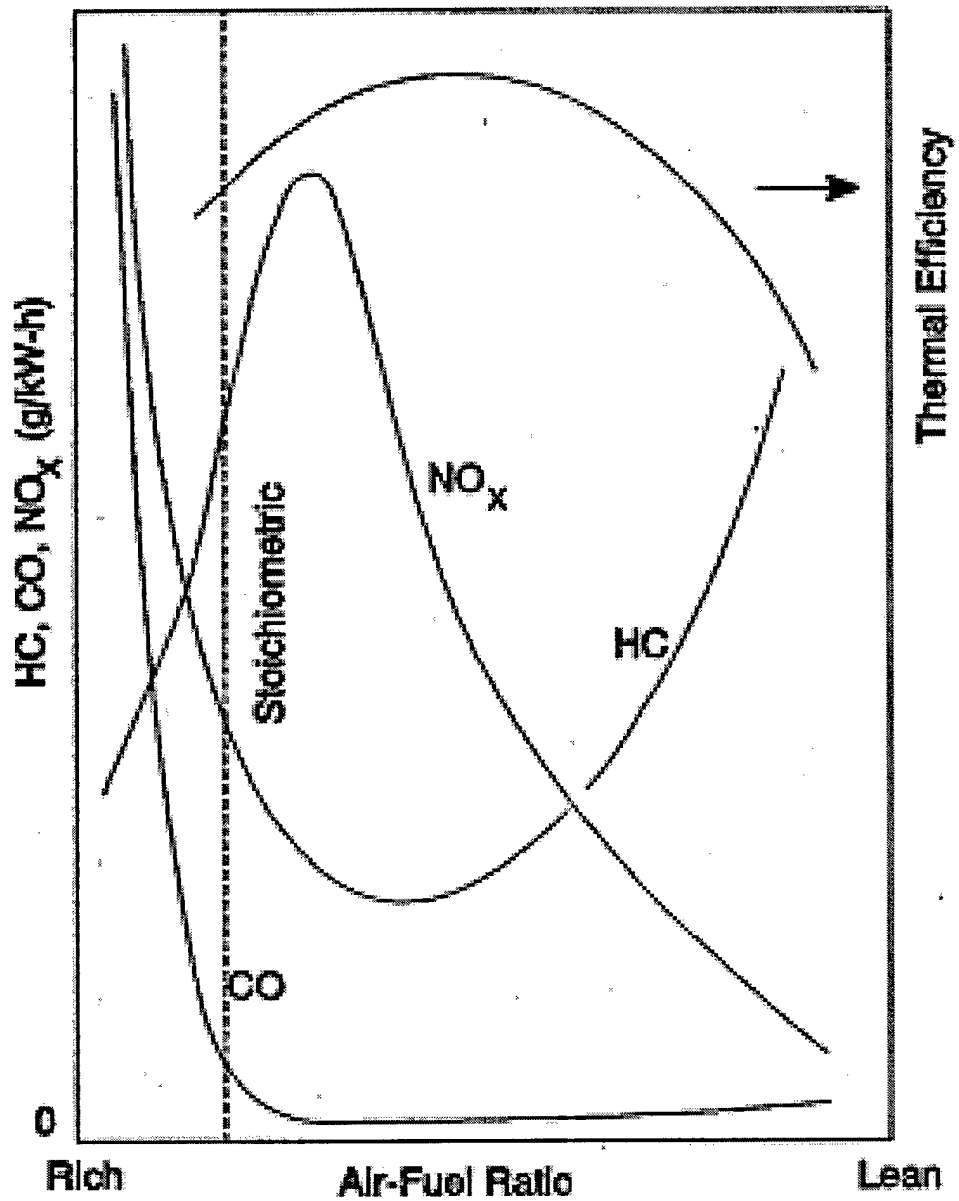


Figure 1-2. Production of hydrocarbons, carbon monoxide, and nitrogen oxides as a function of A/F ratio (Heywood, 1988).

Prompt NOx

Another mechanism that typically produces a minor portion of NOx during fuel combustion involves combustion-formed hydrocarbon radicals that can split the N₂ triple bond as shown below:



This type of reaction can proceed at a relatively low activation energy and may precede the Zeldovitch mechanism thus, the term “prompt.” The contribution of prompt NOx to the overall NOx emissions is usually small for most combustion processes (Buonicore et al., 1991).

Detrimental Effects of NO and NO₂

Biological Effects

Nitrogen dioxide (NO₂) is the most toxic of the NOx species. Its primary effect on mammals is lung damage. At concentrations greater than 100 ppm NO₂ is lethal to most exposed mammals, 90% being subject to pulmonary edema (US EPA, 1993). Short-term non-lethal exposures to NO₂ have been shown to cause pulmonary-function change in the lungs of monkeys (Henry et al., 1965). Pathological lesions have been observed in lungs of animals after short- and long-term NO₂ exposures. Similar symptoms to chronic lung disease have been observed in animals after NO₂ exposure suggesting that chronic effects on humans may result from long-term low-level NO₂ exposures. Exposure of

monkeys to 15 to 50 ppm NO₂ for two hours produced damage to the lungs, heart, liver, and kidneys, and pulmonary changes resembling human emphysema (US EPA, 1993).

Epidemiological surveys for residential areas in Chattanooga, Tennessee, showed an increased occurrence in acute respiratory illness after 6 months of 24-hr averaged concentrations from 0.109 to 0.062 ppm NO₂. The frequency of infant acute bronchitis cases also increased in the same area of Chattanooga for NO₂ concentrations in the range from 0.063 to 0.083 ppm over a 6-month period (Shy et al., 1970).

Detrimental effects of exposure to NO are less well studied. A 12-minute exposure of mice to 2500 ppm NO proved lethal (Flury and Zernick, 1931). Exposure to lower NO concentrations (~ 20 ppm) appeared to inhibit bacterial enzymatic activity (Krasna and Rittenburg, 1954). Although toxicological effects have been demonstrated for NO exposure, the detrimental health effects potential of NO at ambient concentration result primarily from its oxidation to NO₂ (US EPA, 1993).

Effects of plant sensitivity to NO_x have been separated into three categories: (1) acute injury, (2) chronic injury, and (3) physiological effects. Acute injuries in which necrotic patterns result within 48 hours have been observed on agricultural crops exposed to 1 ppm NO₂ for 48 hours (Van Haut and Stramann, 1967). Such conditions are expected only for direct exposure near stationary sources. However, greenhouse studies simulating smog conditions in the Los Angeles basin have suggested that NO_x, not ozone, contributes to significant leaf-dropping (Glater, 1970). Detrimental physiological effects of exposure to NO and/or NO₂ appear to be reduced photosynthesis and CO₂ fumigation (Hill and Bennett, 1970).

Material Effects

Loss of color has been observed in cotton and rayon fabrics due to NO_x (0.6 to 2 ppm) created from natural gas-heated domestic dryers (McLendon and Richardson, 1965). Cotton and nylon textiles fibers can deteriorate from exposure to elevated ambient NO_x concentrations (Morris et al., 1964). Increased metal failures, which were observed in the Los Angeles area, were suspected to be due to elevated particulate nitrate and NO_x concentrations (Hermance et al., 1970).

Government Regulations Related to NO_x Control

A decisive impetus for NO_x-control research was the development of government regulations. Currently federal and state agencies enforce NO_x-related regulations that have been promulgated by legislative acts. The effects of NO and NO₂ as precursors to photochemical smog and contributors to acid rain as well as their being a public health threat have led to NO_x regulation for both ambient concentration levels and point and mobile source emissions. Federal NO_x-related regulations established by the United States Environmental Protection Agency (US EPA) are based on the Clean Air Act (CAA) of 1963 and subsequent amendments promulgated in 1970, 1977, and 1990.

The 1970 CAA amendments established the national ambient air quality standards (NAAQS) which set primary and secondary standards for ambient NO₂ concentrations of 100 µg/m³ (annual arithmetic mean). Areas exceeding the NAAQS standard were designated as "non-attainment." Within areas attaining the standard, new or modified major sources were subject to best available control technology (BACT) standards and were defined as being a listed source with the potential to emit more than 100 ton/yr of an

individual pollutant or emitting 250 ton/yr total pollutants (Buonicore et al., 1991). Through negotiations with regulating agencies, a major-source operator will select the BACT technology through evaluation of various contemporary control technologies, estimation of the reduction of emissions, energy consumed, and cost per pollutant removed. New source performance standards (NSPS) that were established under section 111 of the 1977 CAA amendments generally include the BACT requirements for sources and assist in the decision process.

In non-attainment areas NO_x pollution controls were required to achieve the lowest achievable emission rate (LAER) for new or modified major sources and reasonable available control technology (RACT) for existing sources. The technology decision process was similar to BACT negotiations (Heinsohn and Kabel, 1999).

The 1977 CAA amendments established a classification of major urban areas based on their degrees of non-attainment with deadlines set to reach attainment. State implementation plans (SIPs) were created by state governments to achieve attainment. Title IV of the 1990 CAA amendments addresses the acid-rain issue and requires NO_x reductions in two phase-in periods for coal-fired utility boilers generating electricity exceeding 25 MW, to cut NO_x emissions by 30% from 1980 levels by the year 2000 (Grano, 1995).

Title II of the 1990 CAA amendments sets forth mobile-source regulations that are directed toward improved fuels and advanced sensor-activated controls for combustion and exhaust conditions. The application of catalytic converters, while greatly improved over past years, is limited because of narrow operational conditions (A/F ratio, temperature, etc.) and expensive precious metals that can be poisoned. While sorbent

techniques have been evaluated for certain unique semi-mobile sources (Nelson et al., 1994), inherent difficulties in the application of sorbent methods for NO_x control have not been thoroughly investigated to provide practical applications to mobile sources. Space limitations and sorbent regeneration are key issues to be addressed.

States may establish stricter regulations than the federal government. California, for example, is commonly known to have some of the nation's strictest air pollution standards, because four of the top five non-attainment areas in the US are located in California (Heinsohn and Kabel, 1999). To further address the seemingly persistent air quality problems, California legislation has considered controls for various uncommon NO_x sources, such as small marine-vessel and lawn mower engines.

The current nature of governmental regulation is becoming more regionally oriented in both control and implementation of air pollution programs. Observations that there is considerable transport of ground-level ozone and ozone precursors (NO_x and volatile organic compounds (VOC)) between states has become increasingly evident (US EPA, 1998). Realizing that several states would not meet the 1-hr ozone standard by the November 1994 deadline set forth in the 1990 CAA Amendments, The US EPA extended and reconsidered the deadline. The Ozone Transport Assessment Group (OTAG) was formed in 1995 in response to the ozone non-attainment situation as a partnership between US EPA, the Environmental Council of the States (ECOS) and various industry and environmental groups. The goal of this partnership is to develop an assessment and a consensus for reducing ground-level ozone and the pollutants that cause ground-level ozone, including NO_x. OTAG explicitly addresses ozone transport over the Eastern United States.

Recommendations from OTAG in its final report guided a recent ruling by US EPA mandating reduction of NO_x emissions in 22 states and the District of Columbia to reduce regional ozone transport and help areas reach the new NAAQS ozone standard (US EPA, 1998). Significant, smaller sources of NO_x that were identified by OTAG include, non-utility boilers, reciprocating internal combustion (IC) engines, gas turbines, residential fuel combustion, cement manufacturing, metals processing, wood/pulp/paper manufacturing, oil and gas production, and waste incineration. Despite the fact that these sources operate at greater variability in conditions compared to larger stationary sources, suggested controls in the OTAG final report for most of these sources, which are primarily combustion sources, are NO_x-reduction techniques. The report recognizes the inadequacies of conventional reduction technologies under highly variable operating conditions that are more typical for smaller sources, but does not provide specific methods to improve existing NO_x-reduction techniques.

In the future, regulating agencies may require NO_x controls on smaller and non-conventional NO_x-sources if current regulations fail to achieve the desired goals. One study of non-conventional NO_x sources for which control ideas have been thoroughly investigated by the United States Air Force (USAF) is jet engine test cells (Kimm, 1995; Kimm et al., 1995; Kittrell, 1991; Nelson et al., 1989, 1992, 1993, and 1994; Petrik, 1991). Thus, novel control methods are likely to be of commercial interest based on past and present trends in NO_x regulations. Control of NO_x from non-conventional sources may be economically feasible only if an effective and inexpensive control technology is available that is capable of functioning over varied combustion and exhaust conditions.

NOx Control Technologies

NOx control technologies may be conveniently divided into two major categories: combustion modification and flue gas treatment. In addition, hybrid systems have evolved, which include a variety of NOx control methods that in combination provide enhanced NOx control and system flexibility.

Combustion Modification

The formation of NOx in combustion processes, as previously discussed, is a complex phenomenon based on three mechanisms: thermal NOx, fuel NOx, and prompt NOx. The relative contribution from each of these mechanisms to the overall NOx in exhaust gases must be determined to evaluate beneficial combustion modifications. The following factors affect the amount of NOx formed from combustion: the air-to-fuel (A/F) ratio, the nitrogen content of fuel (fuel-bound nitrogen (FBN)), the amount of pre-mixing of reactants, burner design, and gas residence time in the high-temperature zone of combustion.

For fuels that have little to no fuel-bound nitrogen (FBN) the formation of NOx is dominated by the Zeldovitch mechanism (reaction (1-1)). To reduce combustion-formed NOx according to the Zeldovitch mechanism implies a reduction in peak flame temperature, limiting gas residence time at peak temperatures, and reducing the concentration of atomic oxygen at the peak temperature. Common methods that apply these concepts are flue gas recirculation, reducing the combustion load, lower combustion air preheat temperatures, water injection, and reduced excess air (US EPA, 1993).

Combustion modification methods for NO_x control of fuels with high FBN include limiting available oxygen to the FBN evolved during combustion. Applications that limit available oxygen include fuel-rich firing, staged combustion or burner designs that control the mixing rate of fuel and air streams.

Prompt NO_x is a function of hydrocarbon radicals and molecular nitrogen. Unlike the Zeldovitch mechanism prompt NO_x forms at lower temperatures and at rates similar to the oxidation process. Thus, controlling prompt NO_x cannot be achieved as effectively by methods recommended for thermal NO_x. However, limiting the available oxygen in the gas will prevent the formed N species from reacting with the oxygen. Thus, fuel-NO_x control mechanisms should help limit prompt NO_x.

Flue-Gas Treatment

In the past, combustion modification has been the method of choice to reduce NO_x emissions in commercial applications. Combustion modifications are less expensive than flue-gas treatments if they provide initial reductions of near 50% (Buonicore et al., 1991; Staudt, 1996). However, certain economic and/or physical limitations may render combustion modification impractical (Staudt, 1996).

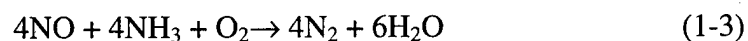
The two general chemical mechanisms for flue-gas NO_x control are reduction and oxidation. These mechanisms have evolved into a variety of processes that may include both oxidation and reduction reactions with various system configurations. The final goal of any of these processes is to convert the flue-gas NO_x to either inert gases or to a palpable (liquid and solid-phase) product. Catalysts are commonly used to improve the rate of the desired reaction.

Sorbents are common commercially-applied for SO₂ control and have also been studied to provide combined SO₂/NO_x control in recent years. Hybrid systems as well have grown in use that encompass various flue-gas treatment systems as well as combustion modifications. One of the most common NO_x control methods involves the reduction of NO_x to inert species.

Reduction Methods

Major NO_x sources, such as power plants, that operate at close to steady-state conditions typically employ selective reduction methods for flue gas treatment. The methods are “selective” to reactions only with NO_x and the reaction reduces the NO_x species to molecular nitrogen (N₂) and other inert species. The two selective reduction methods differ by either exclusion or inclusion of a catalyst (commonly zeolite, titanium, tungsten, and/or vanadium oxides) in the reaction. The methods are called SNCR (selective non-catalytic reduction) and SCR (selective catalytic reduction) methods, respectively (Cooper and Alley, 1986). The catalyst acts to reduce the required reaction temperature and increase the overall removal efficiency, but introduces additional costs and operational limitations. Selective reduction methods are highly temperature sensitive and operate in the ranges 400-300 °C (dependent of catalyst type) and 900-800 °C for SCR and SNCR, respectively.

The typical NO_x-reduction reaction uses ammonia (NH₃) and is represented by



Various reducing compounds (such as NH_3 , CO , H_2 , and urea) have been evaluated for this application (US EPA, 1994). Assuming that the gas-phase reduction in reaction (1-3) is conducted stoichiometrically and with complete mixing, the emission products will be N_2 and water. However, adequate gas mixing and injecting the correct ratio of reducing gas is critical and difficult to achieve under variable NO_x concentrations and emission rates. The result of not achieving these requirements is the emission of additional NO_x from oxidation of the reducing gas or the emission [“slip”] of reducing gas, which itself is a pollutant.

Some inexpensive solid materials have been tested that can perform at lower temperatures with reducing gas, to provide cheaper alternative NO_x reduction methods. Activated carbon has been tested at 230-220 °C with NH_3 injection to simultaneously reduce NO_x to N_2 and oxidize SO_2 to H_2SO_4 (Cooper and Alley, 1986). Copper oxide-impregnated alumina in the presence of SO_2 and O_2 will form copper sulfate and either material acts as a catalyst for reducing NO_x with NH_3 . This control method has been applied in oil-fired boilers in Japan with 90% SO_x removal and 70% NO_x removal (Cooper and Alley, 1986; Markussen and Livengood, 1995).

The Parsons Process simultaneously and catalytically reduces SO_2 to H_2S and NO_x to N_2 in a hydrogenation reactor using steam-reformer gas. Removal efficiencies for a high-sulfur coal pilot plant were 98% for SO_2 and 96-92% for NO_x (Markussen and Livengood, 1995).

Disadvantages of selective-reduction methods include combustion must be performed at known steady-state conditions, catalyst deactivation through continued use and/or poisoning from other flue-gas constituents (particulate, etc.), high start-up capital

costs, and continual reducing-gas costs. Regarding SCR, the required reaction temperature usually mandates that the catalyst be placed in-line prior to particulate control treatment and thus particulate poisoning becomes a major detriment to catalytic activity.

Sorption Methods

Sorption is essentially a process to reversibly collect gaseous NO_x species onto a solid surface or into a liquid. For both wet and dry sorption, the oxidation of NO to NO₂ vastly enhances the removal of NO_x (Cooper and Alley, 1986). After collection the trapped NO_x species can be handled under specified conditions outside the exhaust gas system. An added benefit of sorption methods is that both SO₂ and NO_x can be removed simultaneously using certain sorbent materials with possible synergistic effects on removal efficiency.

Wet Sorption

Wet sorption has been applied to SO₂ control with considerable success and is a standard control technology. However, the solubility of SO₂ in water is much higher than that of NO. While NO₂ is soluble in water it is typically only a small fraction (approx. 5%) of the total amount of NO_x in combustion exhaust. Nitric acid manufacturing typically applies wet scrubbing of NO₂ to produce nitric acid. Counce and Perona (1980) have studied in detail the NO_x-HNO₃-H₂O process in nitric acid manufacturing. However, the concentrations are much higher and temperatures much lower than those experienced in combustion-exhaust NO_x. Chemical enhancements have been studied to improve the solubility of NO, that include KMnO₄/NaOH and Na₂SO₃/FeSO₄ solutions

(Cooper and Alley, 1986). However, due to various limitations, this particular technology has not gained widespread acceptance. Some metal chelates, such as Fe(II)•EDTA have been found to readily remove any absorbed NO and allow for the maximum absorption driving force. Problems have occurred with oxidation of the iron to the inactive ferric state. Antioxidants are added for improved performance. In pilot-scale tests at a 1.5-MW plant, nitrogen oxides were reduced 60% and SO₂ near 100% (Markussen and Livengood, 1995). Wet sorption of NO_x produces a liquid product that cannot be handled as easily as a dry material for on-site or off-site transportation and disposal. Typical costs of water treatment are higher than land disposal for non-hazardous wastes. Additional regulations may be imposed for wet solution supply, storage and handling.

Measurement methods for NO_x were developed using wet sorption, and suggested possible interaction with alkaline materials. A method developed by Jacobs and Hocheiser (1958) collected ambient NO₂ gas by absorption into a solution of NaOH. Standard wet sorption methods for the detection of NO_x have been under development since the beginning of this century (Keiser and McMaster, 1908, Cook, 1936, Jacobs, 1949).

Dry Sorption

Dry sorption methods have been studied using a variety of materials. The advantages of dry sorption include operational simplicity, ease of waste effluent handling, inexpensive sorbent cost (depending on regenerability of sorbent) and low maintenance costs. Dry sorption is essentially gas filtration achieved by chemically sorbing NO_x to the sorbent surface.

Past research and application work has shown that dry sorption methods have the potential to effectively control NO_x. Ganz (1958) evaluated NO_x removal by various compounds including activated carbon, aluminosilicate, silica gel, manganese oxide, copper dioxide and coke. He found aluminosilicates to be the most efficient NO_x sorbent. James and Hughes (1977) used calcined limestone and dolomite to remove high-concentration NO with good results. A review of dry basic sorbents suggests that other materials such as MgO and ZnO are possible sorbents of NO_x (Kompapa, 1986). Kimm researched NO_x sorption to MgO-coated vermiculite (MgO/v); specifically, his results showed the MgO/v sorption of NO₂ (Kimm, 1995, Kimm et al., 1995).

Patented processes for sorbent NO_x control are numerous and point to the generally perceived benefits of dry sorption. Lott et al. (US Patent 5,795,553, 1998) has patented a material comprised of (potassium or sodium) alkali metal and copper-doped hydrous zirconium oxide that is coated on to a honeycomb cordereite monolith to adsorb NO_x emissions under lean-burn operations of mobile sources. Golden et al. (US Patent 5,779,767, 1998) describe the use of an adsorbent of alumina/zeolite treated with basic alkali metal compounds to control NO_x. The most preferred treatment material in this process is potassium carbonate. Bortz and Podlenski (US Patent 5,165,902, 1992) apply injected dry sodium (NaHCO₃ and/or other basic sodium materials) additives, under controlled moisture additions, to remove NO₂ and SO₂ emissions from stationary sources. Lever et al. (US Patent 5,096,871, 1990) patented a procedure for making a general acid-gas adsorber consisting of activated alumina and an amorphous alkali aluminum silicate. Materials capable of sorbing acid gases have been considered using activated alumina with additions of alkali metal materials (US Patent 5,096,871, 1992). Additions of iron

oxide to synthetic layered double hydroxide sorbents to enhance oxidation greatly improved the utilization of sorbents. The sorbents include varying amounts of aluminum, carbonates, and hydroxides (US Patent 5,116,587, 1992). Nelli and Rochelle have studied the combined removal of NO_2 and SO_2 using a patented mixture of calcium hydroxide and silicate (Nelli and Rochelle, 1998).

Cryogenic gas-purification patents for the removal of oxides of nitrogen apply alumina and zeolite adsorbents (US Patent 5,779,767, 1998) with additions of alkali hydroxide materials to improve the removal of unwanted gases, including NO_x . Many other applications relating alumina to cryogenic-gas purification can be found in this patent.

Polymeric materials have been tested for the removal of NO and NO_2 . Kikkinides and Yang (1991) tested a weak-base macrorecticular resin to simultaneously remove NO_2 and SO_2 .

Applied methods of dry sorption

The ADVACATE process uses an activated sorbent of lime and fly ash that has been pilot-scale tested for SO_2 control. However, laboratory studies have found that significant NO_x control may also be possible (Nelli and Rochelle, 1996).

The NOXSO process uses sodium-impregnated alumina beads of sorbent in a fluidized bed system (Ma et al., 1995). Removal of SO_2 and NO_x has been studied in small-scale process tests where 90% SO_2 and 90-70% NO_x removals were observed. Adsorbed NO_x is removed by heating the sorbent to 600 °C in a second fluidized bed. After heating, the sorbent is treated with a reducing gas, such as methane and steam to produce SO_2 and H_2S that can be converted to elemental sulfur via the Claus process.

Reburning of the desorbed concentrated NO_x-laden gas from the saturated sorbent has also been a process which was recommended over conventional adsorption/catalytic methods (Regalbutto, 1994). Improvements upon this process have been achieved and described in a patent in which additions of silica as a strength enhancer and hydrothermal stabilizer is included with an active ingredient of an alkali or earth alkali material (US Patent 5,585,082, 1996).

The LILAC process uses a sorbent composed of fly ash, lime, and gypsum. The sorbent is injected into the flue gas duct. Solids are collected in either a baghouse or ESP. Pilot-plant tests in Japan showed removal of 75% SO₂ and 55% NO_x using a 2.9 Ca/S weight ratio (Markussen and Livengood, 1995).

NaTec Resources Inc. has tested dry sodium carbonate injection into coal-fired boilers at commercial installations in several industrial sites. Removal efficiencies for SO₂ and NO_x were near 70% and 40-0%, respectively, in systems equipped with electrostatic precipitators (ESPs). Systems with baghouses showed removals of SO₂ and NO_x near 90% and 25%, respectively (Markussen and Livengood, 1995).

Spray dryer FGD technology utilizes alkali sorbent in the form of a slurry injected into the flue gas and collected as dry particulate. The particulate is collected and disposed of in landfills. Very little NO_x is removed under normal conditions but researchers at the Pittsburgh Energy Technology Center (PETC) have found that additions of NaOH promote significant NO_x removal at elevated dryer-exit temperatures (Markussen and Livengood, 1995). Demonstration tests at 20-MW high-sulfur burning coal plants with 10 to 3 % weight additions of NaOH reduced the required lime and improved NO_x

removal to near 35%. Removal occurred mostly in the baghouse over extended intervals. NOx removal was higher under higher SO₂/NOx ratios.

Small-scale sorbent systems for domestic coal-fired combustors were designed by Arthur D. Little Inc. (Benedeck, and Flytzani–Stephanopoulos, 1994). Of the sorbents considered, copper–alumina was the most promising. The NOx/SO₂-control units are designed for domestic use in coal-fired combustors and are applied in the form of a cross-flow filter unit.

The USAF has promoted a number of studies for controlling the highly variable emissions of NOx from jet engine test cells (Kitrell, 1989; Lyon, 1989, 1991; Nelson et al., 1989, 1992, 1993, and 1994; Petrik, 1992). From these studies, a dry sorbent material of magnesium oxide coated onto vermiculite (MgO/v) was found to be effective in controlling NOx emissions. Development of this sorbent material was the impetus for the current research that has expanded on previous sorbent research in this laboratory.

Adaptation of these dry sorption methods has demonstrated that the practical application of NOx sorbents is possible. The greatest benefit derived from dry sorption in comparison to other methods is their lack of sensitivity to highly variable operational conditions. The output NOx concentration, gas flowrate, and temperature fluctuations need only be monitored to track the amount of sorbent necessary to maintain a desired removal efficiency. Supplies of reducing gas are not necessary. Thus, the emission of ammonia or other reducing gas is not an issue. Sorbents can perform over a range of temperatures that are lower than those required by SCR and thus allow the system to be located after flue-gas particulate controls. This feature reduces the effect of particulate on reactive gas sorption. Sorbents are normally regenerable and with further research the

number of cycles of use may be improved and thus sorbent consumption reduced. Dry material handling and simple system structure design have obvious benefits over wet sorption methods. The design of sorbent controls for smaller systems can be quite simple and thus reduce start-up cost in comparison to other reduction methods.

Hybrid Systems

Hybrid systems have been under investigation from laboratory-scale up to full-scale studies. The benefits of combining technologies of combustion modification with flue-gas treatment has enabled >95% removal of NO_x. Described below are several of the better developed and field-tested applications.

A 32-MW "Federal Cogeneration" natural-gas turbine power plant facility owned by Sunlaw Cogeneration Partners in Vernon, California uses a hybrid system of water injection and a patented "SCONOX" process to achieve NO_x emissions less than 2 ppm. Water injection reduces the exhaust NO_x to near 25 ppm. The SCONOX process uses catalytic oxidation of exhaust CO to CO₂ followed by catalytic oxidation of NO to NO₂ (US Patent 5,607,650). The oxidized NO₂ then adsorbs to a bed of potassium carbonate-treated alumina. The sorbent is regenerated with H₂ and CO₂ to emit H₂O and N₂ and regenerate the K₂CO₃. This system has been acknowledged by the EPA as having achieved the Lowest Achievable Emission Rate (LAER) for combined-cycle gas turbine systems firing natural gas. A more recent patent describes a combined catalytic/adsorber in which an alkali or alkaline earth carbonate or bicarbonate, preferably potassium carbonate, is coated to a platinum coated high-surface area alumina (US Patent 5,665,321, 1997). This material performs in a similar manner to layered double-hydroxide sorbents (US Patent 5,116,587, 1992).

Integrated dry injection using low-NO_x burners, dry injection of alcohol-water hydrated lime for SO₂ capture, and dry injection of commercial-grade sodium carbonate for additional SO₂ removal and NO_x removal has been tested. Research-Cottrell Environmental Services and Riley Stoker achieved 90% SO₂ and 15% NO_x removal using a proof-of-concept unit following low-NO_x burners (US DOE, 1997).

The LIMB (Limestone Injection Multistage Burner) process uses Ca(OH)₂ injected dry sorbent to control SO₂ with low-NO_x burners for NO_x control. The system has been pilot-scale tested on coal-fired boilers with 70% NO_x and SO₂ control using a combined improved removal system by adding NaOH or Na₂CO₃ to the injected sorbent (US DOE, 1997).

Other processes include the SNRB process which combines sorbent injection with a hot catalytic baghouse to adsorb SO₂ and convert NO_x to N₂ and water (Markussen and Livengood, 1995). The SNOX process catalytically removes SO₂ and NO_x in the flue gas while producing salable concentrated sulfuric acid. Selective catalytic reduction of NO_x to N₂ and water using NH₃ is followed by catalytic oxidation of SO₂ to SO₃. The SO₃ is hydrated in a glass condenser and the exothermic process energy recouped. A 30-MW petroleum-coke fired boiler in Italy maintains greater than 96% removal of both SO₂ and NO_x. A demonstration project as part of a DOE Clean Coal Technology Program has continued to show 95% SO₂ and 94% NO_x removal. A similar process called DESONOX uses a single tower containing both reduction and oxidation catalysts. Removals for low-sulfur coals are near 80% for NO_x and 94% for SO₂ (Markussen and Livengood, 1995).

Related SO₂-Control Methods

The efforts to control SO₂ emissions from various sources are more detailed and extensive than research for improved NO_x control. This difference in research efforts is partly due to the historically known effects of SO₂ sorption relative to studies of NO_x sorption. The research on SO₂ control is related in several ways to NO_x control. A number of control application sorbents apply to both SO₂ and NO₂ through observed performance measures (US Patents 5,665,321, 1997, 5,585,082, 1996 5,165,902, 1992, 5,120,508, 1992, 5,116,587, 1992, 5,096,871, 1990, 4,721,582, 1987). Gaseous SO₂, NO and NO₂ are considered "acid" gases in that hydration of these gases result in acid formation. The United States Bureau of Mines has investigated the use of alkalized alumina for the control of SO₂ emitted from coal-fired power plants (Murphy, 1973). Regeneration temperature of the alkalized alumina destroyed the material and thus further studies were not pursued. Numerous patents have been granted for various aluminas and alkali and alkaline-earth treatments (US Patents 2,992,884, 3,501,264, 3,8535,031, 3,699,037, 3,974,256, 4,002,720, 4,259,179, 5,002,742) to control gaseous sulfur emissions.

Other NO_x-Control Methods

Electron beam irradiation initiates reactions that oxidize SO₂ to SO₃ and NO to NO₂ (Cooper and Alley, 1986). The oxidized compounds are easily reacted further to form salts. However, the cost of the energy required is significantly higher than for other methods. Methods are under investigation to reduce these additional energy costs.

Given the variety of methods being tested and those currently in use, improved system design has become a very specific practice according to the type of combustion

process being considered. If current regulation strategies require stricter NO_x controls for combustion sources having more-variable outputs, single, conventional NO_x reduction methods will be ineffective and either hybrid systems or new technologies will be needed. A dry filter material may serve to provide NO_x control that could be regenerated on a regular basis.

Research Justification

Past research of solid sorbent materials indicates that practical application of sorbent materials is possible despite the limited understanding of current sorbent material sorption properties. The various pilot-scale studies have indicated that a sorbent material has distinct advantages over conventional NO_x control methods. Also, laboratory studies related to this topic have proposed various mechanisms of NO_x sorption by solid sorbents. No other research has provided an in-depth study of the mechanisms involved in NO_x sorption to such common material as untreated γ -alumina, K₂CO₃-treated alumina, and KOH-treated alumina. The kinetics of the sorption process has not been studied from both gas- and solid-phase analyses. The stability of these compounds has not been studied at temperatures experienced under real conditions. In addition, tests of the effects of other gases on NO_x sorption have not been performed for these materials in a comprehensive manner. Applicable improvements to solid-sorption control of nitrogen oxides must be accompanied by fundamental research on the sorption processes.

Research Objectives

Based upon the justification for this basic research, the objectives of this study are as follows:

- Qualify and quantify NO_x sorption for the most promising sorbent materials.
- Evaluate the controlling mechanism(s) of sorption (diffusion or reaction).
- Determine controlling factors in the sorption potential of alkali compounds
- Evaluate and compare saturation characteristics of sorbents.
- Evaluate the progression of gas and solid conditions over exposure time.
- Measure nitrogen surface species formed on sorbent materials.
- Determine the affects of additional gases, such as O₂, CO₂, SO₂, and H₂O on the NO_x sorption process.

CHAPTER 2 EXPERIMENTAL

Fixed-Bed Reactor System

Laboratory experiments to measure NO_x sorption to solid sorbents were performed using a fixed-bed reactor system. The design of the fixed-bed reactor system was modified during the course of experimental work. A reactor system, that was used by a previous researcher (Kimm, 1995), was initially used in this research for comparison of data with the results of Kimm. Studies of magnesium oxide-coated vermiculite (MgO/v) sorbent with added water were performed using the redesigned system, including a redesigned sorbent reactor tube. After the study of added-water effects on MgO/v sorbent was completed, the redesigned system was modified once more to accommodate three sorbent reactor tubes in parallel in the furnace. The experimental errors associated with these three system designs differ and are discussed within the detailed description of each system.

Initial Fixed-Bed Reactor System

Initial studies of NO_x-sorption onto MgO/v were performed using a laboratory-scale, single fixed-bed reactor system operated under isothermal conditions. The system has been previously described (Kimm, 1995). This laboratory system is shown in Figure 2-1. Certified cylinder gases (BOC Gases, Murray Hill, New Jersey) sources consisting of diluted NO and NO₂ (balance N₂) are mixed/diluted by measurement of flow

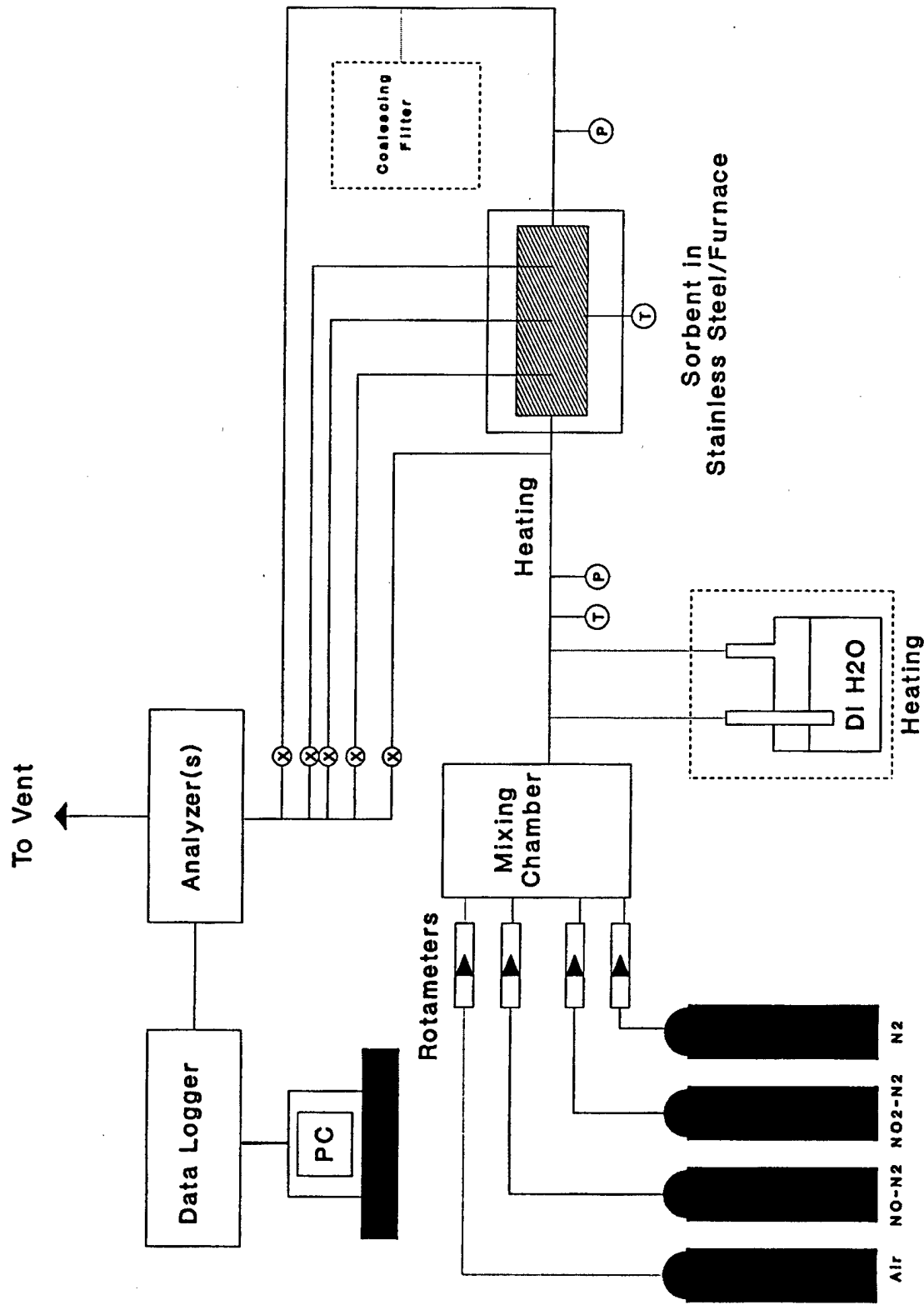


Figure 2-1. Experimental system developed by Kimm (1995) to study NOx removal by magnesium oxide coated vermiculite (MgO/v) sorbent.

through in-line calibrated rotameters (Omega Engineering, Inc., Stamford, Connecticut) prior to entering the bypass line or the reactor bed. Rotameter calibrations were performed regularly on a quarterly basis using a primary standard bubble meter (Gillibrator, Gillian Instrument Inc., Wayne, New Jersey). The reactor bed enclosure is a 1-in. diameter, 18-in. long 316 stainless steel tube fitted with NPT-Swagelok[®] fittings and placed vertically inside a tubular furnace (Model 421135, Thermolyne, Dubuque, Iowa). A type-K thermocouple (Model KQSS-116 -24 and -18, Omega, Stamford, Connecticut) is clamped to the outside of the reactor tube to measure the reactor bed temperature. Sorbent material was weighed and then poured down into the reactor tube to rest upon a 316 stainless steel mesh wire (Tyler screen size 325) support. The tube was flushed with deionized water and air dried before each test. Preliminary measurements were made to quantify the possible interaction of gases in a clean reactor bed. After cleaning the reactor bed outlet concentration was 99+% of the bypass line concentration. For quality assurance purposes, the latter test was performed periodically.

Gas can be continuously sampled for NO and NO₂ content from the bypass or the bed outlet line using a chemiluminescent NO_x analyzer (Model 42H, Thermo Environmental Inc., Franklin, Massachusetts). NO_x concentration checks are performed before and after each test using the NO_x-test gas concentration flowing through the bypass line. Daily NO_x analyzer calibrations were performed with N₂ (zero value) and NO and NO₂ gases certified by manufacturer analysis having a concentration of near 80% of analyzer full-scale range (span value). Control charts of zero and span check values were created and used such that values diverging more than three standard deviations from the mean without an acceptable reason required recalibration of the analyzer. The

response times of the NO_x analyzer in measuring gases flowing from the bed were delayed for about 30 seconds to one minute, depending on flow rates, and data were corrected for the delay.

Three forms of graphical information are used to describe data collected from fixed-bed reactor experiments. One format provides qualitative comparisons of the data collected from the reactor bed gas (NO and NO₂) as bed outlet concentration of gases. A second format of graphics gives quantitative information of the data as accumulated moles of gas sorbed or produced per mass of bed (μmole/g). The third format shows the rates of gas sorbed/produced to indicate trends of gas conversion.

Redesigned System: Single and Triple Bed

The original laboratory-scale single fixed-bed reactor (Kimm, 1995) was redesigned to improve the operation, reliability and performance of the system. The redesigned system is shown in Figure 2-2.

System features can be described using Figure 2-2. Gas flows are obtained from certified gas cylinders as in the original system. Five rotameters, having various flow ranges, that are used to mix the gases, are placed on a supporting frame with quick-connect fittings to the inlets. One rotameter can supply N₂ gas to the H₂O saturation vessel for water vapor-effect studies. A mass flow meter (Model FC-280, Tylan, Rancho Dominguez, California) is set in line following the mixing rotameters to measure total gas flow. A three-way valve allows the gas to flow either to the bypass line or to the reactor beds. A quick-connect fitting was added to the line for flushing the reactor bed(s) without

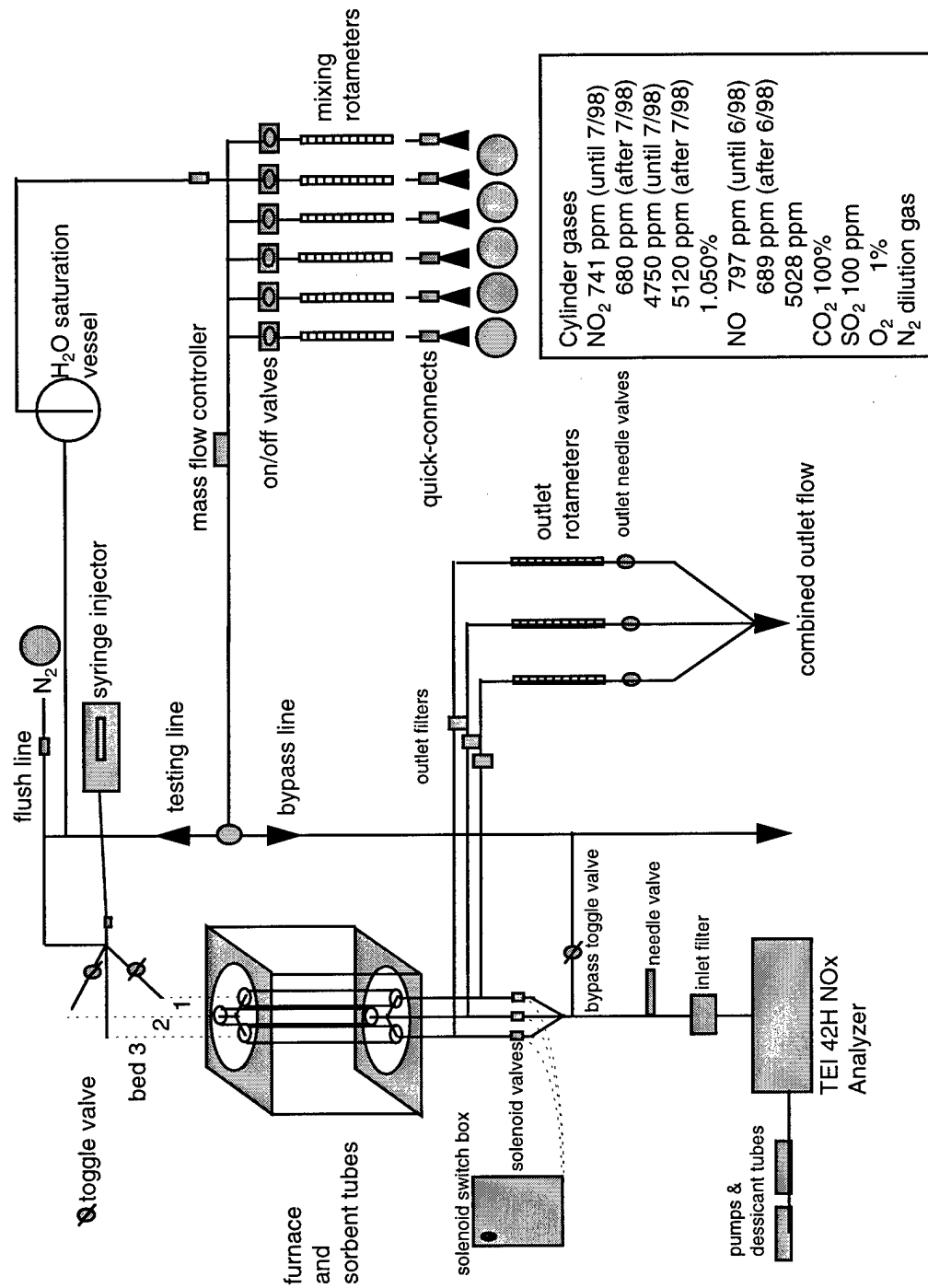


Figure 2-2. Redesigned experimental arrangement for fixed-bed reactor system.

interfering with the inlet mixing gas that is directed to the bypass line. A clam shell type furnace (Model F79325, Thermolyne, Dubuque, Iowa) was purchased to replace the original smaller tubular furnace.

Triple bed

Initially, the redesigned system included only one redesigned sorbent reactor tube. The studies of MgO/v with added water (see Results and Discussion) were performed using the single redesigned sorbent reactor tube. The redesigned reactor tube was a 0.65 in. I.D., 18-in. long 316 stainless steel tube (0.049 in. thickness) with airtight thermocouple insert ports located above and below the 4-in. bed.

Following the MgO/v-H₂O study, the single-bed tube reactor configuration was replaced with three parallel reactor bed tubes. In addition, the single inlet line was modified to incorporate a three-way manifold. Reactor bed #3 had an optional connection to be used for water injection. Inlet lines leading to beds #2 and #1 had on/off toggle valves to allow the use of either one or two beds at a time. A remote controlled solenoid valve was placed at the outlet of each reactor bed to sample effluent gas from that bed. The sequence and time of gas sampling from each bed was adjusted using developed computer software programmed in Visual Basic™. The flow of gas leaving each bed was measured using an outlet line rotameter. Inert filters (47 mm diam., 5 µm pore size, PTFE, Gelman Sciences, Ann Arbor, Michigan) were placed after the sampling lines to trap particulate material that escaped from the beds and might have contaminate the rotameters and the NOx analyzer. The outlet tubing configuration also helped prevent particulate entering into the gas-sampling solenoid valves.

Adjustable features were one of the primary benefits derived from the redesigned reactor system. Additional cylinder gases could be easily added to the existing gas mixtures via Swagelok™ quick-connects to one of the five inlet rotameters.

Water injection

Water vapor would be added to the gas mixture via two optional connections. A syringe could be used [as needed] to inject additional water vapor into the gas via bed #3. Also, bed #3 had a heat-tape-wrapped injection line that would be activated when introducing a known amount of water vapor. The heat rising from the furnace further ensured that the water vaporized. Furthermore, lesser amounts of water vapor could be added to the gas mixture via an alternative connection in the reactor line. Here the water vapor was produced using the saturation pressure of deionized water in a glass bulb with a fritted-bubbler. A portion of the inlet N₂ gas was diverted through the glass bulb to obtain the desired low-concentrations of water vapor. Measurements were made to ensure complete N₂ gas saturation with water at the flow rates used. The theoretical saturation water vapor pressure was obtained within experimental error.

System automation

Certain aspects of the reactor system were automated. A computer data acquisition card (Model PC-LPM-16, National Instruments Inc., Austin, Texas) was purchased to allow for automatic collection of data from the NO_x analyzer and the thermocouples, and for switching of the solenoid valves. A Microsoft® Visual Basic™ program was created to control the DAQ card and provide for collection of data.

To ensure that the computer recorded accurate data from the NO_x analyzer, voltage output settings on the analyzer were initially adjusted and checked on a quarterly

basis. No observable errors have occurred in collected computer data when compared to the displayed NOx analyzer concentration readings. The thermocouple signals were attenuated with additional equipment obtained from the thermocouple manufacturer (Model CCT-23, Omega, Stamford, Connecticut). The attenuator was adjusted to provide a linear, accurate and measurable voltage signal to the DAQ card. The attenuator was adjusted such that a calibrated, hand-held temperature readout device (Model HH23, Omega Inc., Stamford, Connecticut) matched the computer readout values.

Fixed-bed reactor system: experimental error

Given that the initial reactor system was used only to perform comparative testing with the work of Kimm. Detailed analysis of that system error was less in comparison to later studies.

The systematic errors in the fixed-bed reactor system were due to variations of bed temperature, flow mixing, and analyzer calibration. Temperature measures were obtained using an 18-in. type K thermocouple inserted through the bottom of the temporarily opened end of the sorbent reactor tube. Temperature at the horizontal center of the bed at vertical positions of 8 and 12 in. in the sorbent tube was measured three times at a furnace temperature setting of 170 °C for gas flowrates of 0.3 and 3 standard liters per minute (sLpm), respectively. The 8- and 12-in. average measurements for 0.3 sLpm were 189.6 and 206.5 °C and for 3.0 sLpm 193.8 and 204.1 °C. No alterations to the position of the bed were made because the bed positions were chosen and used in the work by a previous researcher (Kimm et al., 1995) and comparison studies required the system to remain unaltered (Kimm, 1995). Cylinder gas N₂ was used for gas flow variation tests.

Test errors due to flow mixing were found to be the most significant experimental error source when gas dilutions greater than 10:1 were used. One must consider the measurable flow parameters used to perform sorption tests: rotameter values and total flow. To test the effect of flow parameters on the input, NO_x flow control settings were varied over extreme ranges of dilution for typical NO_x concentrations and the NO_x measured. The greatest dilutions were 10:1 for any cylinder gas. Control of dilution is dependent on the precision of the rotameter and the relative position of the rotameter ball. The precision of reading the rotameters was found to be near 1% of full-scale flow. Thus, a maximum dilution of 10:1 would be expected to vary the gas concentration by 10%. Testing of the flow controls showed that a 10% variation does occur at the maximum dilution.

The principal NO_x analyzer parameter that was found to significantly affect NO_x measurements was the supply of dry air to the ozonator. Daily calibrations of the NO_x analyzer indicated that the fluctuation in the daily NO calibrations were subject to the dryness of the analyzer air supply. Desiccant canisters used for drying the input air to the ozonator were set in parallel to provide a longer continuous supply of dry air.

Redesigned system

The temperature profiles in the sorbent tube were obtained at 250 °C using an 18-in. type K thermocouple inserted through the air-tight fittings placed temporarily at the bottom of the sorbent tube. Temperature variations from a bed height of 8.5 to 12.5 in. were found to vary from 240 to 265 °C and 249 to 255 °C with no gas flow and at 2 aLpm, respectively. The variations were less at lower temperatures. Cylinder gas N₂ was used for gas flow variation tests.

The mass flow controller added to the system has a full-scale error of 1% when full scale was set at 3.18 Lpm. Thus, the error at the lowest testing flow of 1.5 Lpm (0.5 Lpm x 3 beds) was approximately 2%.

Temperature measures throughout the redesigned triple-bed reactor were sensitive to gas flowrate in the same manner as observed for the original single-sorbent-tube reactor.

Temperature profiles were measured along the length of the reactor beds using thermocouple inserts into each bed. Temperature measures were obtained at 250 °C using a 24-in. type K thermocouple inserted through the air-tight fittings located temporarily at the top of the sorbent tube. The flow rate of gas was varied from 0.5 to 1 Lpm. Cylinder gas N₂ was used for gas flow variation tests. The temperature profiles in the triple bed across the sorbent tube system are shown in Figure 2-3 for these two flows. The bed temperature profiles varied less at lower temperatures. The temperature profiles of each reactor bed indicated that the variation between beds was less than ± 5 °C during sorption tests. Horizontal variations of the tube temperature were observed to vary less than 2 °C from tube wall to bed center at the maximum sorption testing temperature, 250 °C.

Experimental error in sorption data was evaluated by performing identical tests of NO_x sorption on untreated alumina. The triple-bed system error may be considered to be of two types. Experimental error tests were performed to include simultaneously tested

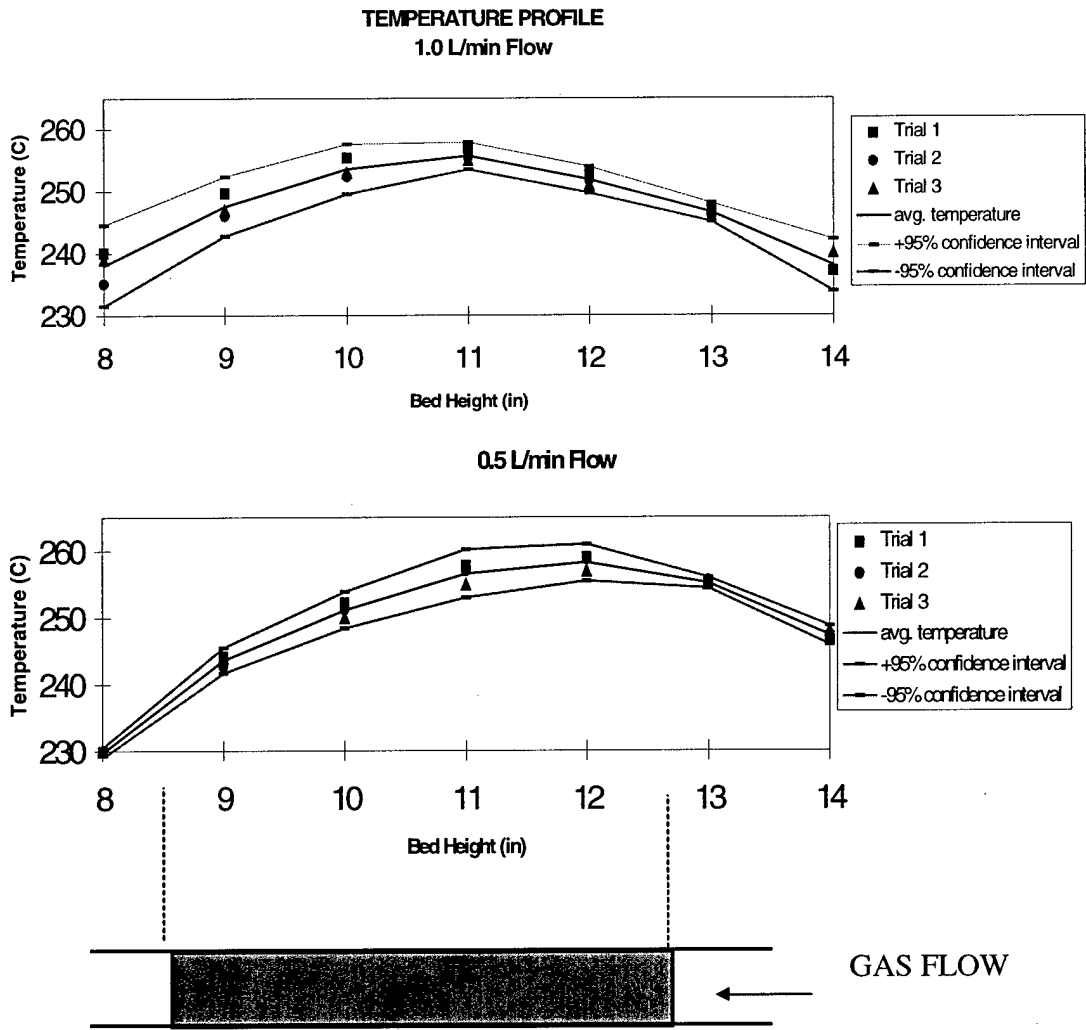


Figure 2-3. Sorbent tube temperature profile of triple fixed-bed reactor system.

Note: sorbent bed position shown.

samples and consecutively tested samples. Figure 2-4 shows the NO and NO₂ outlet concentrations resulting from experimental reproducibility tests of a) simultaneously run samples of untreated alumina, b) consecutively run samples of untreated alumina, for sorption of 50 ppm NO and 500 ppm NO₂ at 200 °C.

General Fixed-Bed Reactor Experimental Procedure

Prepared sorbent material is measured to a specified mass and poured into the reactor tube. The reactor tube is set into the furnace. Gas that has been mixed to the desired concentration is directed to the bypass line. Data collection initially was manually performed. After the system was redesigned, developed in-house software automatically recorded NO and NO₂ measures from the analyzer and temperatures from the thermocouples. The tube furnace temperature controller is set to provide the desired bed temperature. The redesigned system allowed the beds to be flushed (with N₂) prior to testing. Flushing the beds allowed for adjustments to equalize the outlet rotameter readings and to ensure no gas leakage. Once the bed temperature and gas mixture readings stabilized the gas was directed from the bypass line to the reactor bed line. Adjustments of inlet-gas mixing rotameters was performed during the test to ensure a constant gas mixture input. After the desired time of testing, the input gas is redirected to the bypass line for a post-test check of the inlet gas NO_x concentrations.

Experimental Conditions

Fixed-bed reactor system tests of NO_x sorption were performed with atypical ratios of NO₂:NO in gas mixtures. The NO₂:NO ratios used in laboratory tests were in the range of 1:1 to 50:1, whereas the normal ratio of combustion exhaust NO₂:NO is 1:20 (Cooper and Alley, 1986). This divergence from the normal ratio is based on an overall

NO_x-removal concept where NO is oxidized to NO₂ prior to NO_x sorption in flue-gas treatment applications. The mass of material used in the various test series was not constant. Initially the test sample mass was matched to conditions used in previous research (Kimm, 1995). The range of overall flowrates in the reactor beds used in the various test series was 1.0 to 0.5 Lpm. The reactor bed temperature during NO_x exposure tests varied from ambient (23 °C) to 250 °C.

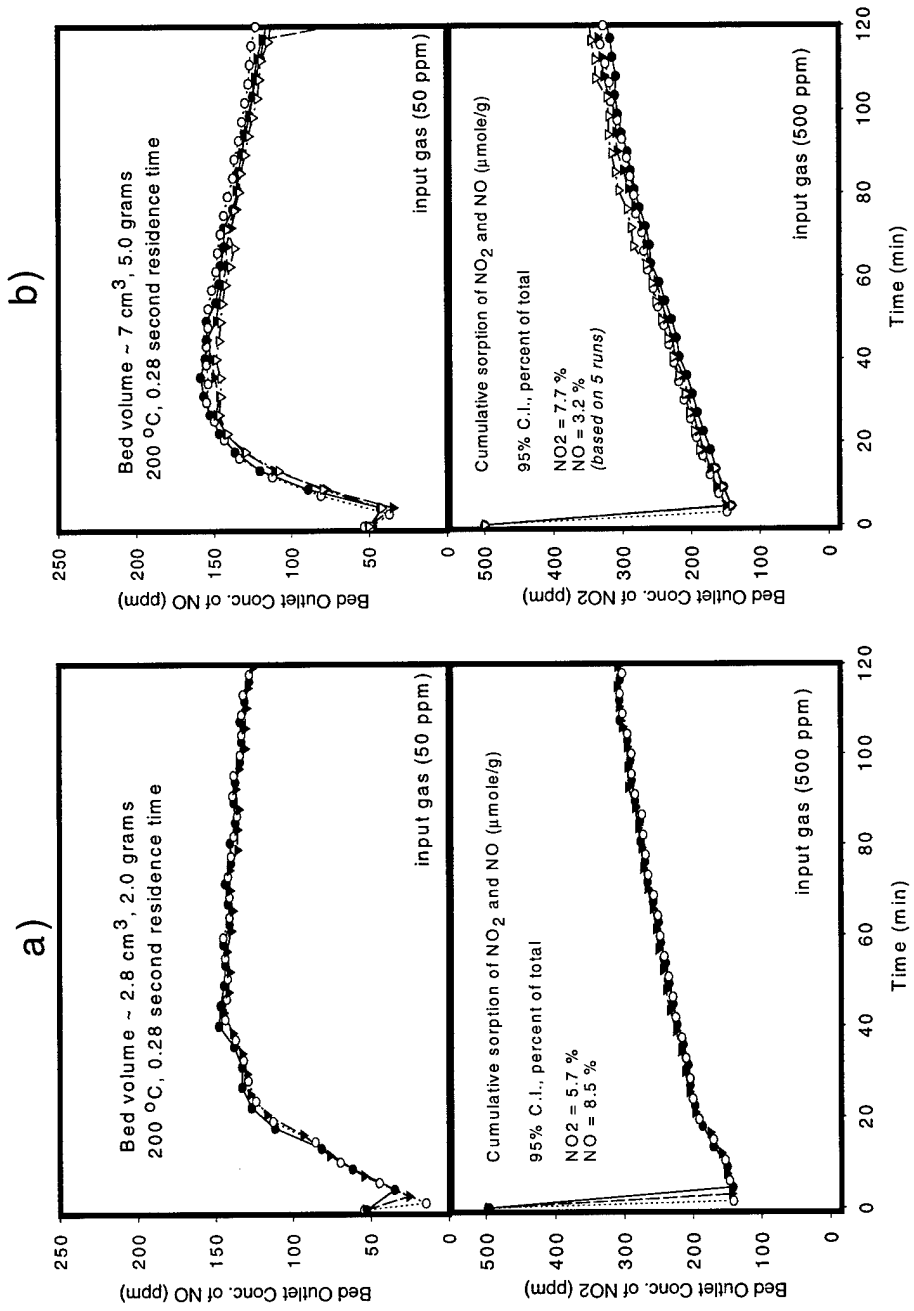


Figure 2-4. Experimental reproducibility tests: a) simultaneously run samples of untreated alumina, b) consecutively run samples of untreated alumina.

Some solid materials were thermally decomposed in the fixed-bed reactor system to observe the nature of decomposition species during a substantial ramp in temperature. Only reactor bed #3 was used to study these solid reactant decompositions and product formation. A set flow of N₂ gas was passed through the reactor bed while the temperature was ramped manually at 10 °C/min to a maximum of 750 °C. Exposed samples of reagent-grade nitrate and nitrite salts were decomposed. The salts proved extremely detrimental to the system in that the vaporized and decomposed salts reformed (condensed) along the outlet tube walls that were at lower temperatures. Thorough cleaning of the entire system outlet lines was required following these tests. However, decompositions of NO_x-exposed sorbent samples did not result in reformation of particulate material along the tube walls. A significant source of error in the results of the decomposition tests was observed following the tests. Reduction of NO₂ to NO by stainless steel is known to occur at temperatures above 500 °C (Sigsby et al., 1973). Tests were performed to observe this effect. The results indicated that measured NO_x species at or above 500 °C would be only NO due to reactor wall reactions. However, NO₂ was observed above 500 °C. This result is addressed later in the Discussion section.

Reproducibility of similarly NO_x-exposed samples of untreated alumina exposed for 2 hours to 500 ppm NO₂ and 50 ppm NO at 0.62 sLpm and 150 °C are shown in Figure 2-5. The results from these untreated alumina samples include errors due to NO_x exposure and, thus, represent a greater error than that expected for decomposition of two similar samples.

Additional gases or vapors tested in conjunction with exposure to NO and NO₂ mixtures include one of the following: water vapor, O₂, SO₂, and CO₂. Water injection was in the range from 1 to 5% of gas volume at temperatures ranging from 25 to 200 °C.

Sample Preparation

A variety of sorbent materials were studied in this research in which the preparation, if necessary, was varied as well. The materials include magnesium oxide-coated vermiculite (MgO/v), untreated γ -alumina, and γ -alumina treated with one of the following compounds: carbonates (Li, Na, K, Rb, Cs), hydroxides (Li, Na, K, Rb, Cs), or sulfates (Na and K).

Magnesium-Oxide Coated Vermiculite (MgO/v)

MgO/v was prepared following the technique used by Kimm (Kimm, 1995). One-kilogram batches were prepared using a 45:55 mass ratio of MgO (Elastomag 170 m²/g, Akrochem Inc., Akron, Ohio) and vermiculite (coarse grade, Stronglite Product Inc., Pine Bluff, Arkansas). Each batch was hand-mixed with a 4:1 mass ratio of deionized water/MgO-vermiculite. Batches were baked at 550°C for 30 min. in a muffle furnace and stored in airtight plastic containers. This preparation method is described in more detail in the patent description held by Sorbtech (US patent 4,721,582, 1987). Sorption

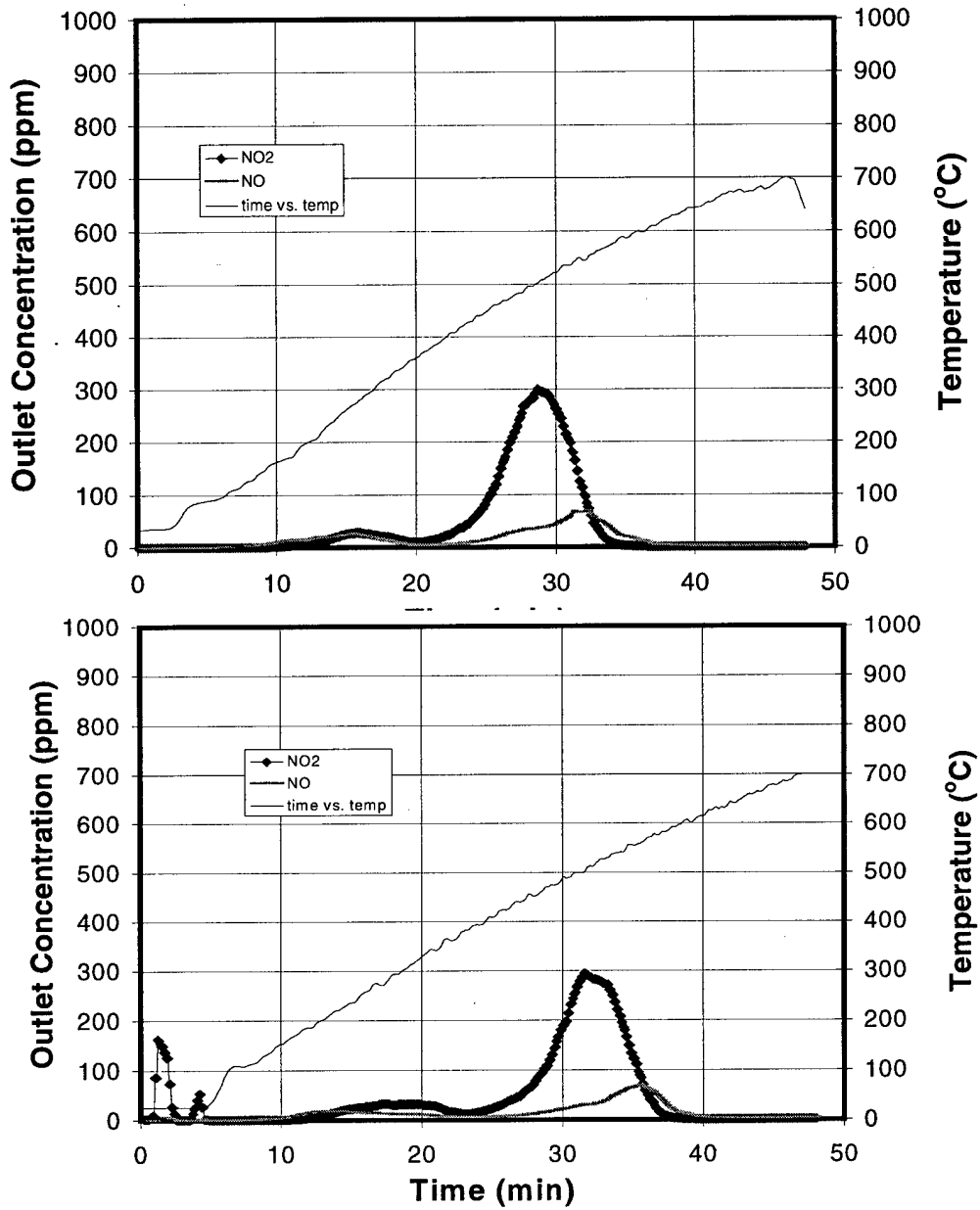


Figure 2-5. Reproducibility of decomposed samples separately sorption tested.

studies of the effects of aging on the MgO/v material stored in airtight containers showed that the stored sorbent performs well without deterioration over a minimum of two years. Storage of MgO/v in ambient air for periods of several weeks also does not appear to alter the NO_x sorption characteristics.

γ-Alumina: Untreated and Treated

Untreated cylindrical pellets (1/8 in O.D. x 1/8 in.) of γ-alumina were obtained commercially (material AL-3438 T, Englehard Corp., Elyria, Ohio) with a nominal surface area of 170 m²/g. Pellets were dried at 150°C for a 24-hour period prior to storage in sealed containers. Reagent-grade chemicals (Fisher Scientific, Pittsburgh, Pennsylvania) were used to make aqueous solutions for treating the alumina pellets. Solution concentrations varied from 1.0 to 0.04 M. Two types of treatment techniques were used: impregnation and precipitation. Most heated material studies have used the precipitate-prepared treated alumina. Impregnated pellets were prepared by flowing the salt solution through the bed of alumina pellets supported on Whatman 41 filter paper for about two minutes. Precipitated samples were prepared by mixing pellets with the salt solution and evaporating the solution to dryness. Both impregnated and precipitated samples were dried for 24 hours at 150°C. Impregnation treatments were performed only for initial comparative studies of treatment techniques. Table 2-1 provides a listing of the physical properties of treated materials as recorded during preparation.

Table 2-1. Physical properties of sorbent materials studied.

Sorbent material	percent	bulk density
MgO/v	MgO(45):v(55)	0.13
untreated Al ₂ O ₃	----	0.70
LiOH-Al ₂ O ₃	7.3	0.59
NaOH-Al ₂ O ₃	10.6	0.77
KOH-Al ₂ O ₃	13.8	0.80
KOH-Al ₂ O ₃	20	0.94
RbOH-Al ₂ O ₃	21.6	0.86
CsOH-Al ₂ O ₃	33	0.98
Li ₂ CO ₃ -Al ₂ O ₃	7.3	0.71
Na ₂ CO ₃ -Al ₂ O ₃	10.6	0.65
K ₂ CO ₃ -Al ₂ O ₃	13.8	0.79
K ₂ CO ₃ -Al ₂ O ₃	24.7	0.85
Rb ₂ CO ₃ -Al ₂ O ₃	21.6	1.01
Cs ₂ CO ₃ -Al ₂ O _{3p}	33	1.15
Cs ₂ CO ₃ -Al ₂ O _{3p}	29	
Cs ₂ CO ₃ -Al ₂ O _{3p}	23	

The nature of the containers (glass or ceramic) used to prepare treated samples does not appear to alter NO_x sorption behavior. NO_x sorption tests on precipitated alumina pellets having similar loading of KOH but prepared using different solution concentrations demonstrated that they have similar NO_x removal characteristics as seen in Figure 2-6.

Ion-Specific Electrode (ISE) Measurements

ISE methods were developed to measure hydronium (H⁺), nitrite (NO₂⁻), and nitrate (NO₃⁻) ions from extracts of NO_x-exposed alumina sorbents by David Pocengal (Pocengal, 1999). Separate methods were developed for NO_x-exposed untreated, K₂CO₃-treated, and KOH-treated alumina sorbents. NO_x-exposed sorbent samples were placed

in deionized water solution, adjusted for solution *pH* with sulfamic acid, and adding interference suppresser as necessary. Solution concentrations were in the range from 1×10^{-2} to 10^{-5} *M*. A *pH* electrode (model 13-620-AP50, Accumet, Pittsburgh, Pennsylvania) and portable *pH* meter (model AP-61, Fisher Scientific, Pittsburgh Pennsylvania) were used to measure the *pH* of aqueous-solution extracts. Ion-specific electrodes that measure nitrite (model 93-46, Orion, Beverly, Massachusetts) with a double-junction reference electrode (model 90-02, Orion) and nitrate (model 93-07, Orion) with a double reference electrode (model 09-01, Orion) were used to analyze sample extracts in aqueous solution. A *pH/mV* meter was used for nitrite and nitrate measurements (Model 245, Corning, New York). After NO_x-exposure, samples of treated or untreated alumina were ISE analyzed or stored in plastic vials (catalog # 14809B, Fisher Scientific, Pittsburgh, Pennsylvania). For certain samples, a portion (~0.5 g) was stored so that additional analyses of the sample could be performed if needed.

Measurement error of the developed ISE method was evaluated by splitting individual sorbent samples exposed in the fixed-bed reactor system into three

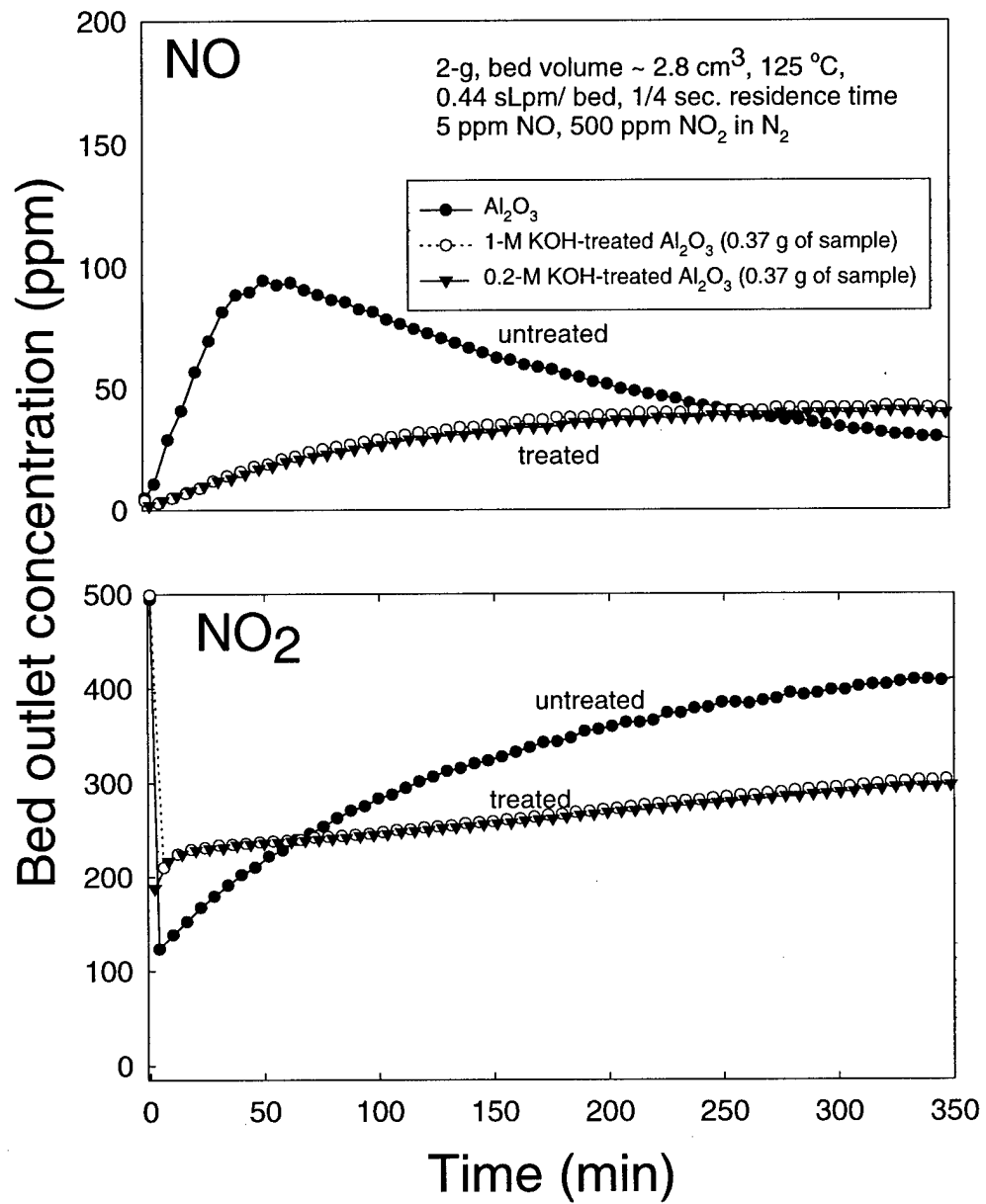


Figure 2-6. Samples prepared by different coating methods with similar mass amounts of coating showing similar NO_x sorption characteristics

1-gram samples and performing ISE analyses of each 1-gram sample. Error analysis was performed on NO_x-exposed untreated, K₂CO₃-treated, and KOH-treated alumina samples. The solution concentrations of the 1-gram sample extracts were near the lower concentration range applied in ISE measurements (1×10^{-4} to 10^{-5} M). Table 2-2 provides results of these tests. Other NO_x-exposed KOH-treated alumina samples were similarly ISE analyzed and results are shown in Table 2-2. The two additional KOH-treated alumina samples were exposed for varied time periods to evaluate the change in the nitrite-to-nitrate ratio with exposure. These tests are further discussed in the Results And Discussion chapter. The cumulative (NO + NO₂, and nitrite + nitrate) 95% confidence interval (95% C.I.) is calculated using the Student-t test with a cumulative standard deviation (*Stotal*) as

$$Stotal^2 = Sa^2 + Sb^2$$

where *S* is the standard deviation and *a* and *b* represent NO and NO₂ or nitrite and nitrate.

The ratio of measured ISE nitrogen to measured NO_x sorbed is used to express a fraction of recovery. Given the calculated 95% C.I. in Table 2-2, the ISE measurements of total nitrite and nitrate are in the range of measured NO_x sorption for all three sorbent materials. Using the 95% C.I., the fractional amount of error for cumulative nitrite and nitrate by ISE measurement on K₂CO₃-treated alumina is (47.2/203.4) 23%. Thus the high fractional NO_x/NO_x recovery of 1.19 is within the 95% C.I.. The ISE measurements indicated that recovery for untreated alumina, K₂CO₃-treated alumina, and KOH-treated alumina discussed in the Results and Discussion chapter, Gas and Surface Profile for the Sorption Process section were approximately 70 %, 120%, and 100%,

respectively. ISE measurements indicated that recovery of NO_x sorbed onto untreated alumina decreased with increased time between exposure and ISE analysis. This observed reduction of recovery is further discussed by Pocengal (1999). The reduced recovery affected the average recovery described in the Gas and Surface Profile for the Sorption Process section. Thus, these error-analysis tests, in which ISE analysis was performed immediately after NO_x exposure, represent a more accurate recovery. In addition to the effects on recovery of time between exposure and ISE analysis, nitrate and nitrite on untreated alumina was found to be difficult to transfer from the solid to liquid phase. Mechanically crushing the untreated alumina pellets and sonication of solution enhanced recovery and was performed. The high recovery of K₂CO₃-treated alumina is caused by extract solution ionic activity being greater than that in standard solutions and is further discussed by Pocengal (1999).

Cumulative errors were evaluated for collaborative work of sorbent samples similarly exposed in the fixed-bed reactor system followed by ISE measurement. An evaluation of cumulative errors was performed of NO_x-exposed untreated, K₂CO₃-treated, and KOH-treated alumina samples. The fixed-bed reactor system was used to simultaneously expose three samples using similar conditions used for evaluating the sorption mechanisms discussed later (see Gas and Surface Profile for the Sorption Process section). Three-gram samples of untreated, K₂CO₃-treated, and KOH-treated alumina were simultaneously exposed to 1950 ppm NO₂, residual NO (10 ppm) flowing at 0.885 sLpm per bed at 25 °C. The 30-minute exposures were performed three times and

Table 2-2. ISE measurement error of NO_x-exposed untreated, K₂CO₃-treated and KOH-treated alumina samples.

Coating material	Cumulative NO _x (μmol/g)			Cumulative nitrite and nitrate (μmol/g)			Recovery NO _x ⁻ /NO _x
	fraction error	NO	NO ₂	total NO _x	NO ₂ ⁻	NO ₃ ⁻	
untreated	-97.7	325.4	227.7	8.3	197.0		
				13.1	195.0		
				13.4	185.0		
mean				11.6	192.3	203.9	0.90
95% C.I.				6.48	14.6	15.9	
error fraction						0.08	
K₂CO₃	-5.6	177.1	171.5	108.0	106.0		
				84.4	85.7		
				113.0	113.0		
mean				101.8	101.6	203.4	1.19
95% C.I.				34.6	32.1	47.2	
error fraction						0.23	
KOH	-5.0	153.0	148.0	82.5	66.3		
				80.9	64.5		
				82.8	72.1		
mean				82.1	67.6	149.7	1.01
95% C.I.				2.3	9.0	9.3	
error fraction						0.07	
KOH	46.0	56.7	102.7	103.0	11.5		
short exp.				82.2	9.6		
				94.6	9.3		
mean				93.3	10.2	103.2	1.01
95% C.I.				23.7	2.7	23.8	
error fraction						0.23	
KOH	-363.9	1440	1076	134.0	609		
long exp.				318.0	903		
				279.0	801		
mean				243.0	771.0	1015	0.94
95% C.I.				219.4	337.8	402.8	
error fraction						0.40	

each sample was immediately ISE analyzed. Sorbent samples were not split for ISE analysis but analyzed as one measurement sample each. Based on the triplicate tests Table 2-3 includes results of measured NO_x sorption and ISE analyses of nitrite and nitrate. Similar results to the ISE measurement error tests (Table 2-2) of K₂CO₃-treated alumina are observed in that recovery is high (1.23). The error fraction of the total nitrite and nitrate by ISE measurement for K₂CO₃-treated alumina using the 95% C.I. is 14%. The error fraction of the NO and NO₂ sorption measurements for K₂CO₃-treated alumina using the 95% C.I. is 8%. Thus, given the combined error fraction of NO_x sorption measurements and the ISE measurements, a recovery of 123% is possible. The similar error fractions due to NO_x sorption or ISE measurements in Table 2-3 suggest that errors due to either NO_x-sorption or ISE measurement were not dominant. Also, comparing the error fraction of the ISE measurements in Table 2-2 and Table 2-2, one observes that ISE measurement fraction error varies from 0.14 to 0.23, respectively. The higher variation of error fraction of ISE measurements, alone (Table 2-2) indicates that ISE measurements are the same if not greater than error of NO_x-sorption measurements.

X-ray Photoelectron Spectroscopy

Certain features of sorbent samples of interest were further studied using X-ray photoelectron spectroscopy (XPS), courtesy of Professor G. Hoflund and his group, Chemical Engineering Department, University of Florida. This ultra-high-vacuum technique uses X-rays to bombard a material that will emit detectable photoelectrons of characteristic energies. Ultra-high vacuum (10^{-10} torr) is necessary to reduce the interference of gases during X-ray bombardment of the material. Upon bombardment, the

Table 2-3. Cumulative measurement error of fixed-bed reactor testing and subsequent ISE measurement of three samples of NO_x-exposed untreated, K₂CO₃-treated and KOH-treated alumina.

Coating material	Cumulative NO _x (μmol/g)		total NO _x	Cumulative nitrite and nitrate (μmol/g)		total NO _x ⁻	Recovery NO _x ⁻ /NO _x
	NO	NO ₂		NO ₂ ⁻	NO ₃ ⁻		
untreated							
mean	-114.8	335.0	220.2	8.9	181.3	190.2	0.86
95% C.I.	4.4	15.8	16.5	0.7	13.5	13.5	
error fraction			0.09			0.07	
K₂CO₃							
mean	-29.7	289.2	259.4	143.3	176.0	319.3	1.23
95% C.I.	5.1	20.2	20.8	6.9	43.7	44.2	
error fraction			0.08			0.14	
KOH							
mean	-25.8	284.1	258.3	146.0	144.0	290.0	1.12
95% C.I.	0.9	19.4	19.4	14.1	13.6	19.6	
error fraction			0.08			0.07	

elemental species will characteristically interact with the X-ray and may emit a photoelectron that is then measured for intensity.

Prior to XPS analysis, alumina pellets are crushed to expose the inner surface, placed in an aluminum cup, pressed into a new pellet, mounted on a stainless steel sample holder, and inserted into the ultra-high-vacuum chamber. This procedure exposes the pore walls for analysis. XPS is performed using a double-pass cylindrical mirror analyzer (CMA) (Perkin-Elmer PHI model 25-270AR, Eden Prairie, Minnesota). Survey spectra are taken in the retarding mode with a pass energy of 50 eV, and high-resolution XPS spectra are taken with a pass energy of 25 eV using Mg K α X-rays (Perkin-Elmer PHI

model 04-51 X-ray source). Data collection is accomplished using a computer-interfaced, digital pulse-counting circuit (Gilbert et al., 1982) followed by smoothing using digital filtering techniques (Savitsky and Golay, 1984). Since XPS is performed using a flood source, the XPS data represents an average over the area analyzed (~ 4 mm diameter). The reproducibility of survey spectra was evaluated for several samples. Figure 2-7 shows spectra of two separate samples of untreated alumina and separate samples of KOH-treated γ -alumina that were individually NO_x saturated. Survey scans of the individually NO_x-saturated samples include errors from KOH-treatment, and fixed-bed reactor exposure to saturate with NO_x, as well as sample preparation for XPS analysis.

BET Analyses

A few samples were tested to determine surface adsorption properties using the Brunauer–Emmett–Teller (BET) technique (Brunauer et al., 1938). The surface properties are measured by observed changes in pressure upon physical sorption of N₂ to the sorbent. Material surface-area measurements were performed on all supplied samples and pore size distributions were obtained on a few samples. Professor B. Moudgil, Materials Science and Engineering Dept., University of Florida, provided access to a BET analyzer (Model Nova 1200, Quantachrome, Boynton Beach, Florida) using system software.

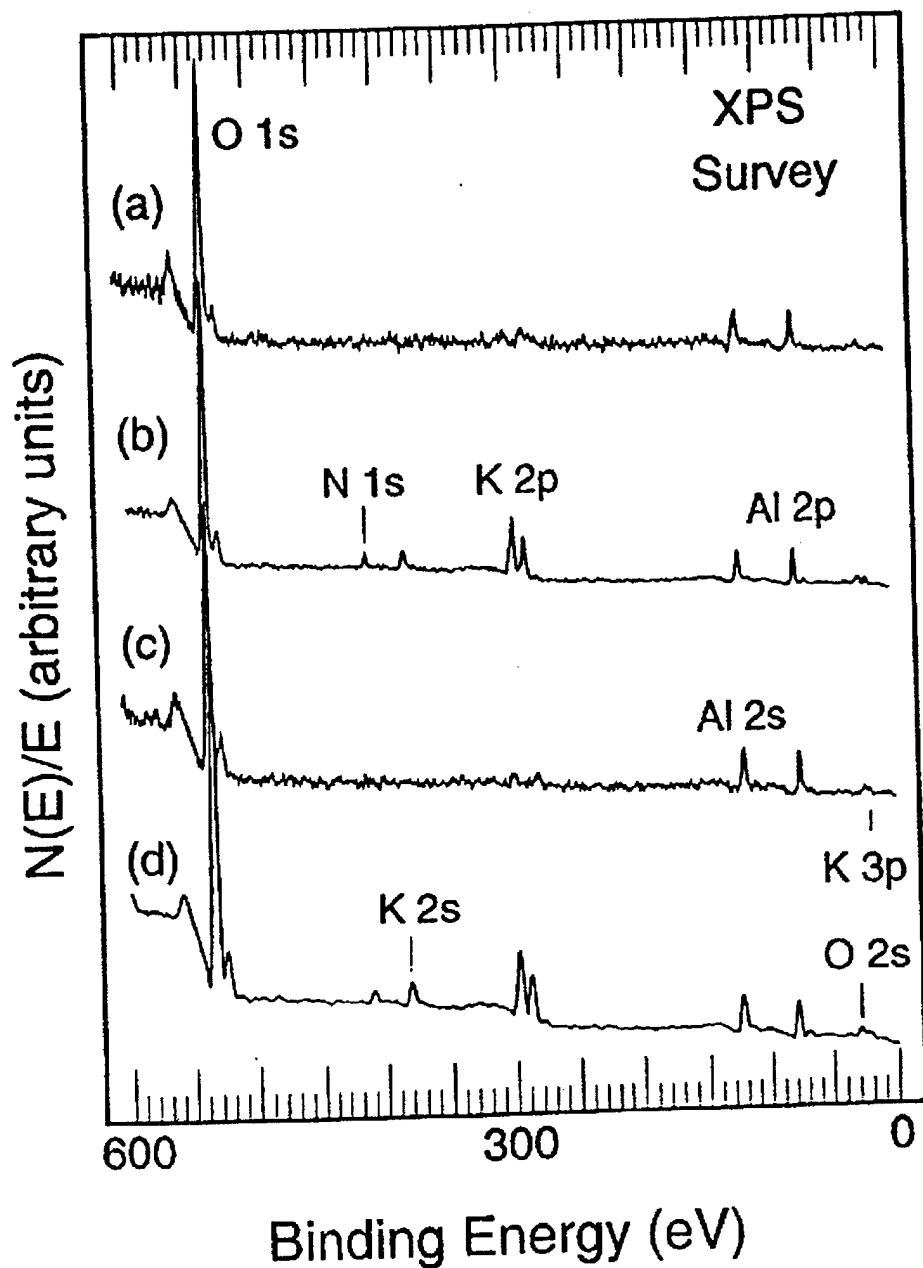


Figure 2-7. XPS survey spectra obtained from (a) untreated γ -alumina, NO_x saturated (b) untreated γ -alumina after KOH-coating and NO_x-saturated (c) untreated γ -alumina, NO_x saturated (d) untreated γ -alumina after KOH coating and NO_x saturated.

The BET sample tube is inserted into the analyzer sampling port where a canister of liquid nitrogen is placed around the testing tube. The canister of liquid nitrogen is necessary to maintain the sample near the condensation temperature of N₂ during testing. Certified high-purity N₂ cylinder gas (Grade 5.0, BOC Gases, Riverton, New Jersey) is used to sorb to the analyzed material. A standard set of five pressure point values are collected and converted into surface area measurements by the analyzer. The pressure values are typical for BET analysis from 0.05 to 0.30 fraction of total pressure.

Pore-size distributions were performed by desorbing an N₂-saturated sample. Twenty pressure points (increments of 5% of total pressure) are collected during desorption. The amount of gas desorbed from the sample is converted by the analyzer to provide an estimate of pore size distribution and pore volume.

Tests were performed to observe possible measurement errors due to variations in the BET analyzer sample preparation procedure. Samples are placed in pre-weighed calibrated glass test tubes, initially vacuum-outgassed for at least 6 hours, and heated to 150 °C to remove trapped gases and vapors within the solid material. The vacuum is set at near 10 Torr. Longer heating time periods do not significantly affect the reproducibility. After outgassing, the samples were weighed. Reproducibility error is found to be most significant for similarly prepared and NO_x-sorption-tested treated alumina samples (5% relative std. dev.). Repeated analysis of the same sample indicates insignificant variation (<1% at 95% C.I.).

Fourier Transform Infrared (FTIR) Analyses

A Fourier transform infrared spectrometer (FTIR) (Model 5PC, Nicolet, Madison, Wisconsin) was used to perform further analyses of NO_x-exposed sorbents, courtesy of Professor K. Williams, Department of Chemistry, University of Florida. This technique measures the infrared absorption (4000 to 400 cm⁻¹ wavenumber) by a material surface in which the absorption is characteristic of that material. The sorbents studied before and after NO_x exposure were powdered by placing in a container and crushing with a rod made of 316 stainless steel. Powdered samples and reagent-grade materials were stored in plastic vials prior to transport and analysis by FTIR. During FTIR analysis the materials were held in a ZnSe-windowed container. A gas purging system (Model 53-152, Barnstead, Boston, Massachusetts) reduced the amount of gases within the chamber. PC software (Nicolet PC/IR ver. 3.2) was used to collect, display and store data from the FTIR. In order to obtain reproducible spectra of a single sample periodic scans (two-minute intervals) were performed until the background CO₂ gas peak (2550 cm⁻¹) was constant. Reproducibility testing was performed of the same sample powder that has been mixed between scans. The FTIR reproducibility scans are seen in Figures 2-8.

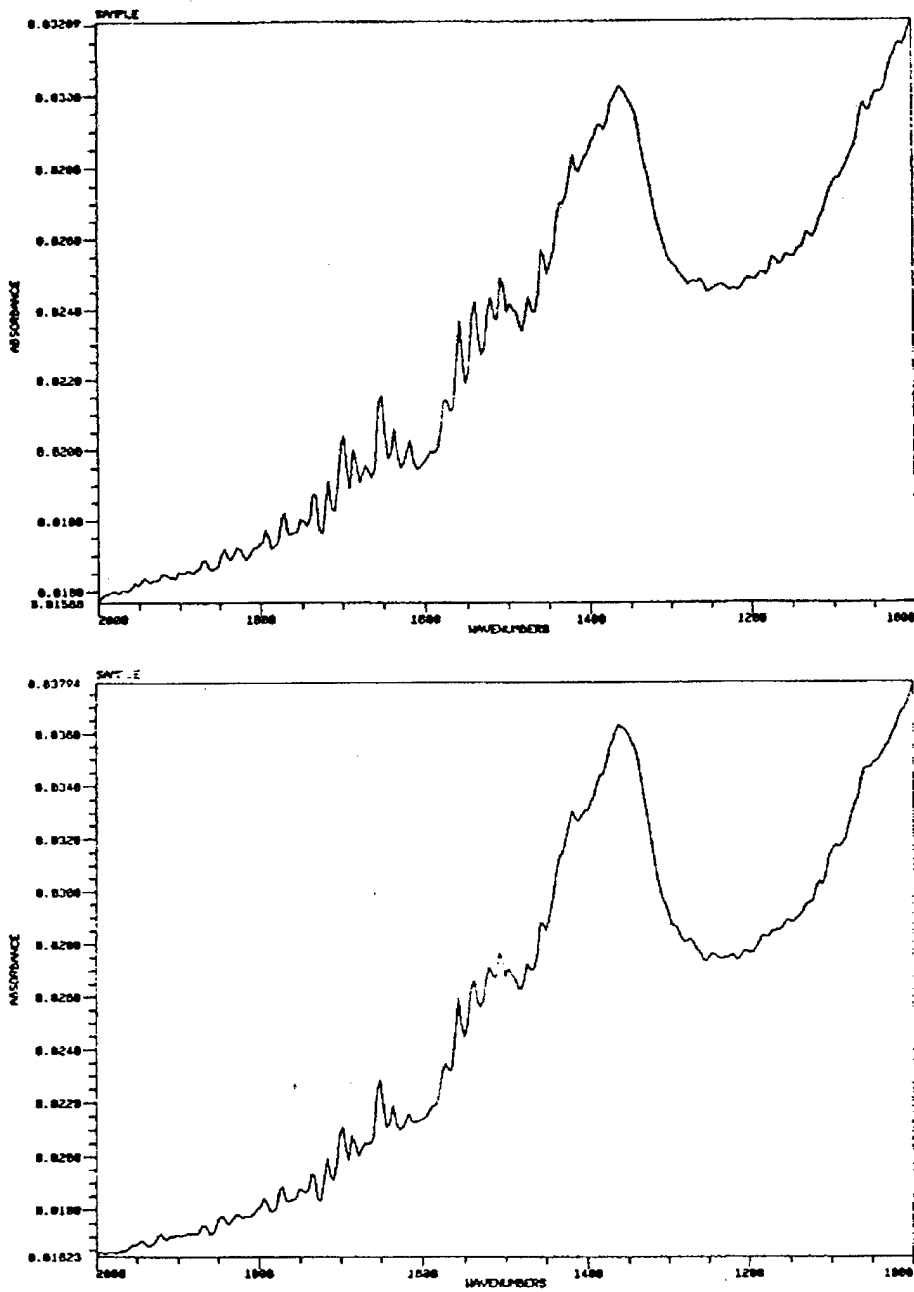


Figure 2-8. FTIR reproducibility of Cs_2CO_3 -treated alumina a) initial survey, b) second survey after mixing sample.

CHAPTER 3 RESULTS AND DISCUSSION

Methods of solid sorbent control of nitrogen oxides have been studied by many other research groups (Murphy, 1972; Nelson et al., 1989; Ma et al., 1995; and Nelli and Rochelle, 1998). From this previous research it is apparent that group-I compounds have been used successfully to sorb NO_x. Some researchers have proposed mechanisms for the surface reactions occurring during NO_x sorption. However, an in-depth analysis to quantify the sorption process has not been performed that is crucial to improving sorption properties. Initial studies are described that have led to questions concerning previously proposed mechanisms. Further research is described which identifies multi-step mechanisms of NO₂ sorption and suggests that the process is limited by the formation of nitrate and nitrite that is further converted to nitrate for the group-I compounds. In addition, group-I compounds remove both NO and NO₂ in the early stages of sorption.

A fixed-bed dynamic reactor system was constructed to serve as the main experimental method to study NO_x interactions with solid sorbents. Other analytical methods used to study sorbent exposed to NO_x include XPS (X-ray photoelectron spectroscopy), FTIR (Fourier-transform infrared spectroscopy), BET (Brunauer et al., 1938) surface analysis, and ion-specific electrodes. Initial experiments were based on the evaluation of magnesium oxide-coated vermiculite (MgO/v) and the effects of other gas constituents on NO_x sorption. As the research progressed to studies of other sorbents, the use of alumina pellets and group-I-compound coated γ -alumina were determined to be

superior to MgO/v and research became focused on the latter materials. The errors of an analytical technique dictate the quality of experimental data and the resulting conclusions. Therefore, an evaluation of the errors is included in the experimental techniques section of Chapter 2.

Studies of untreated alumina showed that the manufacturer or surface acidity of γ -alumina did not differ in sorption of NO_2 . XPS analysis of NO_x -exposed γ -alumina indicated that potassium impurities interact with NO_2 sorption. Potassium hydroxide was coated on alumina and found to remove both NO_2 and NO . Given the success of KOH-treated alumina, tests of sulfate, hydroxide, and carbonates in the form of sodium and potassium compounds, were coated in varied amounts onto alumina. Tests showed that potassium compounds improved NO_x sorption and carbonate coatings performed better per mole than hydroxide while sulfate compounds performed poorly. Next, group-I, lithium through cesium hydroxides and carbonates showed improved NO_x removal with decreasing ionization potential of the alkali metal element. A series of fixed-bed reactor experiments in which the concentrations of NO or NO_2 were varied over temperatures from ambient (25°C) to 250°C , indicated that NO_x sorption improved with temperature. Specifically, increased NO removal occurred at higher temperatures.

Proposed mechanisms of sorption of NO_x were formulated based on fixed-bed reactor tests and ion-electrode measures of nitrites and nitrates formed. Mass balance estimates for NO_x sorbed and surface nitrogen species produced were used to calculate reaction rates of the slowest stage of a multi-step mechanism. Confirmation of ion-electrode measures of surface nitrite and nitrate was accomplished using FTIR studies. Thermal decomposition of NO_x -exposed sorbent indicates that differences exist

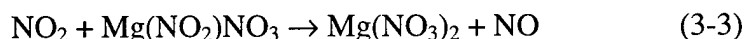
in the quantities of surface nitrate and nitrite formed in comparison to bulk salt compounds.

Initial MgO/v Laboratory Experiments

Initial NO_x-sorption experiments were conducted on MgO/v in the single fixed-bed reactor system designed by Kimm (1995). The NO_x sorption potential of magnesium oxide-coated vermiculite (MgO/v) had been shown to be feasible in pilot-scale applications (Nelson et al., 1992, 1993, 1994). Field experiments performed to control NO_x emissions from a jet engine test cell at Tyndall AFB used MgO/v. Depending on the operational conditions, NO_x removals were in the range from 40 to 70% (Nelson, 1992). The benefits of MgO/v as a NO_x sorbent were several. Low cost, easier handling than wet materials, less start-up cost, and ease of scaling to various applications are some of the benefits. The cost of MgO/v is comparable to other high-volume usage sorbents. Kimm performed laboratory experiments on MgO/v (Kimm, 1995). Vermiculite was shown by Kimm to act essentially as a support material with minimal NO_x interaction. Also, previous flue-gas studies had shown minor NO_x interaction with vermiculite (Nelson, 1989). The formation of magnesium nitrate through sorption of NO₂ onto MgO/v was proposed by Kimm (1995). As vermiculite is a naturally occurring mineral that is commonly used as plant-potting material, the end product fertilizer consisting of magnesium nitrate and vermiculite was considered a useful product. Alternatively, the regeneration of MgO/v was found to be possible by heating in a reducing atmosphere (Nelson, 1989).

NOx Sorption: MgO/v

Laboratory experiments by Kimm showed negligible removal of NO when it is the only NOx species present. Kimm's research suggested that only NO₂ removal is possible by MgO/v. Because field experiments indicated that NO is removed by sorption to MgO/v further tests to include the presence of other flue gas constituents were suggested. In addition, Kimm showed that NO₂ sorption resulted in a 1-to-3 ratio of NO production to NO₂ removal. He proposed the following sequential mechanism for the sorption of NO₂ to MgO/v:



Samples of MgO/v that were NOx saturated were further tested for nitrates using a nitrate-specific ion electrode. The results showed that saturated MgO/v samples accumulated a 3:2 molar ratio of NO₂ sorbed to nitrate formed. This ratio agrees with the above mechanism proposed by Kimm. In addition, Kimm showed that the saturation capacity of MgO/v utilized less than 2 percent of the magnesium oxide available. If the sorptive characteristics of MgO/v were to be improved additional studies of the material would be necessary. Based on the positive findings of Kimm and the growing interest in this application, additional studies were warranted to improve upon MgO/v as an effective NOx sorbent.

Based on research suggested by Kimm (Kimm, 1995) additional MgO/v testing was performed. Laboratory fixed-bed reactor studies were chosen to further describe the

removal of NO_x and the effects of other flue gas constituents. Given that Kimm observed no removal of NO when it was the only NO_x species present, pre-oxidized NO_x conditions were selected for experimentation. Experiments were repeated that showed no measurable interaction of gaseous NO with MgO/v.

Preparation procedures and physical properties of the MgO/v material are described by Kimm (1995). A measure of size distribution was performed to confirm Kimm's data. Also, reproducibility testing was performed to compare the data collected using the modified NO_x-sorption system with the original data collected by Kimm. The reproducibility test results are compared to Kimm's data in Figure 3-1.

MgO/v: Internal Diffusion of NO₂

Kimm notes that the MgO/v material is brittle and MgO powder easily breaks apart from the vermiculite substrate (Kimm, 1995). To test the possible effect of varied particle size on NO_x, tests were performed at similar conditions on MgO/v samples that were sieved into five size categories. The results displayed in Figure 3-2 indicate that no significant differences in NO_x removal occurred for the test conditions. Therefore, effects due to particles crumbling to smaller sizes during handling are considered to be insignificant. Problems did occur, however, from small sorbent particles that were carried with the sampled gas into the NO_x analyzer causing clogging of the capillary tubes. Given the similar results for different particle sizes, a decreased particle size and thus, decreased bed volume for the same mass did not significantly affect NO_x sorption. Therefore, internal (intra-pellet) mass transfer appeared to be negligible for the particle sizes

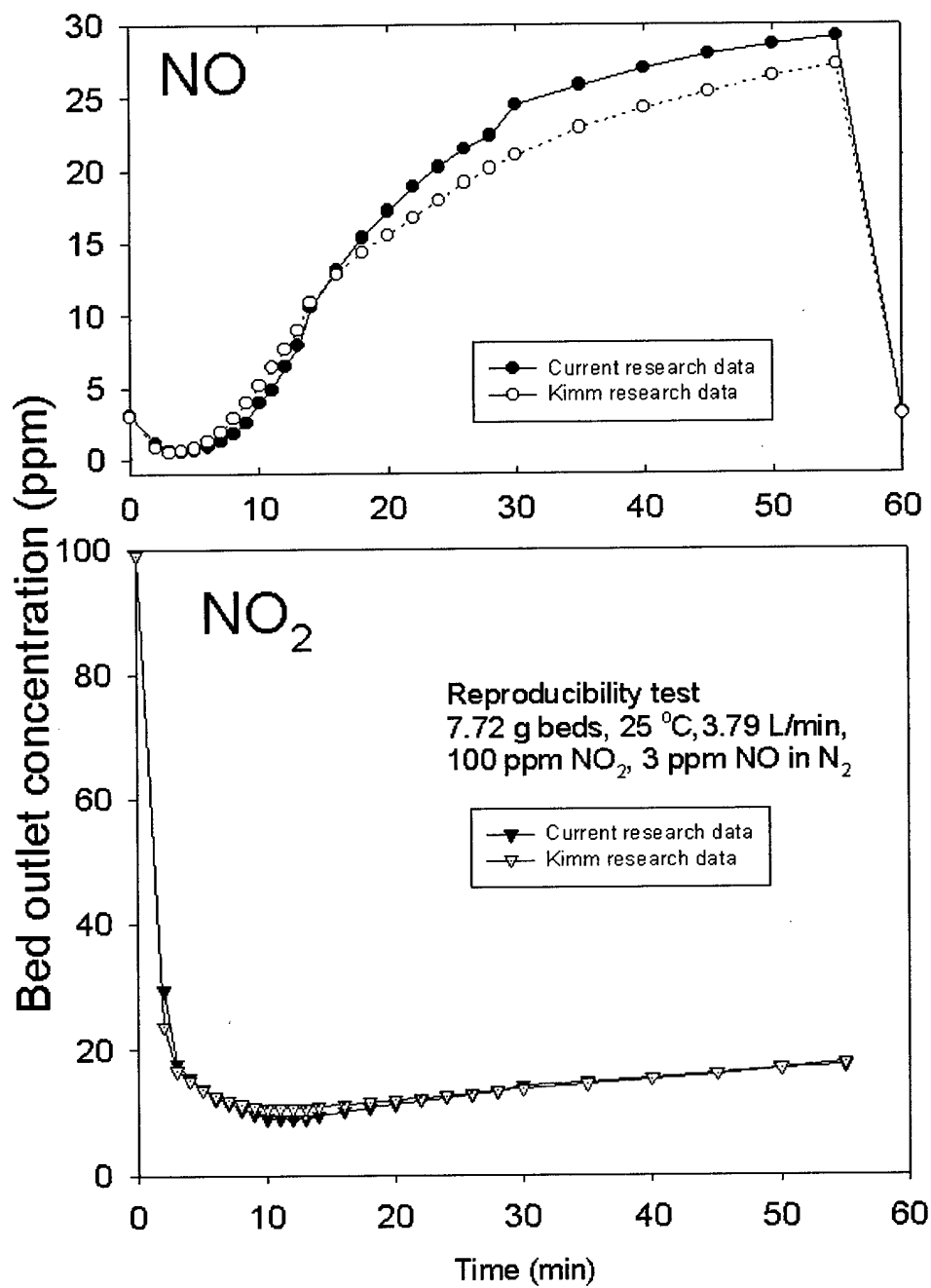


Figure 3-1. NO_x-sorption test for MgO/v compared with Kimm's (1995) data.

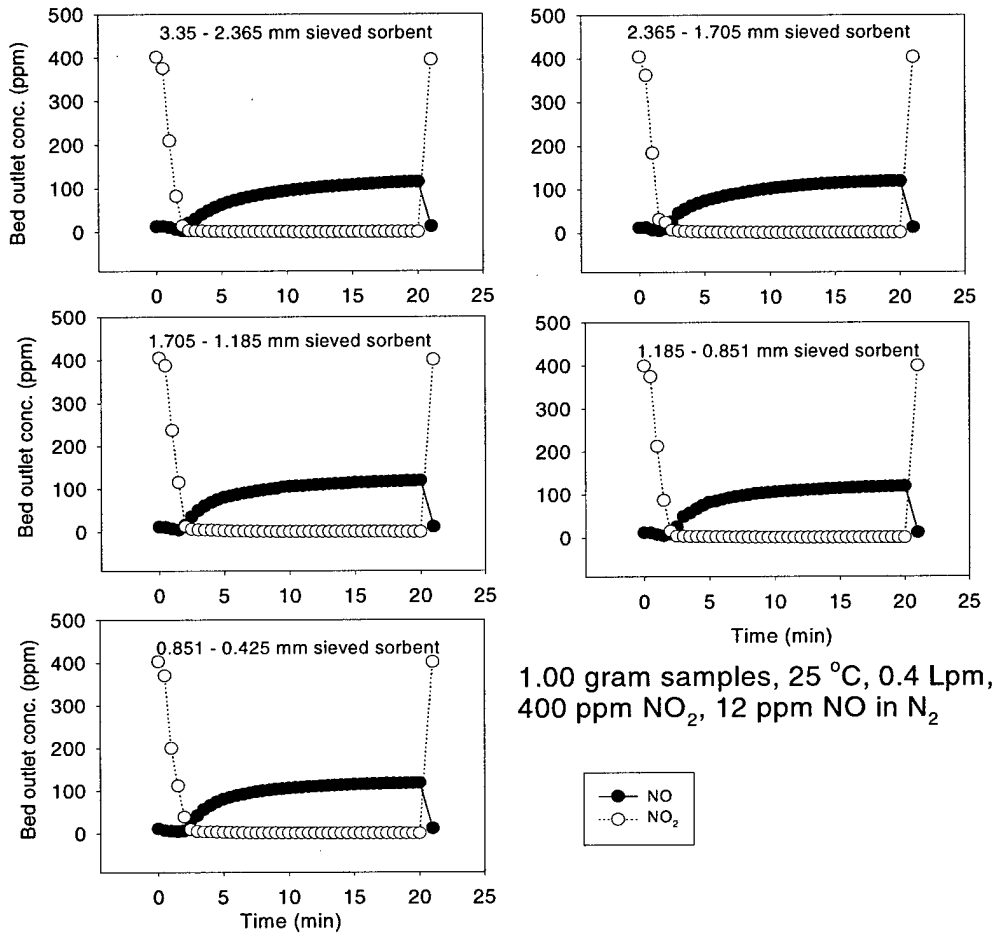


Figure 3-2. NO_x-sorption tests for sieved MgO/v samples

investigated under these test conditions. In addition, this observation supports Kimm's findings that the sorption process is initially reaction controlled and therefore, diffusion into the particle is not rate limiting.

MgO/v: External Diffusion

External (inter-pellet) mass-transfer limitations were evaluated using a method suggested by Ruthven (1968). By varying the face velocity through a sorbent bed while keeping the residence time the same (increasing the volume of sorbent), then similar gas-solid interactions should occur if inter-pellet mass-transfer of the gas is minimized. The data obtained for these tests are presented in Figure 3-3. Kimm's findings for mass-transfer limitations are similar to those reported here (Kimm, 1995).

MgO/v: Sorption of NO

MgO/v was tested for the removal of gaseous NO. A gas stream consisting of 400 ppm of NO in nitrogen (N₂) did not interact with MgO/v. This test supports those performed by Kimm. Discussions with personnel of companies applying this material (MgO/v) to control of NO_x emissions suggested that the sorbent must be interacting with other gases to remove NO (Nelson et al., 1992). Field data consistently showed removal of NO (Nelson et al., 1994). Kimm's research had shown that only NO₂ was removed from gas mixtures containing NO, NO₂ and N₂. NO_x sorption/catalysts (CuO-alumina) required the presence of other gases, such as SO₂, to perform reliably (Cooper and Alley, 1986). Other flue gas constituents were, therefore, considered for comparison testing with the NO_x/MgO/v system.

MgO/v: Effect of Water on NO_x Sorption

Kimm suggested (Kimm, 1995) that future research on the effect of water additions to the NO_x-sorbent system should be performed. A series of tests was performed to evaluate the effect of liquid water added to the sorbent material on NO_x sorption from 50 to 200 °C over a range of flows measured in bed volumes per second (0.5, 1, and 2 bed vol/sec). The effect on NO_x sorption was studied by increasing the fraction of deionized water added by spraying onto MgO/v in amounts from 5 to 25% w/w. Improved sorption of combined NO (50 ppm) and NO₂ (500 ppm) was observed at 50 and 200 °C (Figures 3-4, 3-5, 3-6, and 3-7, respectively). No interaction of NO (balance N₂), when tested alone, was observed over the range of conditions used for these tests.

The maximum amount of added water (25% w/w) to the MgO/v sorbent sample was approximately equal to the amount of sample MgO on a stoichiometric basis. The addition of water was observed to delay NO production, as seen in Figures 3-4, 3-5, 3-6, and 3-7. However, NO_x-sorption tests that saturated MgO/v at 200 °C indicated an increase in the amount of NO₂ uptake and a decrease in NO production (Figure 3-8). Possible interaction of NO₂ and bulk liquid water would explain additional NO₂ removal at temperatures below the boiling point (100 °C) of water. However, the saturation tests were performed at temperatures near 200 °C and, thus, a mechanism involving bulk liquid water does not seem possible.

Other researchers have studied similar group-II materials in this application, and have proposed that the interaction of NO₂ with these metal oxide surfaces is due to

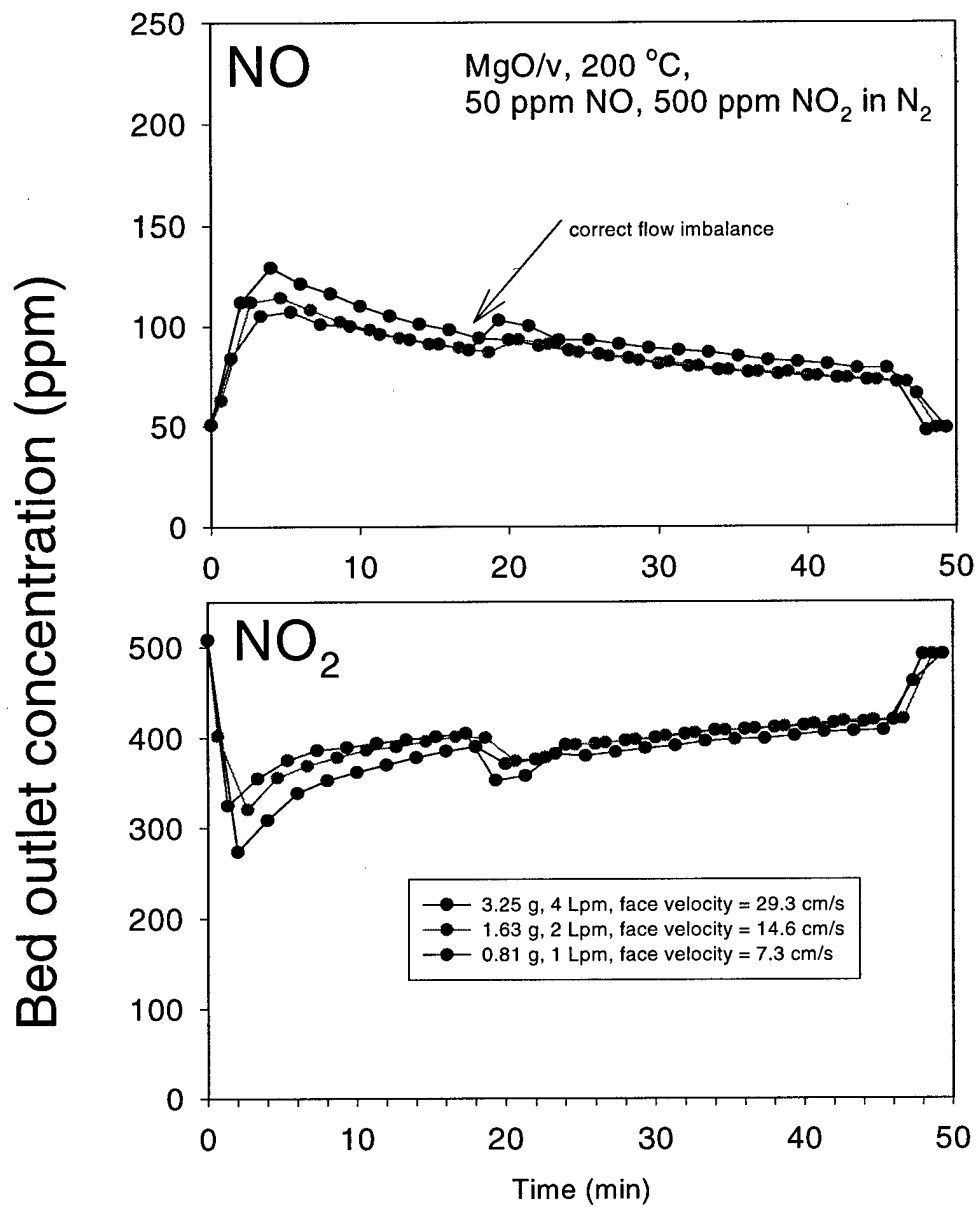


Figure 3-3. External mass transfer test for NO_x sorption on MgO/v.

adsorbed bulk water (Nelli and Rochelle, 1996). Nelli and Rochelle proposed that nitrous acid formed by $\text{NO}_2\text{-H}_2\text{O}$ interaction will further interact with additional NO_2 to form nitric acid and NO . This mechanism is suggested to produce the observed NO .

Furthermore, they proposed that NO_2 interaction with basic surfaces, such as $\text{Mg}(\text{OH})_2$, allows the increased surface pH to prevent association of H^+ and NO_2^- and thus delay NO production.

Additions of liquid water to dehydroxylated MgO has been shown to readily form $\text{Mg}(\text{OH})_2$ species (Fiero, 1990). A monolayer of adsorbed H_2O readily forms when dehydroxylated MgO is exposed to water vapor at 20°C . Adding water to MgO has been shown to increase hydrogen bonding and hydroxyl reaction. Based on this proposal, water added to a surface increases the surface hydroxyl concentration would increase NO_2 uptake and increase, but delay, NO production.

Even though the reported dehydration temperature of $\text{Mg}(\text{OH})_2$ is 350°C , (CRC, 1992) [above 200°C] $\text{Mg}(\text{OH})_2$ should only delay NO production according to the mechanism of Nelli and Rochelle (1996). That no increase in NO production was observed in the latter study suggests that other interactions/mechanisms than those suggested by Nelli and Rochelle (1996) may occur. Given that water added to MgO/v can bind to MgO or vermiculite, speculation on an alternative mechanism seems reasonable. Alternative mechanisms include reactions involving species from sorbed/reacted water/vermiculite.

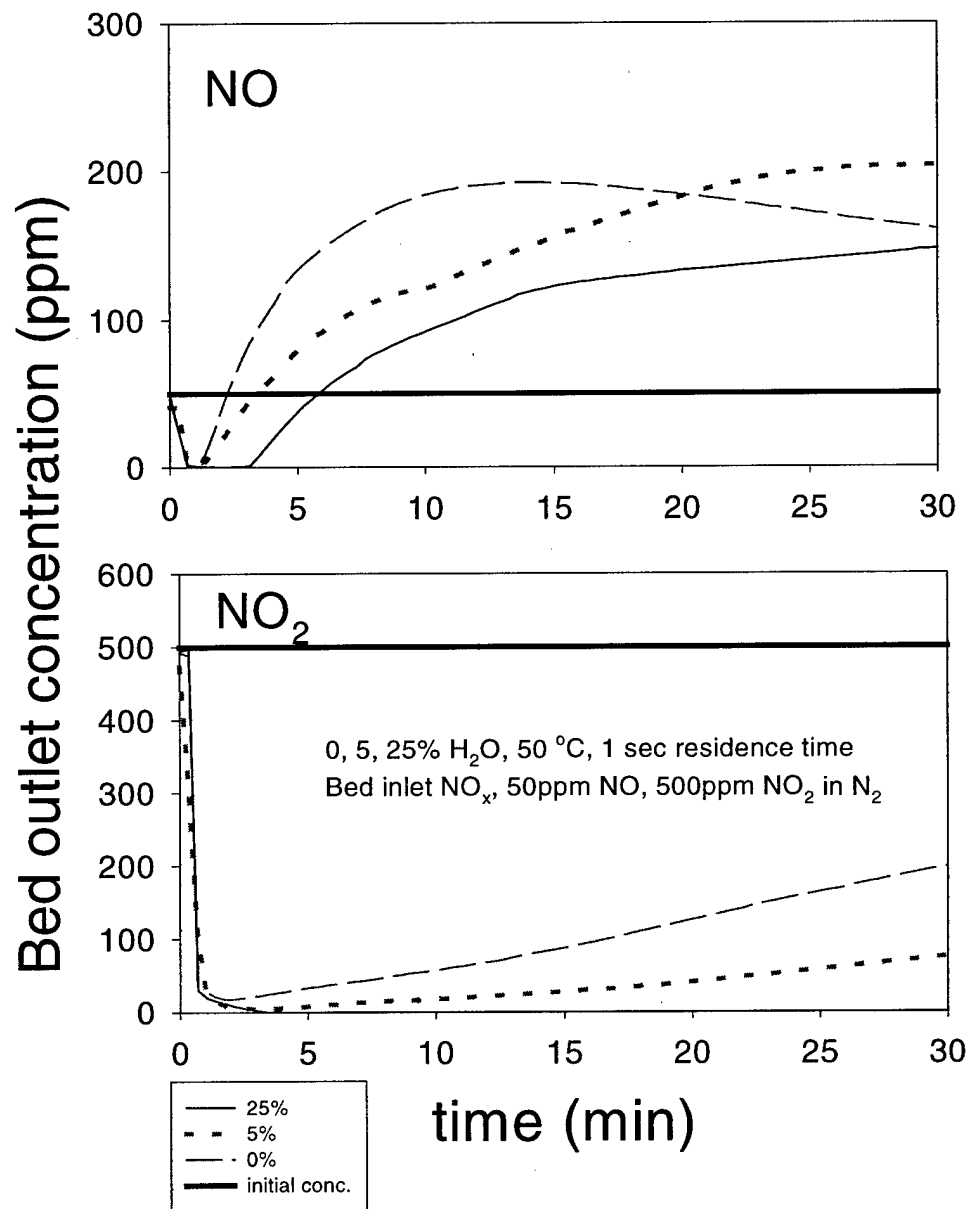


Figure 3-4. Variation of NO_x sorption at 0, 5 and 25% water additions to MgO/v at 1-second residence time at 50 °C

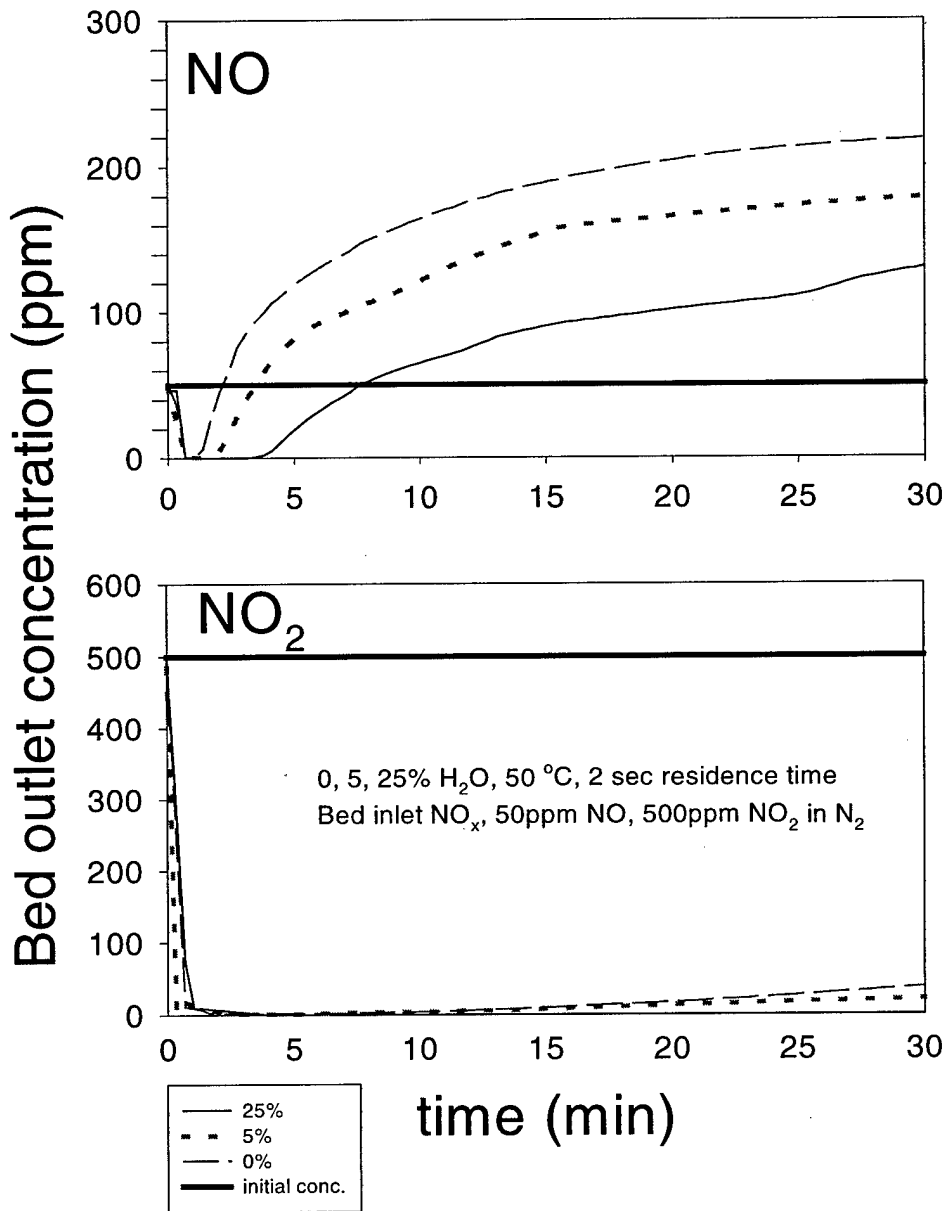


Figure 3-5. Variation of NO_x sorption at 0, 5 and 25% water additions to MgO/v at 2-second residence time at 50 °C

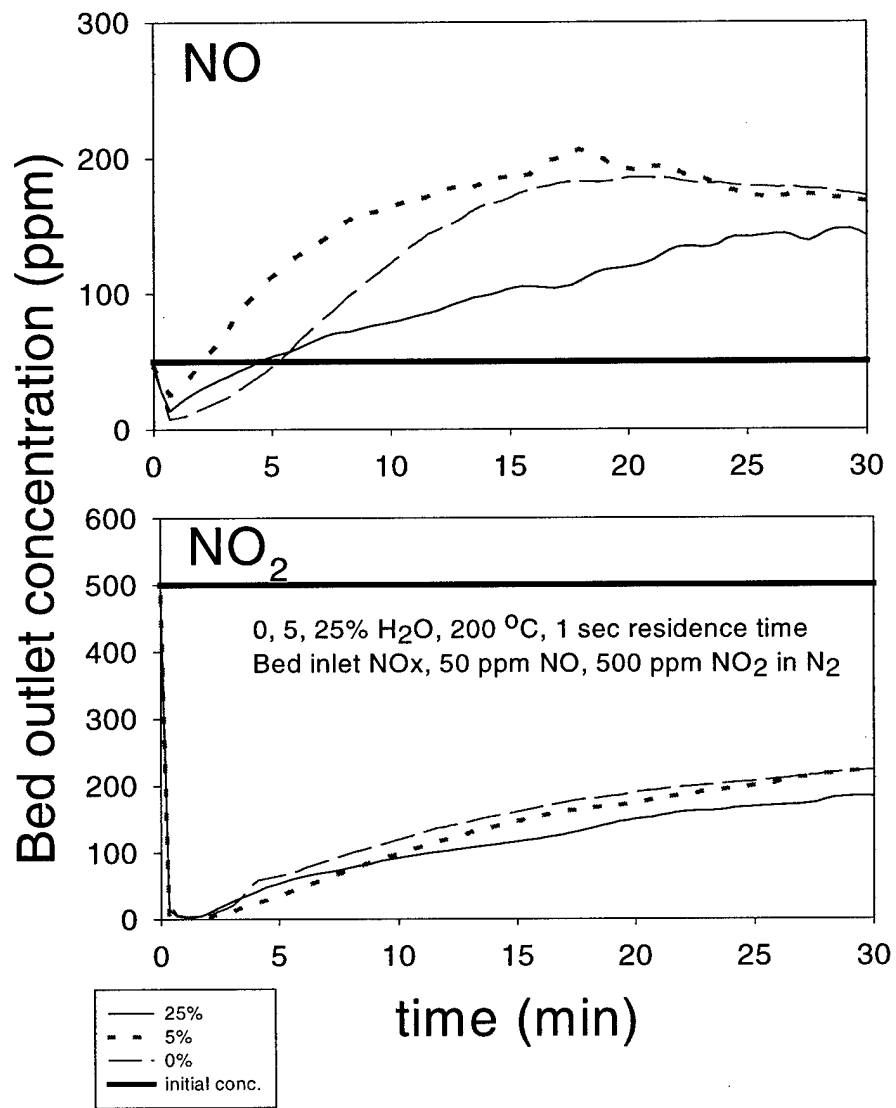


Figure 3-6. Variation of NO_x sorption at 0, 5 and 25% water additions to MgO/v at 1-second residence time at 200 °C

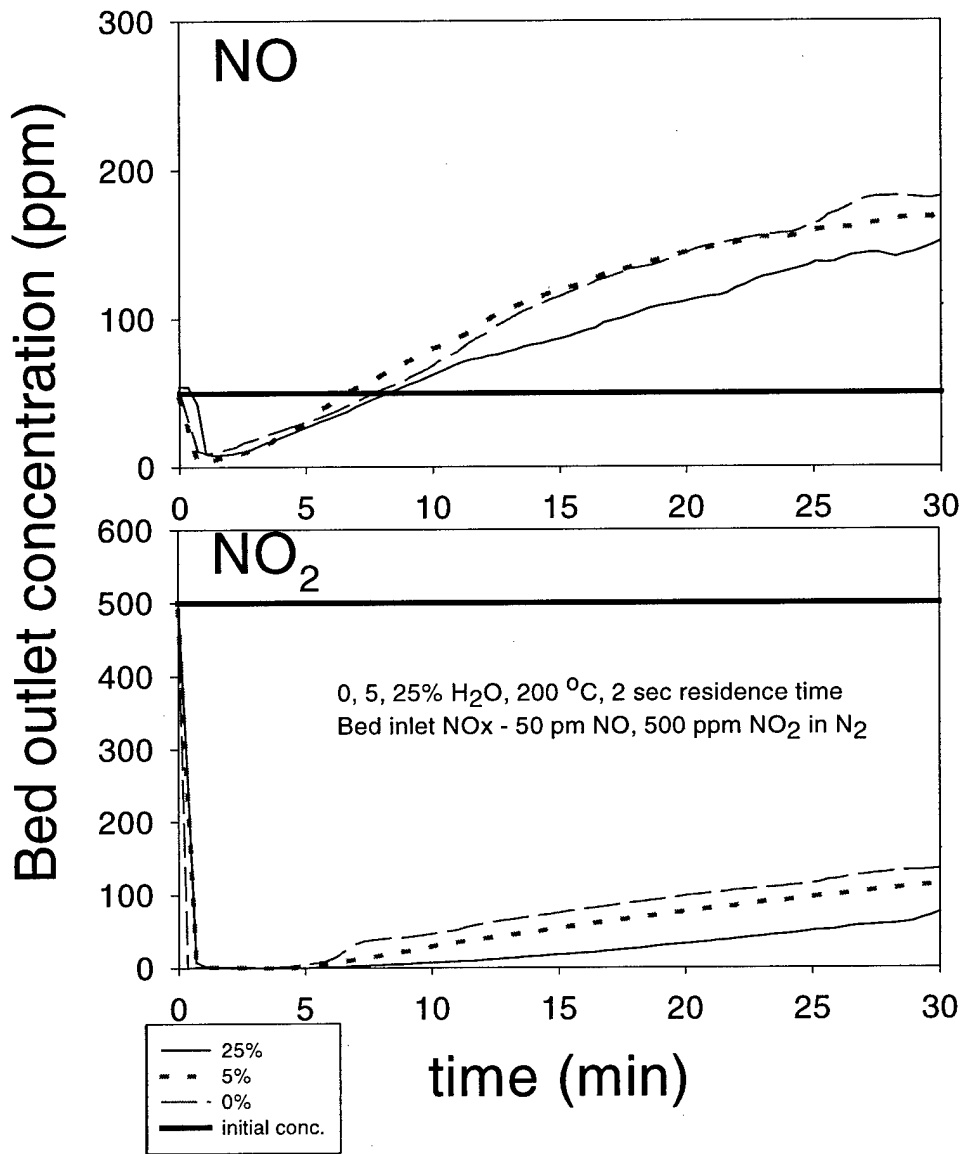


Figure 3-7. Variation of NO_x sorption at 0, 5 and 25% water additions to MgO/v at 2-second residence time at 200 °C.

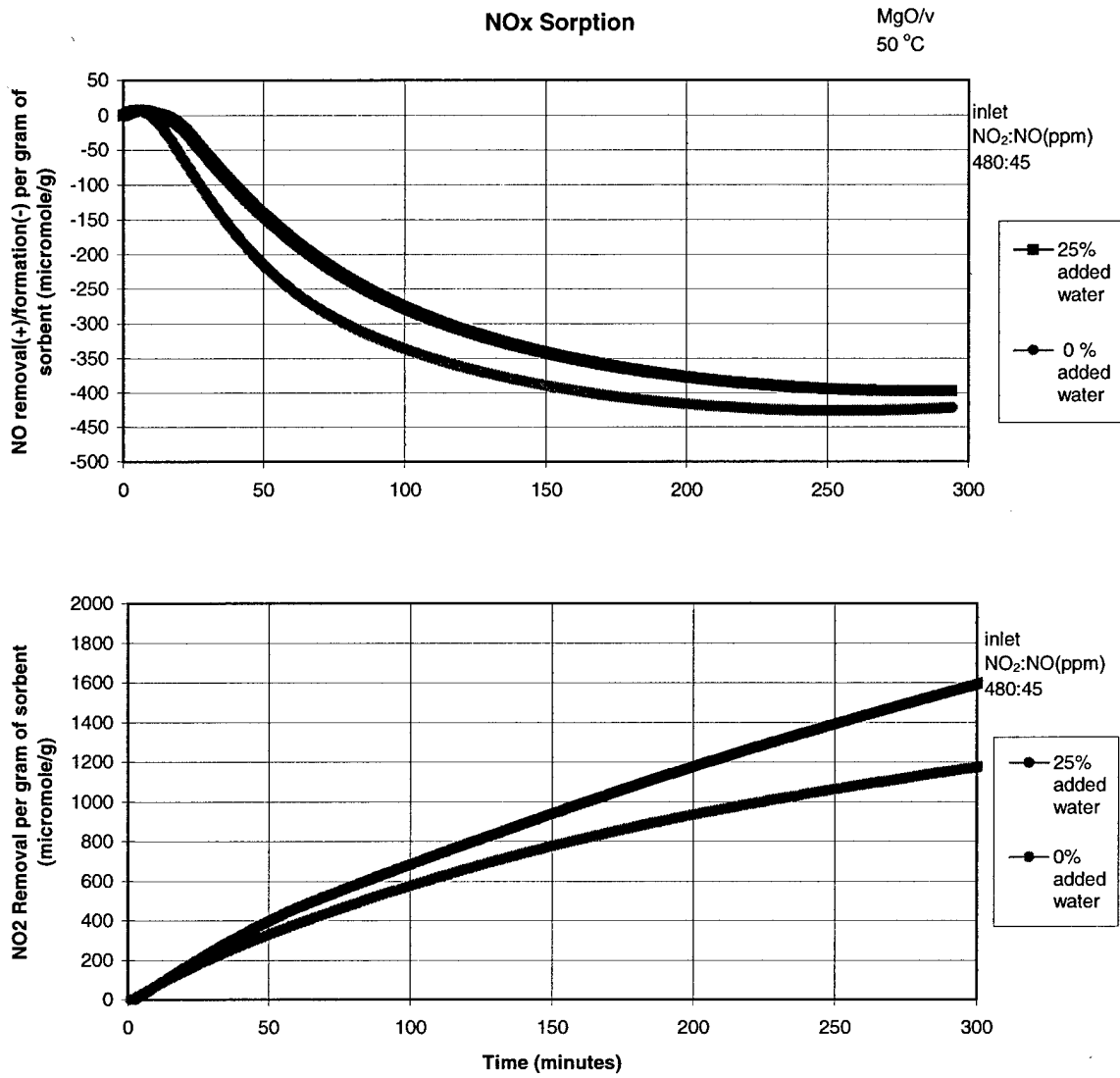


Figure 3-8. NOx-saturation study of MgO/v and added water at 200 °C.

Comparison of MgO/v and Alumina Sorbents

A comparison of MgO/v and alumina (Al_2O_3) sorbents was performed using the modified fixed-bed reactor system. Alumina was chosen for comparison with MgO/v because it has been extensively studied for similar pollutant gas/vapor control processes (Kirk-Othmer, 1992). Also, it is known to have superior sorption properties, it is a structurally more rigid material, and is widely available at comparable costs (Greenwood and Earnshaw, 1989). Alumina is a common material used for numerous industrial process applications from dehydration to catalysis. The material can be purchased in various structural and physicochemical forms. The gamma (γ) form of alumina has a high surface area and is commonly used as a support for catalysts. Its high-surface area provides a high activity for reactions. In addition, pressure drop measurement for similar bed volumes showed that pelletized alumina had on average a 20% lower pressure drop than MgO/v (Tyler size 8 (3.35-2.37 mm) particles).

MgO/v vs. Alumina: NO_x Sorption

Initial comparison tests of Al_2O_3 and MgO/v were performed on equal-volume beds. The sorbents were sequentially exposed to a gas stream containing 500 ppm NO_2 and 50 ppm NO in nitrogen at a temperature of 200 °C. The NO_2 and NO bed outlet concentrations obtained as a function of NO_x-exposure time are shown in Figure 3-9. Following an initial decrease to zero, the NO_2 concentration in the stream leaving the MgO/v bed initially increases rapidly and then more slowly, attaining a value of about 430 ppm after 300 min. After initial fluctuations the NO concentration increases rapidly to a maximum of 190 ppm at 20 min and then decreases slowly to about 50 ppm, which is

the NO feed concentration. The fact that the NO concentration rises above 50 ppm indicates that some of the NO₂ is converted into NO in the bed.

The untreated γ -alumina bed initially removes all NO₂ from the gas stream and then the outlet NO₂ concentration increases gradually to a value of 100 ppm at 300 min. Initially, the γ -alumina removes all of the inlet NO. The NO concentration increases fairly rapidly to a level near 200 ppm at about 100 min, indicating that γ -alumina also allows the formation of NO from NO₂. Untreated γ -alumina and MgO/v actively form significant quantities of NO while removing NO₂.

Given the much greater reactivity of the Al₂O₃ for NO_x for the same bed volume, additional studies of the latter sorbent were warranted. Saturation tests of NO_x with alumina showed that overall a 3:1 ratio of NO₂ uptake to NO production, similar to that for MgO/v, occurs on alumina. However, the amount of removal of NO₂ by Al₂O₃ is six times greater than MgO/v for similar volumes and exposure times. Measures of the surface area of γ -alumina by BET analyses was $170 \pm 3 \text{ m}^2/\text{g}$. Kimm found MgO/v to have a BET surface area of $40 \text{ m}^2/\text{g}$. Given that the saturated samples masses were 5.0 g of alumina and 1.0 g of MgO/v, a comparison by total amount of surface area is 850 m^2 to 40 m^2 , respectively. Despite the overall much higher surface area of the alumina used, alumina shows 20 % greater utilization per gram and thus, a smaller bed volume is required to obtain the same reactivity as MgO/v. In addition, the much greater structural integrity of alumina proved valuable for gravimetric measurement during initial and subsequent analyses. Also, the homogeneity of alumina proves valuable for preparing sorbents of similar characteristics.

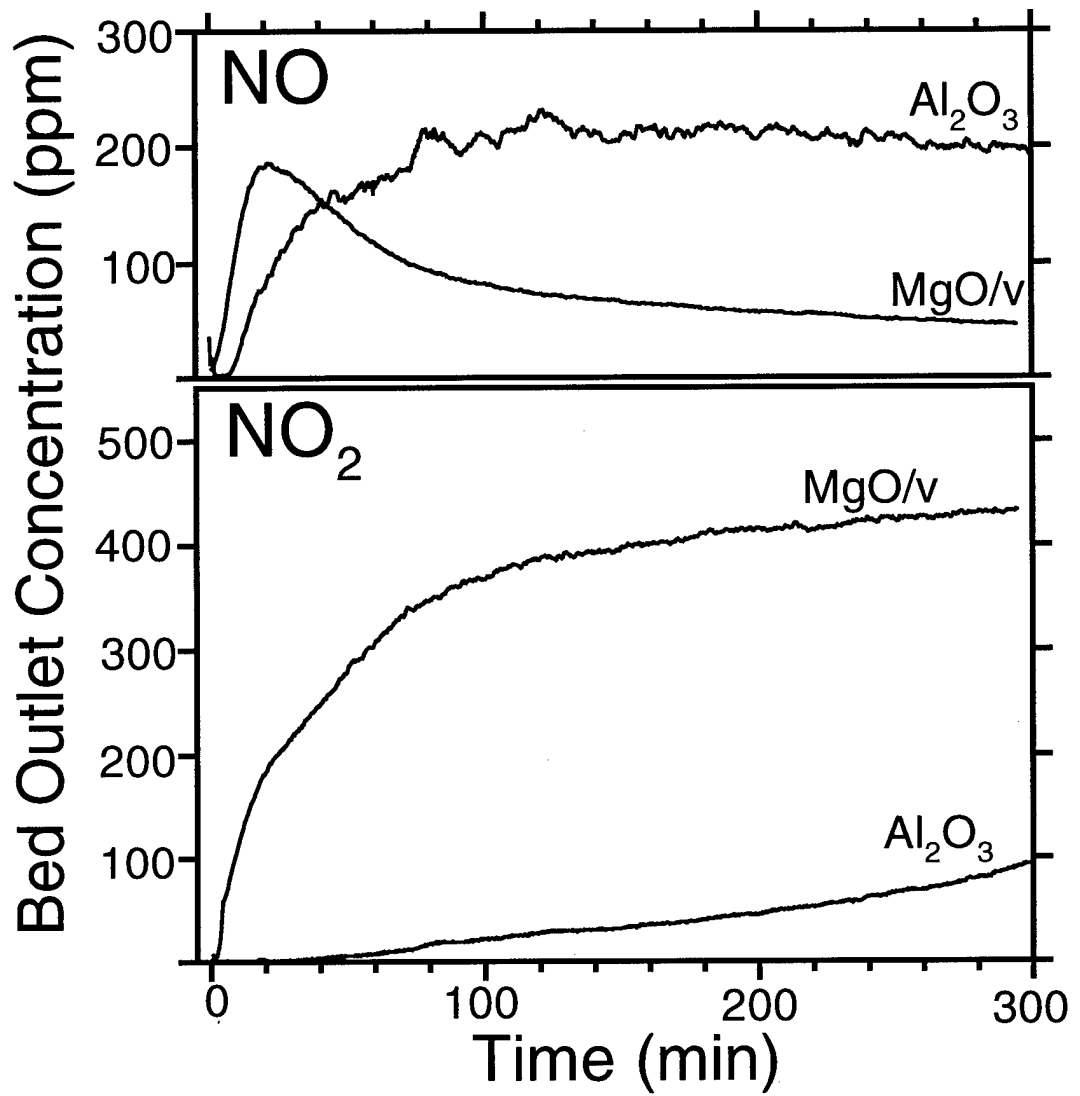
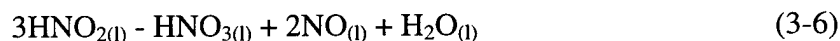


Figure 3-9. NO_x sorption by MgO/v and untreated γ -alumina (Al_2O_3) on equal volume beds (Lee et al., 1998b).

Formation of NO

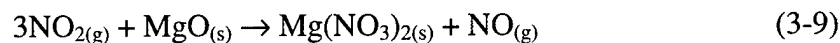
Results shown in Figures 3-9 and MgO/v saturation tests indicate that formation of NO is a by-product of NO₂ sorption on these materials. Nelli and Rochelle (1996) found that 3 mol of NO₂ sorbed to non-alkaline solids and suggested that reaction was with sorbed water to produce 2 mol of nitric acid and 1 mol of NO as follows:



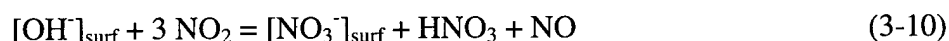
yielding an overall equation



According to Nelli and Rochelle, the rate-limiting step is 3-5. Alkaline solids, such as Ca(OH)₂, buffer the pH of the sorbent surface and delay the formation of NO. Also, Nelli and Rochelle suggest that alkaline materials [such as Ca(OH)₂-coated sorbent] prevent HNO₂ and HNO₃ association and, thus, reduce NO production. Kimm et al.(1995) found that NO₂ sorption to MgO in the absence of oxygen formed NO in the same molar ratio of 3:1 (NO₂ uptake: NO production) and suggested that a 3-step process was involved. They suggested that the overall process was



Both mechanisms, which encompass a temperature range of 25 to 200 °C, also state that 3 moles of NO₂ are removed to form 2 moles of nitrate or nitric acid species (depending on pH) and 1 mole of NO. Boehm (1959) has explained the formation of nitrate ions resulting from NO₂ sorption on alumina as a result of a disproportionation of surface OH⁻ ions with NO₂:



The formation of NO via this mechanism agrees with observations of NO₂ sorption on other oxides and with the reported molar ratios for NO₂ removal to NO formation. Other materials such as AgO have been observed to produce NO from NO₂ sorption in a 3:1 molar ratio in a similar manner (Zemlyanov et al., 1998).

The active sites on alumina are described (Sicar, 1980) as basic (hydroxyl and O²⁻ anion vacancies) and acidic (unsaturated Al³⁺ ions as Lewis and protonated hydroxyl ions as Brønsted acid) sites of various strengths and concentrations. The hygroscopic natures of alumina and MgO have been well documented (Peri, 1965; Knozinger, 1976; Knozinger and Ratnasamy, 1976; Coster and Fripiat, 1995; Sircar et al., 1996) which are known to significantly influence their reactivity. At 50 % relative humidity, activated alumina can adsorb up to 15 % of its own weight of water (CRC, 1980) and a monolayer of surface hydroxyl species can exist on its surface at temperatures of up to 500 °C (Peri, 1965). Thus, the reaction of NO₂ with alumina at the temperatures used in these experiments (200 °C) could involve sorbed water molecules and may be explained by either reaction (3-8) or (3-10). While these reactions are possible for the sorption of NO_x

on untreated alumina, NO_x removal by alkali-treated alumina appears to differ substantially in terms of NO₂ sorption rates, saturation capacity and NO production, as discussed previously.

Initial Studies of Untreated and KOH-Treated γ -Alumina

Different Sources of γ -Alumina

Three different sources of γ -alumina provided sorbent materials for study. The three types of material were obtained from Fisher Scientific Inc. (catal. #, A948 (acid), A941 (basic), and A945(neutral), Pittsburgh, Pennsylvania), Englehard Inc., (catal. # T-3438, Elyria, Ohio), and Edwards High Vacuum Inc., (catal. # H02600055, Liverpool, England).

Fisher Scientific alumina have a Brockman activity of I, meaning the material is heated to have approximately 0% moisture prior to packaging. γ -Aluminas were obtained in three forms described as neutral, acidic, and basic. The manufacturer describes the reactive acidity by suspending the alumina in an 5% w/w aqueous solution and measuring the pH with a hydrogen-ion electrode after 5 minutes. These different acidities are created by adding HCl gas in precise amounts. The three forms (1-gram samples) were tested in this laboratory for the change of the pH of an aqueous solution (50 mL) due to the addition of the alumina. All three materials changed the solution pH as expected (acid, pH 4; neutral, pH 7; base, pH 10). Considering the behavior of the different forms of alumina as Brønsted acidity, the basic alumina must act in aqueous solution to either extract hydronium ions from solution or release hydroxyl groups.

The materials were individually tested to determine the effect of sorbent acidity on the process of NO_x sorption. The powdered materials were individually placed inside the sorbent reactor tubes supported on glass fiber wool. A 4-gram portion of each type of powder was exposed to 500 ppm NO₂ and 500 ppm NO at ambient temperature. The amounts of NO₂ and NO accumulated per sample mass obtained as a function of exposure time are shown in Figure 3-10. All materials showed similar results. Complete removal of the input NO₂ is observed during the exposure period. The NO concentration increases indicating a formation of NO. This increase is due to NO₂ sorption followed by its partial conversion to NO. The proposed equation describing the sorption of NO₂ to MgO discussed previously indicates a 1:3 molar ratio of NO produced to NO₂ sorbed. The removal of NO₂ and formation of NO for all Fisher Scientific alumina materials indicates the same 3:1 molar ratio as that observed for MgO/v. The most interesting feature is that the production of NO is not affected by the acidity of the alumina. The bonding structure of the three forms of alumina is designed to alter the *pH* in aqueous solution. Alumina normally contains some bound hydroxyl groups and bulk water at ambient conditions.

According to Nelli and Rochelle, the formation of NO is based on the surface pH such that a "basic" surface will prevent the association of surface nitrites and nitrates and therefore delay NO production. However, the basic form of alumina did not delay the production of NO. The latter test was performed at ambient conditions and thus the solid alumina should contain some sorbed water and related hydroxyl groups. As no delay in NO production was observed, either the production of NO from the surface is not based on its acidity or basicity alumina does not interact with NO₂ in a similar manner as alkaline materials. Alumina samples from the different manufacturers were tested to

determine if significant differences in the sorption of NO_x are apparent. Preliminary tests showed inefficient NO₂ sorption by the Edwards High Vacuum spherical pellets. The Fisher Scientific alumina sample was shown to remove all NO₂, produced NO in the proposed stoichiometry, and provided evidence supporting the proposed mechanism of reaction. A comparison of the three different manufacturer's materials was made by exposing all three materials to completely remove input NO₂ for a known period of time. If the production of NO is observed to be similar then additional evidence for the proposed stoichiometry would be obtained. To provide complete removal of NO₂ by the three different alumina samples the Englehard and Edwards High Vacuum materials were crushed to fine powders using a marble pestle and mortar. The material was crushed and passed through a Tyler size 200 sieve to remove larger particles. Additional NO_x-sorption testing showed that the 4-gram portion of Edwards crushed powder would not provide complete removal of NO₂. Therefore, the NO_x sorption of the three materials was performed with different material masses to ensure complete NO₂ removal. The accumulated removals of NO₂ and NO by the three different materials are shown in Figure 3-11. All three materials show a similar 3:1 molar ratio of NO₂ sorbed to the NO formed.

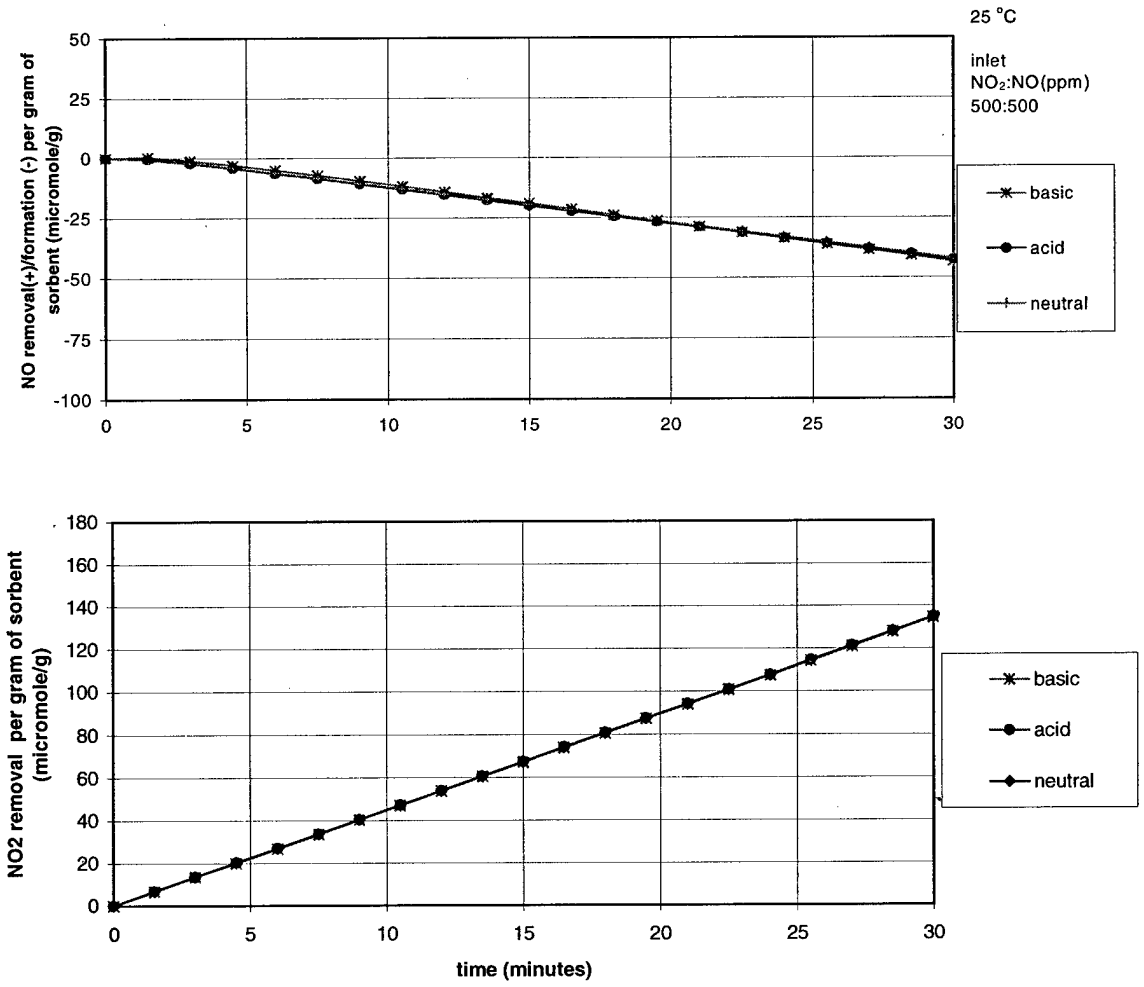


Figure 3-10. Sorption of NO_x to Fisher Scientific[®], acid, basic and neutral “pH” forms of alumina.

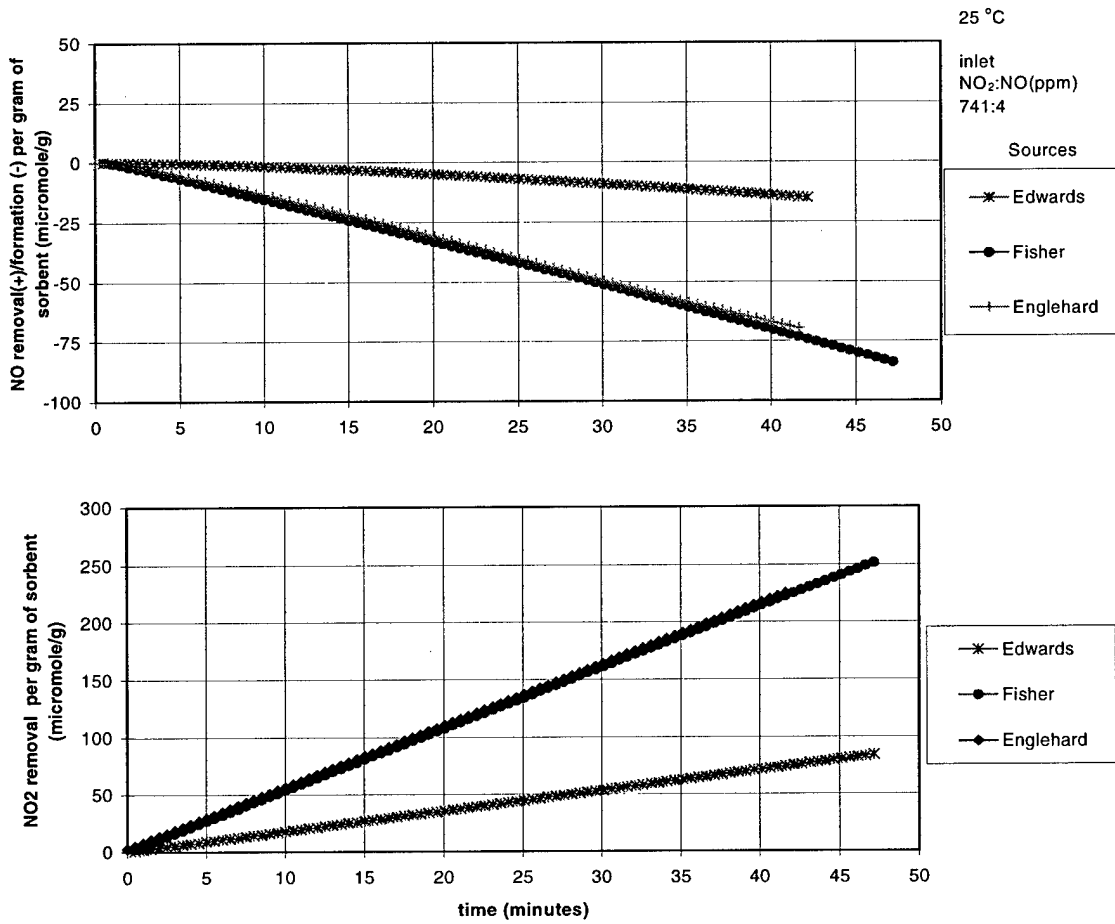


Figure 3-11. γ -Alumina from different sources exposed to NO₂.

Alumina: Removal of Gaseous NO

Tests on alumina similar to those for MgO/v were performed for the sorption of gaseous NO (400 ppm) alone at 25 and 250 °C. No interaction of gaseous NO with alumina was observed. As discussed in the experimental section, simulated preoxidized NOx conditions (high NO₂, low NO) were used for all sorption tests. The molar ratio of input NO₂:NO for testing was varied for certain tests. However, the general premise behind effective NOx sorption remains that initial conversion of NO into NO₂ is essential. A series of tests was performed which altered the ratio of NO₂:NO and the effect on NOx sorption studied. These tests are discussed later.

X-ray Photoelectron Spectroscopy (XPS) Analysis of Untreated γ -Alumina

Unexposed alumina and a NOx-saturated alumina sample were analyzed by X-ray photoelectron spectroscopy (XPS). Survey spectra are shown in Figures 3-12 a and b. Peak assignments pertain to both spectra. The spectra show Al (2s and 2p), C (1s), and O (1s and 2s) peaks. The C (1s) peaks in both spectra are probably due to the presence of about a 2% graphite component from the manufacturing process. The N-(1s) peak is apparent only after NOx exposure in Figure 3-12 b. The small K (2p) peak in Figure 3-12 a is enhanced after exposure to NOx in Figure 3-12 b. Potassium has been identified as a common contaminant in aluminum foils (Jimenez-Gonzalez, 1991). Observation of this significant increase in the K-(2p) peak after chemical interaction between a surface K compound and NOx, provides justification for examining the effects of pretreating γ -alumina with a potassium compound.

Krizek (1966) evaluated absorption of NO_2 by aqueous KOH and found that potassium nitrite is formed. Also, he found that aqueous KOH more efficiently absorbs NO_2 than aqueous NaOH, although the latter has been used for ambient NO_2 measurement in past EPA reference methods (Jacobs and Hochheiser, 1965), and for NO_x flue-gas measurements (Himi and Muramatsu, 1969). Furthermore, Nelli and Rochelle suggested that an alkaline solid, such as $\text{Ca}(\text{OH})_2$, moderates the surface acidity. The surface of the $\text{Ca}(\text{OH})_2$ -buffered sorbent has enough alkaline sites to keep HNO_2 and HNO_3 dissociated, thereby minimizing the production of gaseous NO. Since this previous research has shown that hydroxide compounds can reduce the production of NO, and XPS studies suggest that K compounds and NO_x interact, KOH was chosen for treatment of γ -alumina.

KOH-Treated γ -Alumina: Initial Testing

Given the observed interaction of potassium species with NO_x , potassium hydroxide (KOH) was coated onto alumina from solution of various concentrations by methods of impregnation and of precipitation. KOH-treated γ -alumina was tested for NO_x removal under conditions similar to those used for comparing MgO/v and untreated alumina. The NO_x exposure data obtained for untreated γ -alumina, KOH-impregnated γ -alumina, and KOH-precipitated γ -alumina are shown in Figure 3-13. All three sorbent beds yield very low outlet NO_2 concentrations for the first 40 min of NO_x exposure. After 40 min the outlet NO_2 concentrations are minimal and the same, within experimental error, for KOH-impregnated and -precipitated γ -alumina, and gradually increase to 50 ppm at 300 min. The KOH-impregnated γ -alumina NO outlet

concentration

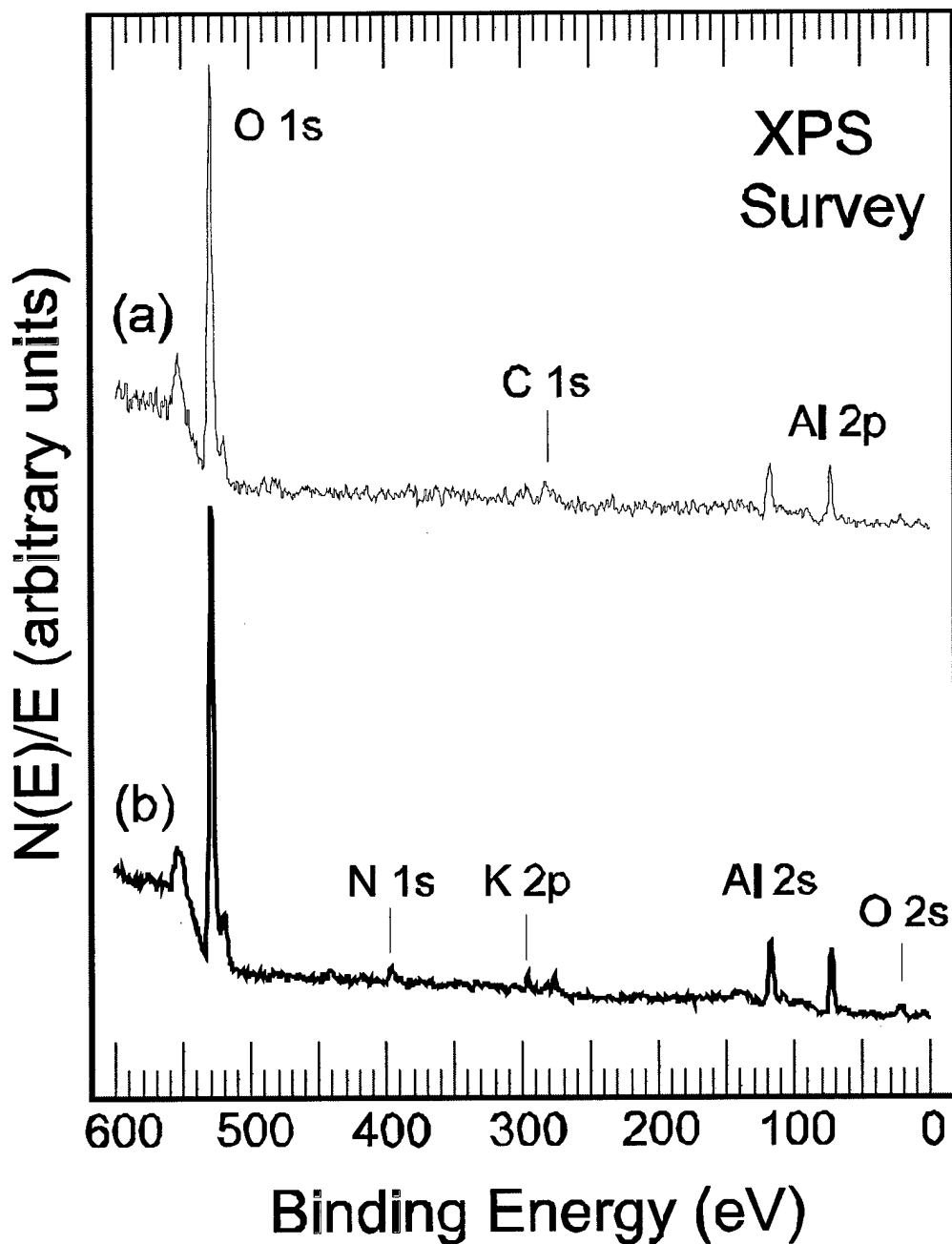


Figure 3-12. XPS survey spectra obtained from (a) fresh and (b) NO_x-saturated γ -alumina pressed powder samples (Lee et al., 1998b). Assignments made pertain to both spectra.

indicates removal of NO for the first 140-min exposure period but increases to about 150 ppm at 300 min, which is lower than that for untreated γ -alumina. KOH-precipitated γ -alumina removes nearly all the input NO over the time period examined. KOH-precipitated γ -alumina exhibits a 90% removal of both NO and NO₂ at 300 min, at which time approximately 12 mol (300 L) of NO_x-containing gas has been treated.

XPS survey spectra obtained from the unexposed KOH-impregnated and NO_x-saturated KOH-impregnated γ -Al₂O₃ are shown in Figures 3-14 (a) and (b) respectively. Peak assignments in Figure 3-14 pertain to both spectra. The Al-(2s and 2p), C-(1s), O-(1s and 2s), and K-(2p) peaks are apparent in these spectra. The surface carbon content of this sample is large since the C-(1s) peak is similar in size to the aluminum peaks and carbon has a low XPS sensitivity.

The K (2p) peak is enhanced after exposure to NO_x, as observed in Figure 3-14 (b). This is consistent with the XPS data obtained from untreated alumina (Figure 3-12). The N (1s) peak is barely apparent after the NO_x exposure. XPS survey spectra obtained for the unexposed 1-M KOH-precipitated and NO_x-saturated KOH-precipitated γ -Al₂O₃ are shown in Figure 3-15 (a) and (b) respectively. Before NO_x exposure the survey spectrum is quite similar to that obtained from the unexposed KOH-impregnated γ -alumina except that this surface appears to contain less carbon. After NO_x exposure, very prominent K (2p and 2s) and N (1s) peaks are apparent, and the C (1s) peak height also is increased.

High-resolution N (1s) spectra obtained from unexposed KOH-precipitated and KOH-precipitated, NO_x-saturated γ -Al₂O₃ samples are shown in Figure 3-16 (a) and (b),

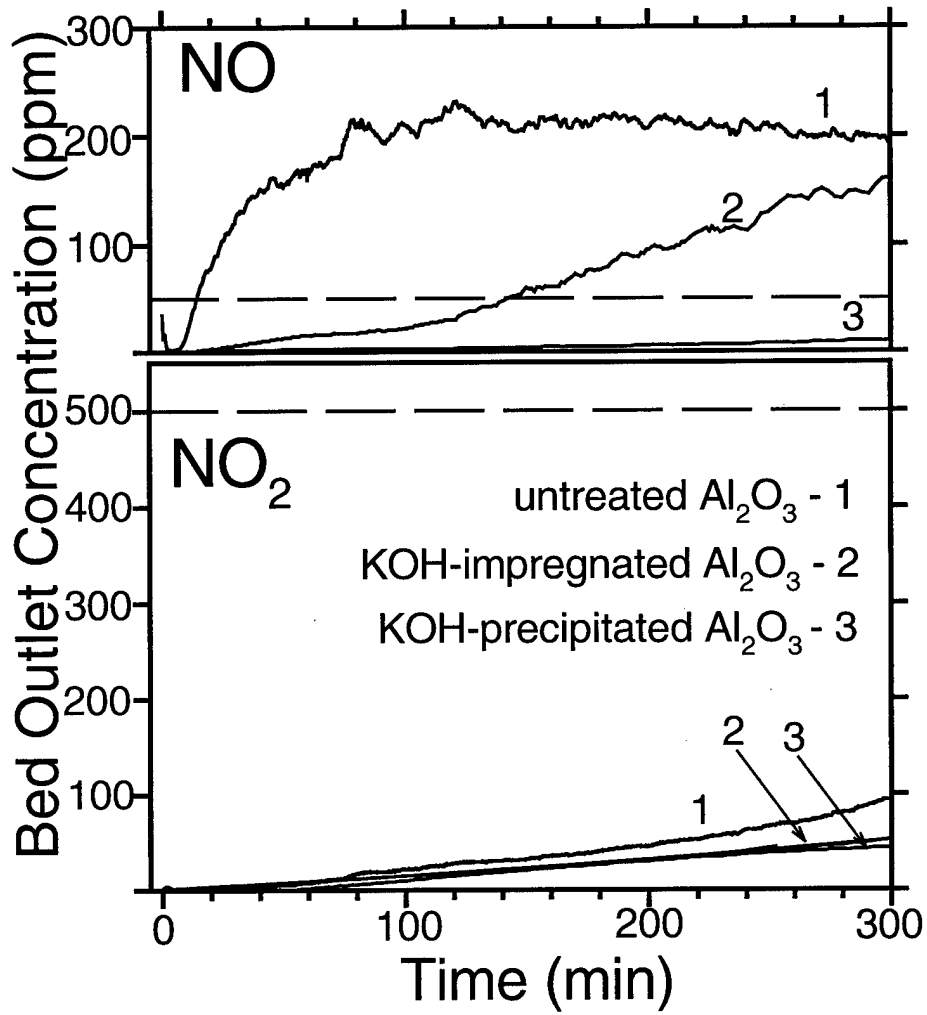


Figure 3-13. Bed outlet NO and NO₂ concentrations as a function of time for untreated and KOH-treated γ -alumina (Lee et al., 1998b).

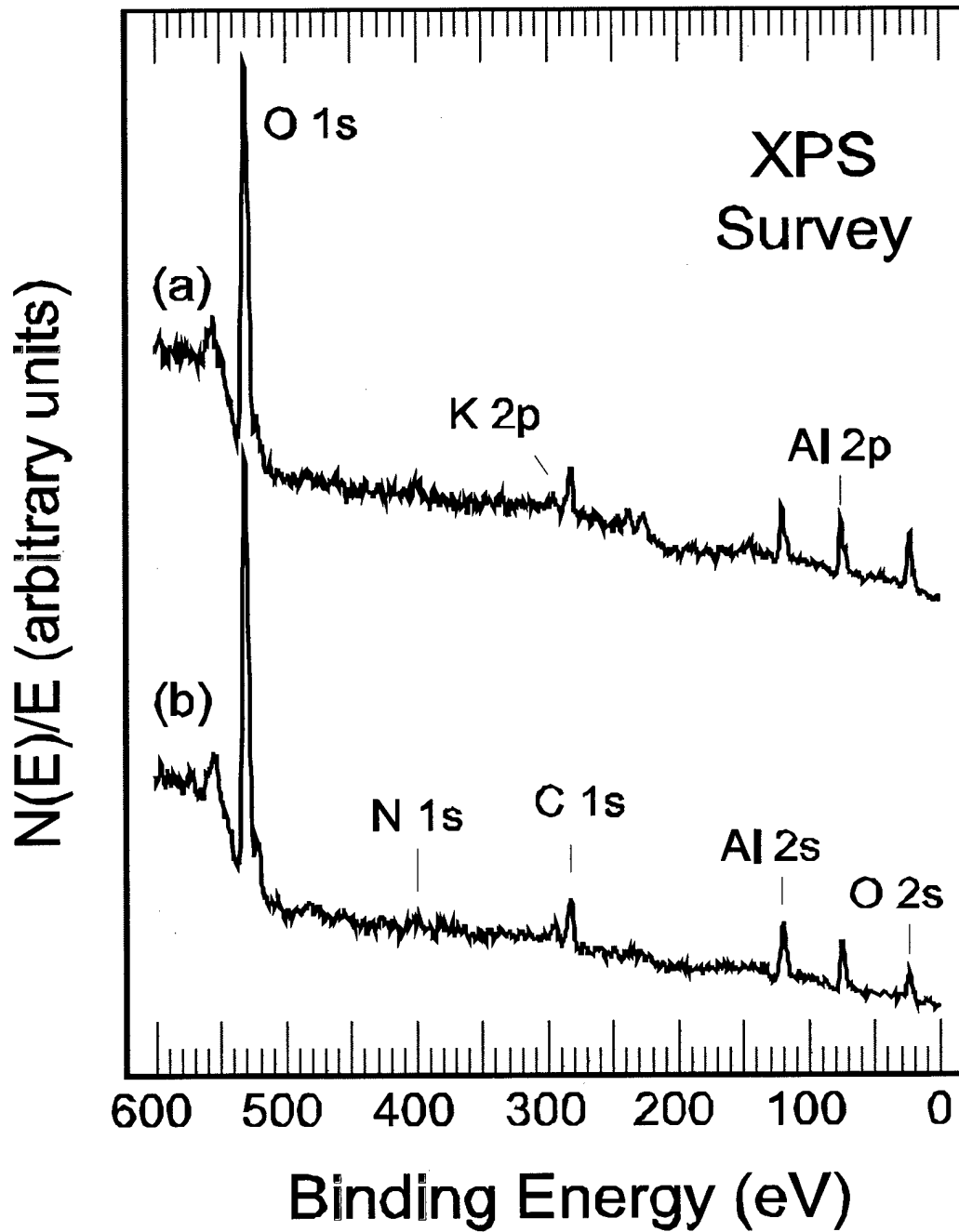


Figure 3-14. XPS survey spectra obtained from (a) KOH-impregnated and (b) NO_x-saturated KOH alumina pressed powder samples (Lee et al., 1998b). Assignments made pertain to both spectra.

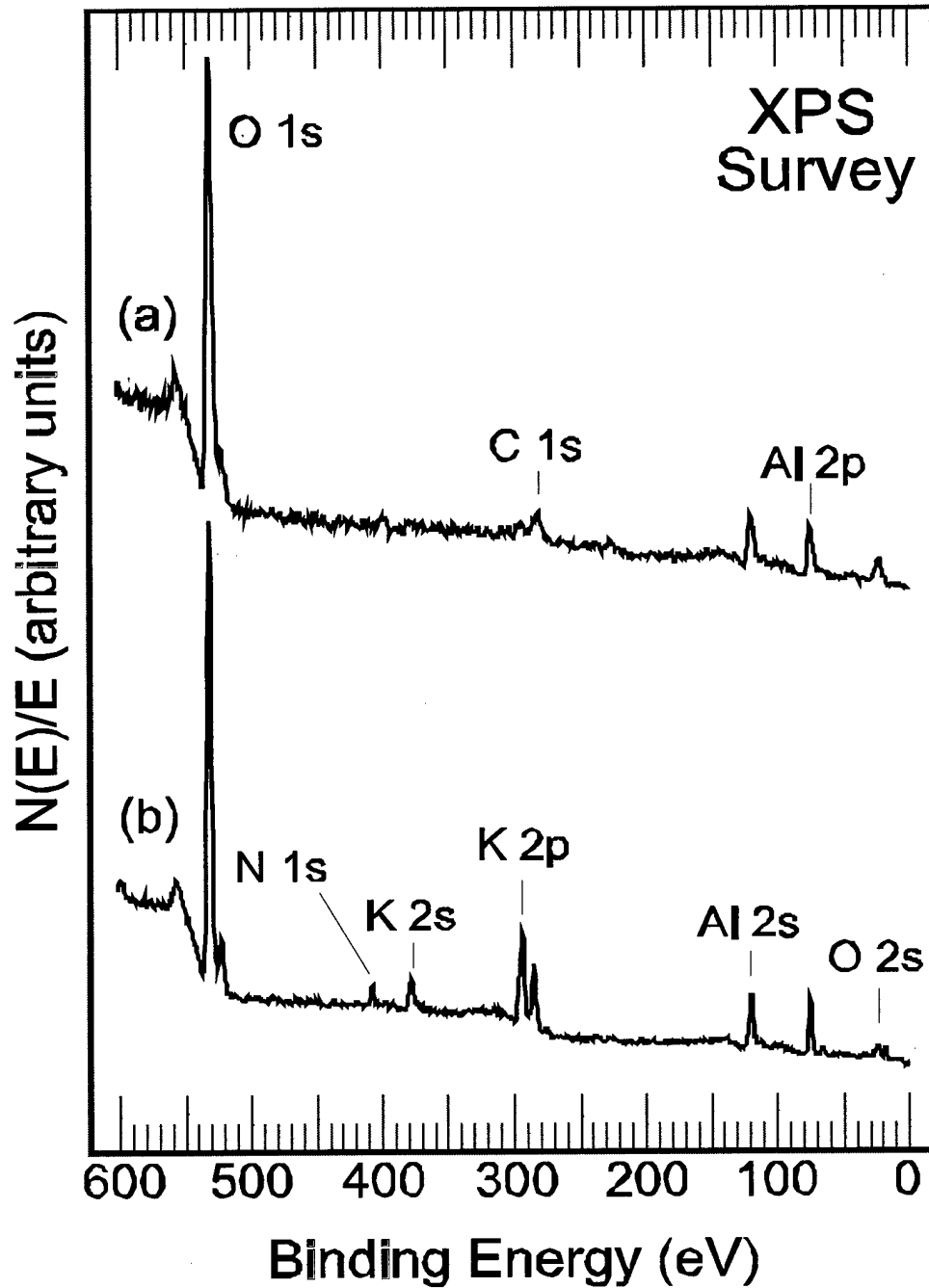


Figure 3-15. Unexposed (a) and NO_x-saturated (b) KOH-precipitated γ -Al₂O₃ pressed powder samples (Lee et al., 1998b). Assignments made pertain to both spectra.

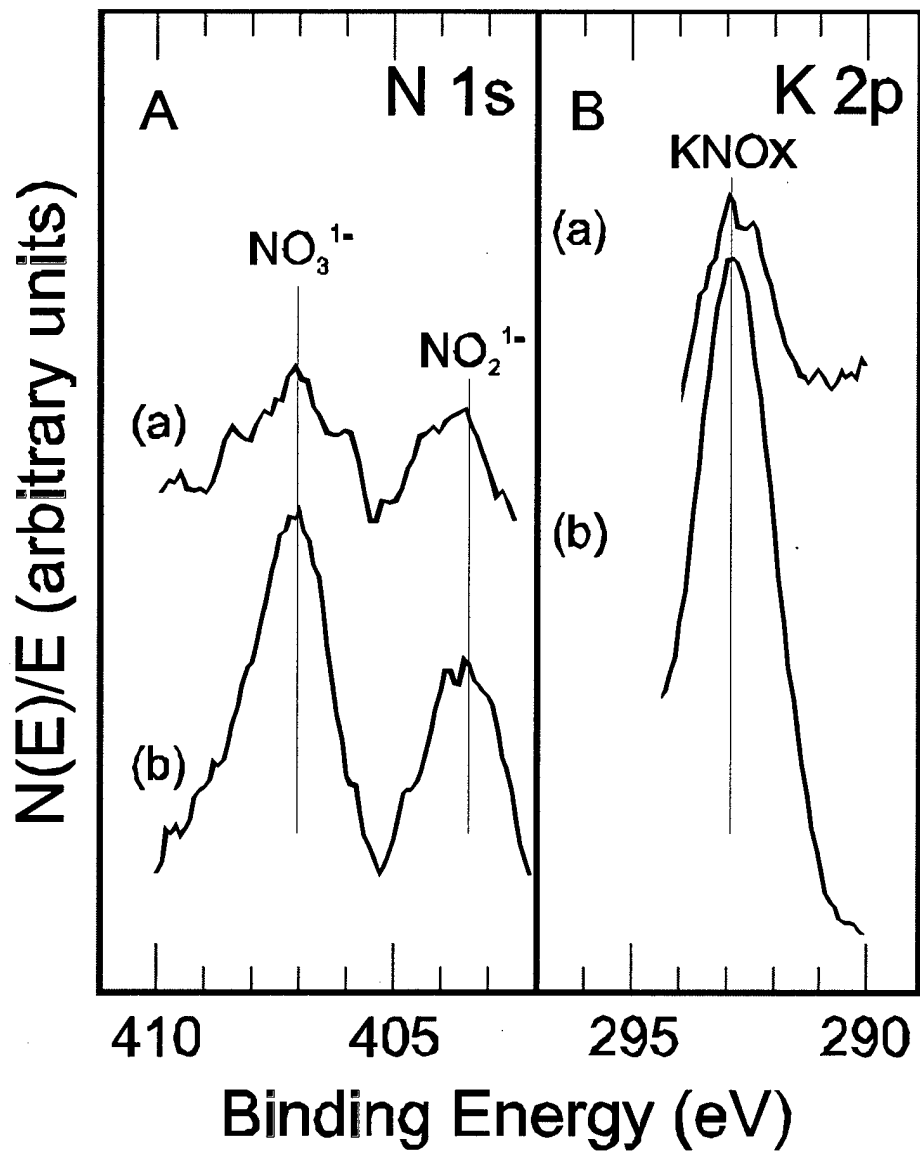


Figure 3-16. XPS (A) N 1s and (B) K 2p spectra obtained from (a) KOH-precipitated and (b) NOx-saturated KOH-precipitated alumina pressed powder samples (Lee et al., 1998b).

respectively. The presence of nitrate and nitrite chemical states are clearly observed. The $\text{NO}_3^-:\text{NO}_2^-$ ratios are approximately 1.5:1 and 2.0:1, respectively, in (a) and (b), indicating that more nitrate forms during the NO_x adsorption. The K (2p) feature is significantly increased in size after NO_x exposure similar to the N (1s) features. The K (2p) peaks suggest that it is present as nitrate and/or nitrite before and after the NO_x exposure, but it may be present as hydroxide before exposure.

As stated previously, Nelli and Rochelle (1996) proposed that a $\text{Ca}(\text{OH})_2$ -buffered sorbent is basic enough to keep HNO_2 and HNO_3 dissociated. They assume that decompositions of HNO_2 and HNO_3 are rate limiting in the mechanism for the overall reaction. Even though buffering compounds such as $\text{Ca}(\text{OH})_2$ or KOH keep HNO_2 and HNO_3 dissociated, results of Nelli and Rochelle demonstrate that NO is eventually formed with continued exposure to NO_2 .

Results of saturation testing in the fixed-bed reactor system containing γ -alumina, in both untreated and treated forms, are shown in Table 3-1. The saturation capacity is defined as that exposure condition at which the bed NO_x outlet concentration does not differ by more than 5% from the inlet concentration. These tests were conducted at the same temperature and NO_x concentration used in previous tests. However, to conserve cylinder gas resources, smaller sorbent sample masses (5 grams) were used. Preliminary tests indicate that the ratio of NO_2 removed per unit sample mass does not vary for different sample masses of untreated alumina saturated with NO_x . The amount of NO_2 removed per unit amount of added KOH is reduced with increased KOH added. BET surface area measurements indicate that the surface area is reduced as the KOH added is

Table 3-1. NO_x saturation capacity of untreated and KOH-treated γ -alumina (Lee et al., 1998b).

γ -alumina	sorbed NO ₂ per NO formed (mmol/mmol)	mass of KOH (w/w% of sample)	mol of sorbed NO ₂ /mol of KOH	BET surface area (m ² /g) nonexposed	BET surface area (m ² /g) NO _x sat.
untreated	1.5/0.54	0	---	170	170
KOH-impreg	1.96/0.65	0.1 g (2%)	1.1	163	154
KOH-precipitat	7.8/2.4	0.96 g (20%)	0.44	98	39

increased and that NO_x exposure further reduces the surface area, which explains the reduction in efficiency. The increased molar volume of nitrate species formed by NO_x sorption has also been suggested as a reason for reduced efficiency (Kimm, 1995).

KOH Treatment Parameters: NO_x-Sorption Effects

The maximum KOH solution concentration that could be applied homogeneously to γ -alumina was found to be 1 g-mol/L (1 *M*). Alumina precipitated in a 2-*M* KOH solution showed a significant decrease in NO_x removal when compared to using a 1-*M* solution. From tests of NO_x sorption on treated Al₂O₃, a trend was observed of increased NO_x removal with increased solution concentrations up to 1 *M* KOH. However, KOH-coated alumina that was prepared using lower-concentration solutions but more solution volume and acquired equal added KOH mass from the treatment. These KOH-treated sorbents performed similarly in NO_x-sorption testing as shown in Figure 2-6. In addition, if the method of treatment [impregnation or precipitation] resulted in similar mass additions, no significant difference of sorption characteristics for NO_x is observed. Therefore, the change in NO_x sorption by KOH treatment proved to be a simple factor of KOH coating mass. An effective maximum addition of KOH to Al₂O₃ was found to be near 20% w/w alumina and was limited by macroscopic surface deterioration and decreased NO_x sorption at higher levels. Further addition of KOH produced a weakly bound coating layer that flaked off when handled (i.e., mechanically unstable). This observation was visible to the naked eye and was studied with a microscope (Bausch and Lomb, Rochester, NY). Concern was raised over the effect of hydration on the sorbent as KOH is a highly hygroscopic material. Samples of treated alumina were exposed to ambient conditions and observed through a microscope over a period of one month. Samples of γ -alumina coated with greater than 1-*M* KOH solution immediately after coating were observed to be brittle and cracks covered the pellets in comparison to

untreated samples. During the month of observations the samples coated with 20% w/w (or less) appeared to maintain a consistent surface integrity.

Preparation variables in the drying atmosphere employed for KOH coatings were varied to evaluate their effect on NO_x sorption. In order to test the effect of the drying atmosphere an inert gas, argon, was chosen. A cylinder of research-grade argon (Bi-Tec Southeast, Inc., Tampa, Florida) was used to supply a 10-mL/min flow into a Griffin beaker containing a preparation slurry of the alumina pellets and KOH solution during the baking process. The flow of argon was assumed to replace the lighter ambient air in the void space above the slurry. After baking, the samples were tested similarly for NO_x sorption. No measurable difference in NO_x sorption was observed due to preparation in an argon atmosphere when compared to ambient air.

The effect of baking temperature was compared from 100 to 300 °C. Samples of prepared slurry were dried at different temperatures for 24 hours and subsequently NO_x-sorption tested. Preparing the sorbent at drying temperatures between 100 and 300 °C did not appear to affect NO_x sorption characteristics. Drying the sorbent at temperatures above 400 °C showed that the alumina pellets became white. Loss of carbon, is suspected to cause the color to change from black to white, which occurred at the temperatures tested from 400 to 800 °C. Alumina manufactured without binder material is white. In addition, the time of drying at these elevated temperatures was a factor in the degree of change in color. Literature on the properties of γ -alumina suggest that the form of γ -alumina will change to a lower surface-area material such as α (alpha)-alumina upon heating to temperatures above about 500 °C.

The time of baking at 150 °C was tested for KOH-treated alumina at 12, 24, 48, and 316 hours. Portions of one batch of KOH-treated alumina were removed at the selected time intervals and stored in air-tight containers prior to testing. Portions of samples from each time interval were divided and thrice NO_x-sorption tested. After all of the material was prepared, samples were tested in random order of bed placement within the triple-bed reactor to examine possible testing errors. The results indicate that NO₂ sorption is unaffected by the time of drying but that NO sorption is enhanced for the samples dried 12 hr. The observed increased removal of NO for the 12-hr preparation sample may be due to changes in surface properties during treatment. Even though a specific reason to explain this effect has not been found, at longer drying times the material appears to stabilize and become more reproducible.

Given that the method of treatment and the time of drying (> 24 hrs.) were found to be inconsequential, preparations of varied coating amounts onto alumina using the latter reproducible conditions were selected in further studies.

Studies of Group-I Treated γ -Alumina

Although previous researchers have studied NO_x removal by γ -alumina treated with various chemicals (Haslbeck et al., 1985; Nelli and Rochelle, 1989; Ma et al., 1995) and NO_x sorption has been achieved using aqueous solutions of alkaline materials (American Public Health Association, 1939-40; Jacobs and Hochheiser, 1958; Krizek, 1966), it seemed that further evaluation of potential coating treatments was warranted. Carbonates, sulfates, and hydroxides of sodium and potassium were studied as potential coating treatments for alumina. Two types of treatment techniques, impregnation and

precipitation, were evaluated for consistency in providing stable added mass and observations were made of adhesion and physical changes resulting from the treatment process used. Treatment by impregnation showed that the added mass varied with solution concentration. However, volumes of solution greater than four times the bulk volume of alumina pellets did not appear to further increase the added mass in impregnation treatments. For precipitated samples, the added mass was a simple function of the volume of solution used to treat the pellets. Observation of precipitation-treated alumina samples showed carbonate- and sulfate-treated samples were limited due to shedding and flaking at high loading, whereas solutions more dilute than 0.04 *M* deposited so little material that the weight difference was obscured by gravimetric measurement error. Tests were performed to study NO_x sorption by alumina, when treated with one of the treatment chemicals listed above either by precipitation or impregnation and producing an equal amount of added coating mass but from solutions of different concentrations.

Tests of alumina samples treated with different added masses of coating material under similar conditions for the sorption of NO_x are shown in Figures 3-17 to 3-20. Data for sulfate-treated alumina samples are not included because the tests showed very low NO_x removal capacity in comparison with other coatings. Each treatment material was tested using three different amounts of coating material. Typical reproducibility data for this study are included for the KOH-treated alumina in Figure 3-17. Also, in Figure 3-17,

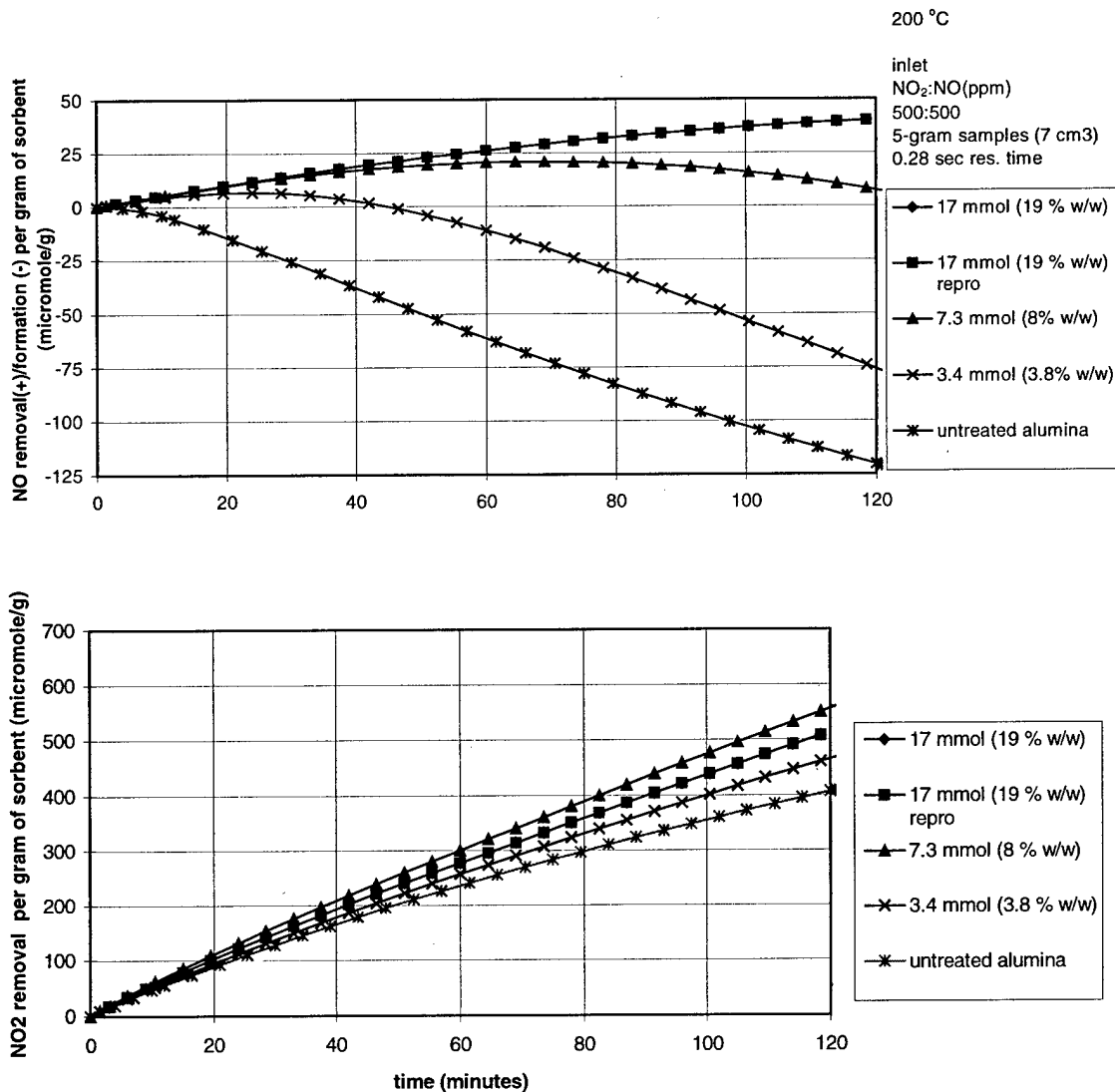


Figure 3-17. NO_x sorption by KOH-treated and untreated alumina samples at 200 °C.

Note mmol (millimole) refers to the amount of treatment material on γ -alumina, “% w/w” indicates the percent of the total sample mass.

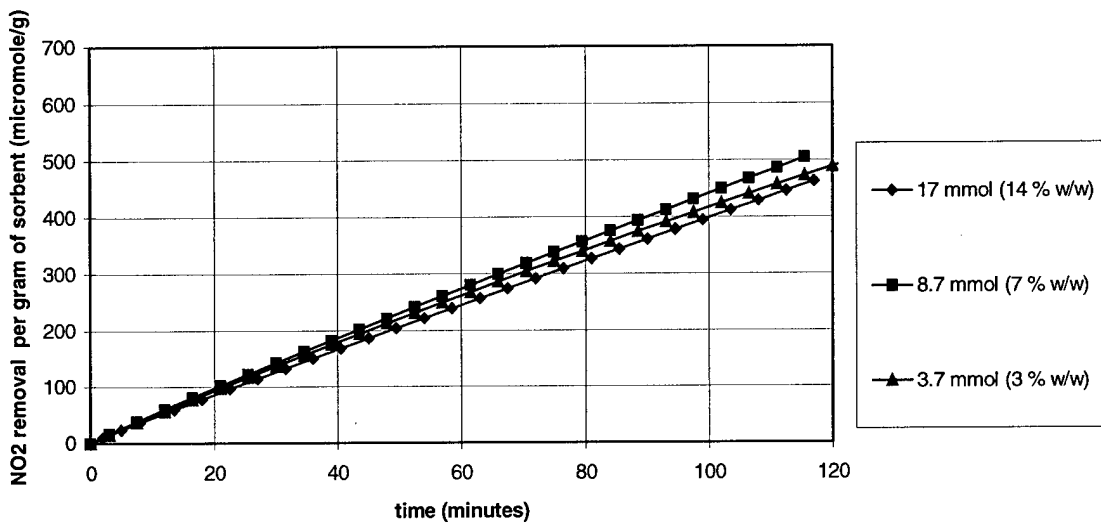
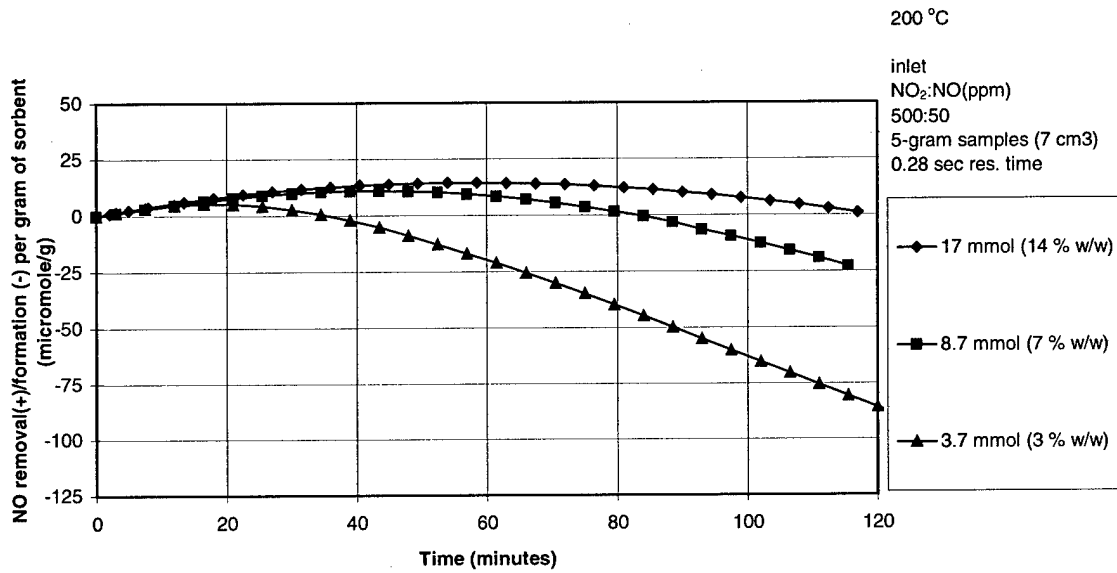


Figure 3-18. NO_x sorption by NaOH-treated alumina samples at 200 °C.

Note mmol (millimole) refers to the amount of treatment material on γ -alumina, “% w/w” indicates the percent of the total sample mass.

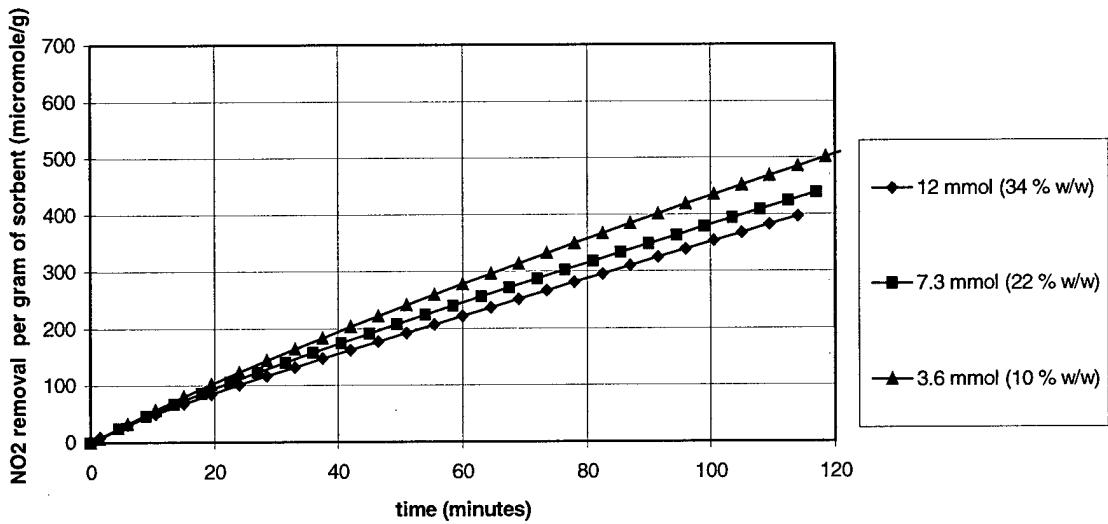
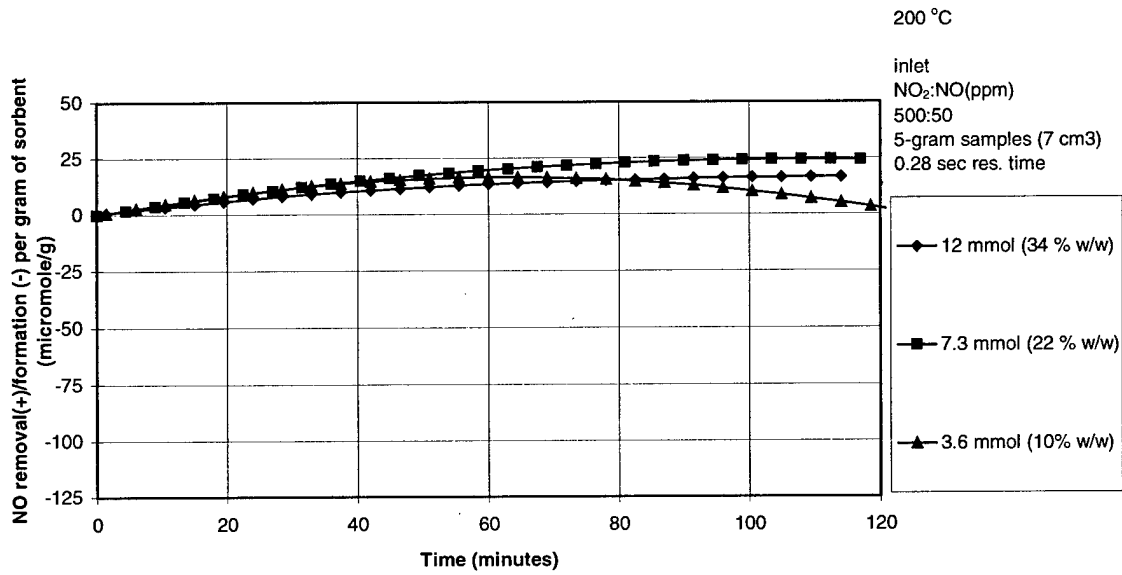


Figure 3-19. NO_x sorption by K₂CO₃-treated alumina samples at 200 °C.

Note mmol (millimole) refers to the amount of treatment material on γ -alumina, “% w/w” indicates the percent of the total sample mass.

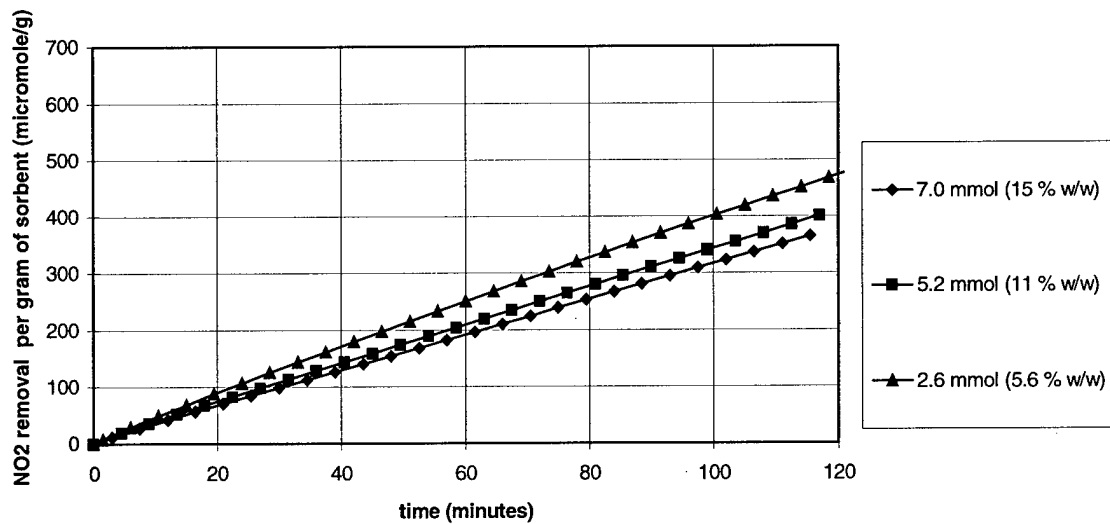
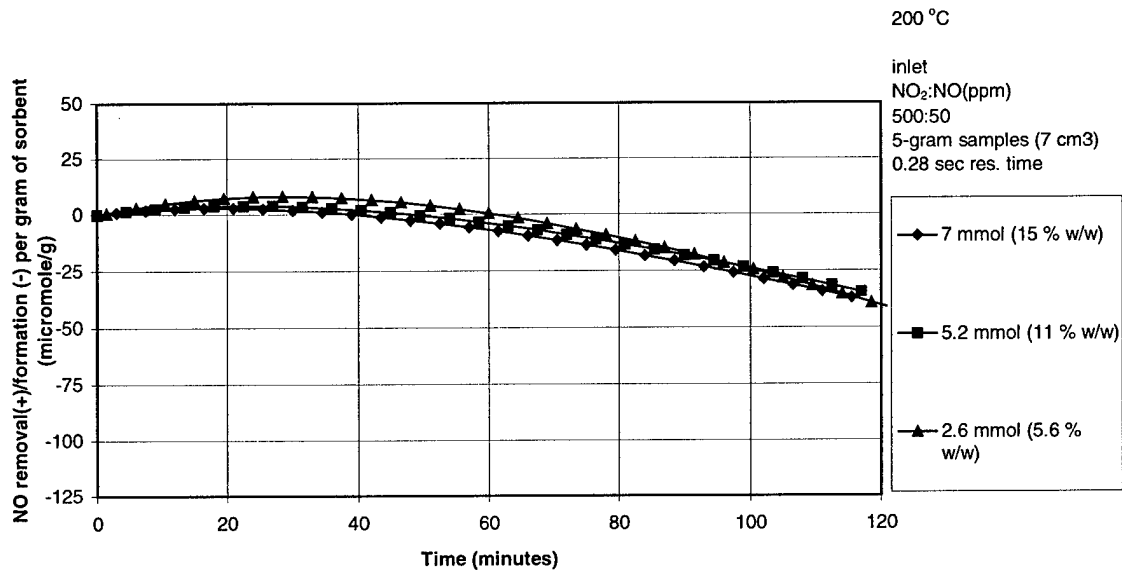


Figure 3-20. NO_x sorption by Na₂CO₃-treated alumina samples at 200 °C.

Note mmol (millimole) refers to the amount of treatment material on γ -alumina, “% w/w” indicates the percent of the total sample mass.

KOH treatment data includes the sorption behavior of untreated alumina. Each treatment material includes the response for the maximum amount of added mass that provided for best binding to alumina. Best binding for each treatment was defined by shaking the tested pellets in a sieve and observing a minimum percent weight loss of the pellets per mass of coating. The minimum weight loss was about 5–1% depending on the coating examined. In addition, pellets were initially visually observed after preparation for the quality of coating to alumina.

For hydroxide treatments (Figures 3-17 and 3-18), the removal of NO is maximized for the highest quantity of coating but NO₂ removal is a maximum for the intermediate coating. Carbonate-treated alumina (Figures 3-19 and 3-20) shows increasing NO₂ removal with decreasing quantity of coating, yet the lowest coating mass shows increasing NO formation. This suggests that the formation of NO by carbonate-treated alumina is directly proportional to the removal of NO₂. However, studies of initial sorption rates show that the fraction of NO₂ removed is not proportional to the percent of coating increase for both hydroxides and carbonates. In comparing NO_x sorption by potassium hydroxide and carbonate for treatment using equimolar amounts (7 mmol), removal of NO by K₂CO₃ is significantly better, while superior NO₂ removal is provided by KOH. On a per-mole basis, potassium compounds generally show better NO removal than sodium compounds under the testing conditions. Variation of NO removal per added amount of hydroxide coating is greater than for carbonate coatings. In comparing NO_x sorption by untreated and treated alumina, decreasing the mass treatments for all chemicals show a gradual trend toward the behavior of untreated alumina. The trend in NO formation for different coating materials relative to that of

untreated alumina is greatest for hydroxides. The greatest combined removal of NO and NO₂ (NO_x) was achieved by KOH-treated (17 mmol) alumina.

NO_x Sorption: Temperature Effects

The temperature of the sorbent bed was varied from 100 to 200 °C to evaluate changes in the rates of NO_x sorption as a function of temperature (Figures 3-21 through 3-24). Two effects are seen from the data shown in these figures, the small overall change in NO₂ sorption rate with temperature and the difference in the rates of NO₂ removal for sodium and potassium-compound treatments. The decreases in the rates of NO₂ removal with an increase in temperature from 100 to 200 °C are small and consistent for all coating materials. This suggests that the process may have a small negative or zero activation energy or that the end product is not thermally stable, as indicated by the production of NO.

NO_x Sorption: Concentration Effects

Tests performed to evaluate the effects of treatment mass and temperature were carried out with different concentrations of NO. Operating conditions for these evaluations were the same except for NO concentration. Comparisons of concentration effects on the sorption of NO_x are shown in Figures 3-25 and 3-26. The amount of treatment in the temperature-evaluation (Figures 3-21 through 3-24) was similar for all materials at 20% by mass. These treatment masses of KOH and K₂CO₃ are within the range of treatments used in the mass evaluation shown in Figures 3-17 through 3-20. Therefore, the effect of lowering inlet NO concentration in the NO_x sorption process for KOH and K₂CO₃ treatments can be observed from the data in Figures 3-17 and 3-21, and

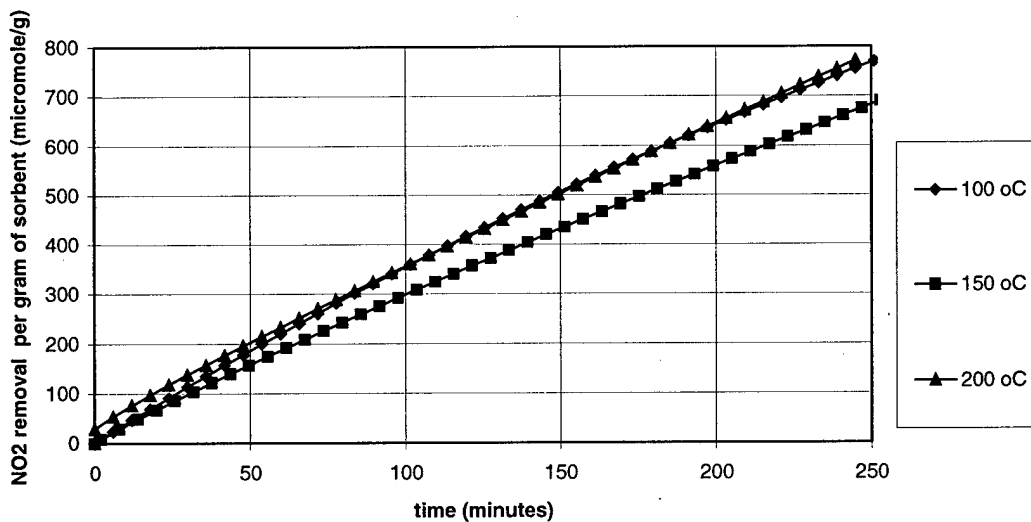
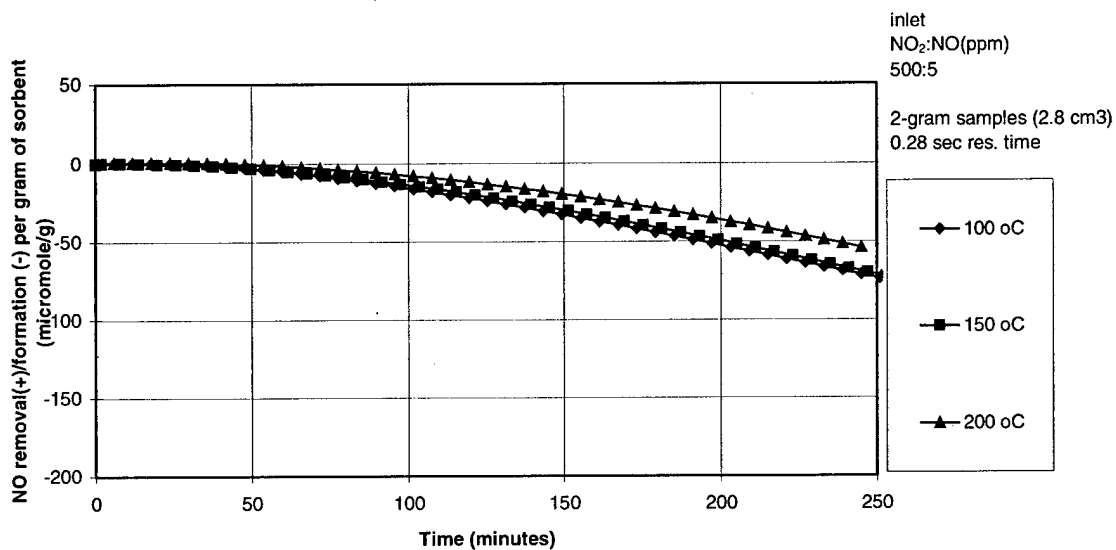


Figure 3-21. Effect of temperature on NO_x sorption by KOH-treated alumina.

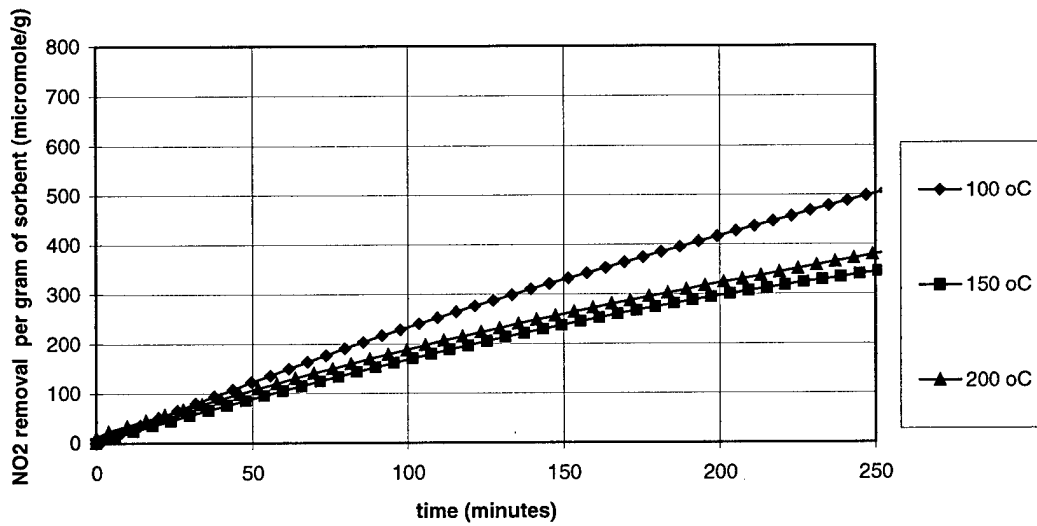
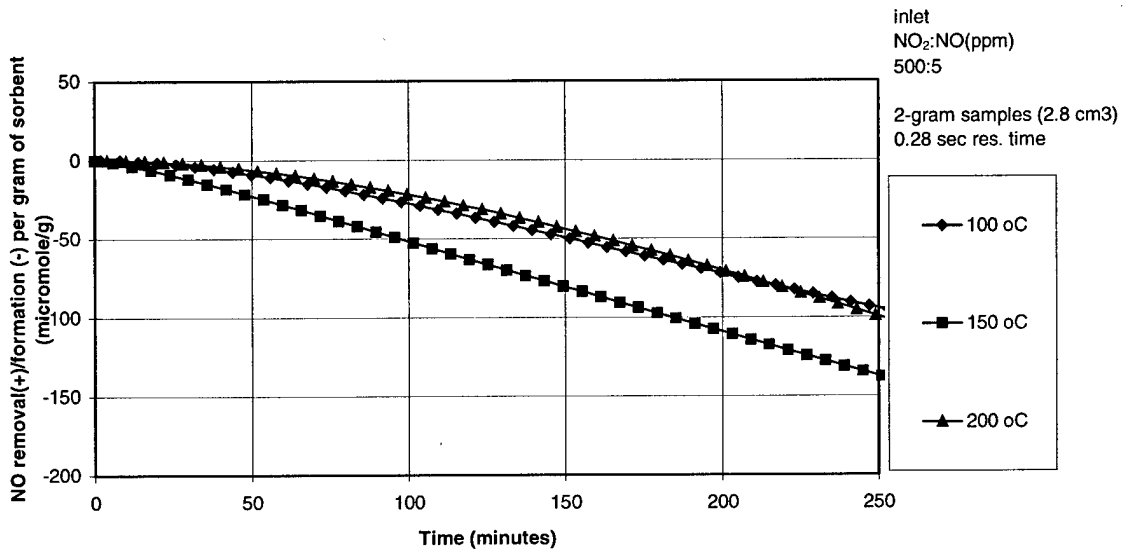


Figure 3-22. Effect of temperature on NO_x sorption by NaOH-treated alumina.

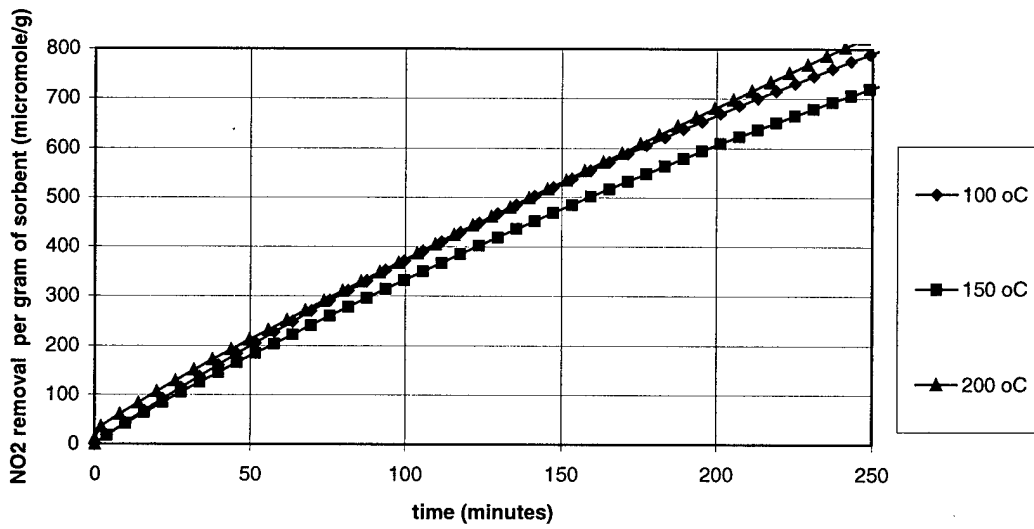
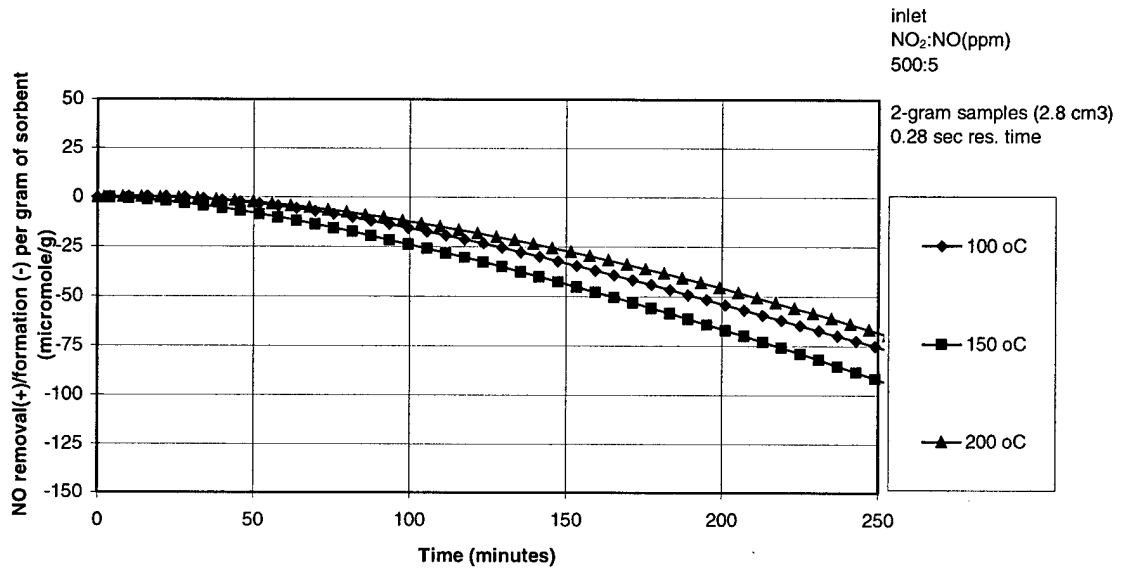


Figure 3-23. Effect of temperature on NO_x sorption by K₂CO₃-treated alumina.

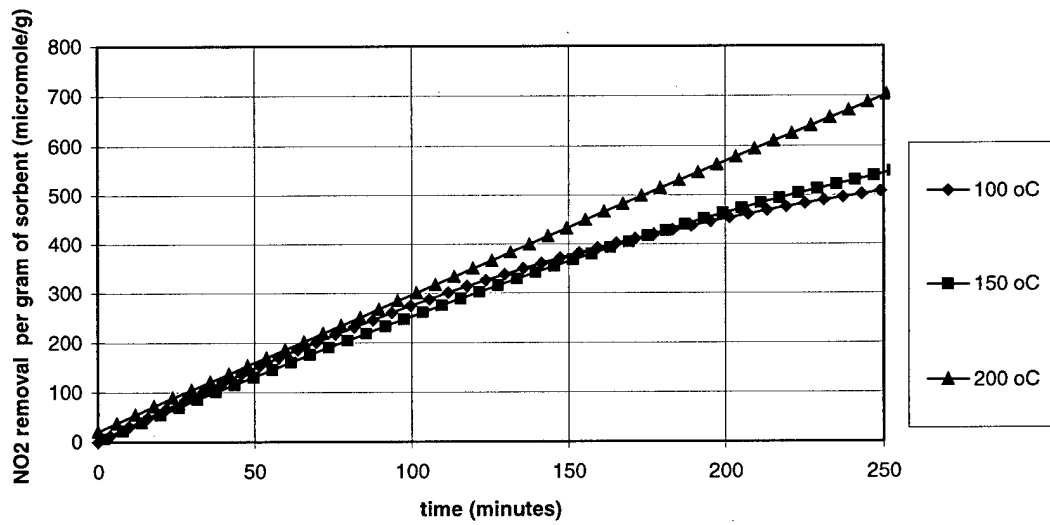
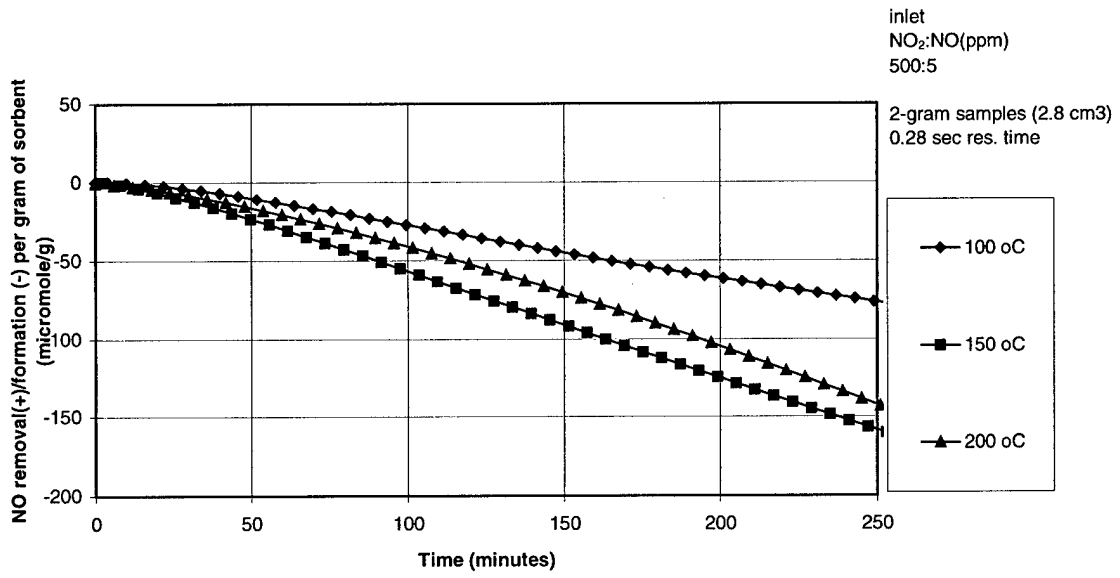


Figure 3-24. Effect of temperature on NO_x sorption by Na₂CO₃-treated alumina.

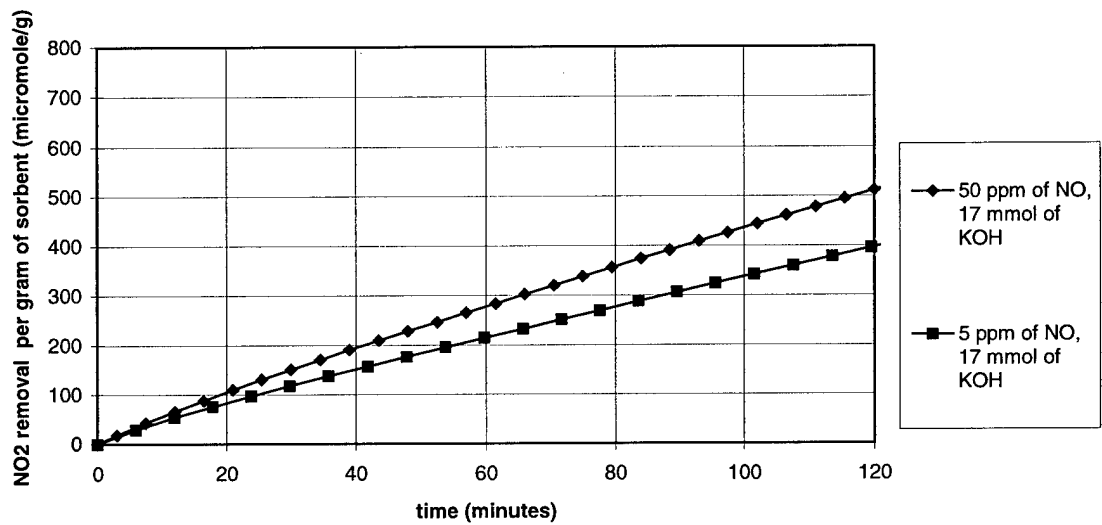
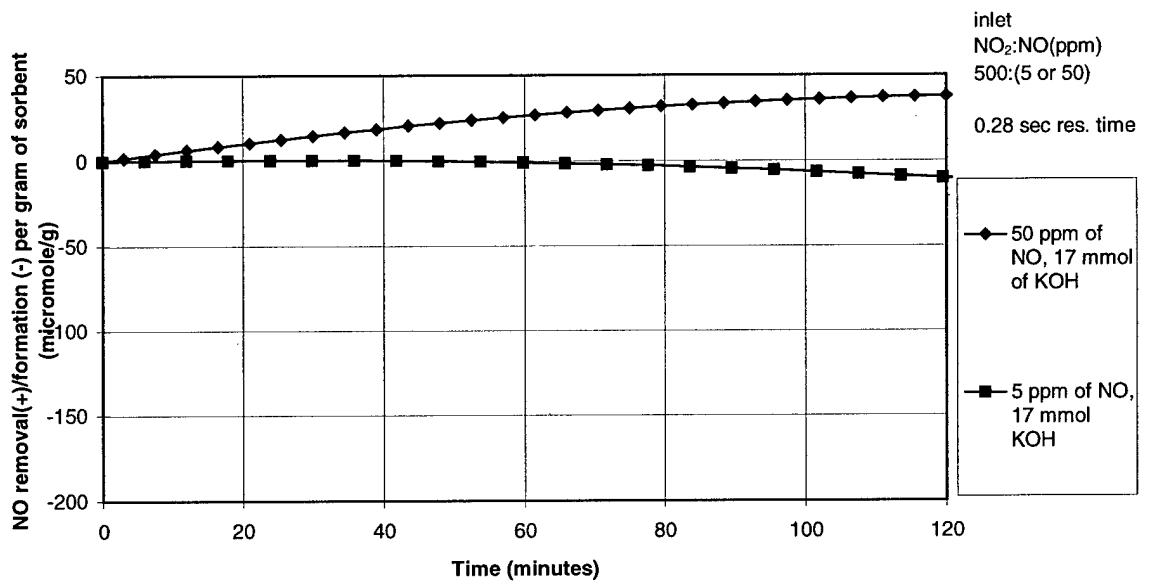


Figure 3-25. Effect of varied NO concentration on the sorption of NO_x by KOH-treated alumina.

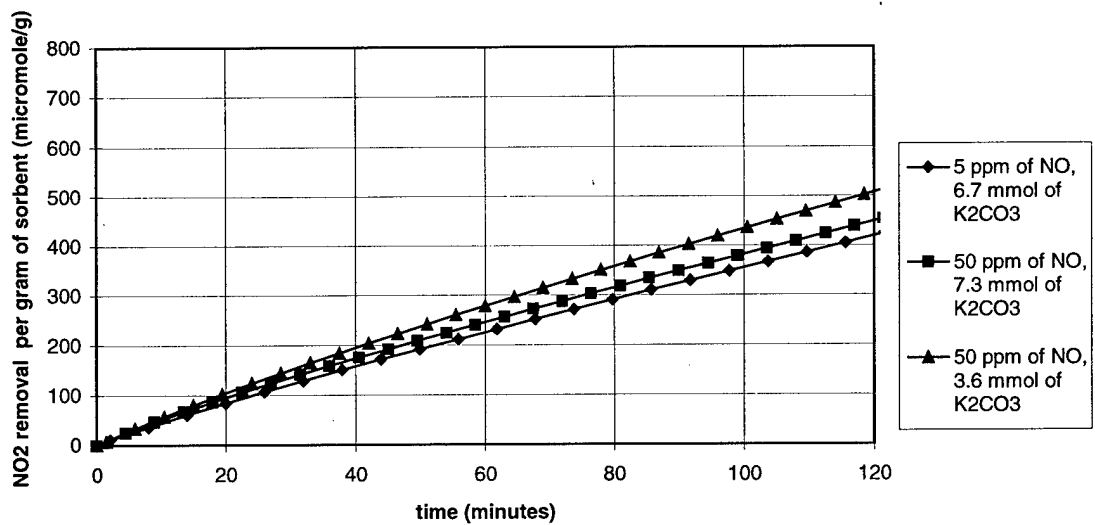
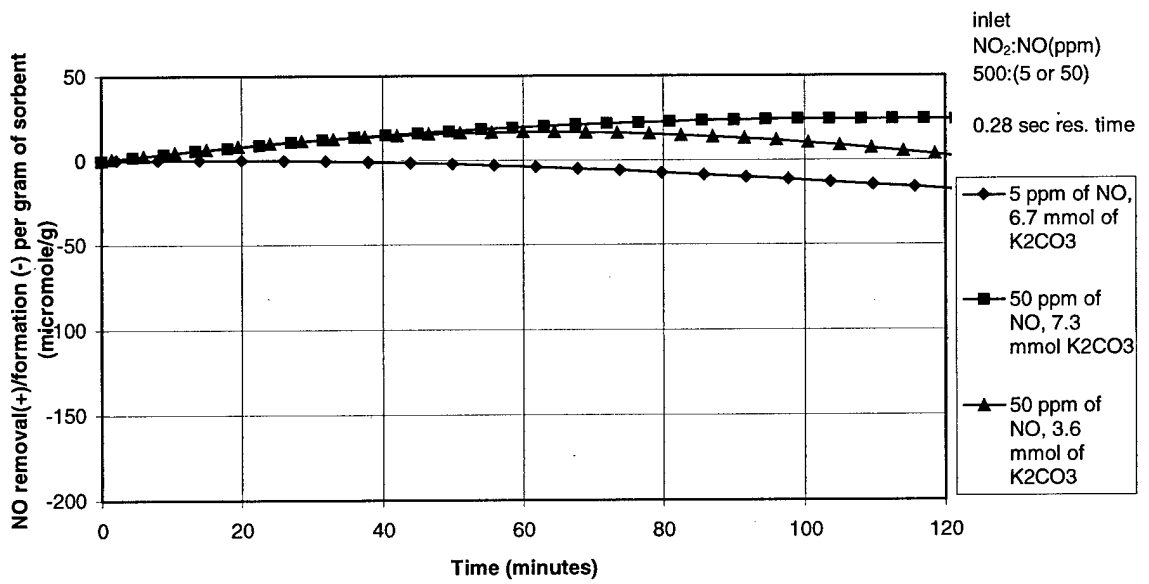


Figure 3-26. Effect of varied NO concentration on the sorption of NO_x by K₂CO₃-treated alumina.

3-19 and 3-23, respectively. The relevant data from these figures are summarized in Figures 3-25 and 3-26. For the KOH-treated (19% by mass) sample in Figure 3-25, removal of NO is small if the NO concentration is 5 ppm but increases at 50 ppm. Furthermore, the removal of NO₂ is significantly less for 5 ppm than for 50 ppm of NO in the inlet gas stream. This observation suggests that the rates of removal of NO and NO₂ by KOH-treated alumina are not independent.

It should be noted that 5-gram samples of sorbent were used in the treatment-mass evaluations but 2-gram samples were used in the temperature evaluations to conserve cylinder gas. However, preliminary testing of NO_x sorption by 2-gram and 5-gram samples using similar residence times showed no significant difference. Tests of 2- and 5-gram samples of untreated alumina under similar conditions are shown in Figure 2-4a) and 2-4b), respectively. Similar observations were made for treated alumina.

Additional sorption tests using a pure gas stream of NO showed no measurable removal by untreated, KOH-treated, and K₂CO₃-treated alumina during a 5-hour period. However, after the 5-hour exposure period, additions of NO₂ to the input-gas showed that treated KOH and K₂CO₃ removed both NO₂ and NO. This observation supports the suggestion that combined gas-solid interaction of NO and NO₂ on alumina is a major factor in the sorption of the two gases. Additional work is necessary to understand this phenomenon and it is important to the detailed understanding of the mechanism of NO_x removal on sorbents.

NO_x Sorption: Saturation

Two-gram treated (20% by mass) alumina samples were saturated with NO_x (500 ppm NO₂ and 5 ppm NO). The results are displayed in Table 3-2. The reproducibility for triple runs of potassium hydroxide-treated alumina samples was low ($\pm 15\%$). However, general trends are observable from the results. Carbonate and hydroxide compounds showed that potassium compounds removed greater amounts of NO_x than sodium compounds. Potassium hydroxide and carbonate performed equally well for similar amounts of treatment mass while sodium hydroxide and carbonate varied greatly. On a molar basis potassium carbonate exhibited the highest efficiency of NO₂ removal. All treatments reduced the amount of NO formed per unit amount of NO₂ removed. Sulfate treatments actually reduced the overall uptake of NO_x compared to untreated alumina, which could be an important feature if sulfur dioxide is a copollutant in the gas stream being treated by a solid sorbent.

Comparison of Alkali Compounds: NO_x Sorption

The alkali elements of Li, Na, K, Rb, and Cs, as hydroxides and carbonates were precipitated onto γ -alumina pellets in equimolar amounts for each element. Laboratory sorption studies of NO and NO₂ were performed in the fixed-bed reactor system followed by either surface area measurement by the BET method or X-ray photoelectron spectroscopy (XPS) analysis.

Sorbent samples were prepared by mixing pellets with solution and evaporating to dryness at 150 °C. Repeated preparations were performed to obtain sorbent samples with equimolar amounts of group-I elements. Thus, a 3-g sorbent sample consists of either

0.14 g of LiOH (6 mmol of lithium) or 1.00 g of Cs₂CO₃ (6 mmol of Cs). The amount of treatment to alumina (6mmol) was based on previous tests that indicated a limiting range of treatment with Na and K hydroxides and carbonates (see Figures 3-17 through 3-20 and discussion thereof).

Alkali-Hydroxide Treatments

The adsorption of NO and NO₂ by alkali hydroxide-treated γ -alumina is shown in Figure 3-27. A clear trend can be observed, increased NO₂ removal with increasing group-I alkali metal atomic weight. While equal molar amounts of hydroxides are present on these sorbents, alkali elements of lower ionization potential show improved NO₂ removal. CsOH is observed to improve removal of NO₂ by 30 % when compared to LiOH.

Alkali-Carbonate Treatments

A similar test series of group-I carbonate-treated alumina samples exposed to NO_x is shown in Figure 3-28. Each of the sorbent samples tested contained 6 mmol of the group-I element. The NO_x sorbent of highest activity is Cs₂CO₃-treated alumina while Li₂CO₃ is the lowest.

Table 3-2. Saturation capacity of treated alumina samples.

Coating material	Time to saturation (hours)	Total NOx removed (mmol) ^a	mol NO ₂ removed /mol NO formed	Coating amount (% by mass)	mol NO ₂ removed/mol of coating
untreated	13	0.36	3.0	0	0
KOH	47	2.09	3.9	20	0.38
NaOH	28	0.59	4.0	20	0.08
K ₂ CO ₃	48	2.12	4.0	20	0.97
Na ₂ CO ₃	37	1.71	3.8	20	0.61
K ₂ SO ₄	10	0.15	3.6	20	0.09
Na ₂ SO ₄	10	0.10	3.7	20	0.05

Based on an average of 3 tests of KOH-treated γ -alumina, the molar ratio of NO₂ removed/NO formed is 3.9 (± 0.5 @ 2 std. dev.). Test conditions: 200 °C, 0.28 sec. residence time, gas input 500 ppm NO₂, 5 ppm NO, 2.8 cm³ bed volume

^a Total NOx removed = mole of NO₂ removed - mole of NO formed

Cesium Treatments

Cesium compounds showed the highest activity of NOx sorption and were further studied. An initial test was performed to show that sorption of NO alone does not occur for CsOH and Cs₂CO₃-treated alumina. Figure 3-29 shows the bed outlet concentration of NO during the test. The slight uptake of NO that is observed during the first 15 minutes

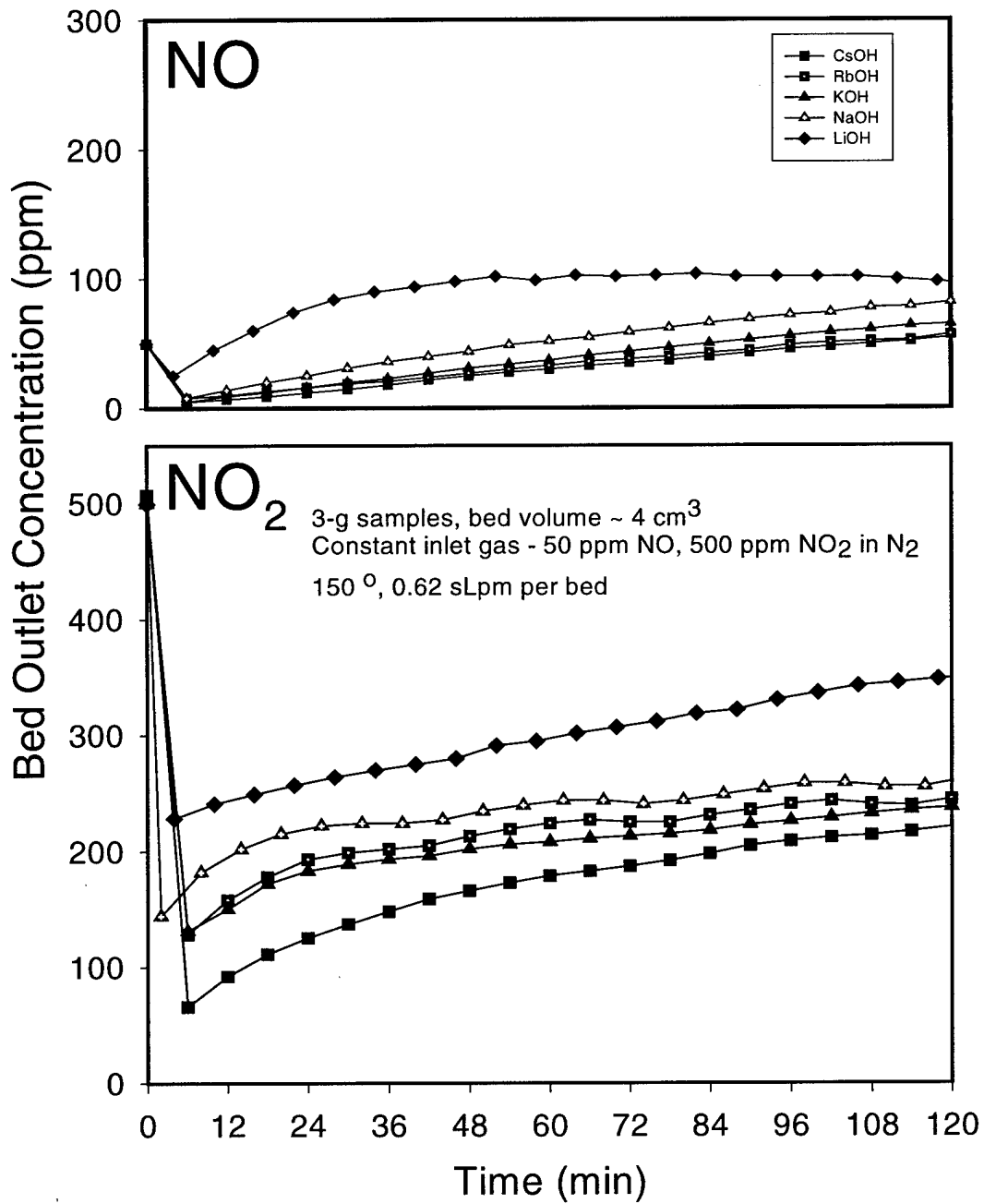


Figure 3-27. Group-I hydroxide equimolar-treated γ -alumina sorption of NOx.

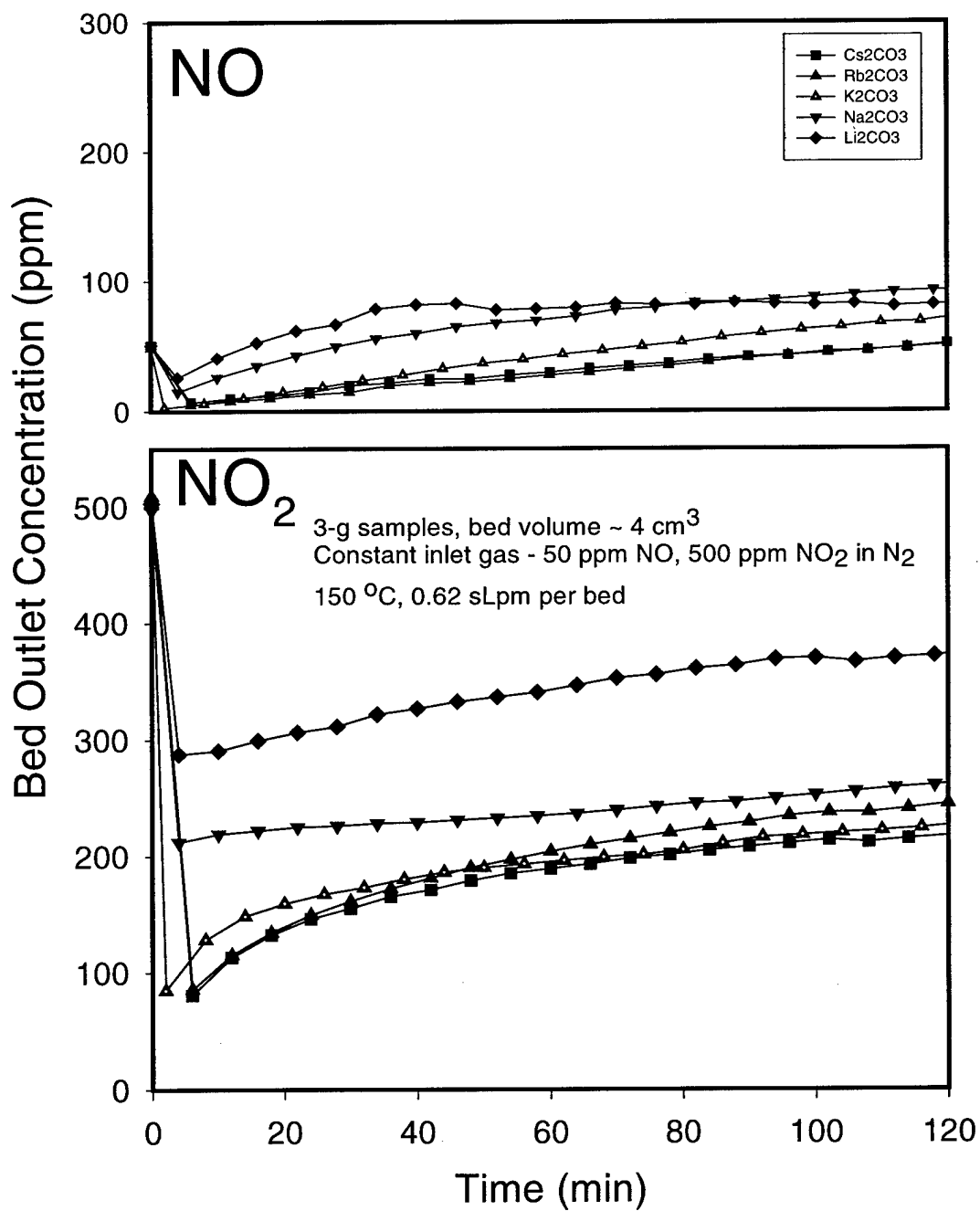


Figure 3-28. Group-I carbonate equimolar-treated γ -alumina sorption of NOx.

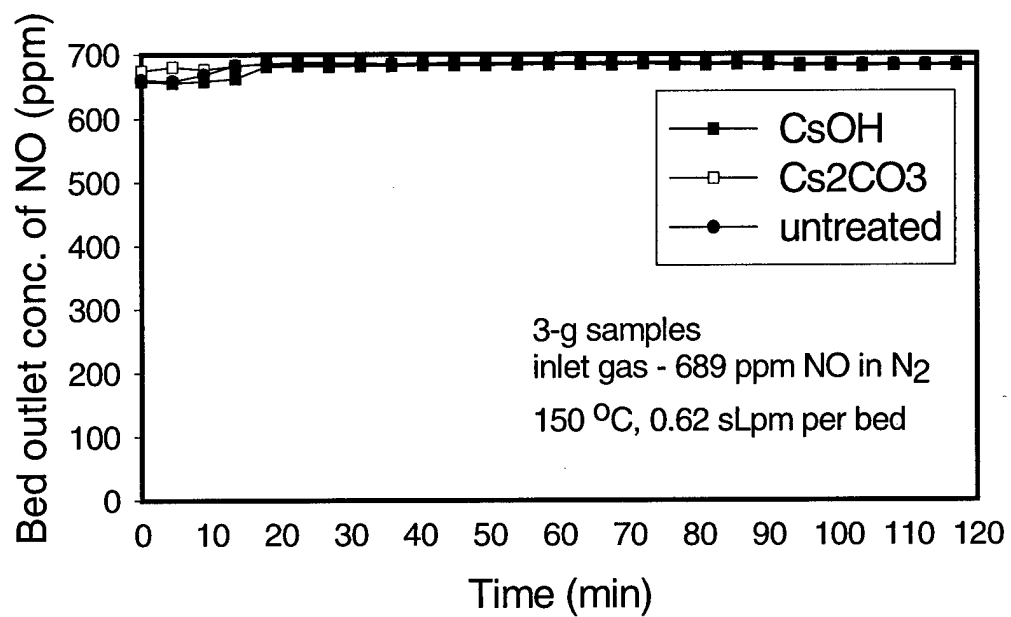


Figure 3-29. Sorption of NO (balance N₂) by untreated and CsOH-treated and Cs₂CO₃-treated alumina.

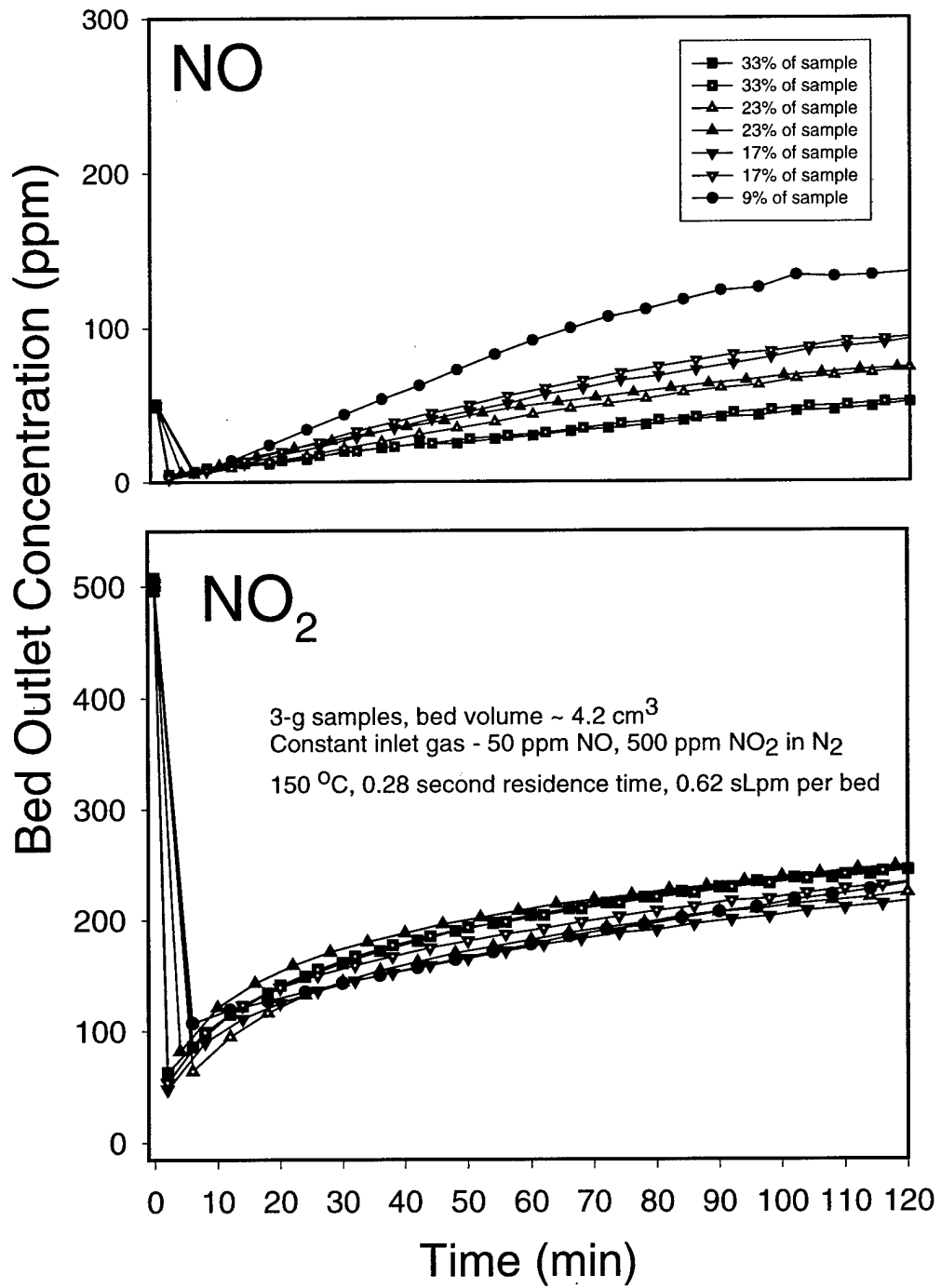


Figure 3-30. Effect of varied amount of cesium carbonate treated onto γ -alumina on the sorption of NO_x.

of the tests is less than 1% of the input NO and within the expected range of experimental error. Previous tests have shown that the uptake of NO by untreated alumina was negligible. Given that in this test the sorption of NO by untreated alumina is observed to perform similarly to the Cs-treated alumina samples it appears that all of these tested materials do not react with NO alone. Varied treatment masses of Cs_2CO_3 were prepared onto alumina and tested for NO_x-sorption. All of these treatments indicate similar NO₂ uptake yet varied NO uptake/production. Based on the rate of NO₂ uptake for all levels of treatment the interaction of Cs_2CO_3 with NO₂ appears to dominate over the uptake of NO₂ by alumina (Figure 3-30). Thus, the production of NO could indicate a faster overall saturation of the surface with production of a stable intermediate presumably CsNO_2 . Build up of nitrites on the surface presumably establish a path to form nitrate and NO.

The Cs_2CO_3 -treated alumina (33 % w/w) sample was XPS analyzed before and after NO_x-exposure. After NO_x exposure no significant peak is observed for nitrogen. This unexpected result was further studied to determine why nitrogen was not observed on the surface.

In the preparation process for XPS analysis the weak bonding force of sorbed gases to Cs was revealed. During the outgassing process to reach 10^{-10} torr, the Cs_2CO_3 -treated sample evolved a large amount of gas. Furthermore, during analysis the x-ray bombardment heated the sample from 25 °C to approximately 50 °C. During this heating an additional amount of gas evolved.

To determine if the outgassing process did in fact remove sorbed nitrogen a subsequent test was performed. A portion of the Cs_2CO_3 -treated sample was placed in the outgassing chamber and the pressure reduced to 10^{-8} torr. The sample was then

removed and stored for further testing. The sample was transported and placed in the fixed-bed reactor. A decomposition test was performed on the sample to determine if any NO or NO₂ species would evolve. The sample was flushed with a constant flow of 1 sLpm N₂. The furnace heating rate was 10 °C /min. The temperature was increased until it was observed that a significant amount of NO was released from the surface. From the decomposition test it was clear that the outgassing process did not remove sorbed NO_x species. Therefore, another explanation for not observing nitrogen species through XPS analysis is necessary. The relative scale of the information collected from the XPS system is a function of the greatest intensity peak. The Cs (3d) peak has an intensity factor of approximately 10 times that of nitrogen. Therefore, detection of the N (1s) peak is presumably decreased due to the large intensity of the Cs (3d) peak.

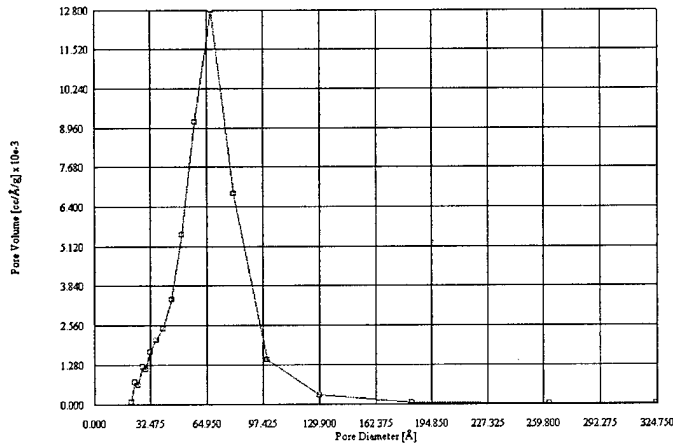
Alkali-Treated Alumina: Surface Area Measurements

Surface area measurement data for the equimolar treated alumina materials are shown in Table 3-3. A trend in decreasing surface area with increasing group-I atomic radius is apparent. Given that these materials have equimolar treatments of each alkali element the differences in the surface area measurement are believed to be primarily caused by the change in the alkali metal atomic radius. Having observed that lithium compounds performed relatively poorly compared to cesium, the surface areas of these materials indicates that the relative activity of cesium is even greater per surface area.

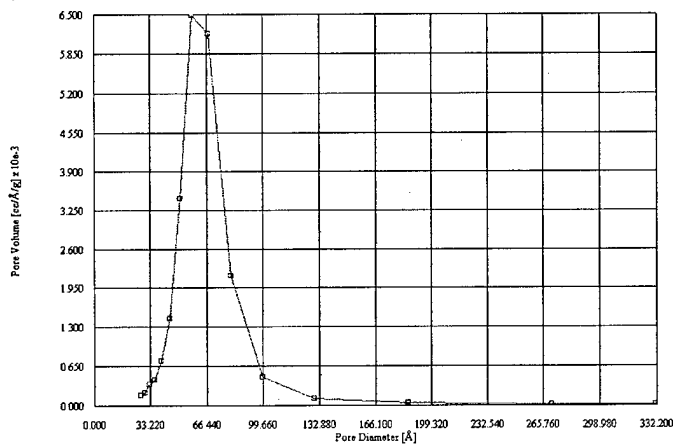
Figures 3-31 a), b), and c) show the pore size distribution for untreated γ -alumina, Cs₂CO₃-treated (33% w/w) γ -alumina, and NO_x-saturated Cs₂CO₃-treated (33% w/w)

Table 3-3. BET surface area measurement of treated γ -alumina sorbents.

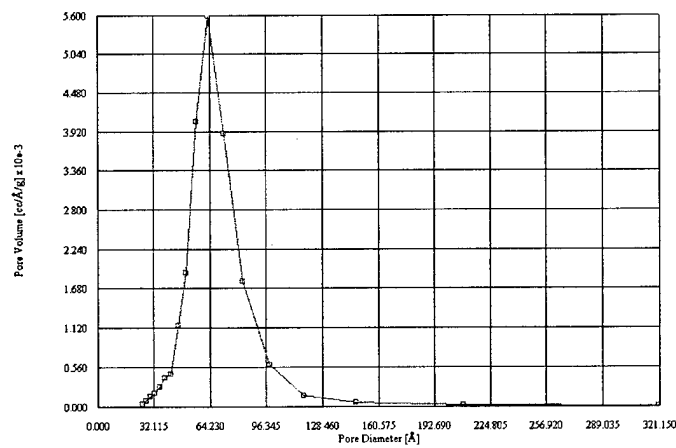
Treatment Compound	coating millimoles per sample	NOx exposure NO ₂ /NO	Surface Area (m ² /g)	Atomic Radius (Å)
Li ₂ CO ₃	3.0	----	157	0.53
LiOH	3.0	----	122	0.53
Na ₂ CO ₃	2.85	----	142	0.67
NaOH	3.0	----	126	0.67
K ₂ CO ₃	3.0	----	120	0.86
KOH	3.0		114	0.86
Rb ₂ CO ₃	2.8	----	85	1.53
RbOH	3.0		83	1.53
Cs ₂ CO ₃	2.95	----	71	1.90
CsOH	3.0	----	71	1.90
Cs ₂ CO ₃	2.95(33% w/w)	saturated	58	
Cs ₂ CO ₃	2.95(33%)	1.2:0.12	61	
Cs ₂ CO ₃	1.40(17%)	----	122	
Cs ₂ CO ₃	1.40(17%)	1.2:0.12	116	
Cs ₂ CO ₃	0.80 (9%)	---	144	



a) Pore size distribution of untreated γ -alumina.



b) Pore size distribution of Cs_2CO_3 -treated (33% w/w) γ -alumina.



c) Pore size distribution of NO_x -saturated Cs_2CO_3 (33% w/w)-treated γ -alumina

Figure 3-31. Pore size distribution of a) untreated γ -alumina, b) Cs_2CO_3 -treated alumina, and c) NO_x -saturated Cs_2CO_3 -treated alumina.

γ -alumina, respectively. Pore size distribution measures of the Cs_2CO_3 -treated alumina (33% w/w) before and after NO_x -exposure compared to untreated alumina indicate that the average pore size is not significantly altered but that overall surface area and pore volume is decreased by treatment and NO_x -exposure. The pore radius increases from 90 to 94 \AA upon coating treatment with Cs_2CO_3 and further increases to 97 \AA after NO_x saturation. The surface area decreases from 172 to 75 m^2/g after coating treatment and reduces to 58 m^2/g after NO_x saturation. The pore volume decreases from 0.388 to 0.176 cc/g upon treatment and reduces to 0.142 cc/g after NO_x saturation. Because there is little change in the average pore diameter yet a decrease in the available pore volume possibly indicates that the pore channels are simply closed by surface treatment and NO_x exposure. The pore closure effect suggests an inefficient use of the total material surface. The molecular size of sorbed particles has been suggested for observed pore closure of Ca_2O when used as a sorbent for SO_2 (Borgwardt and Harvey, 1972). The molecular sizes of group-I nitrate compounds are greater than the corresponding carbonates and this may explain the decreased surface area after NO_x saturation.

A small sample (0.8 g) of Cs_2CO_3 -treated alumina (33% w/w) was set in the sorbent tube such that it formed a one-pellet thick layer of sorbent. This material was to be NO_x -exposed for further study by either XPS, FTIR or ion-selective-electrode. A small sample was used to achieve quick saturation. Also, the thin layer should minimize any secondary effects of NO gas produced by sorbed NO_2 . The tests performed involved

exposing the sorbent to a stream containing 1950 ppm NO₂ at 150 °C. The sorbent was exposed until the NO₂ outlet concentration was 85% of the NO₂ inlet concentration. Only trace amounts of NO were present in the NO₂ gas stream. Unexpectedly, the single-pellet layer bed of Cs₂CO₃-treated alumina immediately produced NO as a result of NO₂ sorption. During 4 hours of exposure the ratio of NO produced approached approximately a 3:1 ratio. This trend is shown in Figure 3-32.

Relation of Alkali Element Ionization Potential to NO_x Sorption

The activities of the group-I alkali metal compounds with NO_x appear to correlate with their ionization potentials. Similar trends are observed for hydroxide and carbonate materials. Table 3-4 lists the ionization potential of each element and the average fraction of NO₂ removed during the NO_x-sorption tests shown in Figures 3-27 and 3-28. Lithium has the highest ionization potential and is least reactive to NO_x, while cesium has the lowest ionization potential and highest reactivity per mole with NO_x.

Sorption Studies of the Effect of Varying NO and NO₂ Concentrations

A series of experiments was performed on untreated, K₂CO₃-treated and KOH-treated γ -alumina to characterize the effect on NO_x sorption of varying the concentrations of NO or NO₂ in the presence of both reactive gases. Previous tests had shown an unexpected increase in NO sorption in the presence of NO₂ for alkaline-coated aluminas. Gaseous NO alone is not removed by any of the sorbent materials studied. Tests in which the NO₂ concentration was held constant while the NO concentration was increased showed an increase in NO sorption (Figures 3-25 and 3-26). Knowing that NO alone is

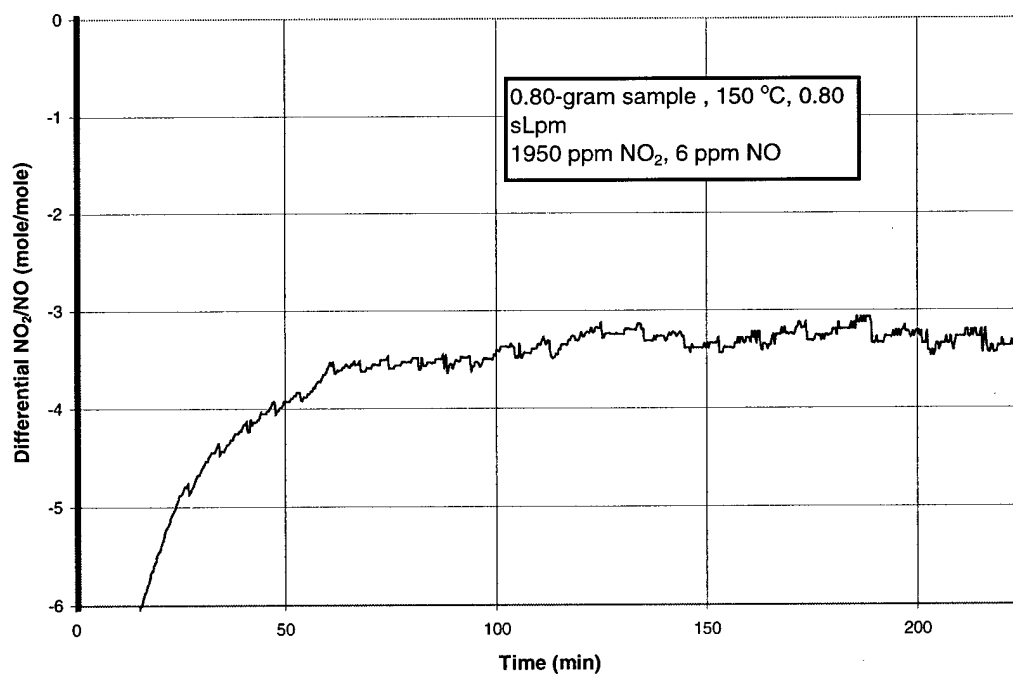


Figure 3-32. Incremental molar ratio of NO₂/NO for Cs₂CO₃-treated alumina sorption of NO₂.

Table 3-4. Fractional NO₂ removal of group-I treated compound alumina and element ionization potential.

Treatment Compound	Fraction of NO ₂ Removed	group-I element Ionization Potential (eV)
LiOH	0.299	5.392
NaOH	0.497	5.139
KOH	0.538	4.341
RbOH	0.541	4.177
CsOH	0.625	3.894
Li ₂ CO ₃	0.287	
Na ₂ CO ₃	0.498	
K ₂ CO ₃	0.585	
Rb ₂ CO ₃	0.595	
Cs ₂ CO ₃	0.600	

not removed, the observation of increased removal of NO with concentration suggested that NO₂ reacted in coordination with NO₂ at the sorbent surface. This should also be confirmed by an increased NO₂ uptake with increased NO as well as increased NO₂-formation.

Initial Tests on Sorption of Gaseous NO

A preliminary test was made to confirm that NO sorption alone did not occur but when combined with NO₂, NO is sorbed. Figure 3-33 shows the NO_x outlet concentrations of K₂CO₃-treated and KOH-treated γ -alumina. The test consists of two segments of a specific inlet feed of NO₂ and NO. Initially NO, alone is directed through the bypass line which is indicated by 50 ppm NO. The feed gas, which is absent of NO₂, is then directed to the sorbent beds. As seen in the figure, the outlet NO concentration during this exposure was the same as the inlet concentration (50 ppm NO). After exposure of the bed to NO for 40 minutes the NO gas was redirected to the bypass and

the NO₂ gas (50 ppm) is added to the NO flow. Upon redirection of the gas mixture flow to the beds, the sorption of NO in the presence of NO₂ is immediately apparent.

Interaction of NO with Sorbents following NO₂ Sorption

Other tests were performed to further identify the process of NO-NO₂ sorption. One question arises as to whether NO sorption is due to a species formed from sorbed NO₂ or by another process. An experiment to answer this question was performed. A fixed-bed reactor test was performed in which the K₂CO₃- and KOH-treated materials were first exposed to NO₂ (689 ppm) at 25 °C. Following NO₂ exposure the bed was flushed with N₂ to remove residual NO₂ gas. The bed was then exposed to NO. Two tests were performed to observe effects of lengthened NO₂ exposures. In Figure 3-34 time-resolved outlet NO and NO₂ concentrations for K₂CO₃/γ-alumina are plotted. The test procedure during the time intervals is described below numerically (1–8).

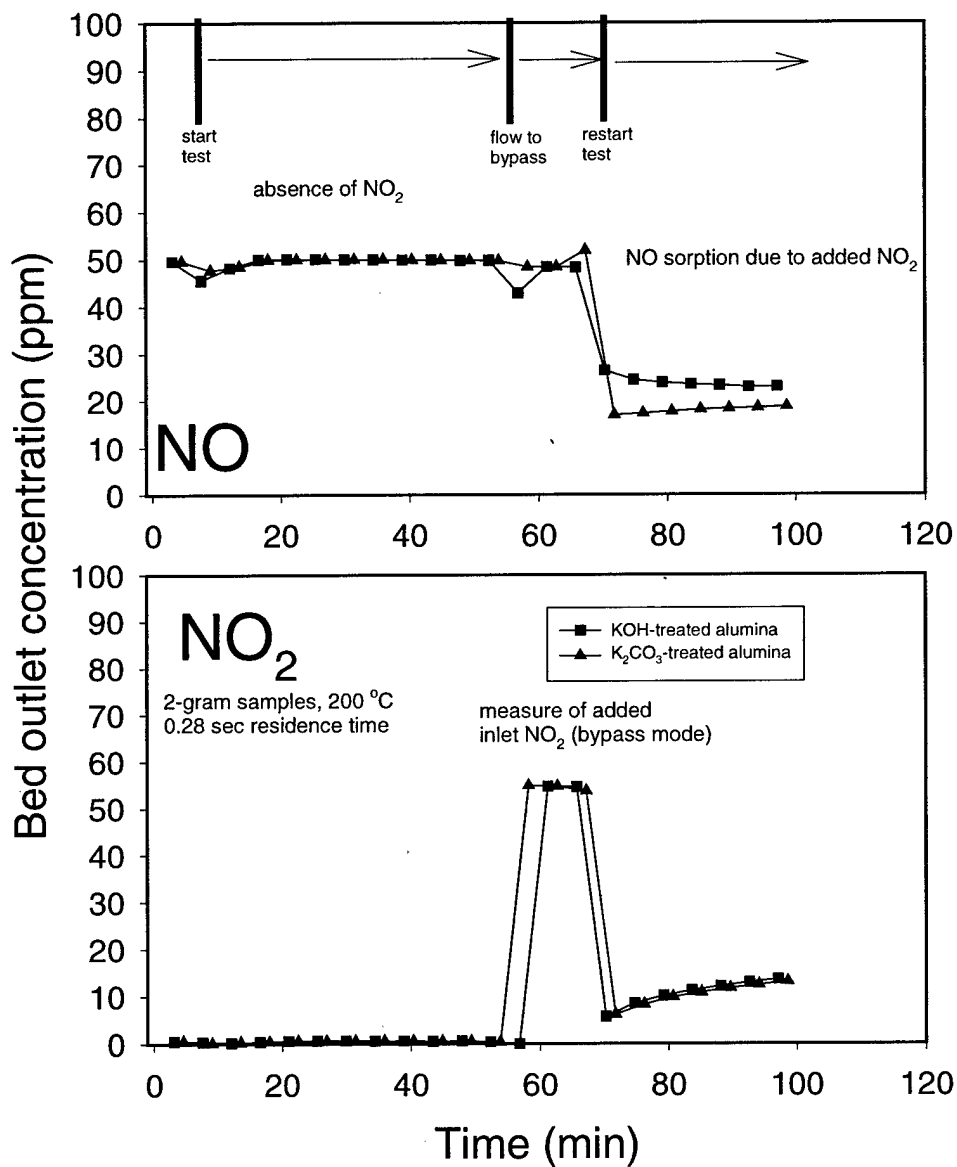


Figure 3-33. Effect of presence of NO₂ on sorption of NO for KOH-treated and K₂CO₃-treated alumina.

1. Certified cylinder-gas NO (680 ppm @ 1 sLpm) is measured in the bypass line.
2. Certified cylinder-gas NO₂ (689 ppm @ 1 sLpm) is measured in the bypass line.
3. NO concentration is measured in the empty reactor tube.
4. NO₂ concentration is measured in the empty reactor tube.
5. The empty reactor tube is removed and filled with 2-g of K₂CO₃-treated (24.7 % w/w) alumina. The filled reactor tube is replaced in the system.
6. The bed is exposed to NO₂ (689 ppm @ 1 sLpm) for 20 minutes (Figure 3-34 a)) or 5 minutes (Figure 3-34 b)).
7. The flow of NO₂ is stopped and the bed is flushed with N₂ (1 sLpm).
8. The reactor bed is exposed to NO until the outlet concentration reaches <1% of empty-tube NO concentration.

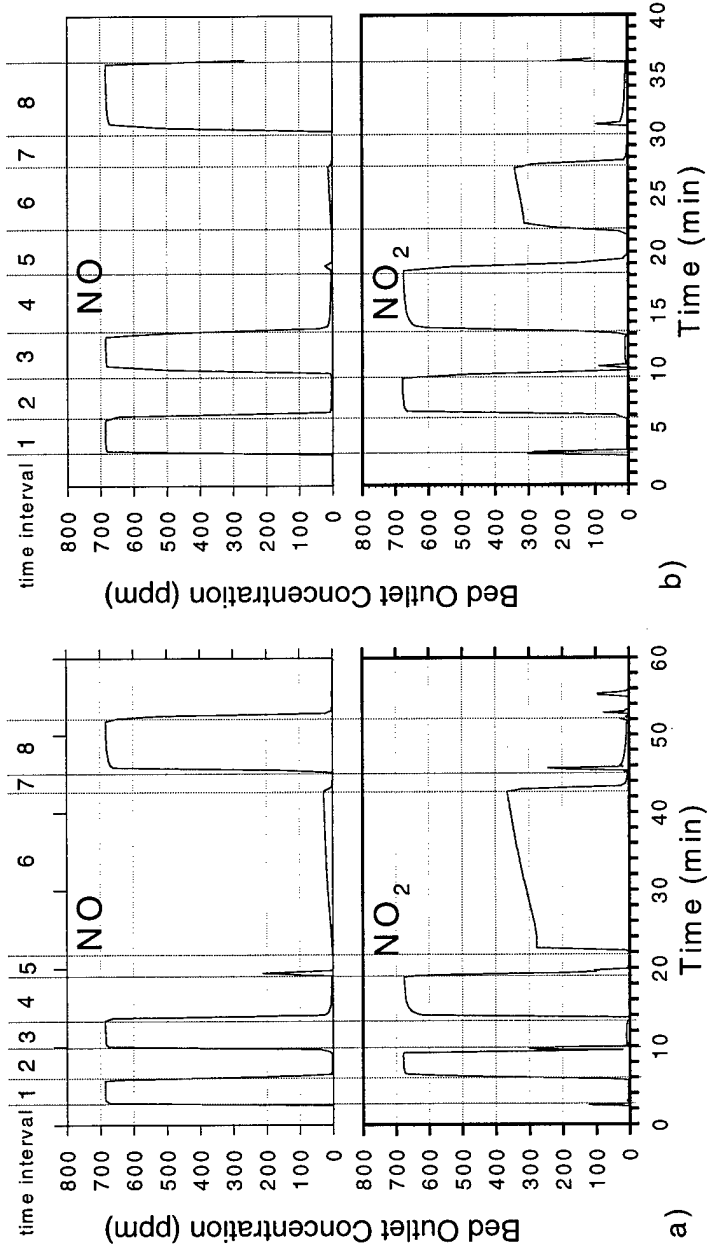


Figure 3-34. Surface interaction of NO following exposure of K₂CO₃-treated alumina to NO₂ at 25 °C.

The test revealed several interesting features. First, after NO₂ exposure to the K₂CO₃-treated alumina, a small fraction of NO flowing through the sorbent bed is observed to be sorbed (Figures 3-34 a) and b), time interval 8.). Comparing Figures 3-34 a) and b), increased amounts of NO sorption occurs that corresponds to increased NO₂ exposure time. The ratio of NO₂ initially sorbed (time interval 6, (41.1 and 143.5 μmole/g sorbent) to the amount of NO subsequently sorbed (time interval 8, (0.78 and 6.89 μmole/g sorbent)) are 2.6 and 4.8 % for the 20 and 5 minute exposures, respectively. Thus, the amount of NO subsequently sorbed is a small fraction of the NO₂ sorbed and does not increase proportionally to the amount of NO₂ sorbed.

Second, an unexpected phenomenon can be observed. NO sorption simultaneously occurs to a production of NO₂ (time interval 8). This corresponding production of NO₂ during NO sorption is proportional to the amount of NO sorbed (time interval 8). The ratio of NO sorbed/NO₂ produced during time interval 8) is 0.88 (20 min (Figure 3-34 a)) and 0.73 (5 min (Figure 3-34 b)). A reason for this observed simultaneous NO sorption-NO₂ production is that the increased concentration of inlet NO (680 ppm) and the absence of NO₂ causes a reversal of a reaction with surface species formed during NO₂ exposure (time interval 6). The surface species formed may then reversibly react to convert NO to NO₂. Similar results were observed for untreated and KOH-treated γ-alumina. Again, untreated, K₂CO₃-treated, and KOH-treated alumina are observed to sorb NO and produce NO₂ in similar tests after NO₂ exposure.

According to the proposed reactions of others (Kimm, 1995; Nelli and Rochelle, 1996), NO₂ can convert to nitrite, nitrate, and NO. This study may indicate a reversal of a reaction, similar to reaction 3-3 or 3-8, that is a reaction of NO with an intermediate

complex nitrate. Thus, it is suggested that the phenomenon described above is the reversal of nitrite to nitrate conversion. However, the small fraction amounts of NO sorbed (time interval 8) suggest a high barrier to reversing the suggested reaction.

To test the proposed reaction, pure KNO_3 was exposed to NO to determine if NO_2 could be produced in a similar manner to that observed in the above study. This test was performed by placing pure KNO_3 within the fixed-bed reactor system and exposing to NO at 25 °C. Production of NO_2 was not observed. In addition, tests with KNO_3 -treated alumina exposed to NO did not produce NO_2 in the fixed-bed reactor. Assuming the reaction proposed above is correct, this result suggests that nitrate species formed by NO_2 sorption may have very different properties from bulk-phase nitrate. Thus, these tests may not be indicative of the proposed reaction. Decomposition tests, that are discussed later (see section entitled Thermal Decomposition Studies), of pure samples of potassium nitrite and nitrate did not similarly decompose as NO_x -exposed sorbents and alumina treated with KNO_3 or KNO_2 solutions.

Effect of Varying the Inlet NO Concentration

A series of fixed-bed reactor experiments was performed on untreated γ -alumina, K_2CO_3 -treated and KOH-treated γ -alumina to measure the effects of increasing NO in the presence of a constant NO_2 concentration. Experiments were performed with the concentration of NO_2 held constant at 500 ppm and varied NO concentrations (10, 50, 200, and 500 ppm) with a constant gas bed residence time at temperatures of 25, 50, 100, 200, and 250 °C. Gas residence time in the sorbent bed has been discussed to significantly effect the sorption behavior of these materials and thus was kept constant during these tests (see Figure 3-3). Therefore, at different temperatures (25, 50, 100, 200,

and 250 °C) the gas flow was varied to provide a similar bed residence time of approximately 0.25 sec. The bed masses were held constant at 3 grams for consistency of comparison by mass. The experimental results are shown as cumulative sorption of NO and NO₂ in micromole/g of sorbent in Appendix A.

Reproducibility tests of three samples each of untreated, K₂CO₃-treated, and KOH-treated alumina show 95% confidence intervals to be 7.6, 8.7, and 7.6 percent, respectively, of the accumulated NO₂ sorbed after 2 hours of NO_x exposure. These tests were performed at 250 °C that have greater errors than lower-temperature tests due to lower flowrates and higher temperature variations. Thus, lower-temperature tests should have greater reproducibility.

The efficiency of NO₂ removal is constant with temperature. However, the reduced molar flow rate of NO_x applied at higher temperatures reduces the amount of cumulative NO₂ sorbed. Treated materials show a significant increase in cumulative NO sorbed with increased temperature. As well, the rate of NO sorption for treated materials becomes more linear at higher temperature. At lower temperature, NO sorption decreases rapidly and production of NO is observed eventually for the treated materials.

Over the tested temperature range, increased NO input appears to increase NO₂ sorption to treated alumina yet is not significant given the 95 % confidence intervals. Based on previously described tests (see Figure 3-25 and 3-26) this result was not expected. Previous tests indicated that the sorption of NO corresponded to additional NO₂ sorption. One may propose that NO and NO₂ interact to provide sorption of both gases. Another sorption process observed may be sorption of NO₂ alone. Given that

these tests did not show increased NO₂ sorption and the extensive coverage of conditions of these tests, sorption of NO with NO₂ may be competitive with sorption of NO₂ alone.

Effect of Varying Inlet NO₂ Concentrations

A similar series of experiments was performed to study the effect of varying NO₂ concentration (10, 50, 200, and 500 ppm) in the presence of constant NO concentration (500 ppm). Tests were performed at the same temperature and flow used for the previously discussed series. Cumulative sorption of NO and NO₂ in $\mu\text{mole/g}$ are shown in Appendix B for this series of tests.

Results from the test indicate the sorption of NO₂ is first order with respect to itself over the range of temperatures. NO sorption trends to a first order relation at higher temperature with respect to input NO₂.

A significant finding is that higher temperature increases cumulative NO sorbed. However, at lower temperatures a maximum cumulative amount of NO sorbed is observed. Also, at lower temperature less cumulative NO sorption is observed for an NO₂ inlet concentration of 500 ppm than 200 ppm. Thus, having observed at lower temperature that increased NO₂ inlet concentration decreases the cumulative amount of NO sorbed suggests a competitive sorption process may occur where sorption of NO₂ is preferred. This preferred sorption may be the sorption of NO₂ alone. Thus, if two sorption processes are proposed to be sorption of NO₂ and NO or sorption of NO₂ alone, a preference is observed for NO₂ alone in tests of 500 rather than 200 ppm NO₂ inlet concentration. Tests with lower NO₂ inlet concentration (200 ppm) increase the cumulative NO sorption because the ratio of NO:NO₂ inlet concentration is higher.

Gas and Surface Profile for the Sorption Process

Preliminary studies of KOH-treated γ -alumina showed both NO and NO₂ sorption for an initial period of NO_x exposure (see Figure 3-7). Thus, a mechanism that includes treated sorbent removal of NO is necessary. Having observed an interaction of NO in the presence of NO₂ by alkali-treated γ -alumina (Figure 3-33), a series of fixed-bed reactor experiments was designed to measure the outlet gas concentrations and surface species formed by NO_x sorption within a sorbent bed of untreated, K₂CO₃-treated, and KOH-treated alumina. These data could give indications of possible reactions that occur on the sorbent surface.

The fixed-bed reactor system was used to expose untreated, K₂CO₃ and KOH-treated alumina (15-gram samples) to a 0.885 sLpm (per bed) flow of NO₂ (1950 ppm) at 25 °C. NO was present in the feed gas as a trace impurity in the NO₂ gas cylinder. After NO_x exposure for a maximum of 2 hours, the 15-gram samples were removed from the reactor and sectioned into 3-gram portions. These 3-gram sections were dissolved in aqueous solution and analyzed by ion-specific electrode (ISE) for nitrite and nitrate concentrations. An in-depth discussion of the data collected and analysis is provided elsewhere (Pocengal, 1999). The total sample mass of 15 grams was chosen to ensure that the individual samples would contain sufficient surface nitrogen species for measurement by ISE analysis. Other 15-gram sorbent samples were exposed to NO_x for shorter time periods of 30, 60 and 90 minutes and were similarly analyzed for nitrite and nitrate concentrations. The ISE analyses can provide the concentration of the formed surface nitrite and nitrate species for the four different exposure times. Nitrite and nitrate

concentrations found at each bed layer for 30, 60, 90, and 120 minute-exposure times are presented in Figures 3-35, 3-36, and 3-37 for the three materials.

Estimated gaseous concentrations of NO and NO₂ within the sorbent bed were obtained by testing sorbent masses of 3, 6, 9, and 12 grams under similar conditions as the 15-gram samples. These measurements of the gas-phase NO and NO₂ concentration profiles throughout the sorbent beds for the three materials are shown in Figures 3-38, 3-39, and 3-40. During the first 30-min exposure period it is seen that essentially no NO₂ or NO gas is emitted from the treated alumina beds. After the 30-min exposure the first layer of all treated materials studied shows a low nitrite-to-nitrate ratio, which corresponds to a high production of NO. Thus, the first layer of all materials appears to be sorbing NO₂ and also converting nitrite to nitrate and NO. For untreated alumina, at longer times of exposure it was observed that continual conversion of a proportional amount of NO₂ into NO occurred throughout the bed (Figure 3-38). As the treated sorbents convert NO₂ into NO in the first and second layers, the NO produced appears to be sorbed within the successive (3rd, 4th or 5th) layers. In Figures 3-36 and 3-37 it is seen that an increased amount of nitrite is formed throughout the bed that corresponds to the subsequent sorption of produced NO. As the beds become saturated over time, the nitrite-to-nitrate ratio in the lower bed layers gradually decreases.

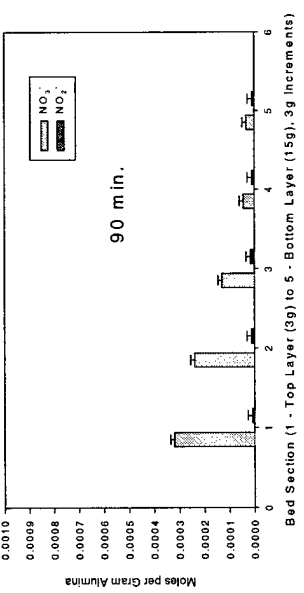
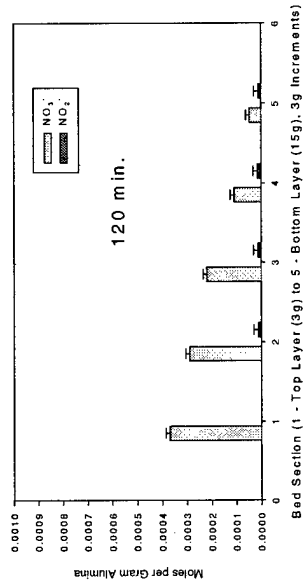
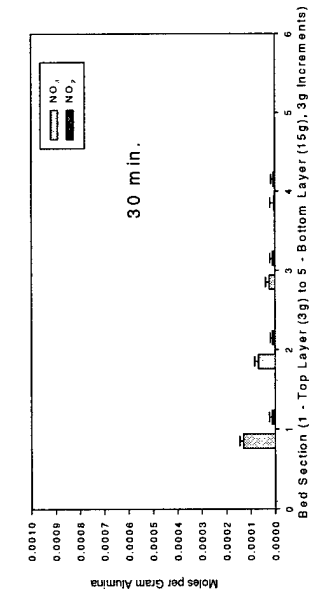
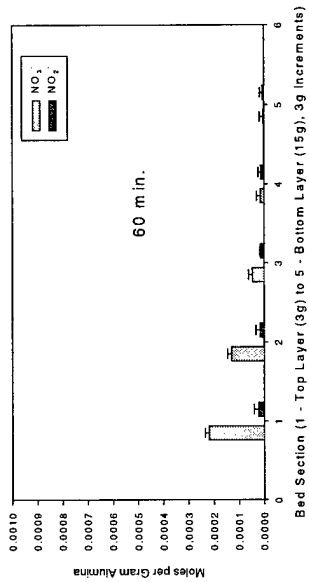


Figure 3-35. Nitrite and nitrate measured on incremental layers of a sorbent bed of untreated alumina.

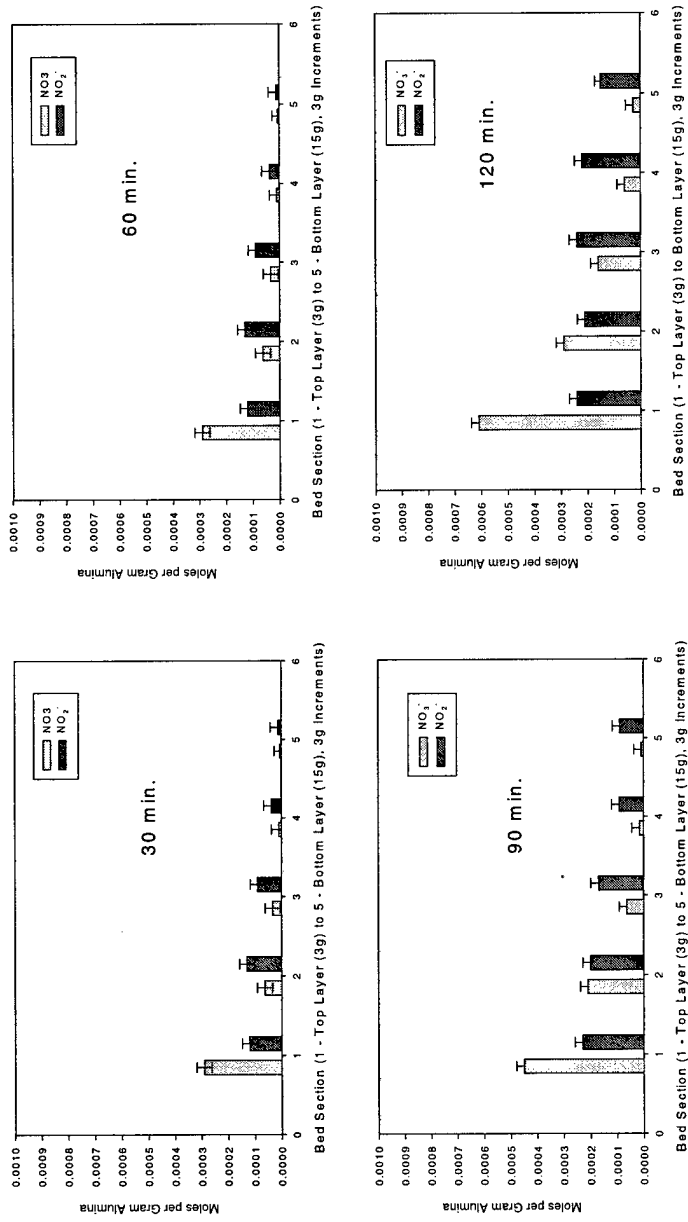


Figure 3-36. Nitrite and nitrate measured on incremental layers of a sorbent bed of K₂CO₃-treated alumina.

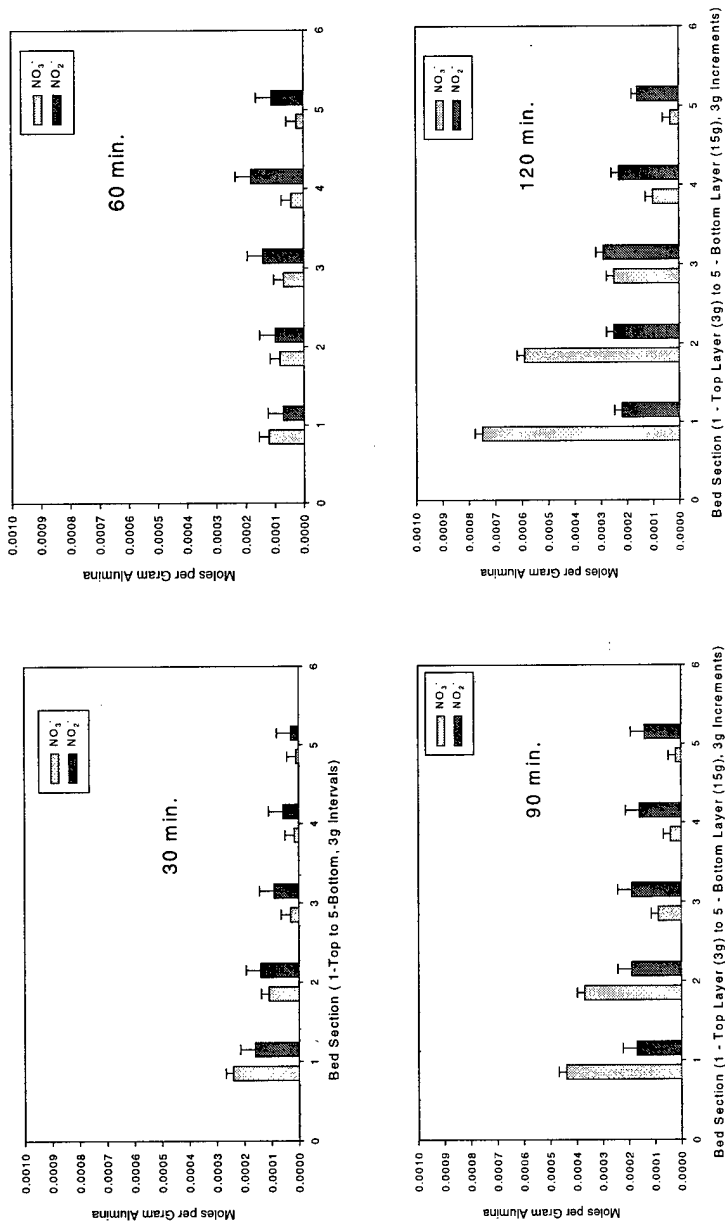


Figure 3-37. Nitrite and nitrate measured on incremental layers of a sorbent bed of KOH-treated alumina.

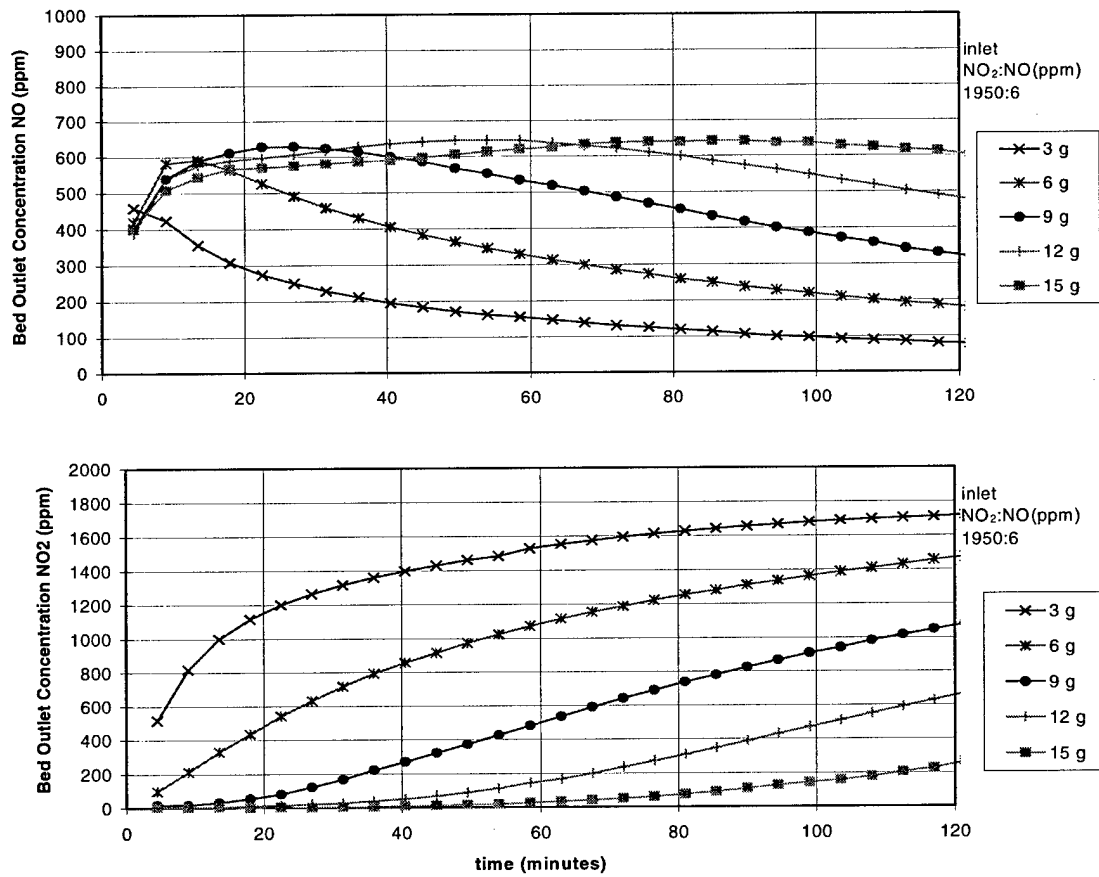


Figure 3-38. Change of NO and NO₂ gas concentrations throughout a bed of untreated γ -alumina.

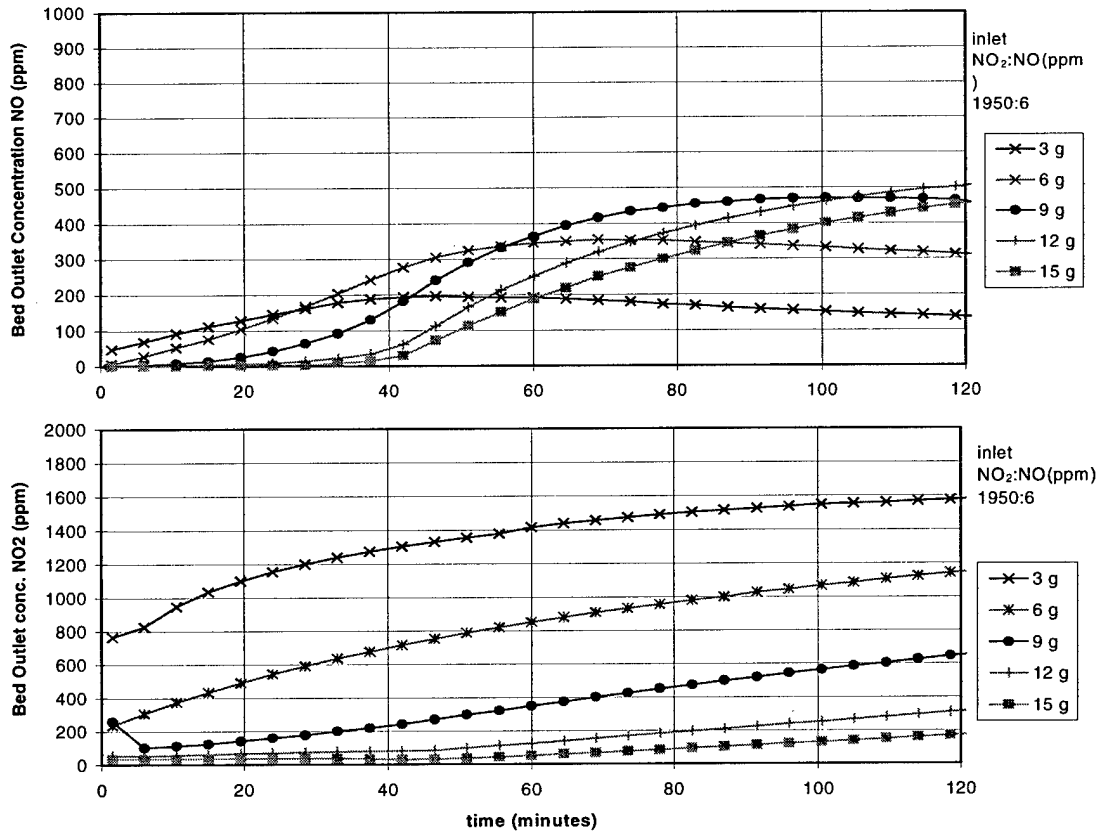


Figure 3-39. Change of NO and NO₂ gas concentration throughout a bed of K₂CO₃-treated γ -alumina.

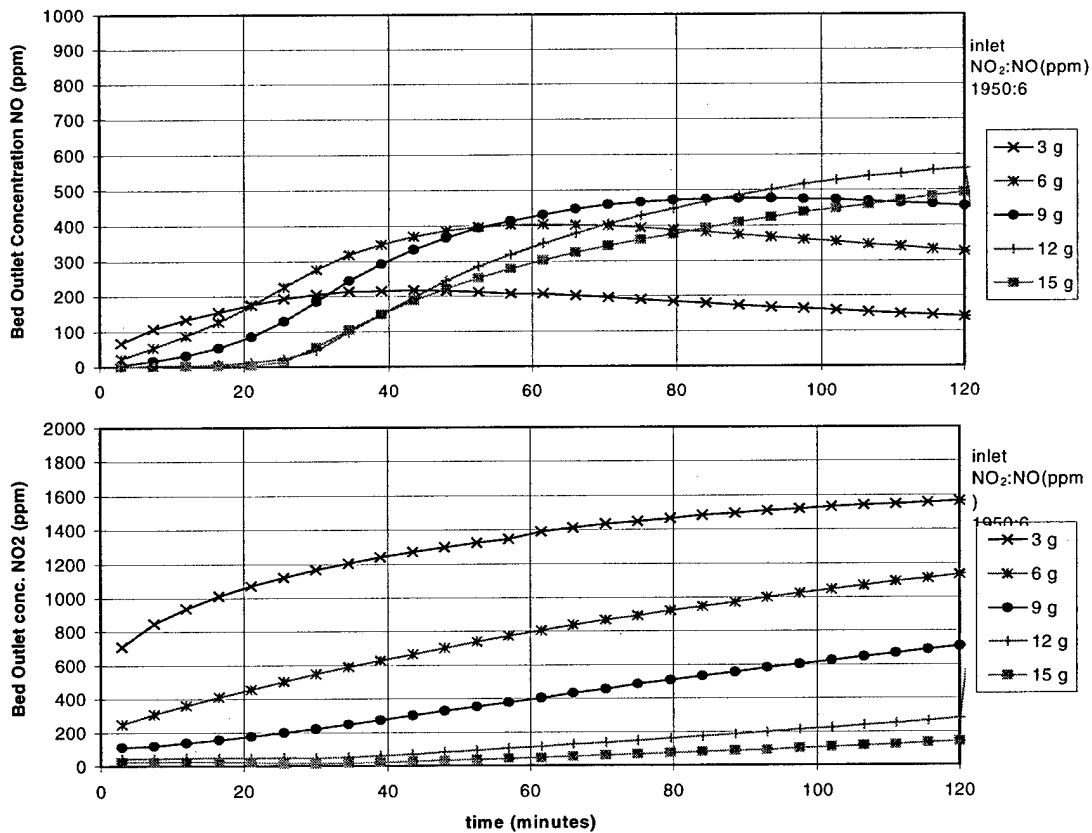


Figure 3-40. Change of NO and NO₂ gas concentrations throughout a bed of KOH-treated γ -alumina.

Molar Ratio of Nitrite to Nitrate

For the treated materials, the reactions that create NO may occur at a slower rate than the process of NO sorption. By observing the ratio of nitrite to nitrate, one may evaluate the rates of NO removal throughout the bed. The molar amounts of nitrite to nitrate throughout the bed for 30, 60, 90, and 120-minute exposure times for the three materials are plotted in Figures 3-35 to 3-37. For the treated materials, one can observe that at the top of the bed nitrate concentrations are greater than nitrite, suggesting that the sorption mechanism at the top of the bed is dominated by reaction with NO₂. However, progressing down the bed, the ratio of nitrite to nitrate increases. As NO is sorbed in these lower layers this suggests that the reaction with NO becomes more active. Also, as the time of NO_x exposure progresses the nitrite to nitrate ratio becomes smaller in the top layers and greater in the bottom layers suggesting that reaction with NO₂ increases the amount of nitrate formed in the top layers. With further exposure the nitrite to nitrate ratio will decrease to where essentially all nitrite becomes constant.

A comparison of the recovery of nitrite and nitrate (moles) to the sorbed NO_x (moles) is presented in Table 3-5. The average molar amounts of nitrite and nitrate are approximately 62, 122, and 100 percent of the sorbed NO_x (NO₂ sorbed - NO_{produced}) for untreated, K₂CO₃-treated, and KOH-treated γ-alumina, respectively. Reproducibility of these data is given in the Experimental section (Tables 2-2 and 2-3-3). A molar balance can be performed throughout the bed given the input NO₂, the accumulated nitrate and nitrite, and the NO produced. In Table 3-5 it can be seen that the molar balance is consistent throughout the bed except for the case of KOH (at 60 min exposure). The data for the latter may be erroneous as ISE analyses are suspect.

Table 3-5. Fractional recovery of surface nitrogen species (NO_2^- and NO_3^-) to sorbed NO_x gas.

column 1-3. Ratio cumulative moles (sum of $\text{NO}_3^- + \text{NO}_2^-$) per sum of (NO_2 sorbed - NO produced).

column 4-6. Ratio cumulative moles (sum of $\text{NO}_3^- + \text{NO}_2^- + \text{NO}$) per sum of (NO_2 sorbed).

layer & exposure time	1 Untreat	2 K_2CO_3	3 KOH	4 Untreat	5 K_2CO_3	6 KOH
1 - 30 min	0.64	1.25	1.37	0.76	1.41	1.32
1 - 60 min	0.72	1.30	0.42	0.82	1.42	0.54
1 - 90 min	0.78	1.37	1.08	0.86	1.40	1.06
1 - 120 min	0.76	1.46	1.35	0.85	1.38	1.25
2 - 30 min	0.58	1.23	1.28	0.72	1.22	1.26
2 - 60 min	0.58	1.30	0.44	0.77	1.26	0.55
2 - 90 min	0.65	1.25	1.10	0.84	1.20	1.07
2 - 120 min	0.75	1.43	1.19	0.84	1.33	1.14
3 - 30 min	0.54	1.17	1.24	0.68	1.16	1.23
3 - 60 min	0.53	1.14	0.53	0.69	1.13	0.58
3 - 90 min	0.64	1.13	1.01	0.76	1.11	1.00
3 - 120 min	0.66	1.26	1.15	0.78	1.21	1.12
4 - 30 min	0.51	1.17	1.23	0.65	1.18	1.23
4 - 60 min	0.51	1.09	0.62	0.66	1.09	0.64
4 - 90 min	0.58	1.10	0.93	0.72	1.09	0.94
4 - 120 min	0.62	1.19	1.03	0.75	1.16	1.03
5 - 30 min	0.48	1.17	1.26	0.62	1.17	1.26
5 - 60 min	0.48	1.13	0.71	0.63	1.12	0.72
5 - 90 min	0.56	1.14	0.97	0.70	1.13	0.98
5 - 120 min	0.58	1.18	1.04	0.71	1.17	1.03
avg.	0.62	1.22	1.00	0.74	1.22	1.00
std. dev.	0.10	0.11	0.30	0.07	0.11	0.26

Trends in ΔNO_2 sorbed/ ΔNO formed: Untreated and Treated Alumina

Trends in the ratio of sorbed NO_2 to NO produced over time for the three types of materials are shown in Figures 3-41, 3-42 and 3-43. Untreated alumina trends to a value near three, which correlates to the overall general reactions expressed for NO_x with metal oxides (Kimm, 1995; Kimm et al., 1995; Knozinger, 1976; Nelli and Rochelle, 1996; Boehm, 1965; Zemlyanov et al., 1998). K_2CO_3 -treated alumina also shows a trend to a value near 3 but the trend is less clear and shows a point of inflection in the ratio that occurs at increased time for increased bed depth. A similar trend in the ratio is seen for KOH -treated alumina. These trends indicate that all of the materials over time show that the amount of NO_2 sorbed becomes proportional to three times the NO produced.

Proposed Reaction Mechanisms of NO_x with Alkali-Treated or Untreated Alumina

Based on the results of this study the delayed production of NO is a function of sorbent surface material. Production of NO from sorption of NO_2 by various metal oxides has been observed (Kimm, 1995; Kimm et al., 1995; Knozinger, 1976; Nelli and Rochelle, 1996; Boehm, 1965; Zemlyanov et al., 1998). A general overall reaction has been proposed for alkaline-earth compounds (Kimm, 1995; Kimm et al., 1995; Nelli and Rochelle, 1996):



where M is an alkaline-earth element, i.e., Ca , Mg .

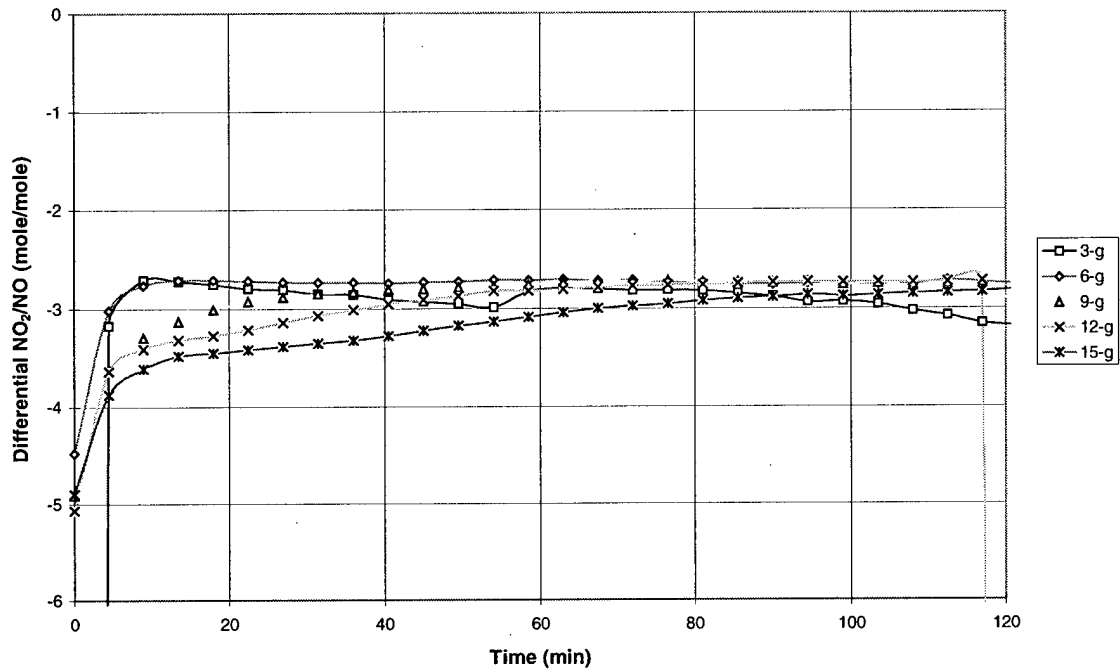


Figure 3-41. Incremental ratio of NO_2 sorbed/ NO formed for successive bed layers of untreated alumina.

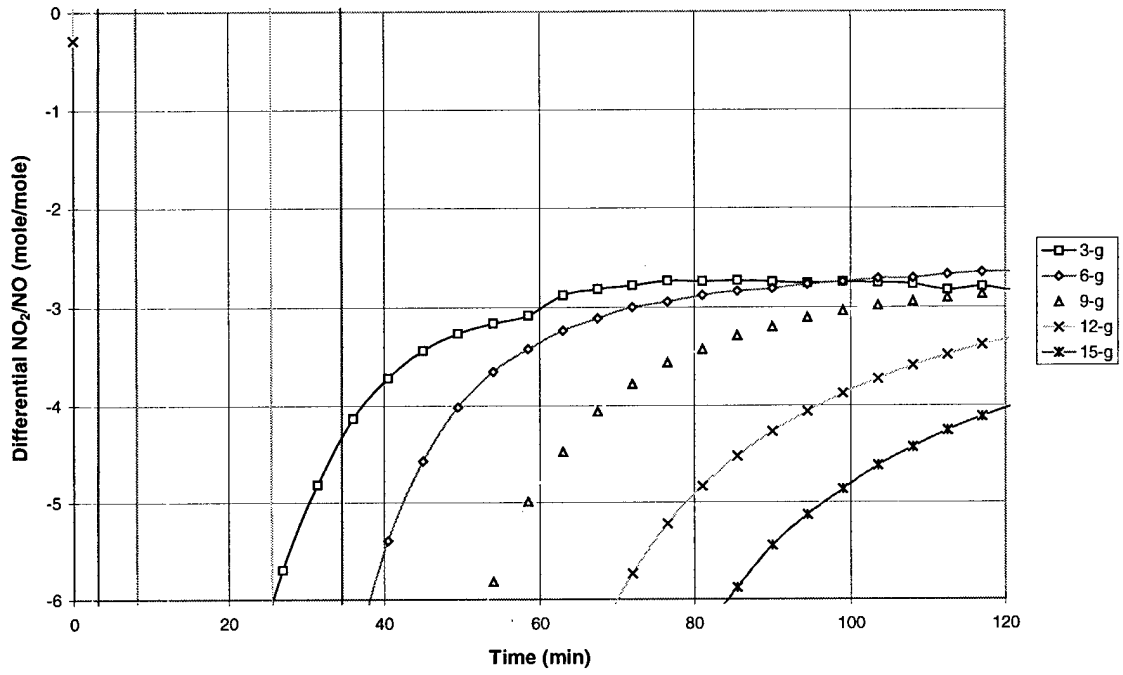


Figure 3-42. Incremental ratio of NO_2 sorbed/ NO formed for successive bed layers of layers of K_2CO_3 -treated alumina.

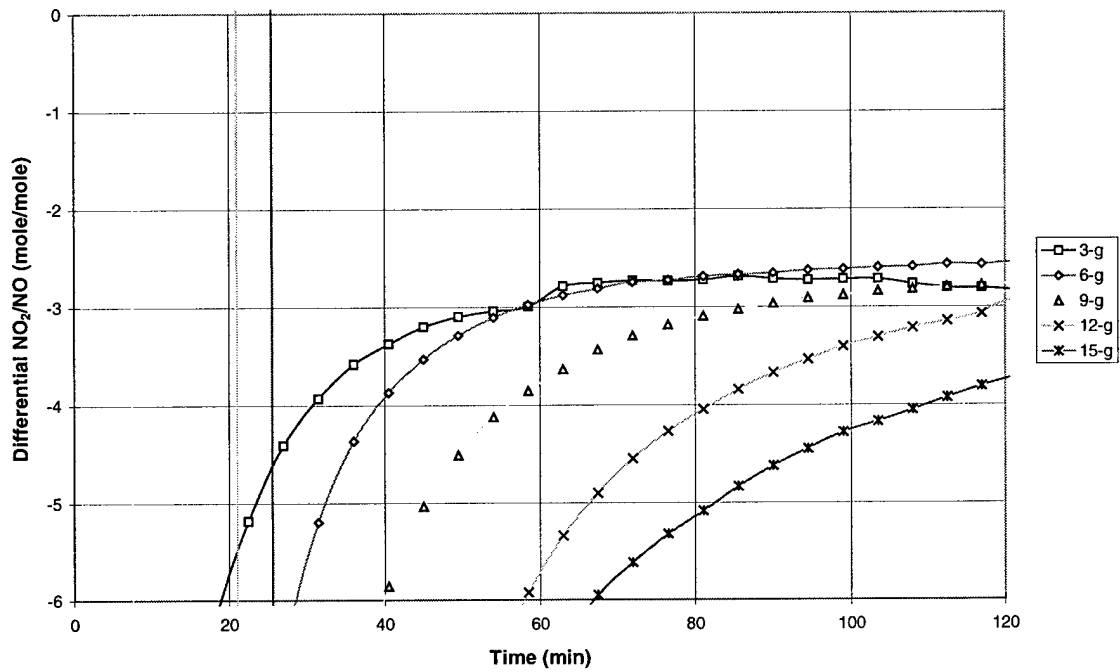


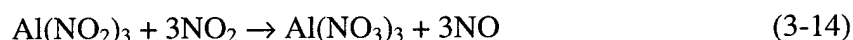
Figure 3-43. Incremental ratio of NO_2 sorbed/ NO formed for successive bed layers of layers of KOH-treated alumina.

Untreated γ -Alumina

In saturation tests the overall stoichiometry (3NO₂ removed per NO formed) has held true for untreated alumina (Lee et al., 1998b). A reaction mechanism is proposed for untreated alumina based on this observation and other properties of exposed γ -alumina. There is no reaction of NO with untreated alumina. The reaction of NO₂ with untreated γ -alumina may proceed as follows because nitrate is a major product. Nitrite achieves a very low steady state concentration and apparently is highly unstable. The equations suggest specific forms of nitrite and nitrate structures which is arbitrary. However, ISE measures and gas-phase data suggests trends of the proposed stoichiometry.



The nitrite formed in (3-12) may react as follows:



Combining reactions (3-12), and (3-13) or (3-14) provides the following overall reaction:

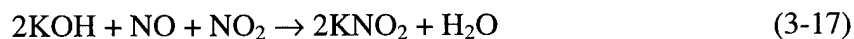
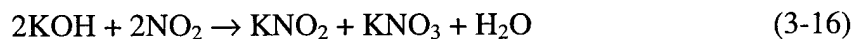


The steady-state nitrite concentration should be small due to the instability of aluminum nitrite. Thus, the proposed reaction (3-13) forms NO₂ and NO, the overall reaction stoichiometry is the same if considering reaction (3-14). The proposed overall reaction predicts a molar ratio NO₂ sorbed to NO formed of 3:1. Aluminum nitrite is not commonly produced like other nitrite salts due to its instability. NO is sorbed by γ -

alumina in minimal amounts in the presence of NO₂ and only for a high concentration ratio of NO:NO₂ feed gas. Sorption of NO by untreated alumina was only observed for an input NO₂:NO ratio of 500:50 and 500:10 with very low efficiencies of less than 5 percent sorption of NO input.

KOH-Treated γ -Alumina

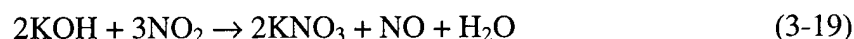
In the case of KOH-coated alumina, experimental data suggest that NO_x interacts strongly with the KOH coating but minimally with the alumina support due to the strong sorption of NO₂ with treated alumina. If this is the case then the following mechanism is possible



These two reactions are proposed because although NO does not react alone, it does react in the presence of NO₂, and in the presence of NO, NO₂ sorption is enhanced. NO production is delayed, which suggests that an intermediate is necessary for production since potassium nitrite is stable. Nitrite formation also is a function of NO₂ and NO concentrations. Reaction with NO₂ is proposed as a source of NO and nitrate in the later stages of reaction.



Based on these reactions the overall reaction can be represented by



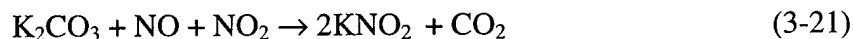
This overall reaction indicates that in the later stages of reaction, when nitrite is at steady state, a 3:1 molar ratio of NO₂ sorbed to NO produced should be observed.

K₂CO₃-Treated γ -Alumina

A similar mechanism is proposed for the reactions of K₂CO₃-coated alumina with NO_x:



and

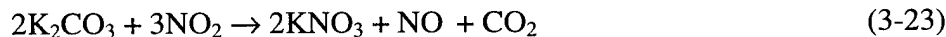


As nitrite builds, reaction (3-20) becomes more important for NO₂ reaction.

Eventually, nitrite will reach steady state.



When nitrite has achieved steady state the overall reaction can be represented by (3-23):



The overall reaction for potassium carbonate coated material predicts a 3:1 molar ratio of NO₂ sorbed to NO formed. In the early stages of exposure reaction (3-21) can remove NO and NO₂ in addition to (3-20) removing NO₂. The question arises as to the extent of these reactions and the reaction rates prior to and at equilibrium. In heterogeneous processes the reaction rate can be affected by the gas-solid transport mechanism. Presumably in this case the sorption is reaction controlled rather than diffusion controlled as discussed previously.

Confirmation of NO Production from Nitrite-NO₂ Interaction

Based on experimental observations, reactions (3-12) through (3-23) were formulated to account for the observed sorption of NO_x by the three sorbents. Two tests

were performed to evaluate the final step in all three mechanisms in which NO_2 reacts with surface nitrite to form NO and surface nitrate. The first test evaluated the differences in NO_2 sorption for untreated and KNO_2 -treated alumina. Similar (mass) samples were exposed to NO_2 gas (741 ppm) at a flow of 0.75 sLpm at 25 °C. The bed outlet concentrations of NO and NO_2 as a function exposure time are shown in Figure 3-44. From this figure it is seen that the amount of NO_2 sorbed is similar for both sorbents. However, the production of NO is much greater for the KNO_2 -treated alumina sample. Also shown in Figure 3-44 are the accumulated amounts of NO_2 sorbed and NO produced by the two sorbents. This test indicated that, indeed, KNO_2 treatment more readily converts NO_2 into NO than does untreated alumina. Another test was performed to measure the concentrations of nitrite and nitrate on KNO_2 -treated alumina at different times of exposure to NO_2 .

Two 5-gram samples of KNO_2 -treated alumina were exposed to a mixture of certified 4750 ppm NO_2 in N_2 gas at a flow of 0.75 sLpm at 25 °C. The NO_x exposure results and data for the measures of nitrite and nitrate on the two samples are shown in Figure 3-45. The results indicate that the nitrite does react to form nitrate and that the nitrite-to-nitrate conversion is proportional to NO_2 sorption.

Fourier Transform Infrared (FTIR) Spectroscopy Confirmation of ISE Measurements

Analysis of samples for surface nitrite and nitrate species was carried out using ion-specific electrode (ISE) methods. The ISE methods require that the sorbent samples be in the form of aqueous extracts and adjusted for pH. The ISE procedure is subject

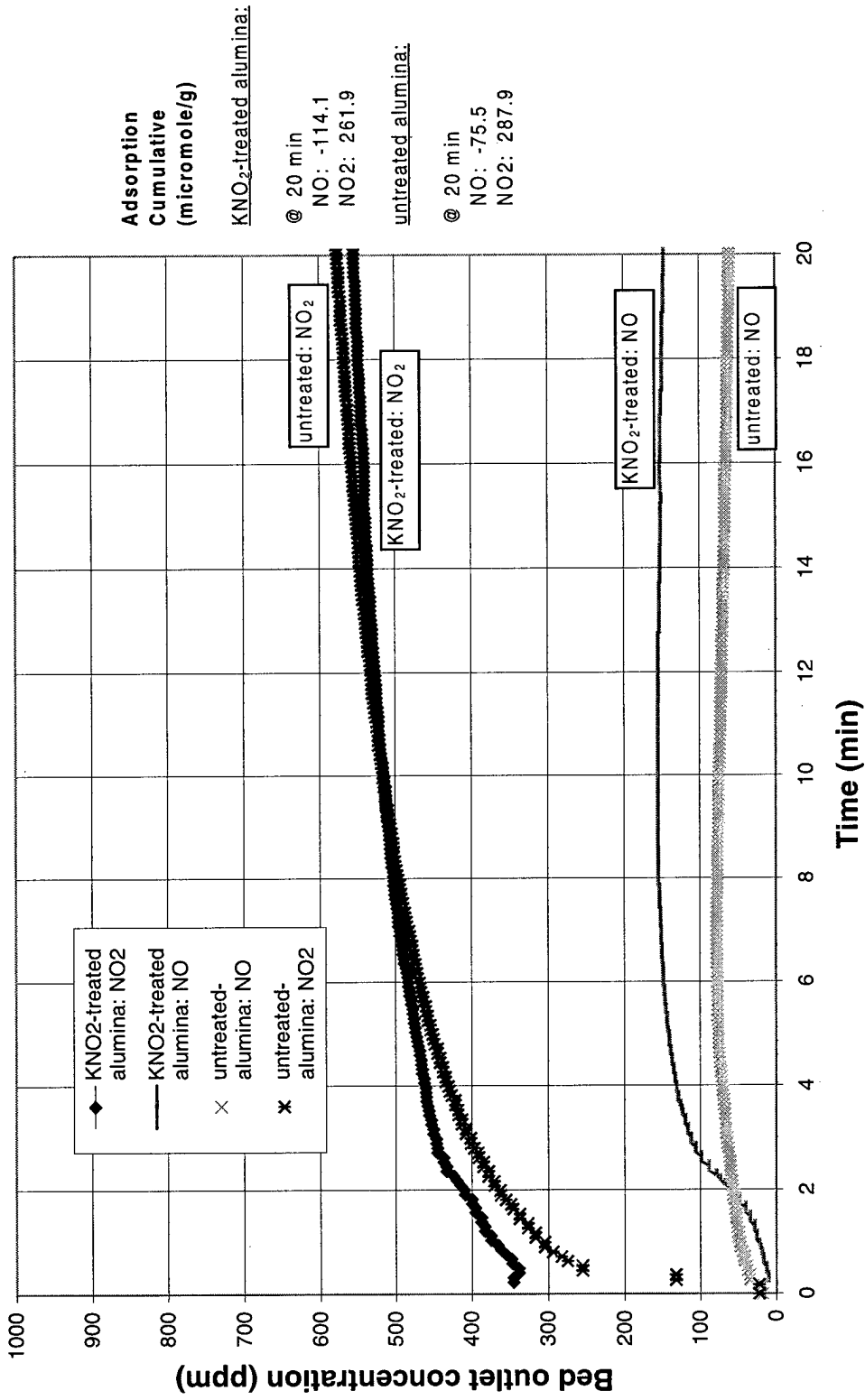


Figure 3-44. NO₂ sorption activity of KNO₂-treated and untreated alumina.

to error due to the possible effects resulting from solution analysis of sorbed ions from a dry or solid material. Therefore, another analytical method that does not require dissolution of the sorbent prior to analysis for surface species was chosen to confirm that the ISE measurements were not affected by the preparation and measurement procedures.

FTIR is a spectroscopic technique that can measure the absorbance of reflected infrared light that is characteristic of the material from which it is reflected. Reference materials included ACS reagent grade KNO_3 , KNO_2 , and K_2CO_3 . Reference literature was used to determine the regions of frequency or wave number that have been established as being characteristic of specific function groups or indicative of a given compound (Nyquist and Kagel, 1971). Sorbent samples before and after treatment and NO_x exposure were analyzed against specific references to determine the changes due to treatment and NO_x exposure. Separate portions of two samples of K_2CO_3 -treated alumina tested in the gas profile study and tested by ISE were analyzed by FTIR for comparison.

First, the reference materials KNO_2 , KNO_3 , and K_2CO_3 were analyzed. FTIR spectra scans of these materials are shown in Figures 3-46, 3-47 and 3-48, respectively. Pure samples of KNO_3 and KNO_2 show low absorbancies for peaks at 1320 cm^{-1} [0.010 absorbance units (au)] and 1210 cm^{-1} [0.0794 au]. These spectra indicate the low sensitivity of the FTIR method for these compounds. Note that absorption peaks for ¹,

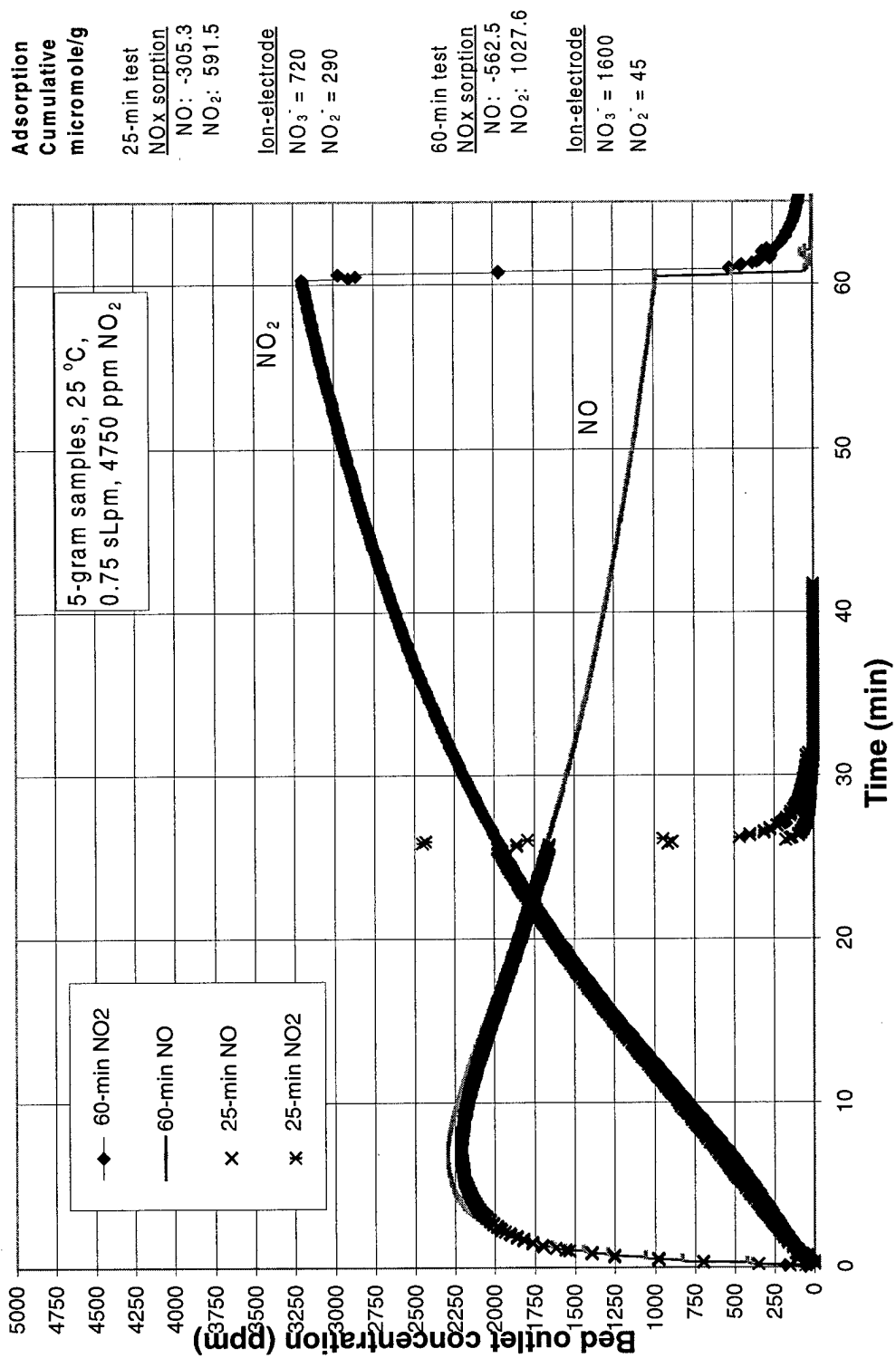


Figure 3-45. Sorption of NO₂ to KNO₂-treated alumina with subsequent ISE analysis.

gaseous CO₂ are typically present in all spectra as background. The gas purge system attached to the FTIR analysis chamber was not able to remove all of the air within the chamber. However absorptions of the common gases H₂O vapor and CO₂ do not occur in the regions of interest. Specific peaks for KNO₃ and KNO₂ are found at 810 and 790 cm⁻¹ respectively. The K₂CO₃ spectrum has a broad absorbance region near 1330 cm⁻¹ and a more specific peak at 890 cm⁻¹.

The spectrum for untreated alumina is shown in Figure 3-49. No specific peaks are identifiable. This spectrum is also used for comparison to K₂CO₃-treated alumina, see Figure 3-50. The spectrum of K₂CO₃-treated alumina indicates a shift in the broad peak for pure K₂CO₃ at 1330 cm⁻¹ to a maximum peak position of 1400 cm⁻¹. This shift suggests that the coating treatment of K₂CO₃ results in a different binding energy than bulk K₂CO₃. Also observable are specific peaks at 1000 cm⁻¹ and 810 cm⁻¹. The reference literature indicates a strong broad absorption at 1320–1530 cm⁻¹, and weak absorptions near 1040-1100, 800-890, and 670-745 cm⁻¹ occur.

Two samples of K₂CO₃-treated alumina that were exposed to NO_x in the gas profile study were analyzed by FTIR (Figures 3-51 and 3-52). The first sample was the same as that from the top layer in the gas profile study (see Figure 3-36, 120 minute exposure, layer 1). The FTIR spectrum of the sample shows increased absorbance in regions near 1350 cm⁻¹ and 1220 cm⁻¹. Also, a peak near 750 cm⁻¹ is observed. Reference literature indicates nitrite broad strong absorption near 1170-1320 cm⁻¹ and a weak bond near 820-850 cm⁻¹. Also published literature indicates that nitrate has a strong, broad absorption near 1280-1520 cm⁻¹ and weak absorptions near 1020-1060, 800-850, and 715-770 cm⁻¹. Measurements of nitrate and nitrite ions on this sample by

ISE indicate that nitrate and nitrite concentrations were 0.75 mmol/g and 0.22 mmol/g, respectively. The second NO_x-exposed K₂CO₃-treated alumina sample analyzed by FTIR was that from the fourth layer in the gas profile study. The FTIR spectrum of the sample showed

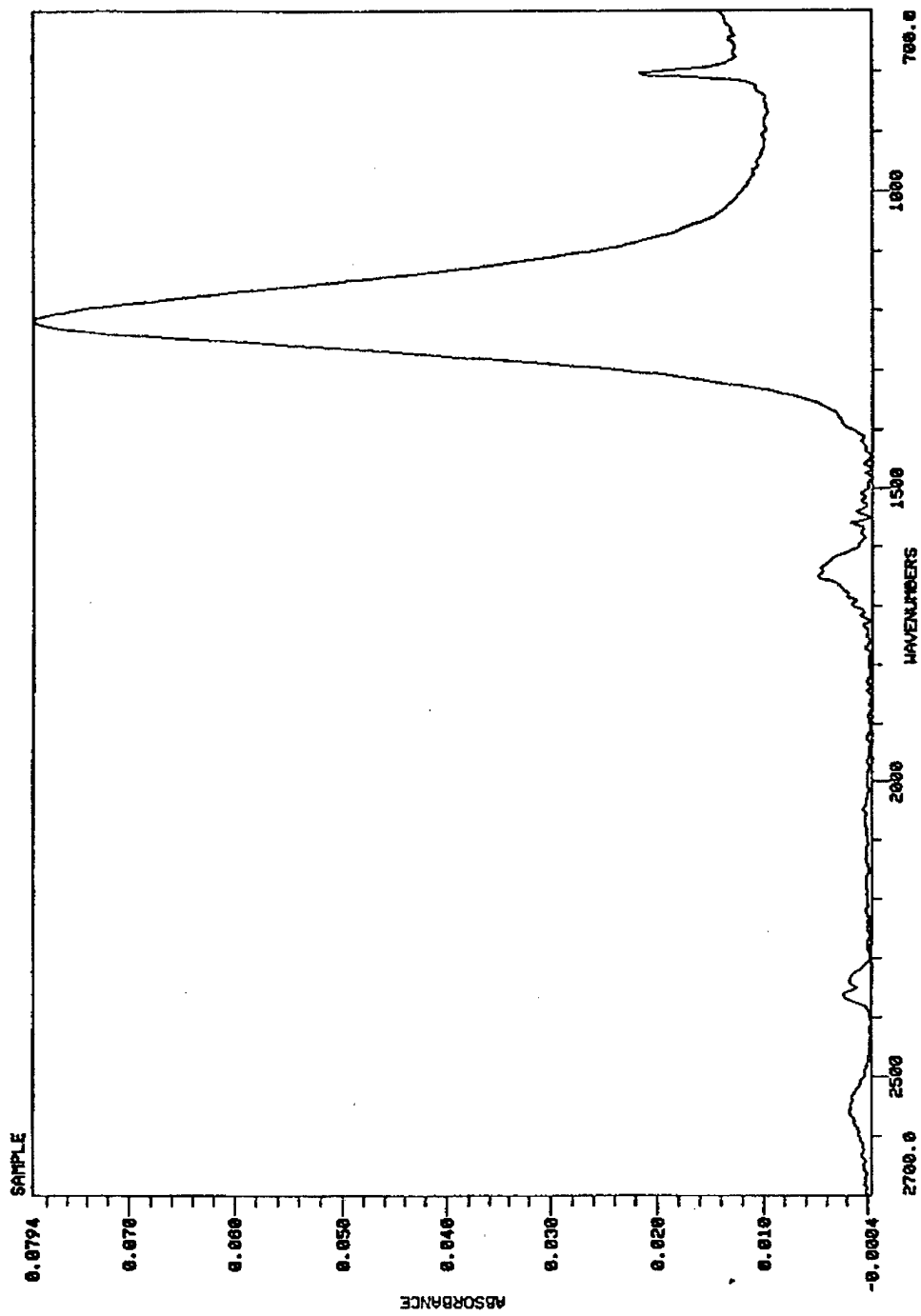


Figure 3-46. FTIR spectrum of reagent-grade KNO₃.

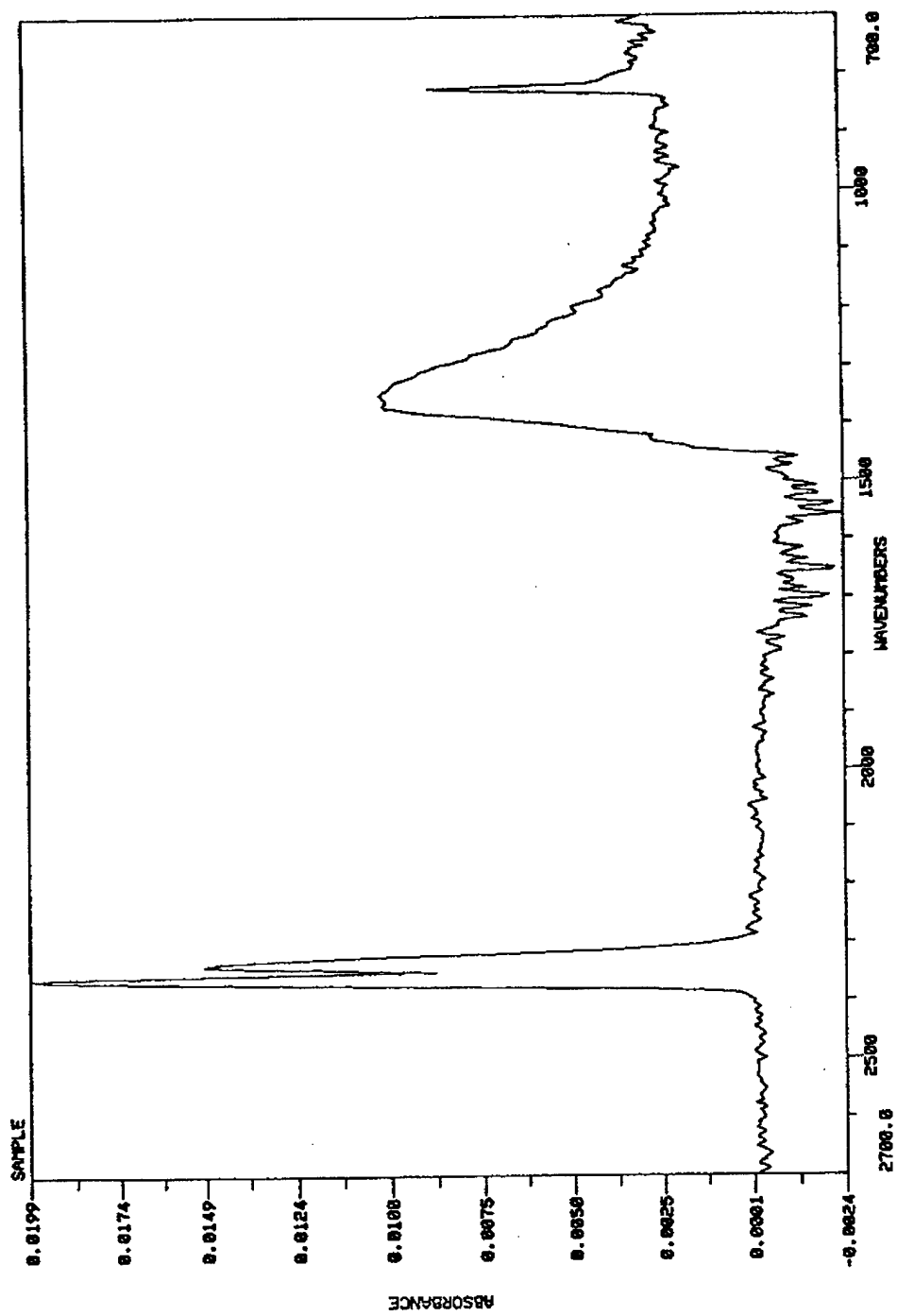


Figure 3-47. FTIR spectrum of reagent-grade KNO₃.

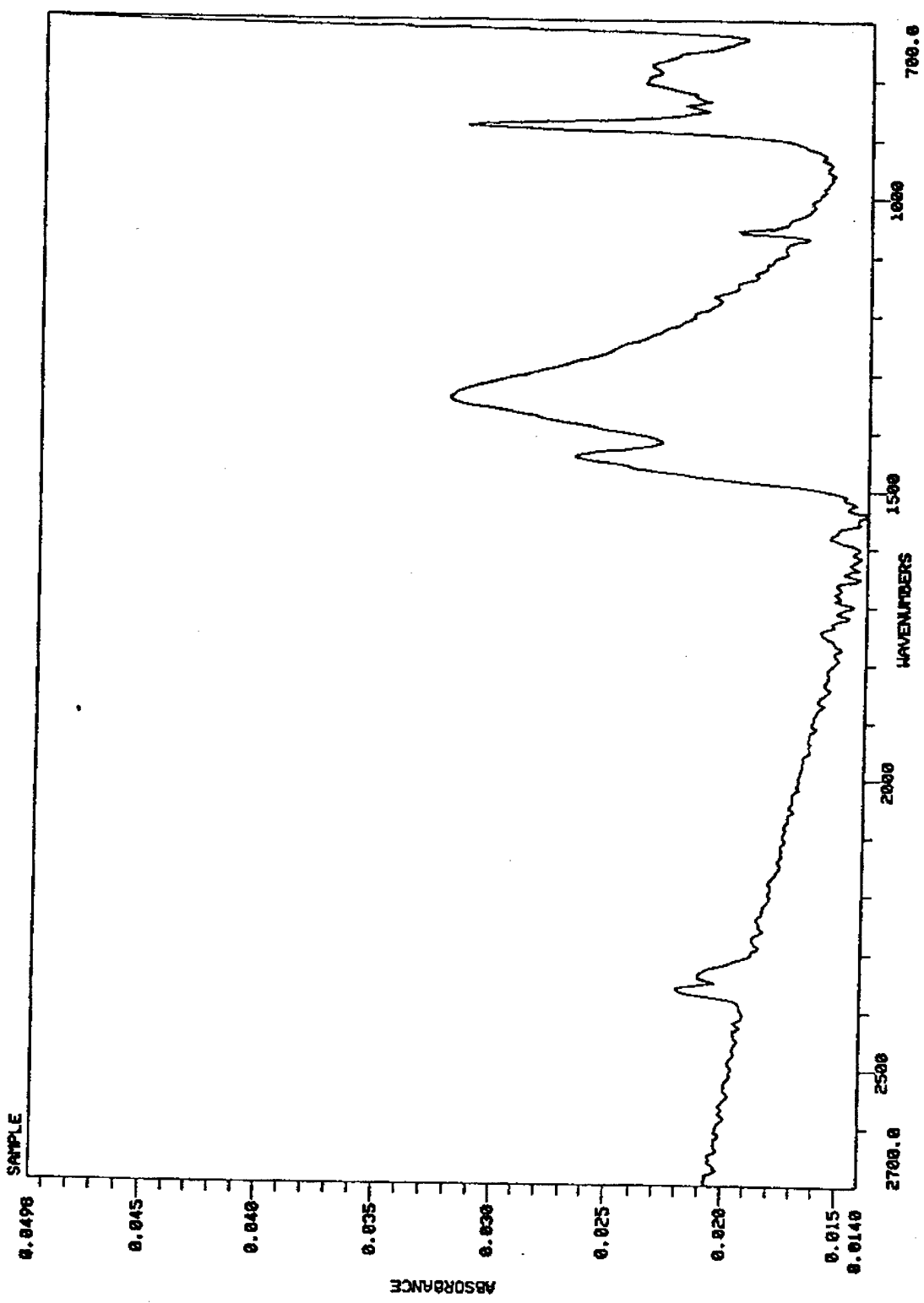


Figure 3-48. FTIR spectrum of reagent-grade K_2CO_3 .

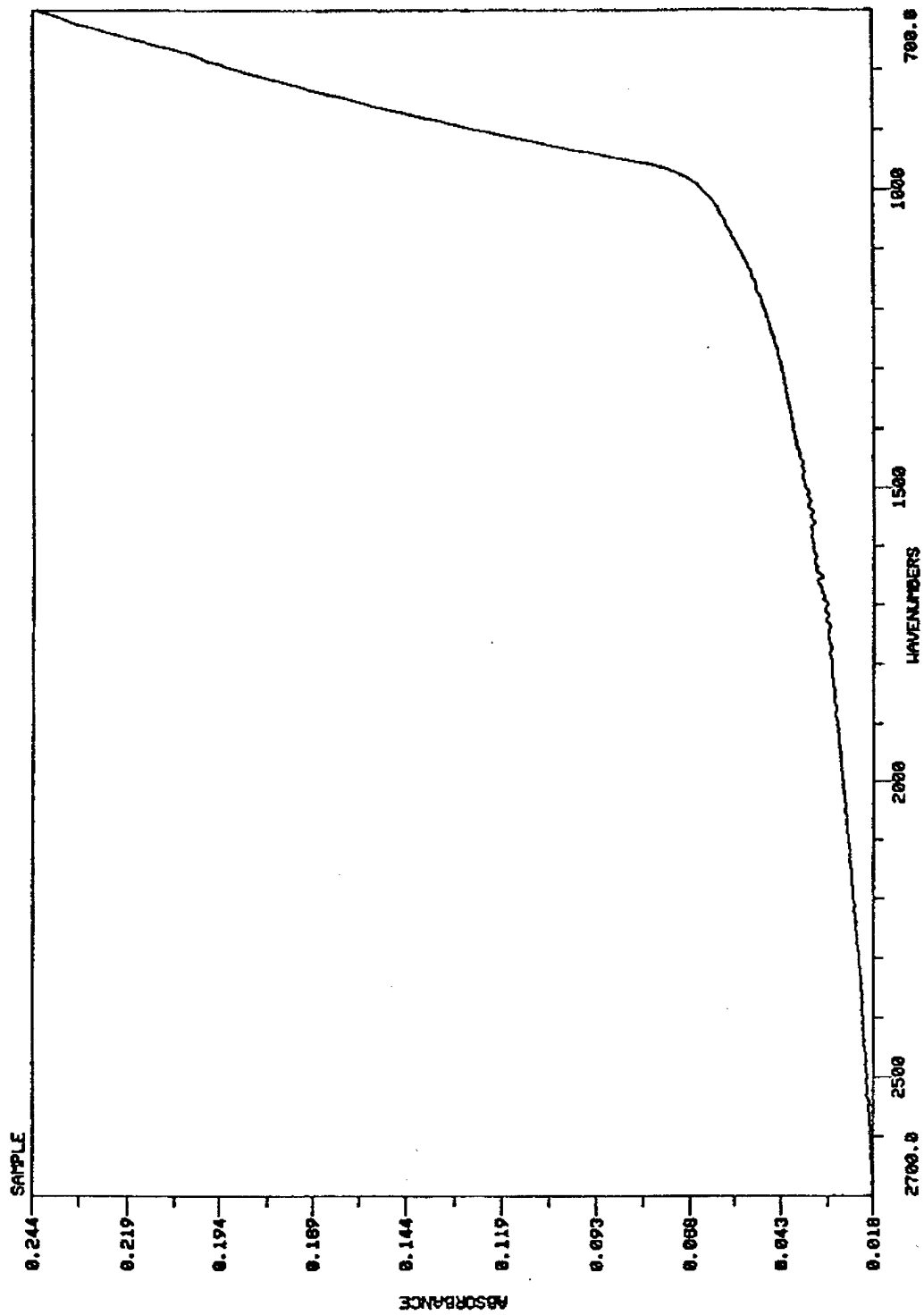


Figure 3-49. FTIR spectrum of untreated alumina.

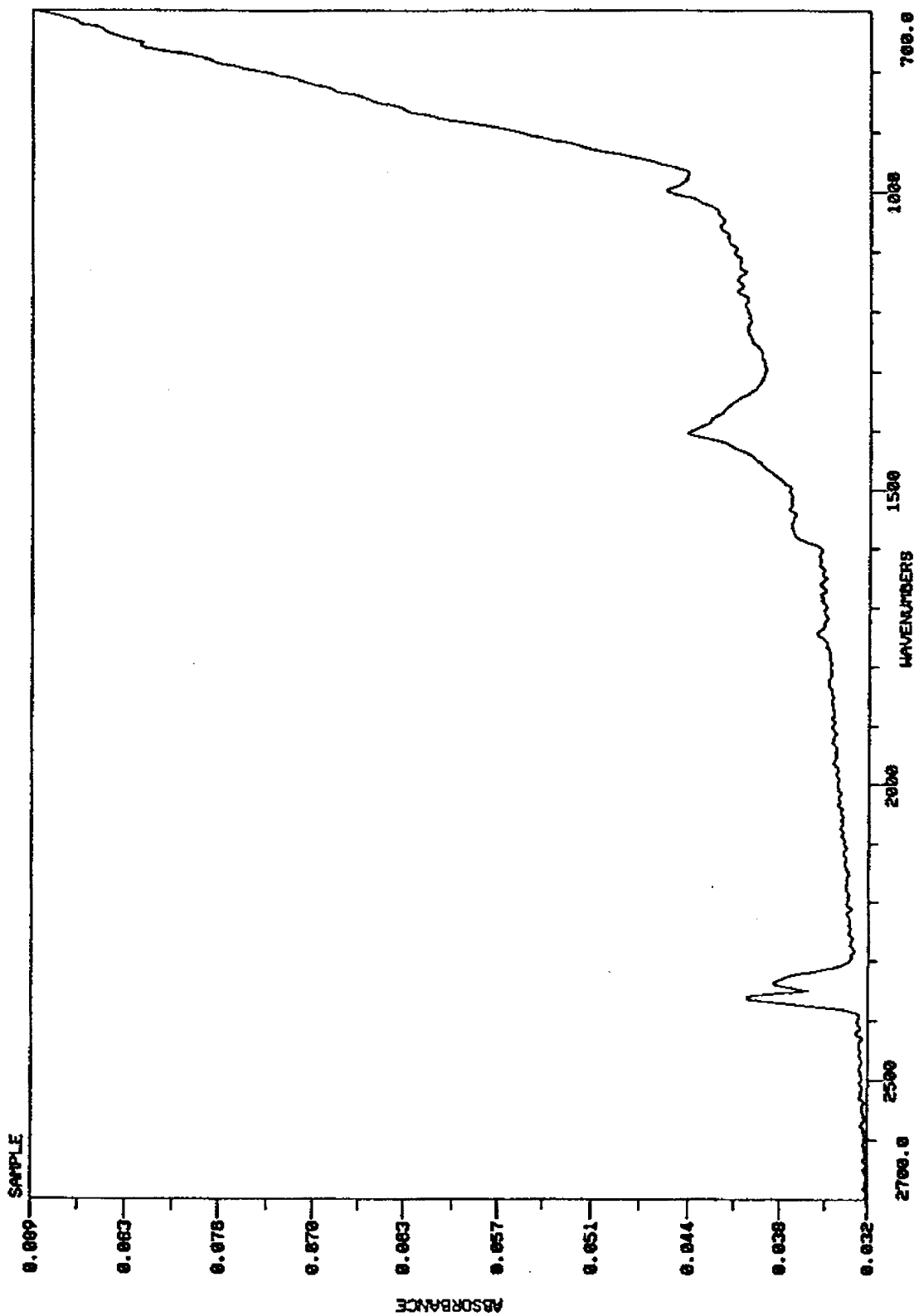


Figure 3-50. FTIR spectrum of K_2CO_3 -treated alumina.

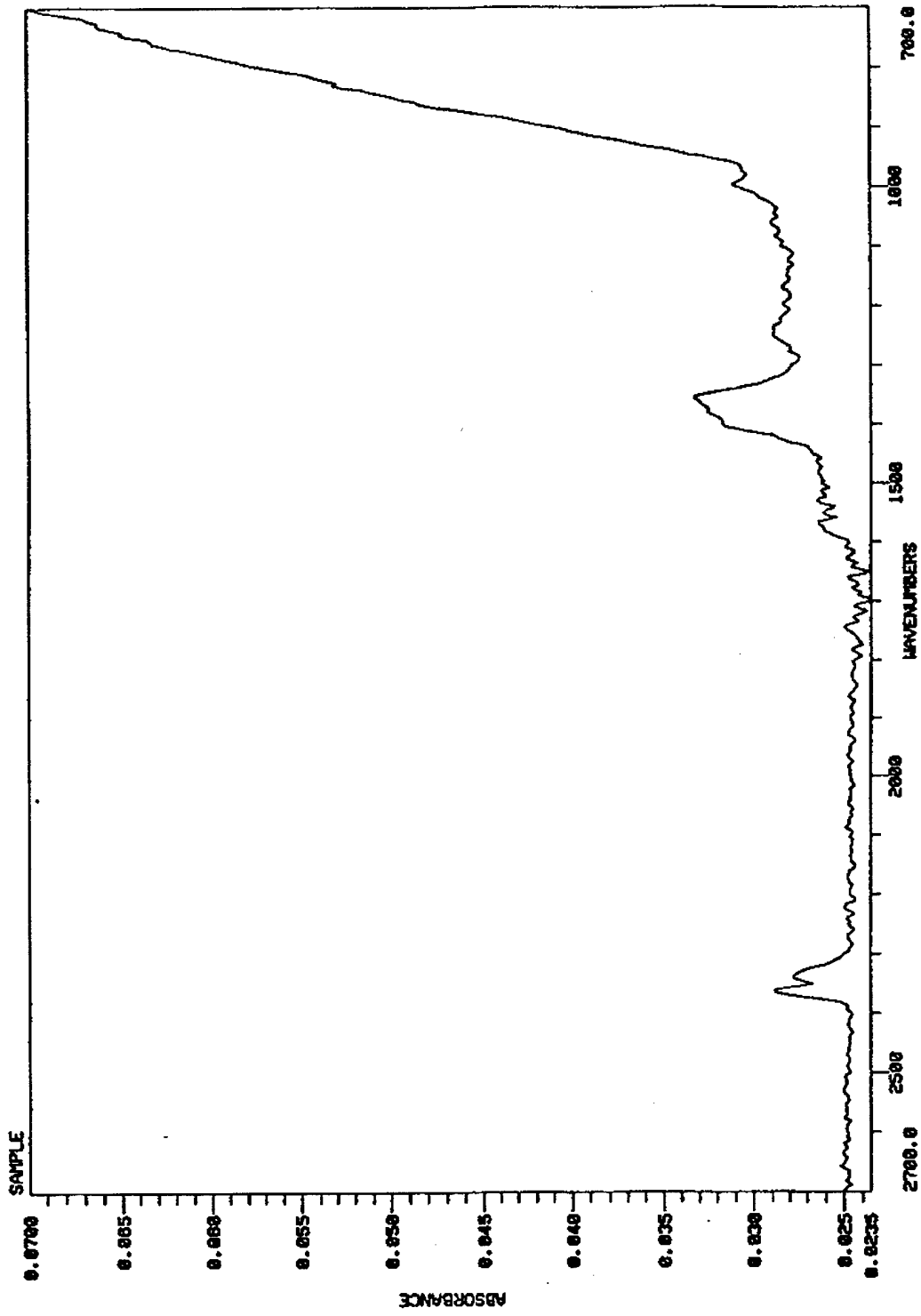


Figure 3-51. FTIR spectrum of K_2CO_3 -treated alumina after exposure to NO_x (1st layer)

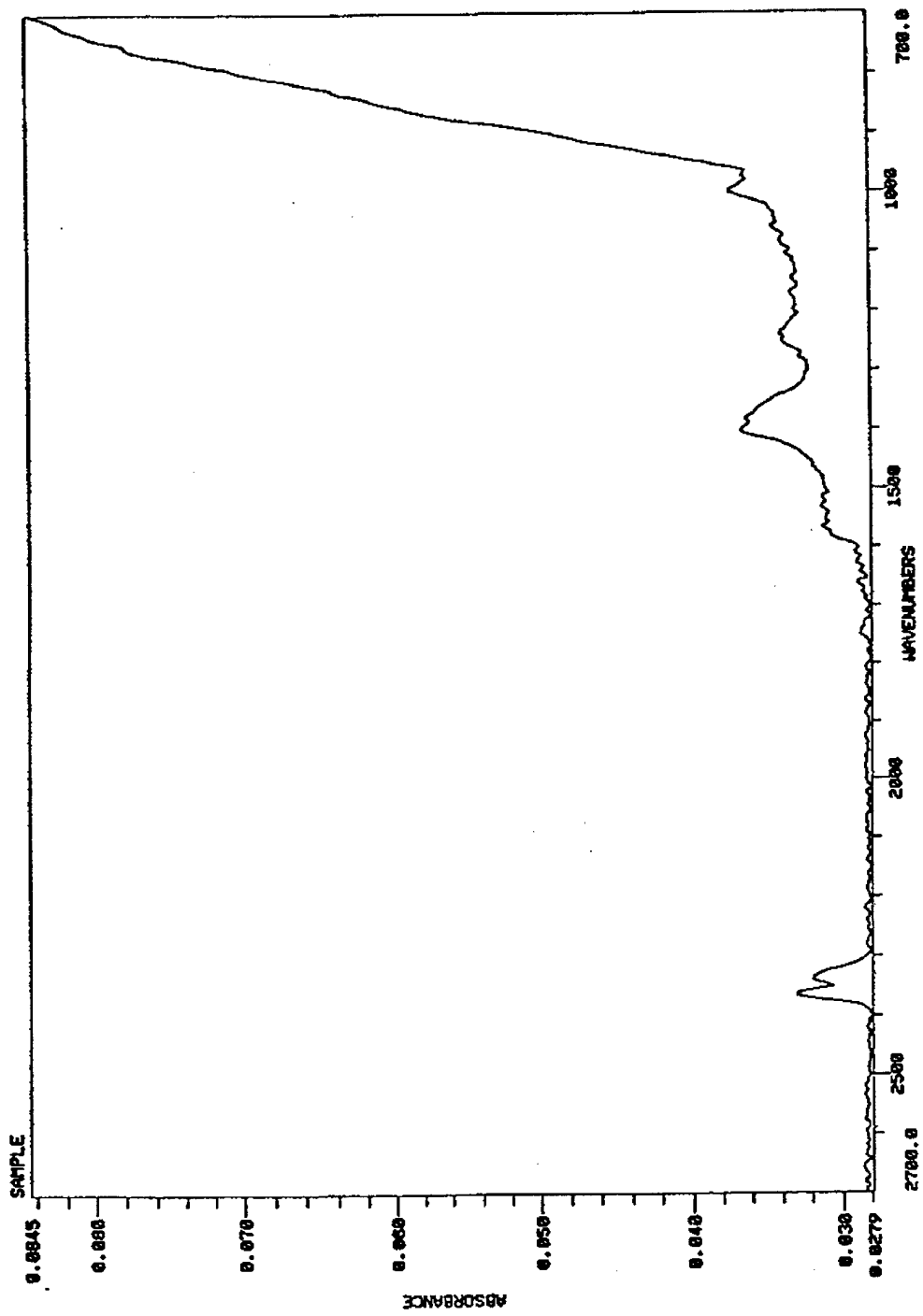


Figure 3-52. FTIR spectrum of K_2CO_3 -treated alumina after exposure to NO_x (4th layer)

decreased absorbance in the region near 1350 cm^{-1} relative to the first sample and that the peak near 1220 cm^{-1} has a similar absorbance. Also, the peak at 750 cm^{-1} on the first sample was not observed on this sample. The ISE measurements for this sample showed nitrate and nitrite accumulations to be 0.01 and 0.23 mmol/g, respectively.

The FTIR results qualitatively indicate that the measurements of nitrate and nitrite by ISE analyses correspond with the FTIR data. However, quantitation of FTIR data is not reliable due to low sensitivity.

Thermal Decomposition Studies

A method to possibly examine surface materials and changes in their properties can be performed by thermally decomposing samples. Specific instruments such as differential thermal analyzers (DTA) based on this principle have been designed solely for this purpose and can be obtained commercially. However, the fixed-bed reactor system can also be used to simulate this method. Samples can be placed in the reactor tubes and gradually heated in a flow of inert gas to carry the gaseous decomposition products to the NO_x analyzer. The decomposition gases can be analyzed for emissions of NO and NO₂. This information may allow for evaluation of changes in properties of sorbed materials during and after NO_x exposure. The decomposition temperature at which NO_x-exposed sorbents release sorbed NO_x should provide knowledge of the limiting temperature at which these sorbent can effectively perform as NO_x sorbents. Reference materials, such as nitrite and nitrate salts can be decomposed and their decomposition properties compared with NO_x-exposed sorbents. Samples of sorbents that have been analyzed by

ISE for nitrite and nitrate can be thermally decomposed to allow for comparative analyses of the sample.

A crucial point should be made prior to discussion of the results of these decomposition tests. After completing the series of decomposition tests indicated that stainless steel reacts with NO_2 at temperatures above 550°C . Sigsby et al. (1973) observed this phenomenon and this property is used in the chemiluminescent detection of NO_2 . Thus, it is expected that decomposition data obtained at temperatures above 550°C maybe affected by this phenomenon and could be invalid. However, in these decomposition tests it is observed that NO_2 is emitted at temperatures above 550°C . The reason for this is probably due to several factors including the physical design of the fixed-bed reactor and flow of gas within the reactor.

During the decomposition of a sample in the reactor bed, the gas decomposes from the sample in the sorbent tube and flows downward into a region of the stainless steel tube where the temperature decreases substantially over a space of several inches. Depending on the flowrate of the N_2 carrier gas, the decomposition products may not have sufficient exposure time at high temperatures to react with the stainless steel walls and convert NO_2 into NO . A test was carried out to observe conversion of NO_2 into NO in the fixed-bed reactor system. It was found that by flowing NO_2 -laden gas through an empty reactor tube, the conversion of NO_2 to NO can occur more extensively as the gas experiences higher temperatures in regions above the sorbent bed and longer residence times in the reactor bed region.

Decomposition of NO₂-Exposed Sorbents: Varied Exposure Time

Three types of materials: untreated, K₂CO₃-treated, and KOH-treated γ -alumina were exposed to NO₂ (500 ppm) for varied lengths of time to observe changes in thermal decomposition products from the sorbents. Three-gram samples were placed in the fixed-bed reactor and simultaneously exposed to NO₂ at a molar flow of 0.098 mol NO₂/min for 10, 15 (only untreated alumina), 30 and 120 minutes. For the shorter time exposure data were not collected during the sorption process as the amount of gas used during the initial exposure was less than that required for the NO_x analyzer. However, the sorption for these short-time exposures can be followed by observing the sorption process at the beginning of exposure for the longer time exposures, during which data were collected. After NO₂ exposure the samples were either stored or immediately decomposed *in situ* by flowing N₂ carrier gas through the bed and ramping the bed temperature. The sorption processes for 120-minute exposure of the three sorbents are shown in Figure 3-53. Corresponding thermal decomposition profiles of samples for the three materials at 10, 30 and 120 minutes NO_x-exposure are presented in Figures 3-54 to 3-62. The decomposition profiles provide the temperature of the bed and corresponding NO₂ and NO concentration over time. It was necessary to control and keep consistent the rate of temperature increase for a comparison of data. All subsequent decomposition tests used a constant temperature ramp of 10 °C/min and N₂ flowrate of 1 sLpm.

As the quantity of decomposition products increased with NO₂ exposure time it was necessary to either decrease the sample size, increase the N₂ flowrate, or decrease the temperature ramping rate. Thus it was decided to well-mix the sample and decompose only a portion of the sample at an increased flowrate of N₂. An added benefit is that

increasing the flow rate improves the resolution of emission peaks. The 120-minute exposure samples were decomposed using 1-gram portions of the total 3-gram sample. Also, the flowrate was increased from 1 to 3 Lpm. The tests had to be predicted for the emission rates of decomposed gas in order to either adjust the sample mass for decomposition or the flowrate of N_2 . Thus, several sample had to be repeatedly decomposed in order to obtain a decomposition profile where the gas emitted remained on the NO_x analyzer measuring range.

Decomposition of the NO_x -exposed untreated alumina samples show three significant regions at 150, 325, and 550 °C for NO emissions and one peak for NO_2 emissions at 500 °C. With greater time of exposure to NO_x the NO_2 peak increases relative to the NO peaks.

Decomposition of K_2CO_3 -treated alumina showed a distinctive peak pattern at 600 to 650 °C that remains consistent with irregardless of NO_x exposure. The peak is forward tailed and may be composed of several unresolved peaks.

Decomposition of the 10 and 30 minute NO_2 -exposed sample of KOH-treated alumina shows a more symmetrical peak pattern than NO_x -exposed K_2CO_3 -treated alumina. The temperature of decomposition is about 600 °C. The 120 minute NO_x exposure with an increased flow provides an emission peak pattern composed of several unresolved peaks major peak.

Decomposition of Pure Compounds Treated onto γ -Alumina

ACS reagent-grade KNO_3 , KNO_2 , and $Al(NO_3)_3 \cdot 9H_2O$ were dissolved in individual portions of N_2 -flushed DI water to provide solutions for coating alumina pellets. The alumina in the treating solution was dried at 150 °C for 24 hours. During drying a slow

flow of N₂ gas was maintained over the solution to prevent oxidation or contamination. These dried synthetic materials supported on alumina were then decomposed to provide the emissions vs. temperature data seen in Figures 3-63 to 3-65. The similarities between KNO₃-treated alumina decomposition pattern (Figure 3-63) and that of NO₂-exposed untreated alumina (Figure 3-56) are noteworthy. A symmetrical NO₂ peak occurs near 500 °C followed by a smaller NO peak at higher temperature (~ 600 °C). The KNO₂-treated alumina shows two NO peaks at 300 and 600 °C. The NO peak at 300 °C is accompanied by a broad NO₂ peak of much lower magnitude. Also, the low-temperature NO peak (300 °C) and accompanying NO₂ peak are similar to the peaks observed for untreated alumina exposed to very small quantities of NO₂ (see Figure 3-54, 10 min. NO_x-exposed untreated alumina). Decomposition of aluminum nitrate-treated alumina shows a peak near 300 °C but its decomposition pattern does not appear to be similar to NO_x-exposed untreated alumina. The only similarity appears to be the NO peak at 300 °C.

Decomposition of Pure Salts

Pure KNO₃ and KNO₂ salts were decomposed in the fixed-bed reactor. KNO₂ did not decompose at temperatures less than 500 °C. Two peaks appeared near 625 and 700 °C. Pure KNO₃ decomposed producing NO₂ at 275 °C followed by a NO peak at 350 °C. The major fraction of these nitrogen salts did not decompose below 600 °C. Decomposition of pure nitrite and nitrate salts resulted in a melt that solidified at lower temperatures. The material that condensed throughout the system was very reactive with NO_x. Thus, the results are not reliable. No further tests of pure salts were carried out. The effect of coating the pure salts onto high-surface area γ-alumina appears to reduce the

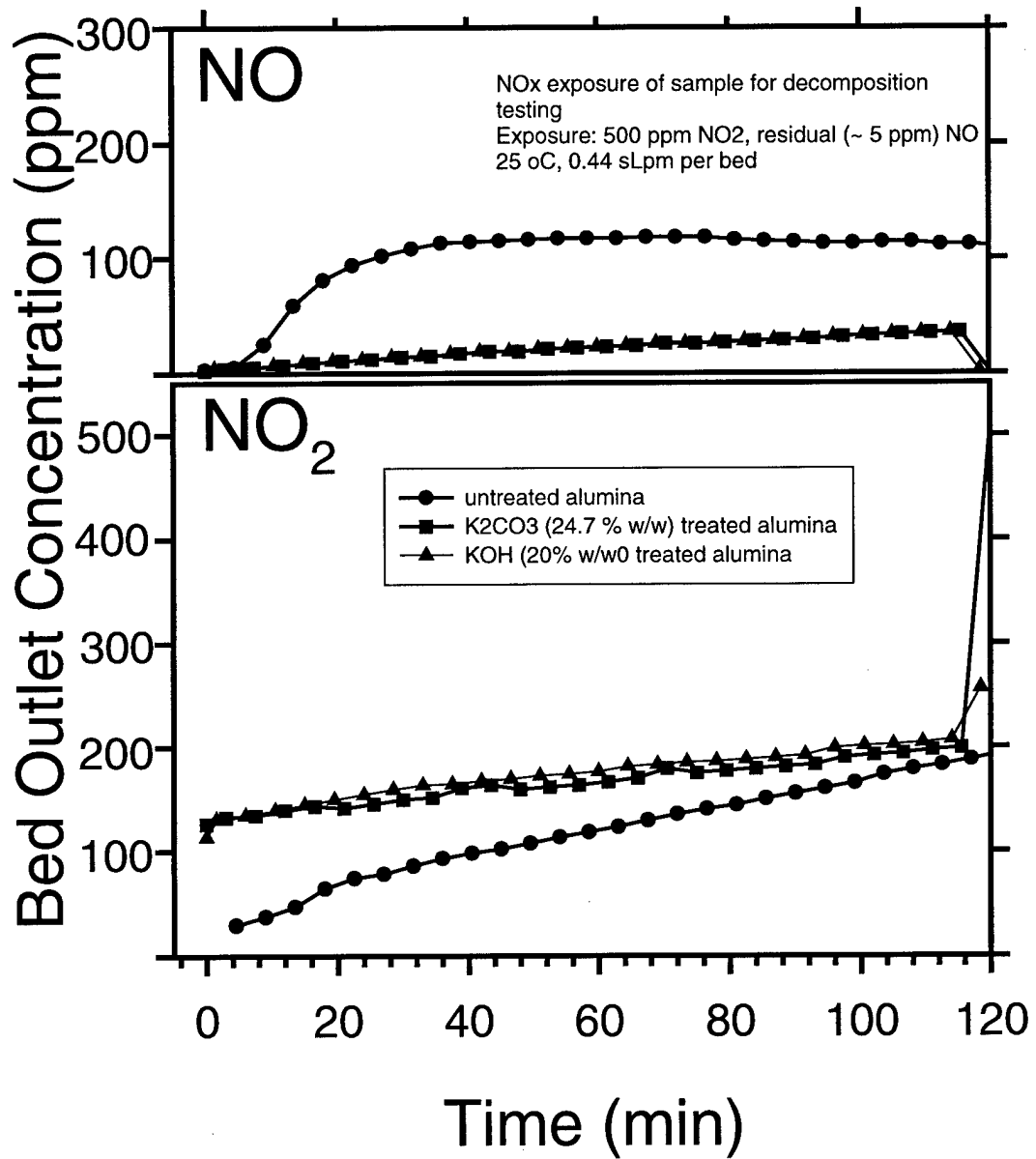


Figure 3-53. Representative NO_x-exposure test for samples decomposed after varied NO_x-exposure times.

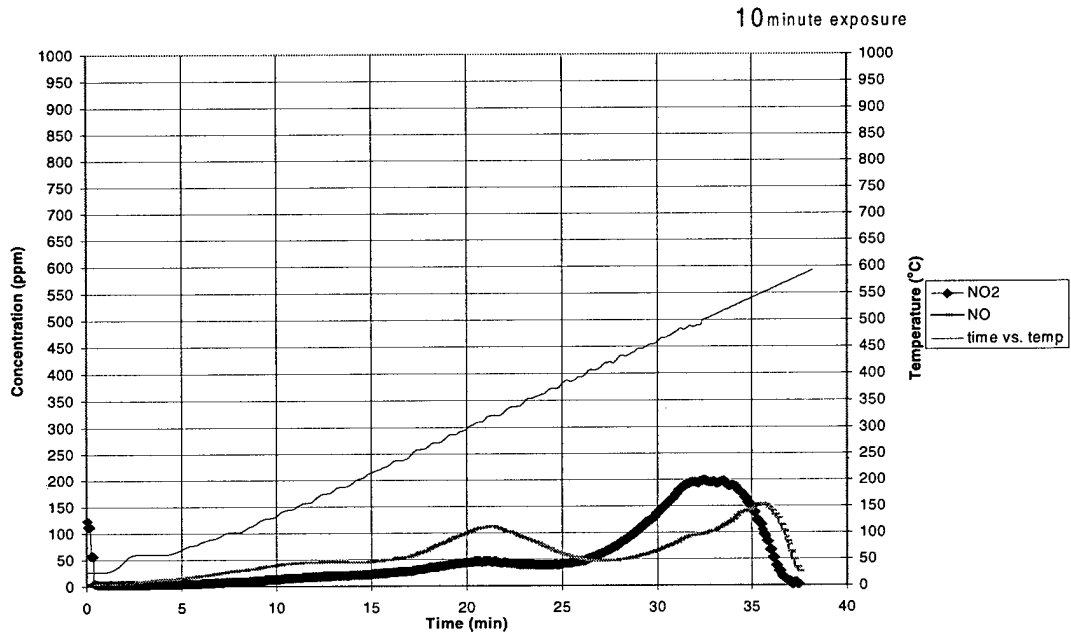


Figure 3-54. Thermal decomposition of untreated alumina after 10-min exposure to NOx.

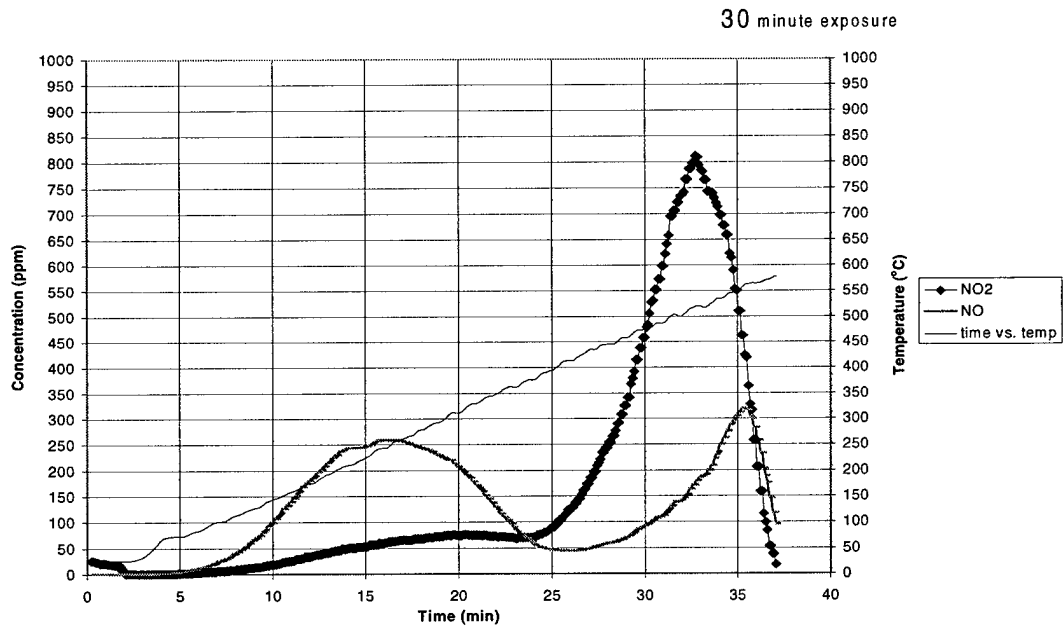


Figure 3-55. Thermal decomposition of untreated alumina after 30-min exposure to NOx.

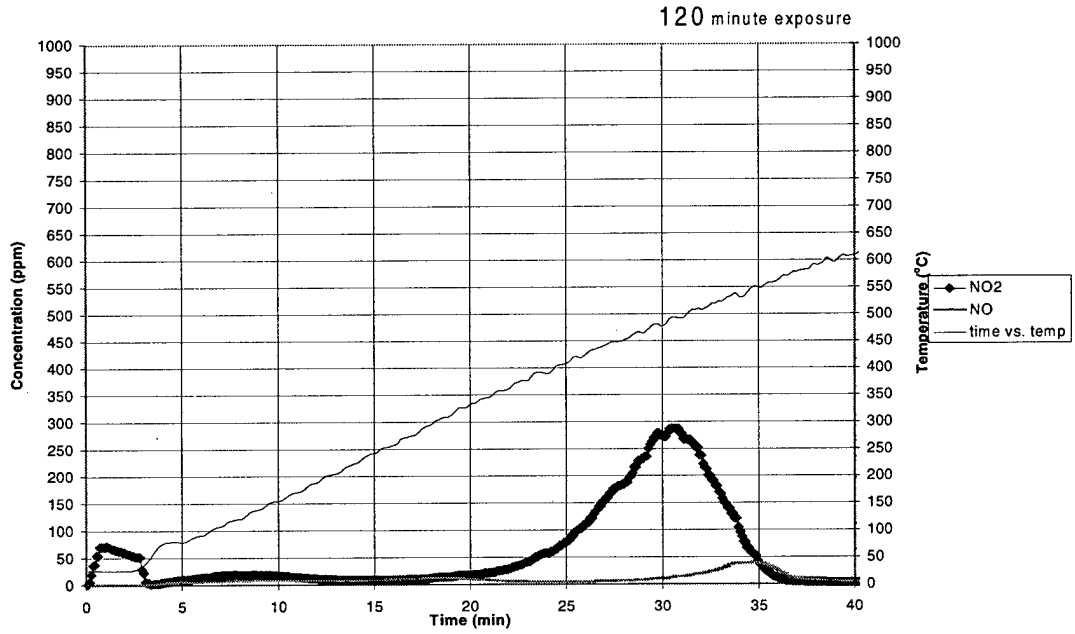


Figure 3-56. Thermal decomposition of untreated alumina after 120-min exposure to NOx.

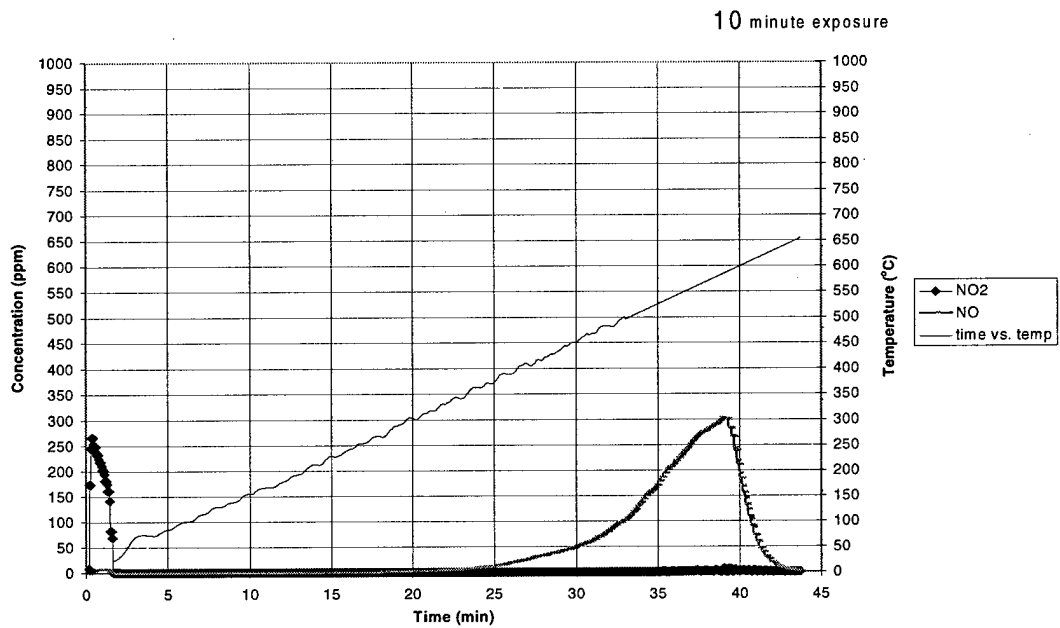


Figure 3-57. Thermal decomposition of K₂CO₃-treated alumina after 10-min exposure to NOx.

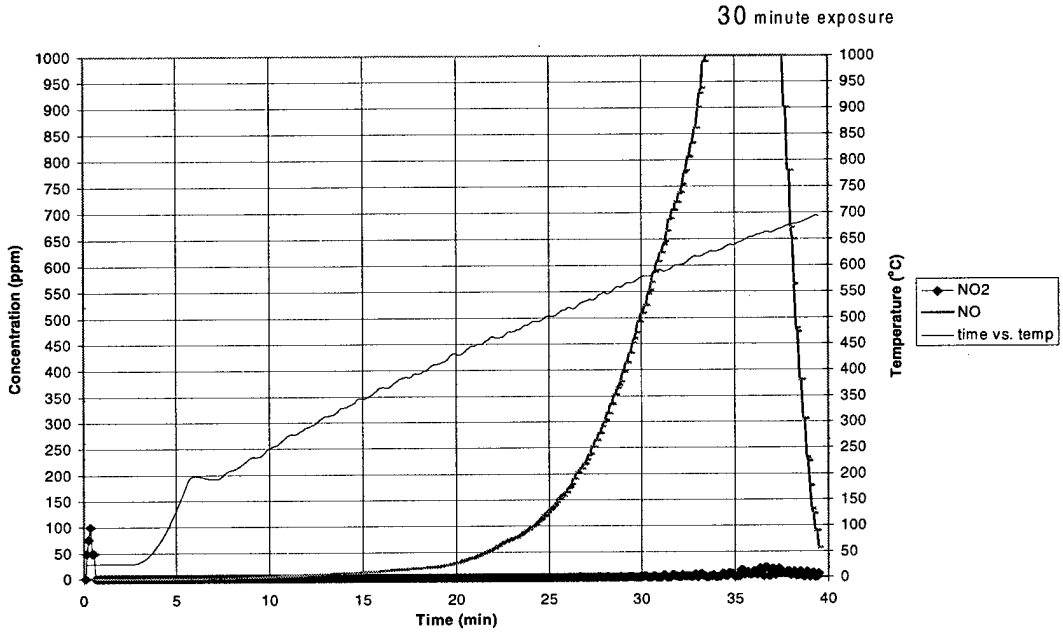


Figure 3-58. Thermal decomposition of K_2CO_3 -treated alumina after 30-min exposure to NO_x .

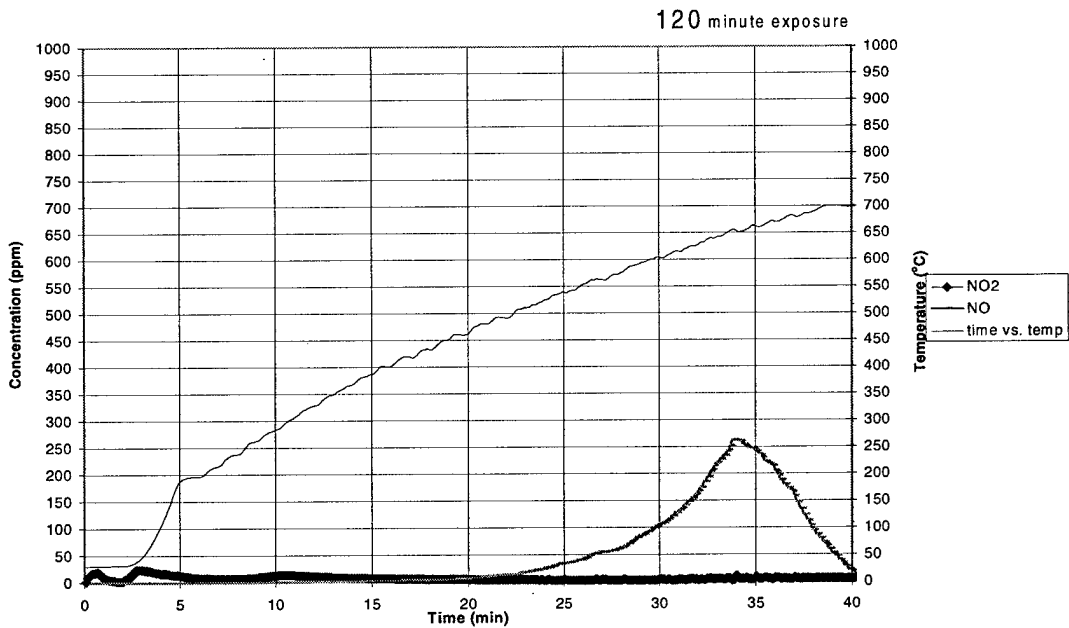


Figure 3-59. Thermal decomposition of K_2CO_3 -treated alumina after 120-min exposure to NO_x .

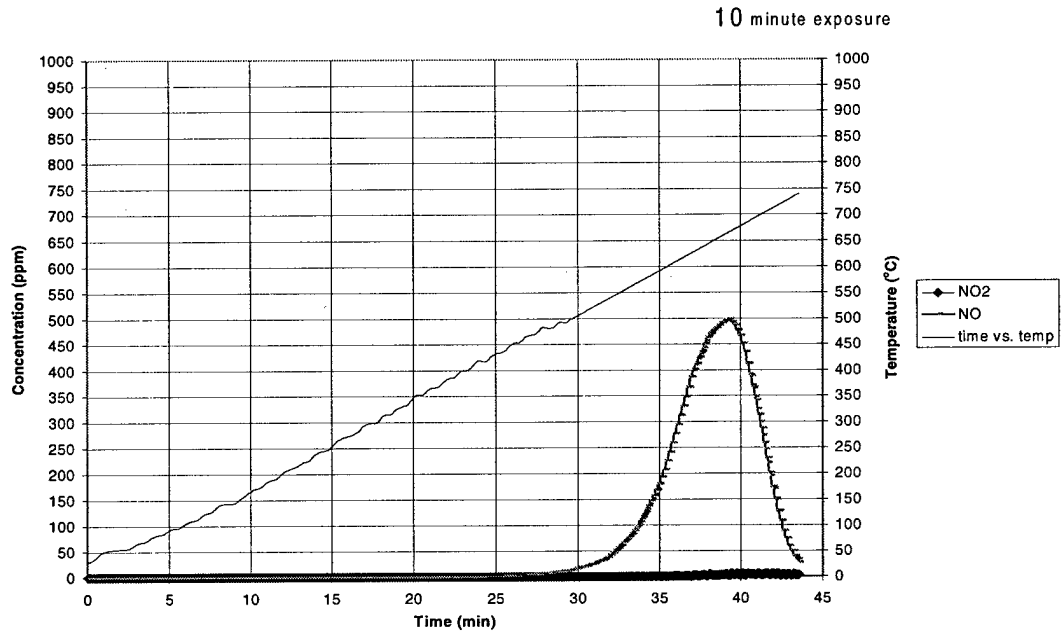


Figure 3-60. Thermal decomposition of KOH-treated alumina after 10-min exposure to NO_x.

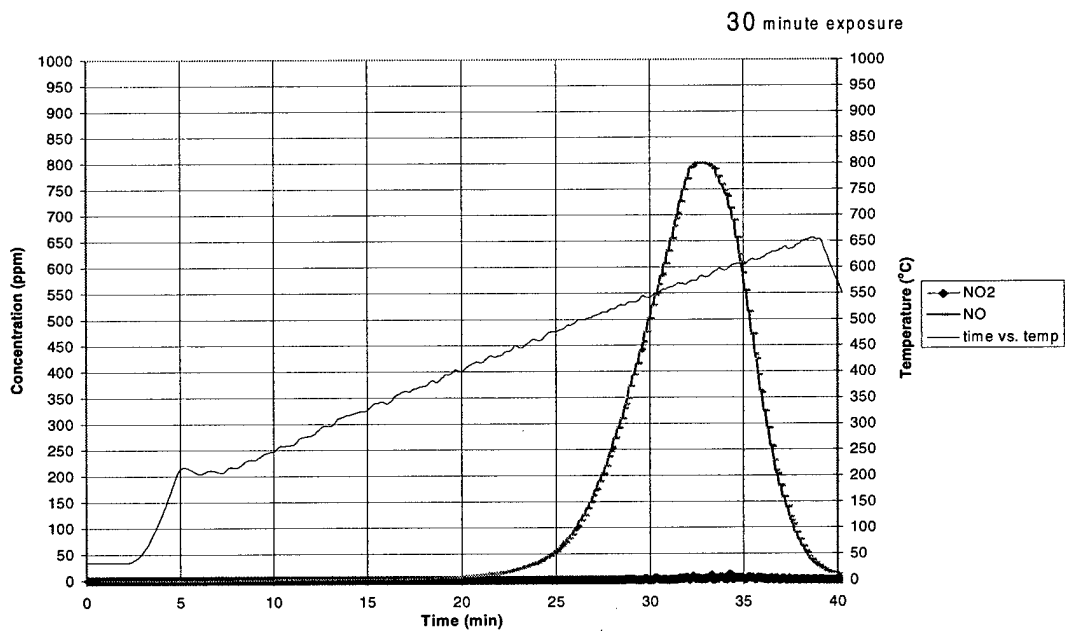


Figure 3-61. Thermal decomposition of KOH-treated alumina after 30-min exposure to NO_x.

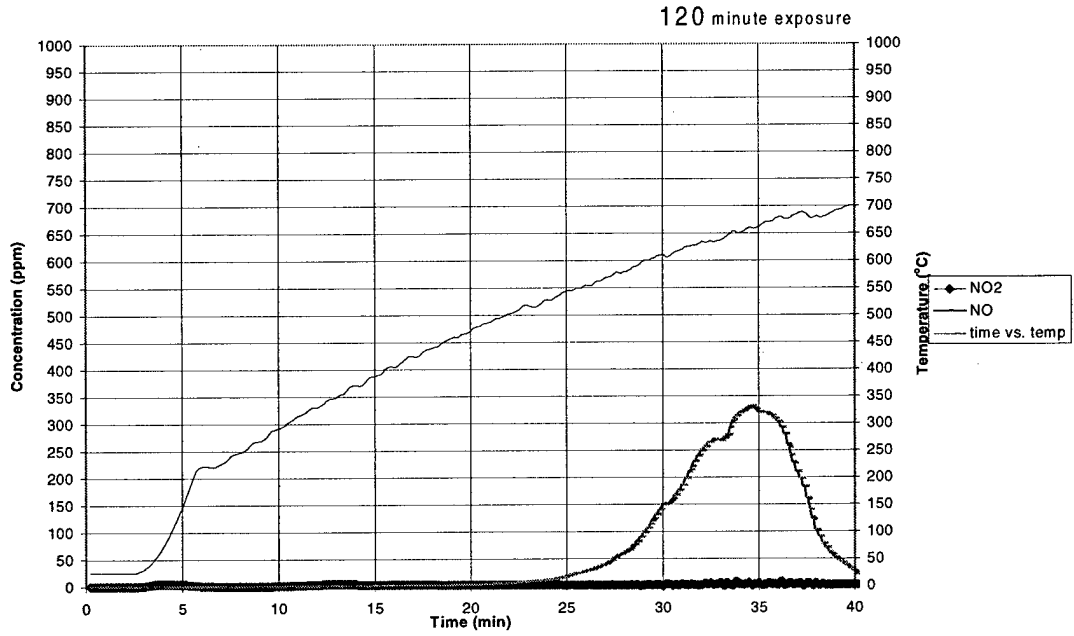


Figure 3-62. Thermal decomposition of KOH-treated alumina after 120-min exposure to NOx.

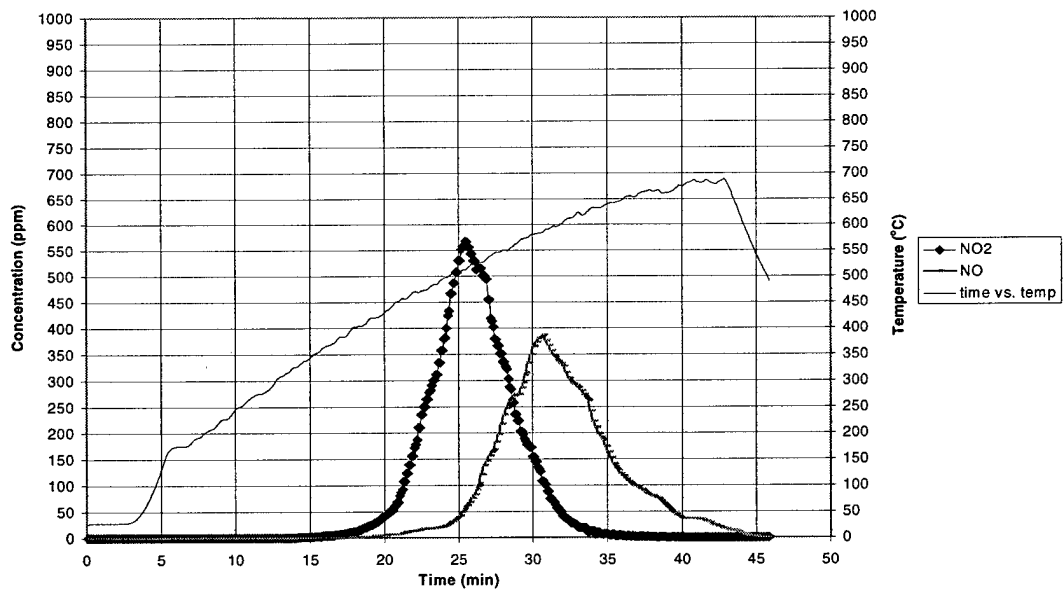


Figure 3-63. Thermal decomposition of KNO₃-treated alumina.

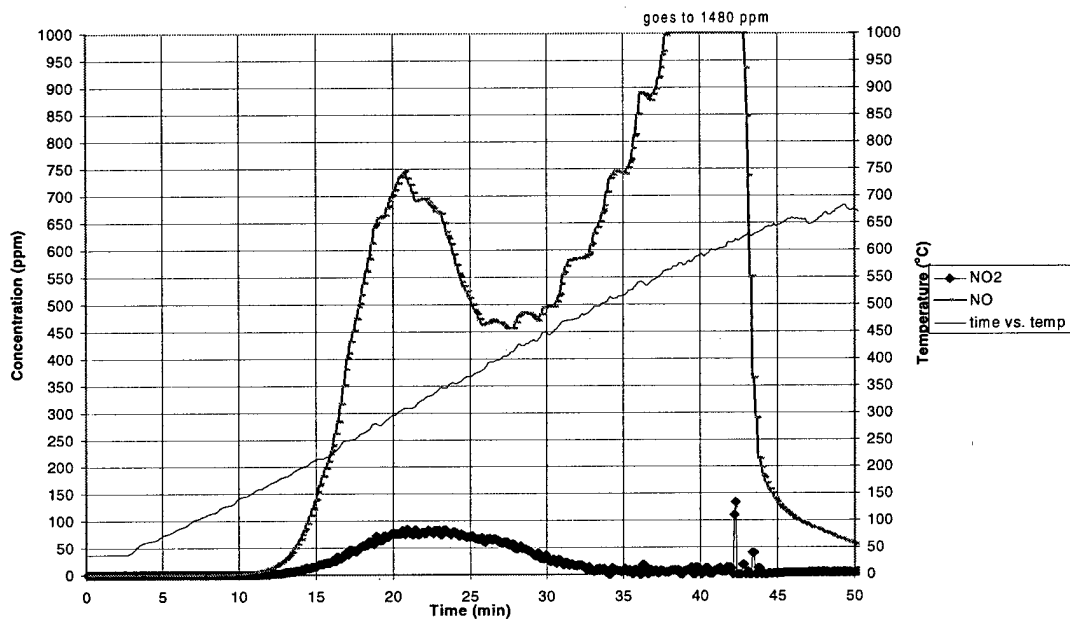


Figure 3-64. Thermal decomposition of KNO_2 -treated alumina.

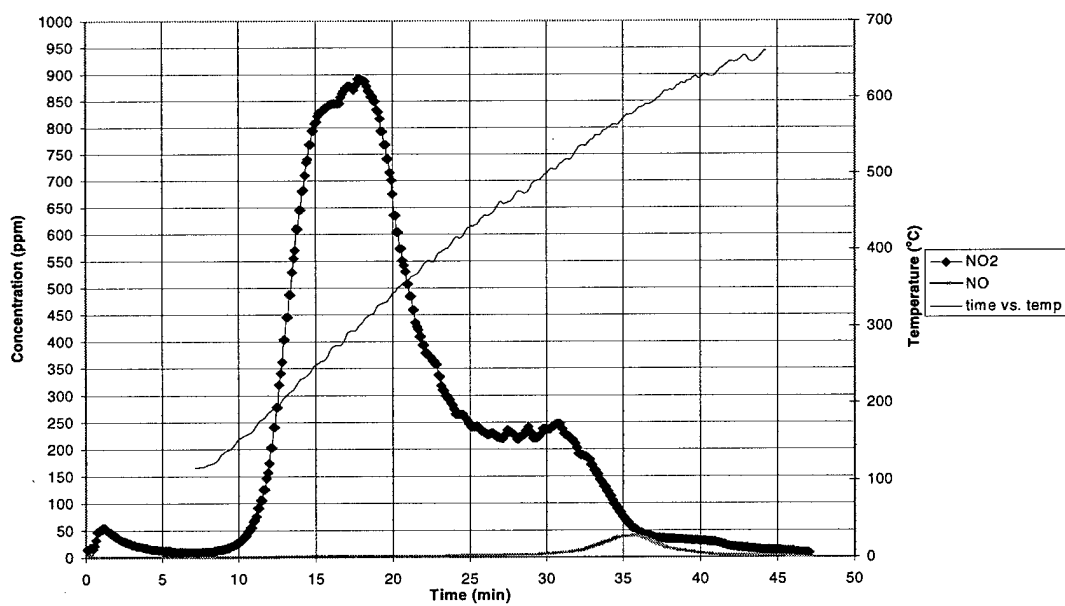


Figure 3-65. Thermal decomposition of aluminum nitrate-treated alumina.

bonding energy as observed by the decreased decomposition temperatures for KNO_2 - and KNO_3 -treated alumina.

Effect of Additional Gases on NOx Sorption

Three types of materials: untreated, K_2CO_3 -treated, and KOH-treated alumina were exposed to NOx (500 ppm NO_2 and 500 ppm NO) and other gases: H_2O vapor, O_2 , CO_2 , and SO_2 in the fixed-bed reactor system at 25 and 250 °C. Certified cylinder gases of O_2 (1% in N_2), SO_2 (100 ppm in N_2), and CO_2 (100% industrial grade) were used to supply the added gases. H_2O vapor was supplied using N_2 flow through water and assuming the saturation vapor pressure of water at a specific temperature. A thermocouple was used to measure the temperature of the water. The temperature was used to find the saturation vapor pressure of H_2O and this vapor pressure was used to calculate the concentration of input H_2O vapor. The saturated gas is mixed with a other gases to produce a gas mixture with the desired NOx concentrations. Concentrations of added gases are estimated by flow rate measurements. The effect on NOx sorption is determined by the NOx analyzer measurements.

Added H_2O vapor

Water vapor was added at a concentration of approximately 23000 ppm. The data from these experiments were compared to similar samples without H_2O vapor. Measurements were also made using an empty sorbent reactor tube at 250 °C. Approximately 5% reduction of NO_2 uptake was observed when the H_2O vapor is present. A correction factor was used in the calculations for the measured NOx sorption in the added water tests due to changes in empty bed residence times at effluent temperatures. Reproducibility tests for each run were carried out. The results in cumulative sorption of NO and NO_2 $\mu\text{mole/g}$ for the three tested materials can be found

in Appendix C. The tests were performed at 25, 100, and 250 °C. In the case of untreated alumina, added H₂O vapor significantly increases the sorption of both NO and NO₂ at 25 °C when the partial pressure of H₂O vapor in the gas is constant. The effect of added water to the sorption of NO₂ and NO is similar at 25 and 250 °C for untreated alumina. The sorption of NO₂ is increased 25% at 25 °C and 250 °C. An unexpected result was observed at 100 °C. The effect of H₂O vapor on NO_x sorption was significantly less than at 25 °C or 250 °C. Given the excellent reproducibility of the data this anomalous effect defies explanation.

For the K₂CO₃-treated (24.7% w/w) and KOH-treated (20 % w/w) alumina the effect at 25 °C of H₂O vapor is most significant in increasing NO sorption. The effect of H₂O vapor is less at 100 °C and further reduced at 250 °C. There is no effect on NO_x sorption at 250 °C for K₂CO₃-treated alumina. NO_x sorption on KOH-treated alumina appears to be more affected than K₂CO₃-treated alumina by the presence of water at higher temperatures.

Added O₂ gas

The effect of added O₂ (8800 ppm) on NO_x sorption was studied for all three materials under the conditions of 500 ppm NO₂ and 500 ppm NO and found to be negligible at both 25 and 250 °C. Multiple runs were performed to confirm the results.

Added CO₂ gas

The effect of added CO₂ on NO_x sorption was studied for all three materials (10% v/v) using 500 ppm NO₂ and 500 ppm NO and found to be negligible at both 25 and 250 °C. Multiple runs were performed to confirm the results.

Added SO₂ gas

The effect of added SO₂ gas (83 ppm) on NO_x sorption was studied using 500 ppm NO₂ and 500 ppm NO. SO₂ concentrations were limited to the certified cylinder gas concentration. The results in cumulative sorption of NO and NO₂ μmole/g for the three tested materials are appended.

At 25 °C SO₂ causes an increase in NO production by untreated alumina. This increase may be due to SO₂ competitively sorbing to available sites to NO_x. Thus, the surface saturation and conversion of formed surface nitrite to nitrate occurs more readily. Results for K₂CO₃-treated alumina indicate NO₂ removal is decreased while NO removal is slightly increased at 25 °C. While the reduction of NO₂ removal may be expected as seen for untreated alumina, the increased removal of NO is curious. This observed increase in NO removal may be due to other surface species formed in coordination with NO. A recent paper (Rochelle and Nelli, 1998) states that improved sorption of NO₂ due to added SO₂ is probably due to the formation of sulfur–nitrogen compounds that effectively sorb NO₂ and do not decompose upon further exposure to NO₂. Thus, both enhanced NO₂ and NO sorption is observed at 25 °C (Rochelle and Nelli, 1998). Results for KOH-treated alumina do not indicate that SO₂ affects the sorption of NO_x. At 250 °C the data do not indicate any effect of SO₂ on NO_x sorption for any of the sorbents. The tests were not reproduced due to experimental equipment constraints.

CHAPTER 4 CONCLUSIONS AND RECOMMENDATIONS

The gas-solid interactions of NO_x and other common combustion-exhaust gases with selected sorbents were studied using an isothermal fixed-bed tubular-flow reactor and supporting analytical methods. The fixed-bed reactor was a specially designed and constructed tubular flow system with automated data collection of NO_x concentrations from the inlets and outlets of three parallel sorbent tubes. Supporting analytical methods included X-ray photoelectron spectroscopy (XPS), ion-specific electrode (ISE) measurements (qualitatively confirmed by Fourier transform infrared spectroscopy (FTIR)), and BET surface-property measurements. In addition, the fixed-bed reactor was used to thermally decompose samples as a method to evaluate the stability and characteristics of surface nitrogen species as well as regeneration capacity.

Initial studies were based on a material previously studied as a NO_x sorbent, magnesium oxide-coated vermiculite (MgO/v). Kimm (1995) has shown that NO, alone, is not sorbed by MgO/v. Kimm's experiments indicated that sorption of NO₂ resulted in NO formation in a 3:1 ratio. Given that NO did not sorb to MgO/v, initial experiments were performed using a feed-gas ratio of NO₂:NO near 10:1. This ratio for combustion exhaust must assume some preliminary method is used to convert NO into NO₂.

Experiments were performed to observe the effects of water-wetted beds of MgO/v. These tests indicated water-wetting increased NO₂ sorption and decreased NO formation. However, as the bed temperature increased from 50 to 200 °C the effect of

water decreased. NO_x-saturation tests of sorbents indicated that water vapor affected NO_x sorption at 200 °C. Previous research on similar solid materials yielded mechanisms that consider sorption of NO_x as a gas-to-liquid (surfacial) interaction (Rochelle and Nelli, 1998). This effect at 200 °C indicates that another form of interaction other than that due to bulk liquid water was possible.

A comparison of MgO/v and γ -alumina sorbents in fixed-bed reactor tests indicates γ -alumina similarly converts sorbed NO₂ into NO in a 3:1 ratio. However, γ -alumina showed a significant increase in NO_x sorption activity while presenting less pressure drop for the material tested. Additional advantages of γ -alumina are that it can be obtained in various forms and with specified chemical and physical properties that are not available for MgO/v.

Subsequent XPS analysis of NO_x-exposed γ -alumina suggested that potassium impurities were active in the NO_x sorption process. A literature search indicated that group-I alkali metal compounds have been tested and used to effectively sorb NO_x originating from various sources (Jacobs and Hocheiser, 1958; Ma et al., 1995; American Public Health Association, 1939–1940). KOH-precipitated onto γ -alumina was tested in the fixed-bed reactor system and sorbed both NO and NO₂. Accordingly, γ -alumina was treated with group-I alkali metal compounds (Na and K carbonates and hydroxides) and comparatively tested for optimum amounts of coating and NO_x sorption over a range of temperatures and varied NO gas concentrations. From these tests it became apparent that the coating amount was limited by a threshold below which the pellets remained structurally stable. Also, greater coating amounts drastically reduced the efficiency of

NO_x removal. Temperature effects on NO_x sorption were small over the range from 100 to 200 °C.

The effect of varying the group-I alkali metal was evaluated for NO_x sorption using lithium, sodium, potassium, rubidium, and cesium as carbonate and hydroxide compounds. These tests indicated that the activity of group-I compounds is related to the ionization potential of the group-I element. Thus, on a molar basis, cesium compounds most effectively sorbed NO_x. Similar to MgO/v, all other sorbents did not sorb NO, in the absence of NO₂. Surface area measurements of these materials and untreated γ -alumina indicated that a decrease in surface area due to treatment was related to the atomic radius of the corresponding element. In addition, BET measures of pore size distributions suggested that sorption of NO_x is limited by closure of the sorbent pores.

After the observation that NO and NO₂ are sorbed by treated materials, two series of fixed-bed reactor tests compared the sorption of NO and NO₂ over a range of temperatures (25 to 250 °C) for three materials: untreated, K₂CO₃-treated, and KOH-treated alumina. The K₂CO₃-treated and KOH-treated were considered as possible NO_x-sorbents because they are better NO_x sorbents than their sodium analogues, and untreated alumina was evaluated as it is the support material. In the first series, the NO₂ concentration (500 ppm) was held constant and NO (10, 50, 200, and 500 ppm) was varied. All tests of the untreated alumina showed immediate NO production in a 3:1 ratio of the NO₂ sorbed. Sorption of NO₂ did not significantly vary as the NO_x concentration was varied. For the two treated sorbent materials, the sorption of NO₂ did not significantly differ as the input NO concentration varied. However, the sorption of NO increased at higher input NO concentration and at increased temperatures such that NO

sorption became unlimited at 250 °C. ISE measurements of the samples exposed at 200 °C indicated a near 2:1 relation of increased nitrite formation to increased NO sorption.

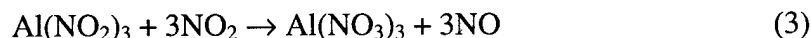
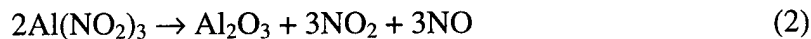
In the second series, the NO concentration (500 ppm) was held constant and NO₂ (10, 50, 200, and 500 ppm) concentration was varied. The treated sorbent materials showed at 25 °C that NO sorption increased with increased input NO₂ concentration except for the 500 ppm input of NO₂. Maximum cumulative NO sorbed was less at 500 than 200 ppm input NO₂ indicating a limit of NO sorption was reached. However, as temperature increased NO sorption increased such that at 250 °C NO sorption was a linear function of the input NO₂ concentration. For the untreated alumina, tests with 500 and 200 ppm input NO₂ showed immediate NO production in a 3:1 ratio. However, minor amounts of NO sorption by untreated alumina were observed for an input NO₂:NO ratio of 500:50 and 500:10 with efficiencies of less than 5 percent of NO input.

Additional fixed-bed reactor tests with supporting ISE analyses were performed as the "longbed" series to help derive general reaction mechanisms for three materials: untreated alumina, K₂CO₃-treated and KOH-treated alumina. The reactor tests exposed large samples of the three materials to 1950 ppm NO₂ and residual amounts of NO (6 ppm) at 25 °C. After exposure the samples were divided into sections and analyzed by ISE for nitrite and nitrate concentrations. Other reactor tests exposed smaller increments of the large sample masses to the same conditions to provide an indication of the change of NO_x concentrations within the bed. These tests were performed over varied time periods to observe gas and solid changes. The proposed mechanisms are given below with supporting evidence.

untreated alumina



In a second reaction the nitrite formed may react as follows



Combining sequential reactions provides the following overall reaction

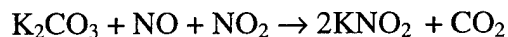


The proposed overall reaction predicts a molar ratio NO_2 sorbed to NO formed of 3:1. This ratio was observed in most tests indicating the second reaction is not limiting. Also, ISE analyses found low or negligible nitrite concentrations on untreated alumina. In addition, instability of aluminum salts was observed in decomposition studies. Thus, the steady-state nitrite concentration should be small. Where the $\text{NO}:\text{NO}_2$ feed-gas ratio was greater than 10:1 minor amounts of NO were sorbed as previously discussed. Under this condition a reversal of the second reaction is thought to occur.

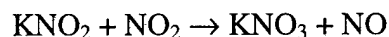
K_2CO_3 -treated alumina



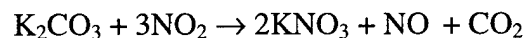
and



Greater concentrations of NO increase the amount of nitrite formed as suggested from ISE analyses. Eventually, KNO_2 will reach a temporary steady state.



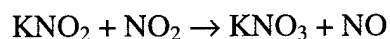
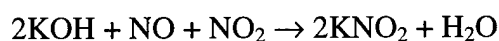
When KNO_2 has achieved steady state the overall reaction can be represented by



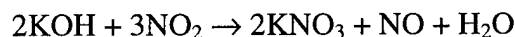
Gas-phase data shows the trend to the 3 NO₂ sorbed: 1NO_{formed} is delayed but eventually occurs for both K₂CO₃-treated and KOH-treated alumina.

KOH-treated alumina

Similar reactions of KOH-treated alumina to that of K₂CO₃-treated alumina are proposed.



For a steady-state concentration of KNO₂, overall reaction can be represented by



This overall reaction predicts that in the later stages of reaction, nitrite reaches steady state and a 3 NO₂ sorbed: 1NO_{formed} ratio should be observed. ISE analyses in the “longbed” series of NO_x exposure of over time indicate a steady nitrite concentration and the gas concentrations trend to a 3 NO₂ sorbed: 1NO_{formed} ratio.

For all of these sorbent materials the overall reaction is similar in that three NO₂ molecules sorb to form two nitrate and one NO moieties. For untreated alumina the proposed mechanism suggests no significant interaction of NO in the presence of NO₂. Also, oxidation of nitrite formed by NO₂ sorption is proposed to occur forming nitrate and gaseous NO or decomposing to NO₂ and NO due to the presumed instability of aluminum nitrite. Alkaline-treated alumina materials react with NO in the presence of NO₂ forming significant amounts of nitrite that increases with temperature. However,

following build-up of nitrite, conversion of nitrite into nitrate with release of NO occurs as observed for untreated alumina.

Feasibility of sorbent regeneration was explored by two methods: washing the sorbent and thermal desorption. Washing the sorbent proved useless as the treatment material was removed and the pellet structure appeared degraded. Thermal desorption of NO_x was applied to a sample of Cs₂CO₃-treated alumina previously exposed to 500 ppm NO₂ and residual NO (3 ppm) at 0.62 Lpm and 25 °C for 2 hours. Upon re-exposure under similar conditions as the initial exposure, NO_x sorption was 93% of the cumulative amount sorbed in the initial exposure. Additional regeneration studies are suggested for further research.

Additional gases such as O₂, CO₂, H₂O, or SO₂ in the NO_x-laden stream were tested to observe their effects on NO_x sorption. The presence of oxygen and carbon dioxide did not affect the sorption of NO_x at 25 and 250 °C. In similar fractional amounts, water vapor improved the removal of NO and NO₂ for the sorbent studied. Sulfur dioxide reduces NO_x sorption to untreated alumina but improves NO sorption to K₂CO₃-treated alumina at 25 °C.

Based on the conclusions presented above and the experience gained in performing this research, recommendations can be made that should further the understanding and application of these sorbent materials to the control of NO_x.

1. The general mechanisms developed for untreated, K₂CO₃-treated, and KOH-treated alumina sorbents are based on gas-phase measurements of NO and NO₂ and subsequent ISE analysis of nitrites and nitrates. A technique to measure the change of the surface species during the sorption process is

Raman spectroscopy. This *in situ* technique could allow one to identify the interactive species more accurately that are involved in this NO_x sorption process. The sensitivity required for this technique may be a limiting factor and should be considered as an element in experimental design.

2. A brief demonstration test indicated that washing of sorbents as means of regeneration is not possible and that thermal desorption in an atmosphere of a reducing gas appears to be effective. Regeneration studies should be performed to demonstrate the long-term effects on sorbent properties of practical regeneration techniques.
3. These coated materials have shown promise as sorbents for use at temperatures well below combustion gas conditions (250 °C). Other uses of this material of interest to the USAF include controlling NO_x (primarily NO₂) exhaust emitted during liquid rocket fueling. Currently, during the rocket fueling process wet scrubbing methods are used to control N₂O₄ emissions. A dry sorption method could easily improve material handling issues as well as improve efficiency using adequate design.
4. Given the observed effects of the copollutants H₂O and SO₂ on the sorption of NO_x, it is recommended that studies be carried out in which these copollutants and their products are analyzed simultaneously with NO_x species. These data will provide needed information to formulate modified or new sorption mechanisms with these gases present. Surface species may be identified by methods such as ion-chromatography or spectroscopic techniques to provide

information about other surface species formed during NO_x sorption in the presence of copollutants.

5. The materials studies can be further improved based on their physical characteristics. Given that pore size distribution measurements indicated that pore closure limited the sorption process, it is recommended that materials of varied physical properties be obtained and tested. As stated earlier, a desirable feature of alumina is that it can be obtained with specified physical properties at reasonable cost. In fact, alumina should allow for easy comparative studies of the effects of surface properties given the observed reproducibility of the obtained manufactured material. For example, because alumina acts as a support rather than sorbent in treated materials, it is important to optimize surface area.
6. The methods of surface treatment should be further studied. Treatment methods can significantly affect the chemical and physical characteristic of the final material. The treatment methods used in this study did evaluate parameters of treatment but other methods of treatment beyond impregnation and precipitation were not considered. Therefore, the common methods of treatment and the expected results from those treatment methods should be analyzed and tested.

REFERENCES

- Benedeck, K.; Flytzani-Stephanopoulos, M. *Cross-Flow Filter-Sorbent-Catalyst for Particulate, SO₂, and NO_x Control*. Final Report, DOE PETC DOE/PC/89805-T9. 1994.
- Berman, E.; Dong, J.; Lichtin, N. N. *Photopromoted and Thermal Decomposition of Nitric Oxide by Metal Oxides*. ESL-TR-91-32, HQ AFESC, Tyndall AFB, Florida. 1991.
- Bienstock, D.J.; Field, J.H.; Katell, S.; Plants, K.D. Evaluation of Dry Processes for Removing Sulfur Dioxide from Power Plant Flue Gases. *J.A.P.C.A.*, **1965**, *15*(10), 459.
- Boehm, H.P. Acidic and Basic Properties of Hydroxylated Metal Oxide Surfaces. *Discuss. Faraday Soc.*, **1972**, *52*, 264.
- Borgwardt, R.H.; Harvey, R.D. Kinetics of the Reaction of SO₂ with Calcined Limestone. *Environ. Sci. Tech.* **1972**, *6*, 350.
- Bortz, S. J.; Podlenski, J. W. *Method and Apparatus for Reducing Nitrogen Dioxide Emissions in a Dry Sodium Scrubbing Process Using Humidification*. US Patent 5,165,902. 1992.
- Bowman, C.T. Kinetics of Nitric Oxide Formation on Combustion Processes. In *Fourteenth Symposium on Combustion*. The Combustion Institute, Pittsburgh, Pennsylvania. 1972. pp. 729-738.
- Brunauer, S.; Emmett, P.H.; Teller, E. Vapor Adsorption to Surfaces. *J. Am. Chem. Soc.* **1938**, *60*, 309.
- Buonicore, A.J.; Theodore, L.; Davis, W.T. *Air Pollution Control Engineering Manual*. Eds. Buonicore, A.J.; Theodore, L.; Davis, W.T. Van Nostrand Reinhold, New York, New York, 1991. pp. 1-13.
- Campbell, L. E.; Danziger, R.; Guth, E. D.; Padron, S. *Process for the Reaction and Absorption of Gaseous Air Pollutants, Apparatus Therefore and Method of Making Same*. US Patent 5,665,321. 1997.

- Carmicheal, G.R.; Peters, L.K. An Eulerian Transport/Transformation/Removal Model for SO₂ and Sulfate - I. Model Development. *Atmos. Environ.* **1984**, *18*, 937.
- Cook, W.A. Chemical Procedures in Air Analysis for Determination of Poisonous Atmospheric Contaminants, *American Public Health Association Yearbook* **1936**; *26*, 3, 80-83.
- Cooper, D.C; Alley, F.C. *Air Pollution Control: A Design Approach*. Waveland Press Inc., Prospect Heights, Illinois, 1986. pp. 451-480.
- Coster, D.J.; Fripiat, J.J. Effect of Bulk Properties on the Rehydration of Aluminas. *Langmuir*, **1995**, *11*, 2615.
- Counce, R.M.; Perona, J.J. A Mathematical Model for Nitrogen Oxide Absorption in a Sieve-Plate Column. *Ind. Eng. Chem. Proc. Des. Dev.* **1980**, *19*, 426.
- CRC, 1992. *CRC Handbook of Chemistry and Physics*, 73rd Edition, 1992.
- Datta, A. Evidence for Cluster Sites on Catalytic Alumina. *J. Phys. Chem.*, **1989**, *93*, 7053.
- Debbage, L.; Kelley, E.; Guth, E.D.; Campbell, L.E.; Danziger, R.N.; Padron, S. *Apparatus for Removing Contaminants from Gaseous Stream*. US Patent 5,607,650. 1997.
- Fiero, J.L.G., ed. 1990. *Spectroscopic Characterization of Heterogenous Catalysts, Part A*. Elsevier. pp. 202-208.
- Flury, F.; Zernick, F. *Schadliche Gas*. Berlin, Springer, 1931.
- Ganz, S.N. Sorption of Nitrogen Oxides by Solid Sorbents. *J. Appl. Chem. USSR*. **1958**, *31*(1), 128.
- Gilbert, R.E.; Cox, D.F.; Hoflund, G.B. Computer-interfaced Digital Pulse Counting Circuit. *Rev. Sci. Instrum.*, **1982**, *53*, 447.
- Glater, R.A. *Smog and Plant Structure in Los Angeles County. Reports Group, School of Engineering and Applied Science*. University of California at Los Angeles, March 1970. Report No. 70-17, pp. 1-39.
- Golden, T.C.; Kalbassi, M.A.; Taylor, F.W.; Allam, R.J. *Use of Zeolites and Alumina in Adsorption Process*. US Patent 5,779,767. 1998.

- Grano, D. *Clean Air Act Requirements: Effect on Emissions of NO_x from Stationary Sources*. ACS Symposium Series, Vol. 587, 1995, p. 14.
- Greenwood, N.N.; Earnshaw, A. Eds. *Chemistry of the Elements*. Pergamon Press, Oxford, 1984, pp. 273–278.
- Grim, R.E. *Clay Mineralogy*, McGraw–Hill Book Co., New York, New York, 1953. pp. 102-103.
- Haslbeck, J.L.; Neal, L.G.; Perng, C.P.; Wang, C.J. *Evaluation of the NO_xSO₂ Combined NO_x/SO₂ Flue Gas Treatment Process*. US DOE Report No. DOE/PC/7325-T2; 1985.
- Haslbeck, J.L.; Wang, C.J.; Tseng, H.P.; Tucker, J.D. *Evaluation of the NO_xSO₂ Combined NO_x/SO₂ Flue Gas Treatment Process*. US DOE Report No. DOE/FE/60148-T5; 1984.
- Heinsohn, R.J.; Kabel, R.L. *Sources and Control of Air Pollution*. Prentice Hall, Upper Saddle River, NJ, 1999. pp. 89-125.
- Henry, M.C.; Ehrlich, R.; Blair, W.H. Effect of Nitrogen Dioxide on Resistance of Squirrel Monkeys to *Klebsiella pneumoniae* Infection. *Arch. Environ. Health*, **1965**, *18*, 580.
- Hermance, H.W.; Russell, C.A. ; Bauer, E.J.; Egan, T.F.; Wadlow, H.V. Relation of Air-Borne Nitrate to Telephone Equipment Damage. *Environ. Sci. Techn.* **1970**.
- Heywood, J.B. *Internal Combustion Engine Fundamentals*. McGraw–Hill Book Co., New York, New York, 1988. p. 571.
- Hill, A.C.; Bennett, J.H. Inhibition of Apparent Photosynthesis by Nitrogen Oxides. *Atmos. Environ.* **1970**.
- Himi, Y.; Muramatsu, F. Sampling Method for Determination of Nitrogen Oxides in Flue Gas. *Japan. Analyst*, **1969**, *18*(6), 710.
- Jacobs, M.B. *The Analytical Chemistry of Industrial Poisons, Hazards, and Solvents*; 2nd ed., Interscience Publishers, New York, New York, 1949; Vol. 1, pp. 79–99.
- Jacobs, M.B.; Hochheiser, S. Continuous Sampling and Ultramicrodetermination of Nitrogen Dioxide in Air. *Analytical Chemistry*, **1958**, *30*, 426.
- James, N.J.; Hughes, R. Rates of NO_x Absorption in Calcined Limestones and Dolomites. *Environ. Sci. Techn.* **1977**, *11*(13), 1191.

- Jimenez-Gonzalez, A.; Schmeisser, D. Preparation and Spectroscopic Characterization of γ -Al₂O₃ Thin Films. *Surface Science*, **1991**, *250*, 59.
- Johnson, S.A.; Katz, C.B. *Feasibility of Reburning for Controlling NO_x Emissions from Air Force Jet Engine Test Cells*. ESL-TR-89-33, HQ AFESC, Tyndall AFB, Florida; 1989.
- Jones, Dale G. *Apparatus for Removing Oxides of Nitrogen and Sulfur from Combustion Gases*. US Patent 5,116,587. 1992.
- Keiser, E.H.; McMaster, L. On the Detection of Ozone, Nitrogen Peroxide, and Hydrogen Peroxide on Gas Mixtures. *American Chemical Society*. **1908**, *39*, 96.
- Kikkinides, E.S.; Yang, R.T. Simultaneous SO₂/NO_x Removal and SO₂ Recovery of Synthesis Gas with Zinc Ferrite. *Ind. Eng. Chem. Res.* **1991**, *30*(8), 1981.
- Kimm, L.T. Control of Nitrogen Oxide Emissions from Jet Engine Test Cell Exhaust using a Magnesium Oxide-Vermiculite Sorbent. Ph.D. Dissertation in Environmental Engineering, University of Florida, Gainesville, Florida, 1995.
- Kimm, L.T.; Allen, E.R.; Wander, J.D. Control of NO_x Emissions from Jet Engine Test Cells. *Proceedings of the 88th Annual Air and Waste Management Association Meeting*; San Antonio, Texas, 1995.
- Kittrell, J.R. *High Temperature NO_x Control Process*. ESL-TR-89-36, HQ AFESC, Tyndall AFB, Florida; 1991.
- Knozinger, H. Specific Poisoning and Characterization of Catalytic Active Oxide Surfaces. In *Advances in Catalysis*, Academic Press, New York, New York, Vol. 25, 1976, pp. 184-267.
- Knozinger, H.; Ratnasamy, R. Catalytic Aluminas: Surface Models and Characterization of Surface Sites. In *Catalysis Reviews: Science and Engineering*, Marcel Dekker Inc., New York, New York, Vol. 17, No. 1, 1976, pp. 31-70.
- Komppa, V. Dry Adsorption Process for Removal of SO_x and NO_x in Flue Gases. *Paperii ja Puu*, **1986**, *5*, 401.
- Krasna, I.; Rittenburg, D. The Inhibition of Hydrogenase by Nitric Oxide. *Proc. Nat. Acad. Sci.* **1954**, *70*, 225.
- Krizek, J. Determination of Nitrogen Oxides in Small Concentrations. *Chem. Prumysl.*, **1966**, *16*(9), 558.

- Lee, M.R.; Allen, E.R.; Wander, J.D. Evaluation of Coated Alumina for the Removal of Nitrogen Oxides (NO_x). *Proceedings of the Air and Waste Management Association*. Paper No. 98-RA93A.03. San Diego, California, June 14-19, 1998a
- Lee, M.R.; Allen, E.R.; Wolan, J.T.; Hoflund, G.B. NO₂ and NO Adsorption Properties of KOH-Treated γ -Alumina. *Ind. Eng. Chem. Res.* **1998b**, *37*, 3375.
- Lever G.; Etchart, C.P.; Tahiani, F; *Alumina-Alkali Metal Aluminum Silicate Agglomerate Acid Adsorbents*. US Patent 5,096,871. 1992.
- Lott, S.E.; Gardner, T.J.; McLaughlin, L.I.; Oelfke, J.B.; Matlock, C.A. *Nitrogen Oxide Adsorbing Material*. US Patent 5,795,553. 1998.
- Lunsford, J.H. A Study of Surface Interactions on γ -Alumina, Silica-Alumina, and Silica-Magnesia using the EPR Spectra of Adsorbed Nitric Oxide. *J. Catalysis*, **1969**, *14*, 379.
- Lyon, R.K. *New Technology for Controlling NO_x from Jet Engine Test Cells*. ESL-TR-89-15, HQ AFESC, Tyndall AFB, Florida; 1991.
- Ma, W.T.; Chang, A.M.; Haslbeck, J.L.; Neal, N.G. NOXSO SO₂/NO_x Flue Gas Treatment Process Adsorption Chemistry and Kinetics. In *Novel Adsorbents and their Environmental Application*. AIChE Symposium Series 309, Vol. 91, 1995, p. 18.
- Ma, W.T.; Haslbeck, J.L.; Neal, L.G.; Yeh, J.T. Life Cycle of the NOXSO SO₂ and NO_x Flue Gas Treatment Process: Process Modeling. *Sep. Tech.*, **1991**, *1*, 195.
- Markussen, J.M.; Livengood, C.D. Alternative Flue Gas Treatment Technologies for Integrated SO₂ and NO_x Control. *Proceedings of the 57th Annual American Power Conference*, Chicago, Illinois; 1995.
- McLendon, V.; Richardson, F. Oxides of Nitrogen as a Factor in Color Changes of Used and Laundered Cotton Articles. *Amer. Dyest. Rep.* **1965**, *54*, 305.
- Morris, M.A.; Young, M.A.; Molig T. The Effect of Air Pollutants on Cotton. *Text. Res.* **1964**, *34*, 563.
- Murphy, J.F. Alumina in Air Pollution Control. *Proceedings of the 102nd AIME Annual Meeting*. Chicago, Illinois, 1972.
- Nelli, C.H.; Rochelle, G.T. Nitrogen Dioxide Reaction with Alkaline Solids. *Ind. Eng. Chem. Res.*, **1996**, *35*, 999.
- Nelson, B.W.; Nelson, S.G.; Higgins, M.O.; Brandum, P.A. *A New Catalyst for NO_x Control*. ESL-TR-89-11, HQ AFESC, Tyndall AFB, Florida; 1989.

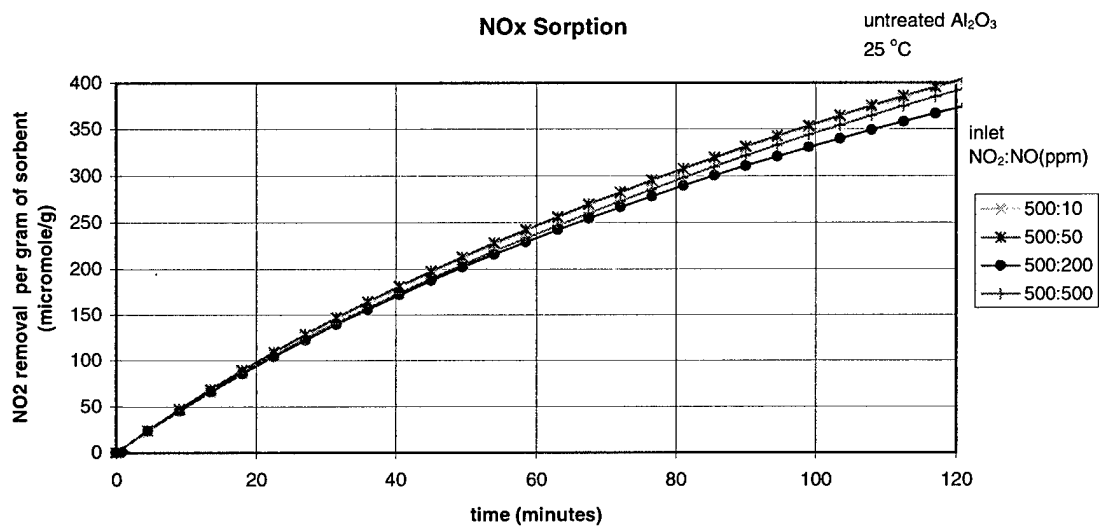
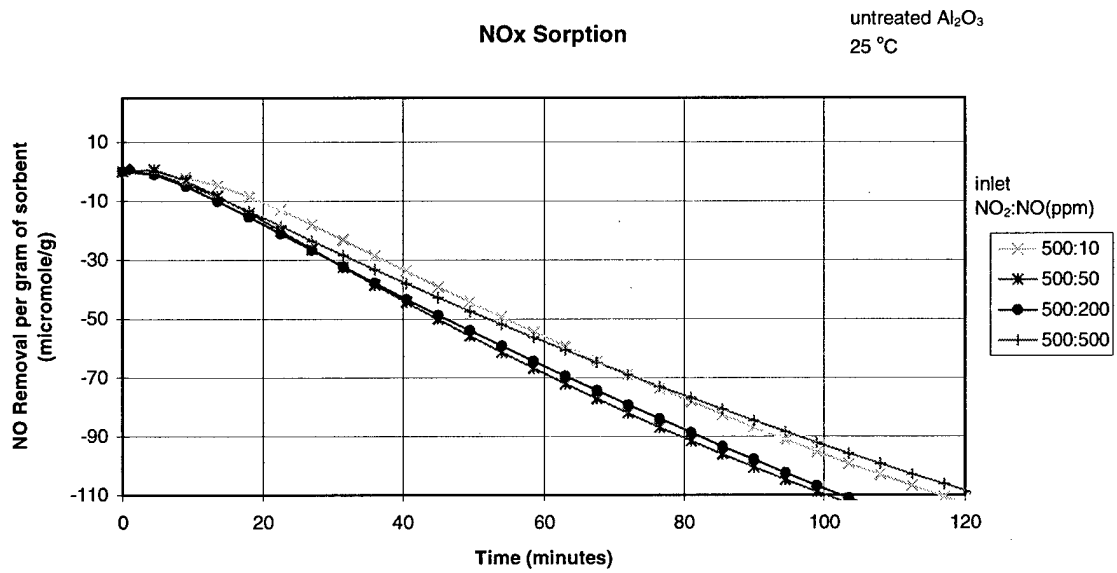
- Nelson, B.W.; Nelson, S.G.; Van Stone, D.A. *Controlling Combustion-Source Emissions at Air Force Sites with a New Filter Concept*. AL/EQ-TR-1994-0006, Armstrong Laboratory, Tyndall AFB, Florida; 1994.
- Nelson, B.W.; Nelson, S.G.; Van Stone, D.A. *Development and Demonstration of a New Filter System to Control Emissions During Jet Engine Testing*. CEL-TR-92-49, HQ AFESC, Tyndall AFB, Florida; 1992.
- Nelson, S.G. *Toxic Gas Sorbent and Process for Making Same*. US Patent 4,721,582. 1987.
- Nelson, S.G.; Van Stone, D.A.; Little, R.C.; Peterson, R.A. *Laboratory Evaluation of a Reactive Baffle Approach to NO_x Control*. AL/EQ-TR-1993-0017, HQ AFESC, Tyndall AFB, Florida; 1993.
- Nyquist, R.A.; Kagel, R.O. *Infrared Spectra of Inorganic Compounds*. Academic Press, New York, New York, 1971.
- Parkyn, N.D. Adsorption Sites on Oxides, Infra-red Studies of Adsorption of Oxides of Nitrogen. *Proceedings of the Fifth International Congress on Catalysis*. Miami Beach, Florida, 1972.
- Petrik, M.A. *Use of Metal Oxide Electrocatalysts to Control NO_x Emissions from Fixed Sources*. ESL-TR-89-29, HQ AFESC, Tyndall AFB, Florida; 1991.
- Pinnavaia, T.J.; Amarasekera, J.; Polansky, C.A. *Layered Double Hydroxide Sorbents for the Removal of SO_x from Flue Gas Resulting from Coal Combustion*. US Patent 5,120,508. 1992.
- Regalbutto, J.R. Comparison of NO_x Abatement Strategies Utilizing Adsorption. In *Final Task Report to the Gas Research Institute*, USDOC PB95-171575, June 1994.
- Rochelle, G.T.; Nelli, C.H. Simultaneous Sulfur Dioxide and Nitrogen Dioxide Removal by Calcium Hydroxide and Calcium Silicate Solids. *J. AWMA*, **1998**, *48*, 819.
- Ruthven, D.M. A Simple Method for Calculating Mass Transfer Factors for Heterogeneous Catalytic Gas Reactions. *Chemical Engineering Science*. **1968**, *23*, 759.
- Savitzky, A.; Golay, J.E. Smoothing and Differentiation of Data by Simplified Least Squares Procedures. *Analytical Chemistry*. **1984**, *36*, 1627.
- Schlesinger, M.D.; Illig, E.G. *The Regeneration of Alkalized Alumina, Attritioning and SO₂ Sorption Rates*. USB.M. Report No. 7275, 1969.

- Shy, C.M.; Creason, J.P.; Pearlman, M.E.; McClain, K.E.; Benson, F.B.; Young, M.M. The Chattanooga School Study: Effects of Community Exposure to Nitrogen Dioxide. Incidence of Acute Respiratory Illness. *J.A.P.C.A.* **1970**, *20*, 582.
- Sigsby, J.E.; Black, F.M.; Bellar, T.A.; Klosterman, D.L. Chemiluminescent Method for Analysis of Nitrogen Compounds in Mobile Source Emissions (NO, NO₂, and NH₃). *Environmental Science and Technology.* **1973**, *7*(1), 51.
- Sircar, S.; Rao, M.B.; Golden, T.C. Drying of Gases and Liquids by Activated Alumina. In *Adsorption on New and Modified Inorganic Sorbents. Studies in Surface Science and Catalysis.* Eds. Dabrowski, A. and Tertykh, V.A., Vol. 99, 1996, p. 629.
- Smith, J.M., *Chemical Engineering Kinetics.* McGraw-Hill Book Co., New York, New York, 1981, pp. 311-333.
- Staudt, J.E. Post-Combustion NO_x Control Technologies for Electric Power Plants. *89th Annual Meeting of the Air and Waste Management Association.* 96-RP139.02. Nashville, Tennessee, June 23-28, 1996.
- Terenin, A.N.; Roev, L. Infrared Spectra of Nitric Oxide Adsorbed on Transition Metals, their Salts and Oxides. *Spectrochimica Acta*, **1959**, *15*, 946.
- US DOE. *Clean Coal Technology Demonstration Program.* Report No. DOE/FE-0351; 1997
- US EPA. *Air Quality Criteria for Oxides of Nitrogen.* Report No. EPA/600/8-91/049aF; 1993.
- US EPA. *Alternative Control Techniques Document-NO_x Emissions from Utility Boilers.* Report. No. EPA-453/R-94-023; 1994.
- US EPA. *The Regional Transport of Ozone.* Report No. EPA-456/F-98-006; 1998.
- Van Haut, H.; Stratmann, H. Experimental Investigations of the Effect of Nitrogen Dioxide on Plants. *Transactions of the Land Inst. of Pollution Control and Soil Conservation of the Land of North Rhine-Westphalia*, **1967**, *7*, 50.
- Yeh, J.T.; Ma, W.T.; Pennline, H.W.; Haslbeck, J.L.; Joubert, J.I.; Gromicko, F.N. Integrated Testing of the NOXSO Process: Simultaneous Removal of SO₂ and NO_x from Flue Gas. *Chem. Eng. Comm.*, **1992**, *114*, 65.
- Zeldovitch, J. The Oxidation of Nitrogen in Combustion and Explosions. *Acta. Physiochem.* **1946**, *21*(4).

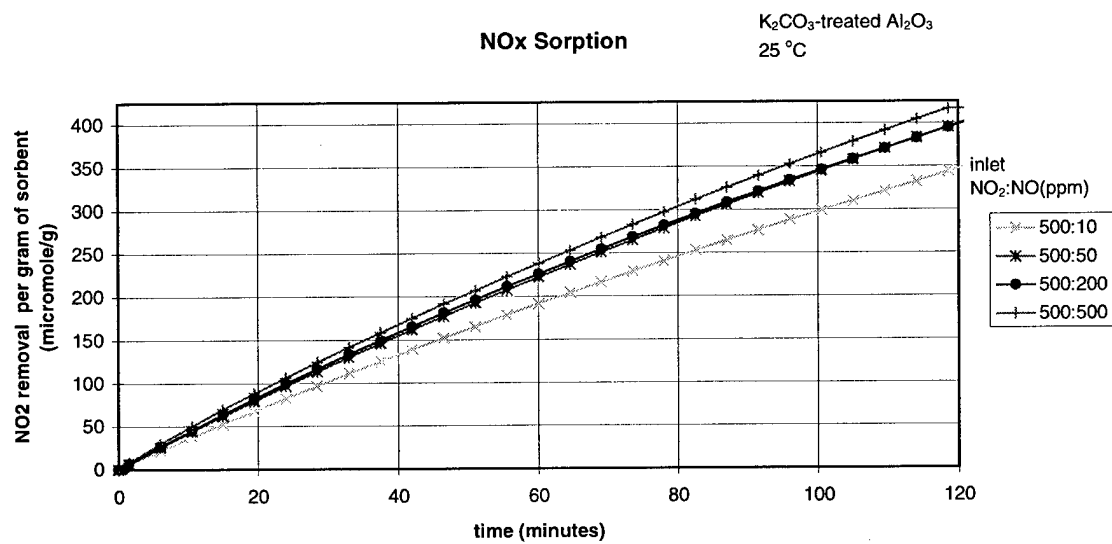
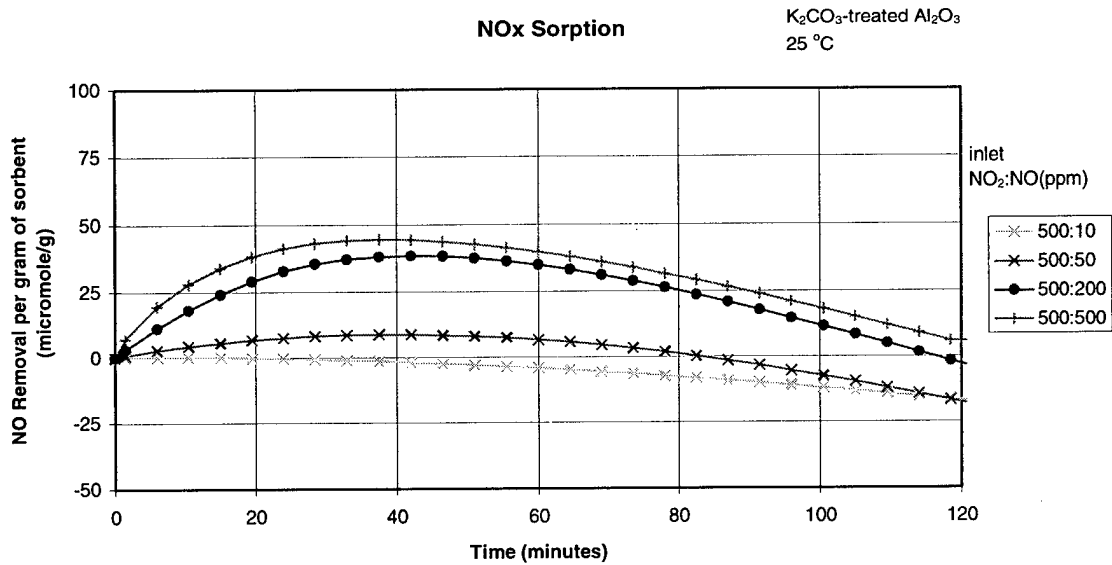
Zemlyanov, D.Y.; Hornung, A.; Weinburg, G.; Wild, U.; Schlog, R. Interaction of Silver with a NO/O₂ Mixture: A Combined X-ray Photoelectron Spectroscopy and Scanning Electron Microscopy Study. *Langmuir*, **1998**, *14*, 3242.

Ziebarth M.S.; Hager, M.J.; Beeckman, J.W.; Plecha, S.. *SOx/NOx Sorbent and Process of Use*. US Patent 5,585,082. 1996.

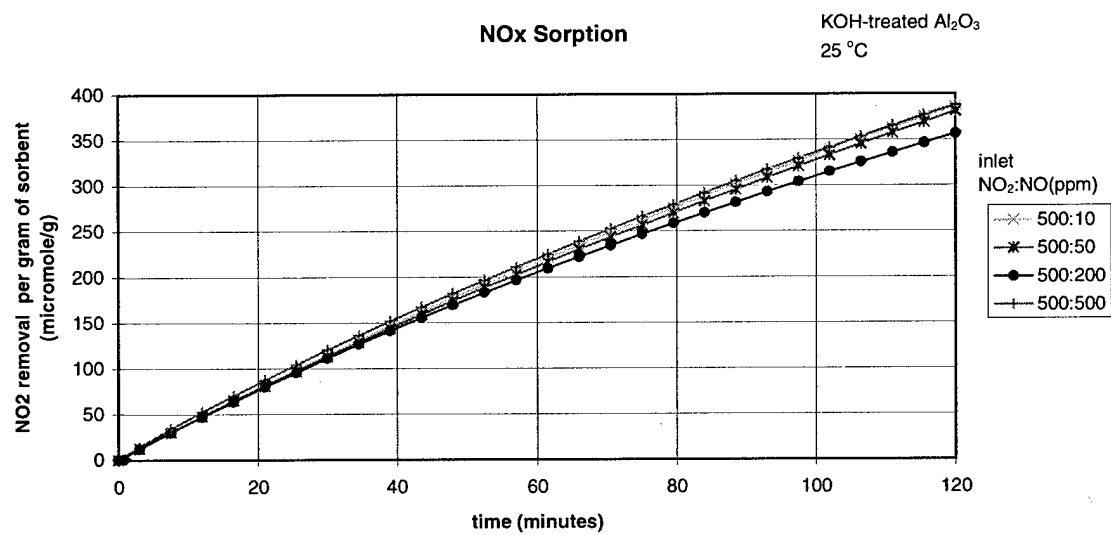
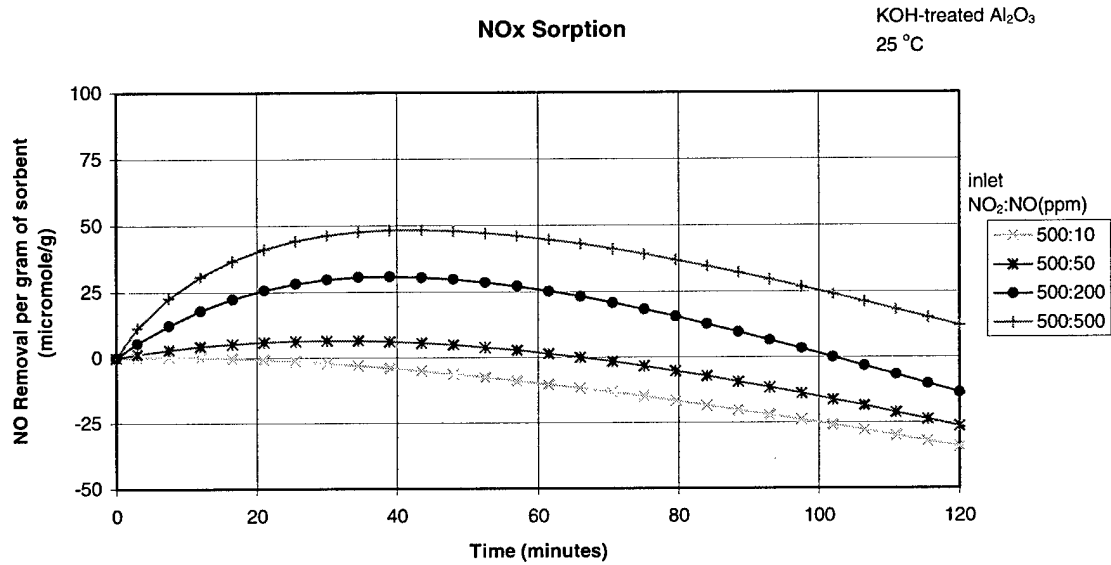
APPENDIX A
NOX SORPTION: CONSTANT NO₂ (500 PPM), VARIED NO CONCENTRATION



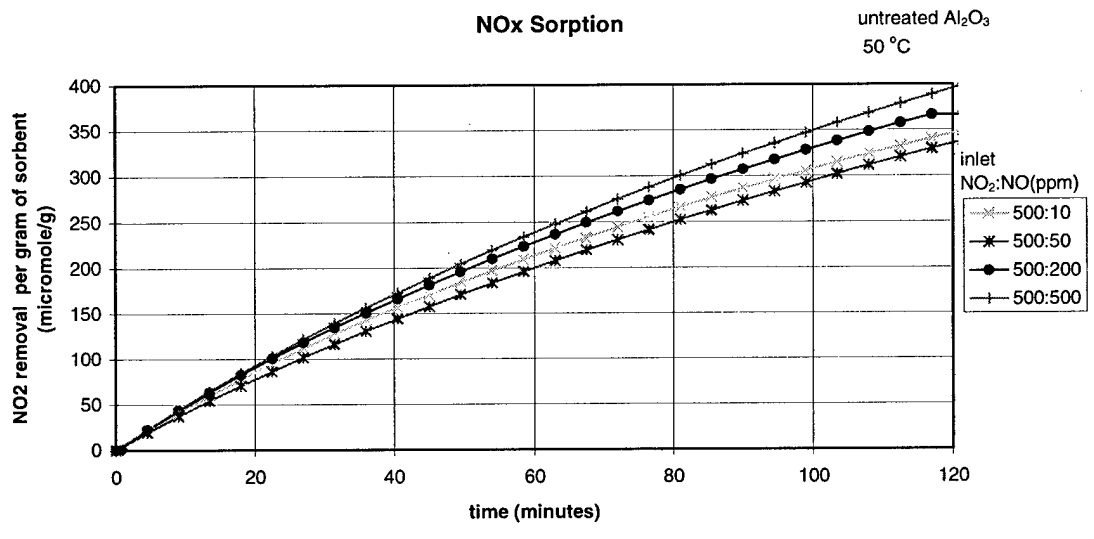
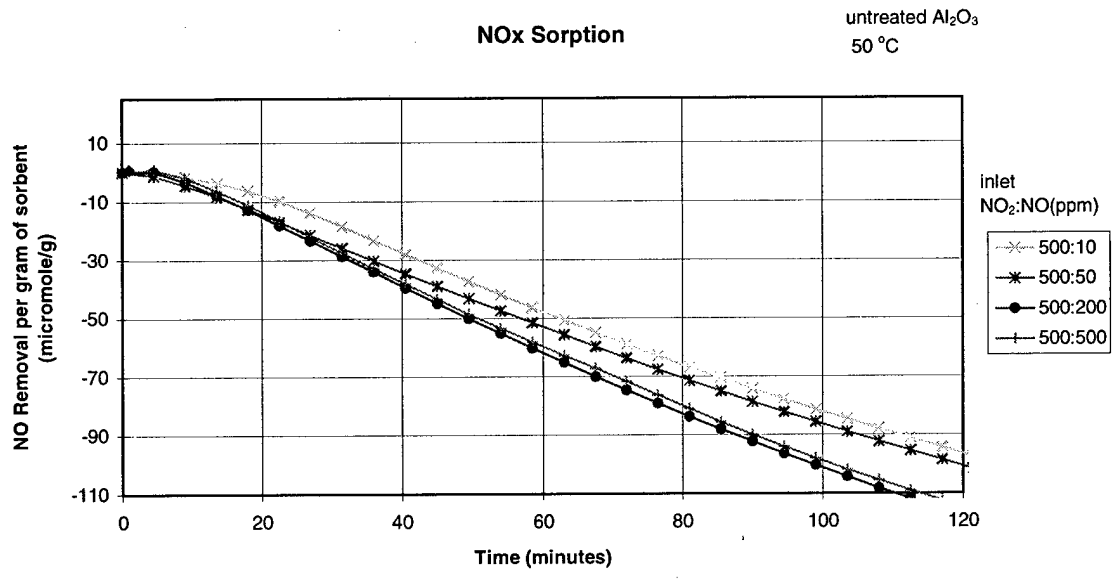
Untreated alumina, 25 °C.



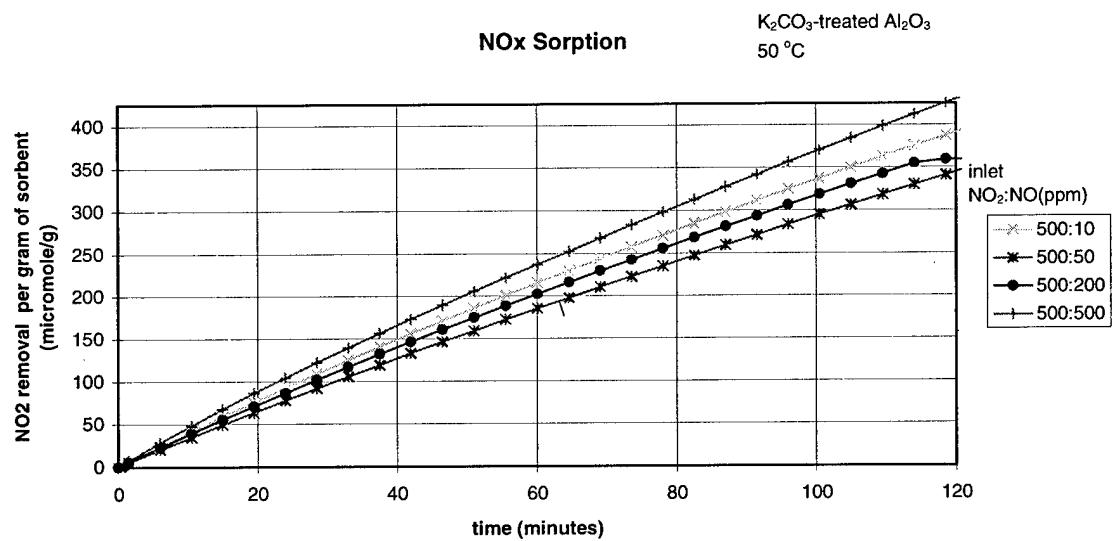
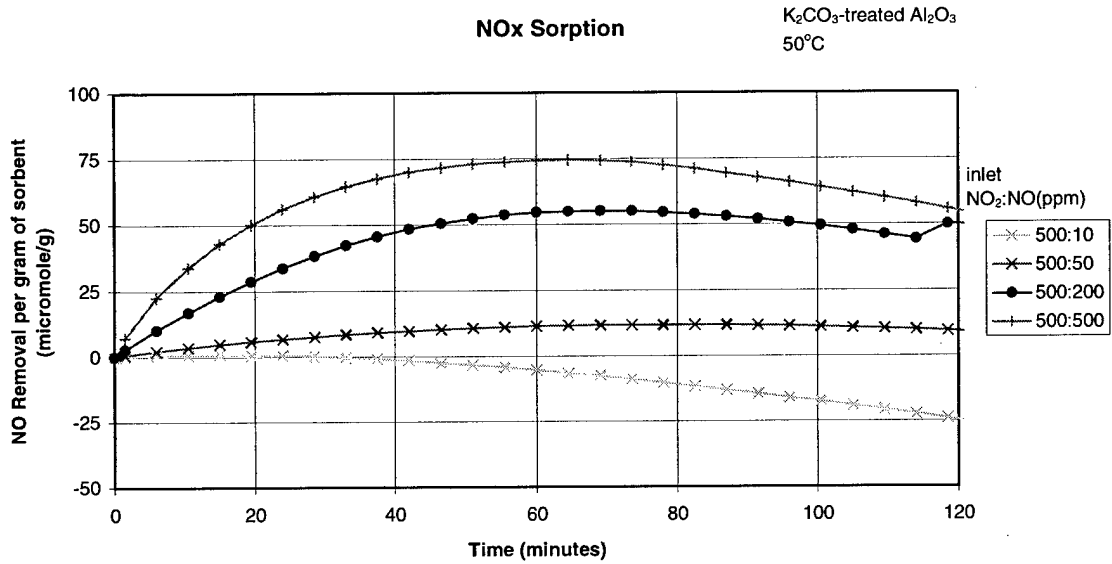
K₂CO₃-treated alumina, 25 °C.



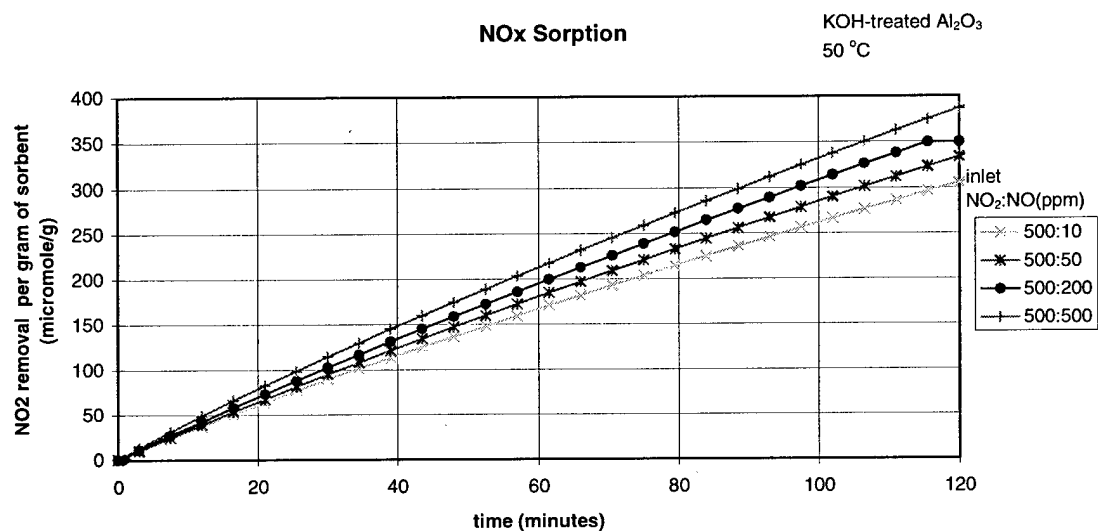
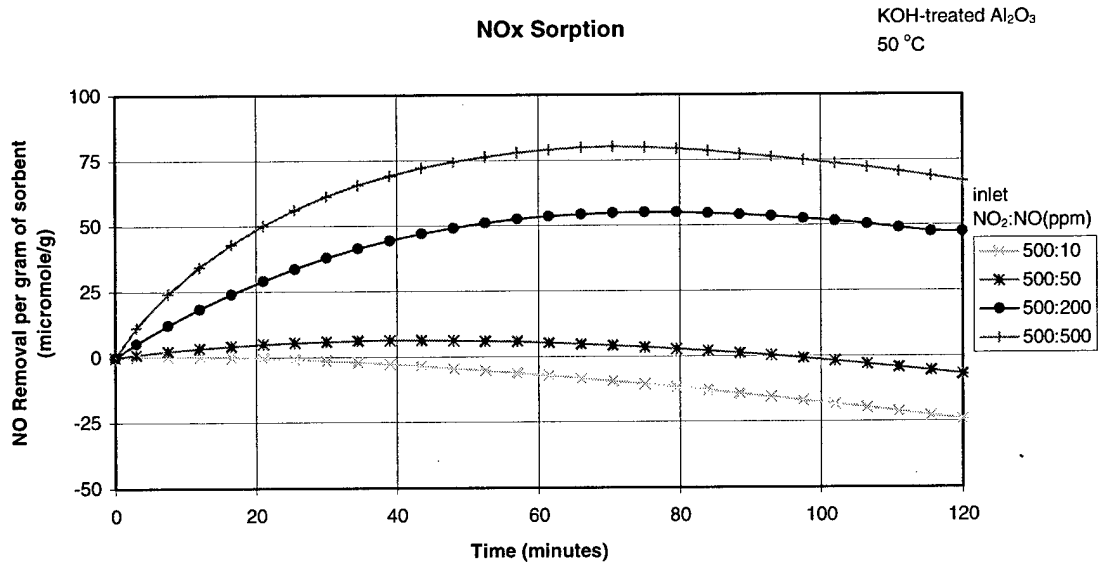
KOH-treated alumina, 25 °C.



Untreated alumina, 50 °C.



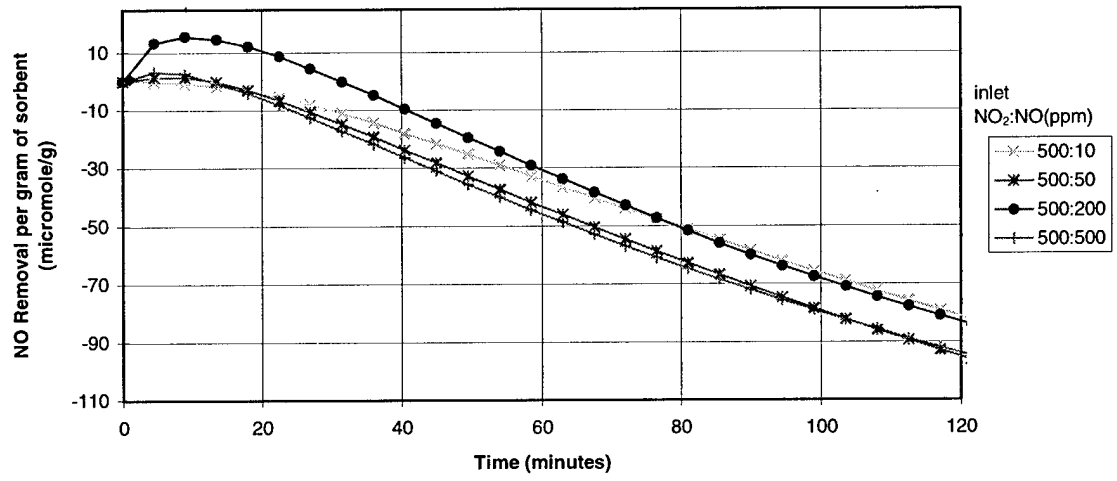
K₂CO₃-treated alumina, 50 °C.



KOH-treated alumina, 50 °C.

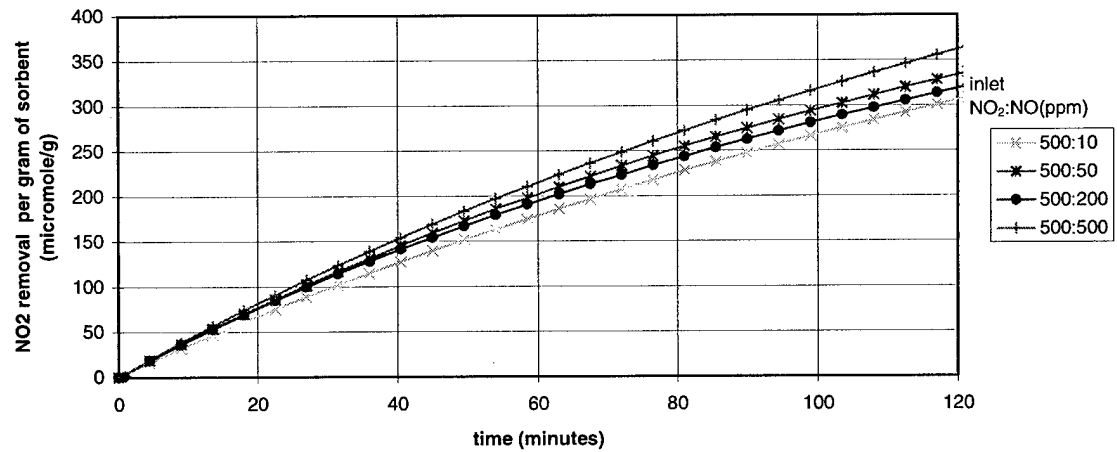
Nox Sorption

untreated Al₂O₃
100 °C

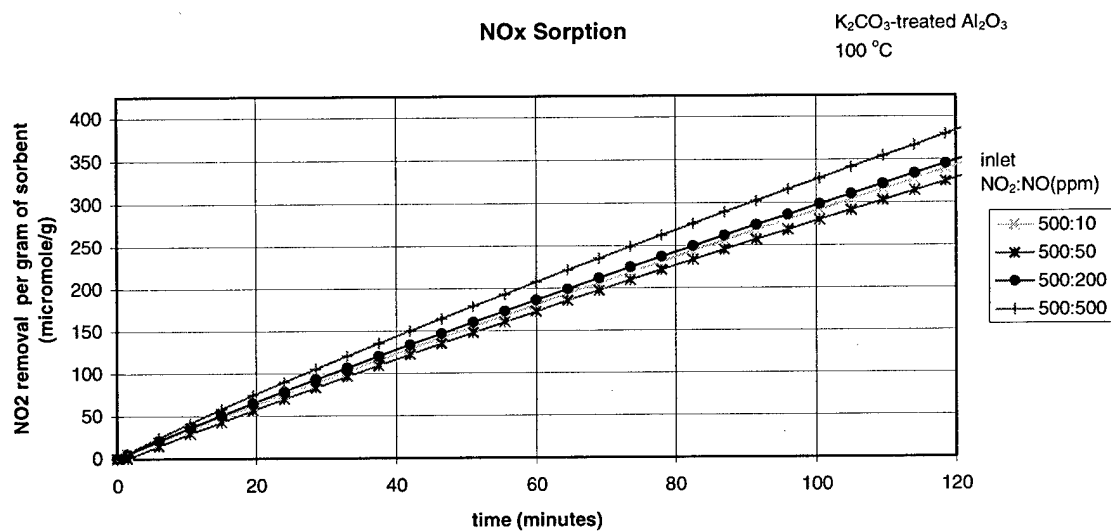
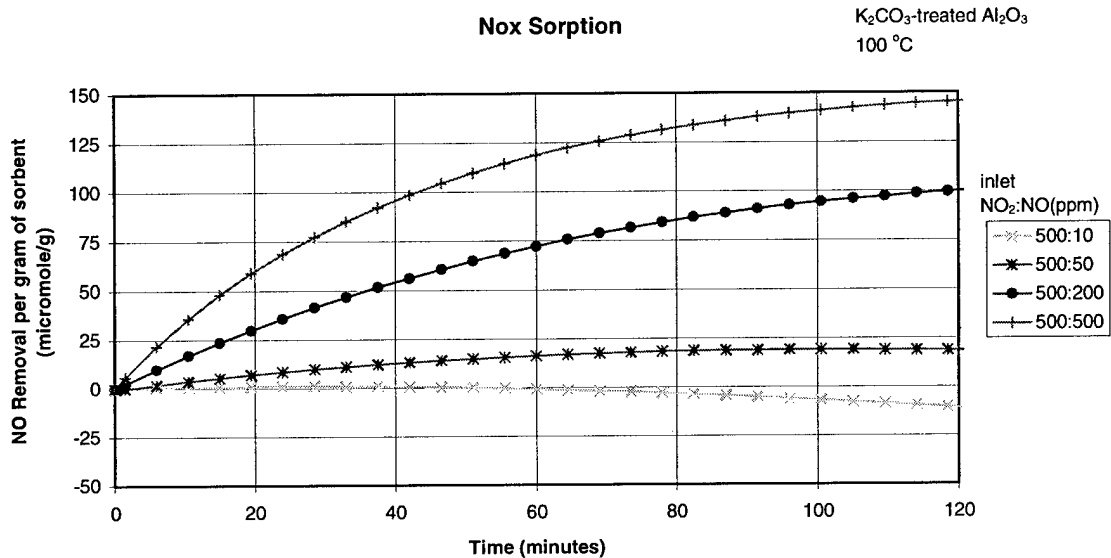


NO₂ Sorption

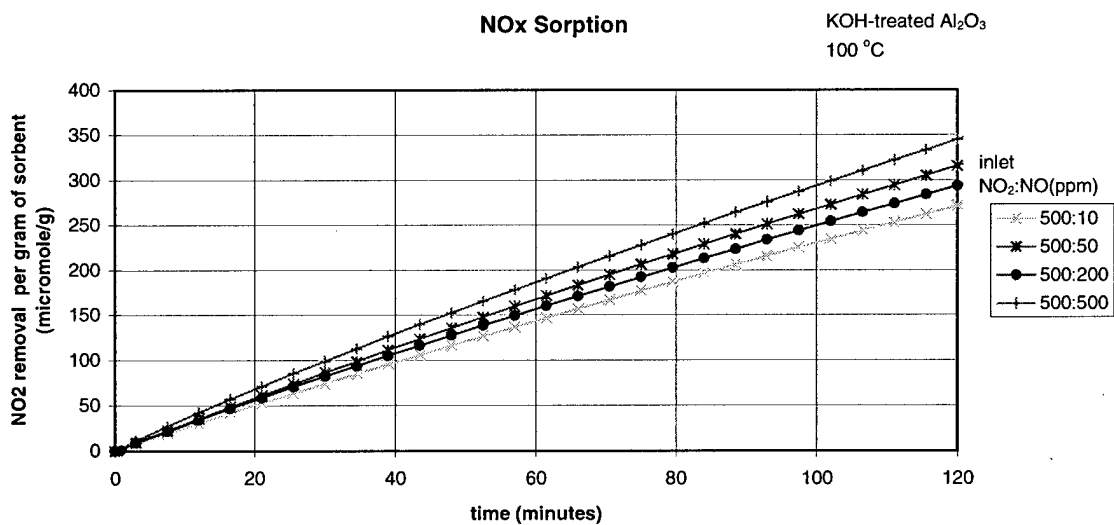
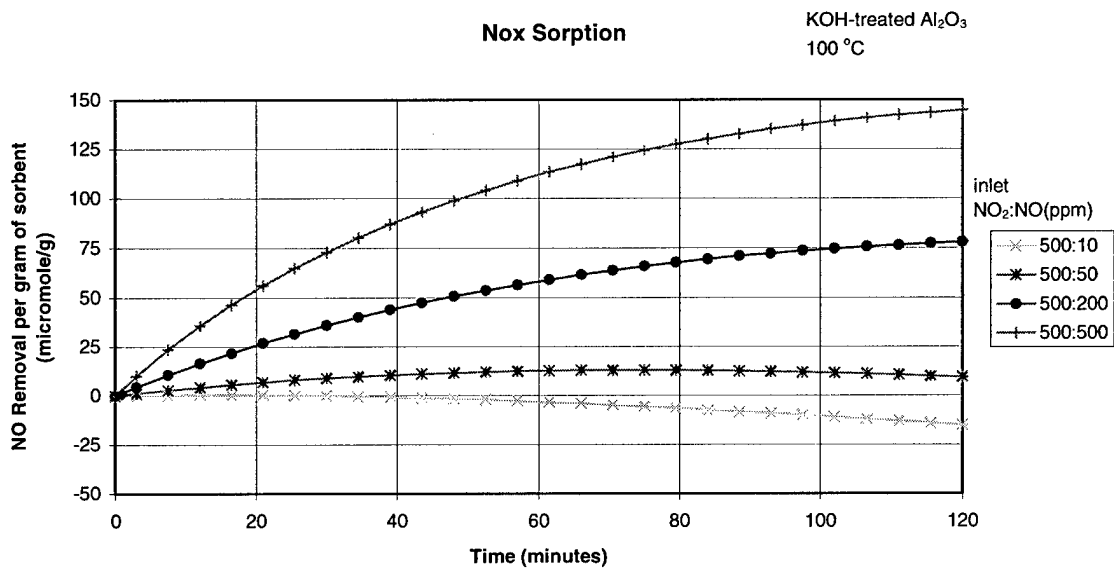
untreated Al₂O₃
100 °C



Untreated alumina, 100 °C.



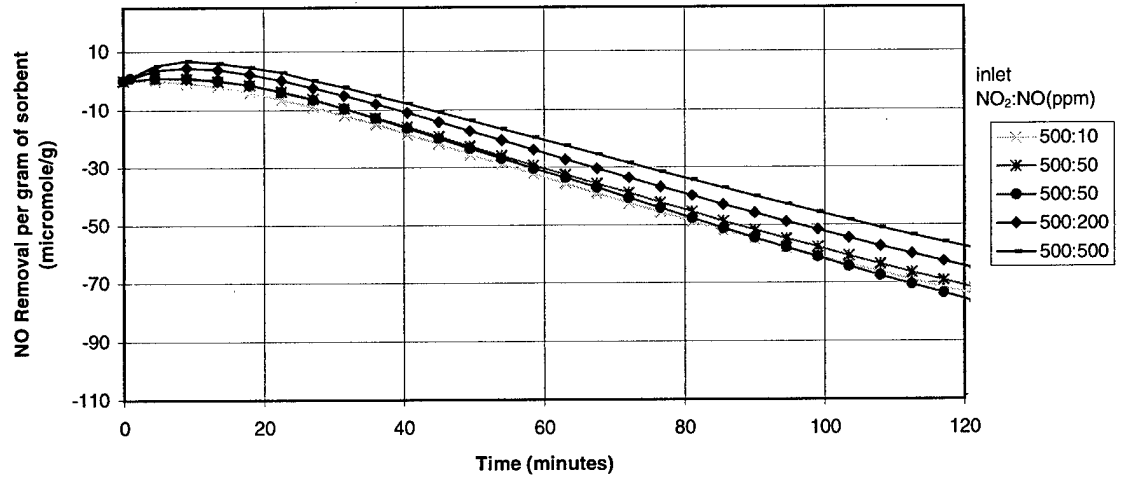
K₂CO₃-treated alumina, 100 °C.



KOH-treated alumina, 100 °C.

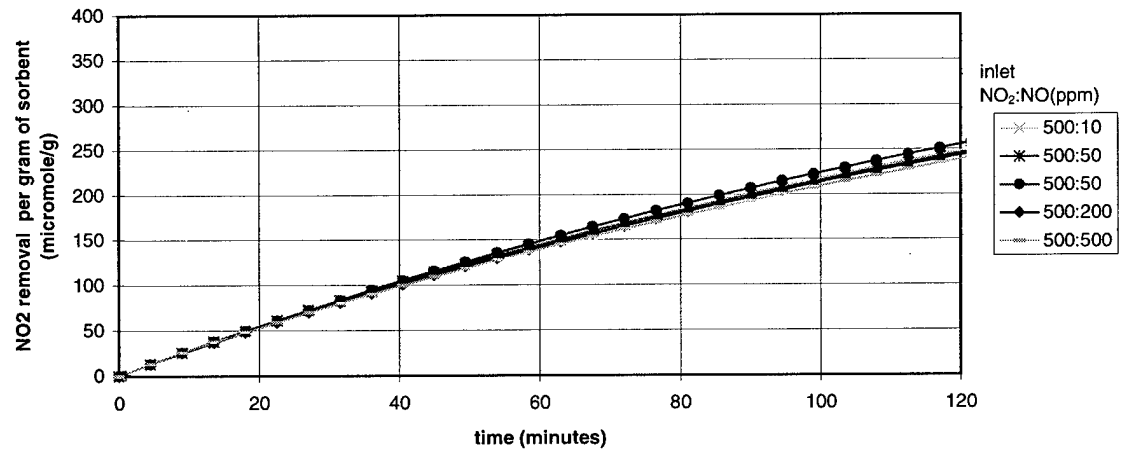
Nox Sorption

untreated Al_2O_3
200 °C

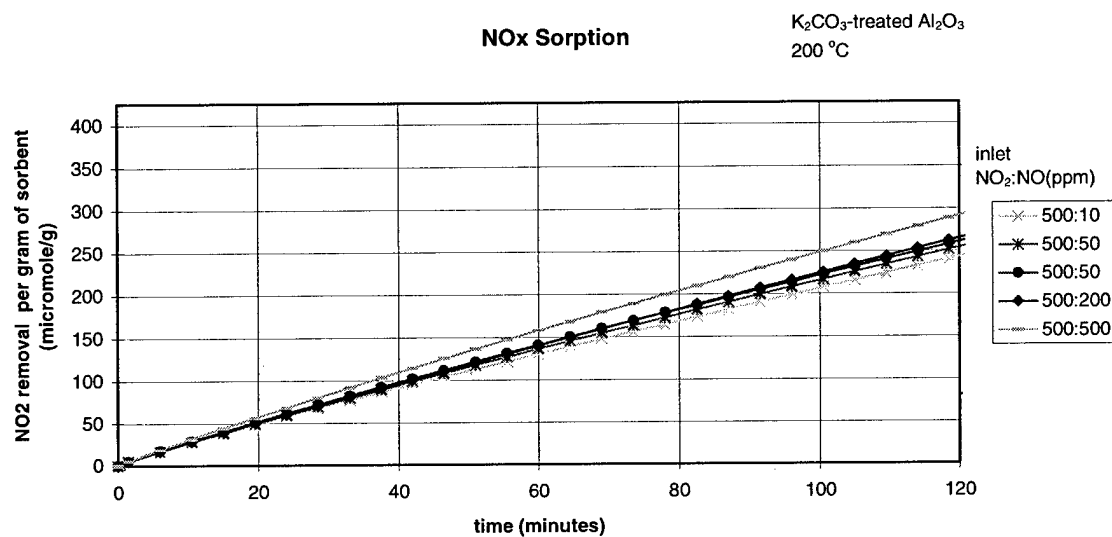
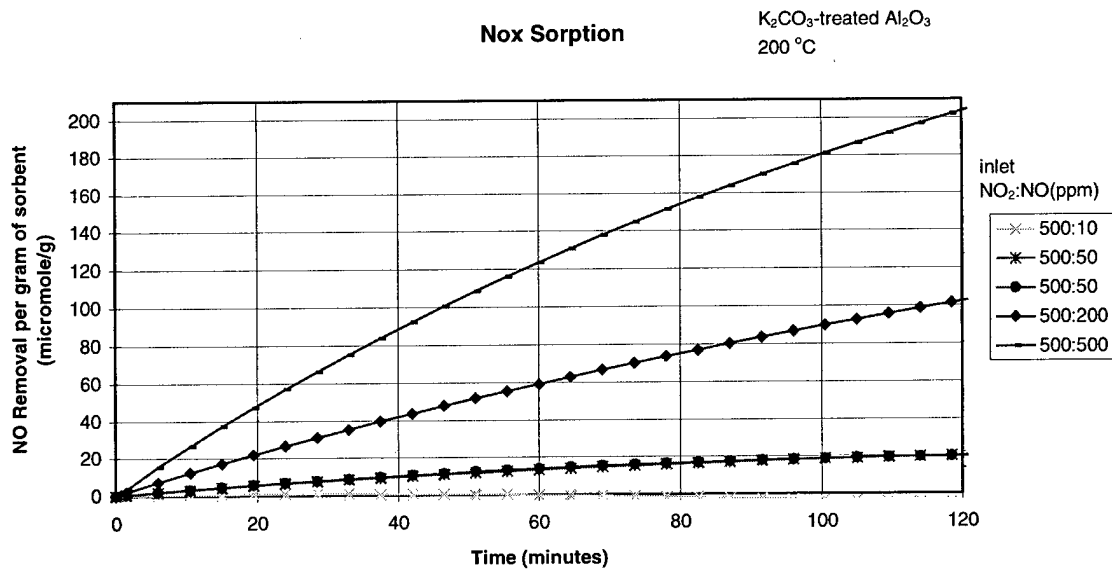


NO₂ Sorption

untreated Al_2O_3
200 °C



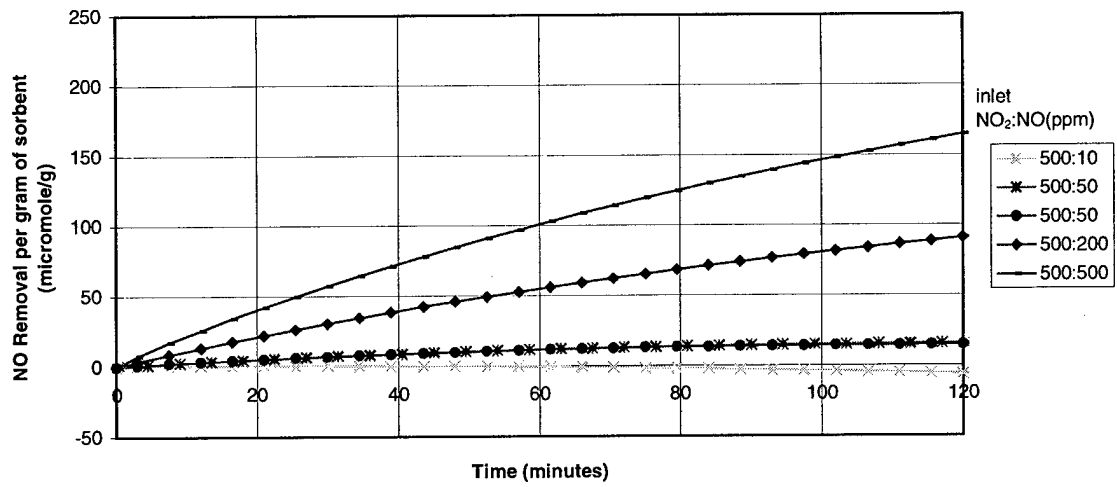
Untreated alumina, 200 °C.



K₂CO₃-treated alumina, 200 °C.

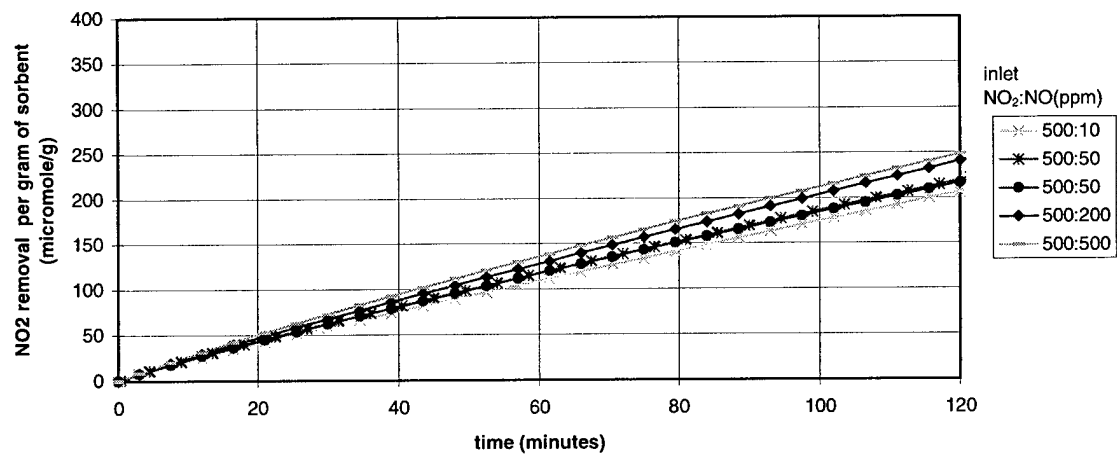
Nox Sorption

KOH-treated Al₂O₃
200 °C



NOx Sorption

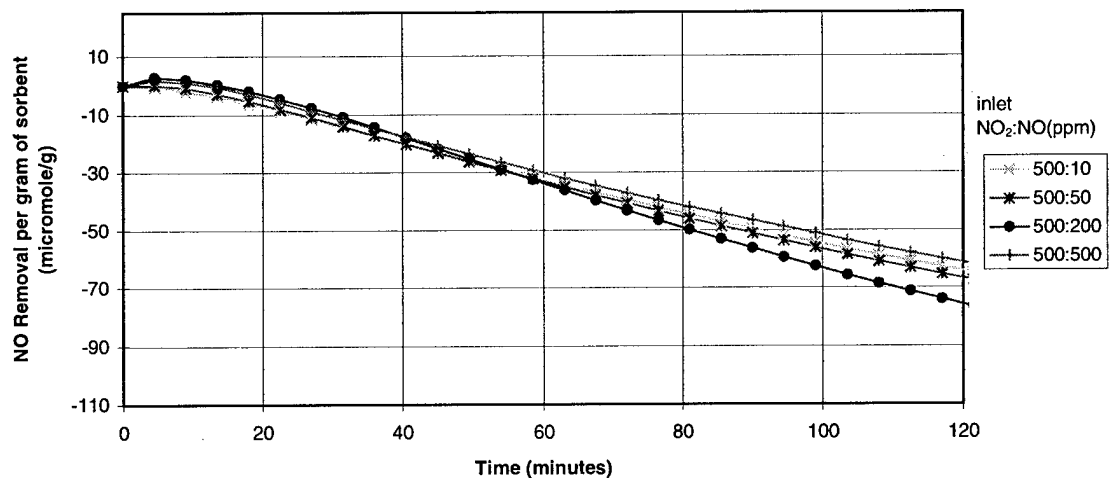
KOH-treated Al₂O₃
200 °C



KOH-treated alumina, 200 °C

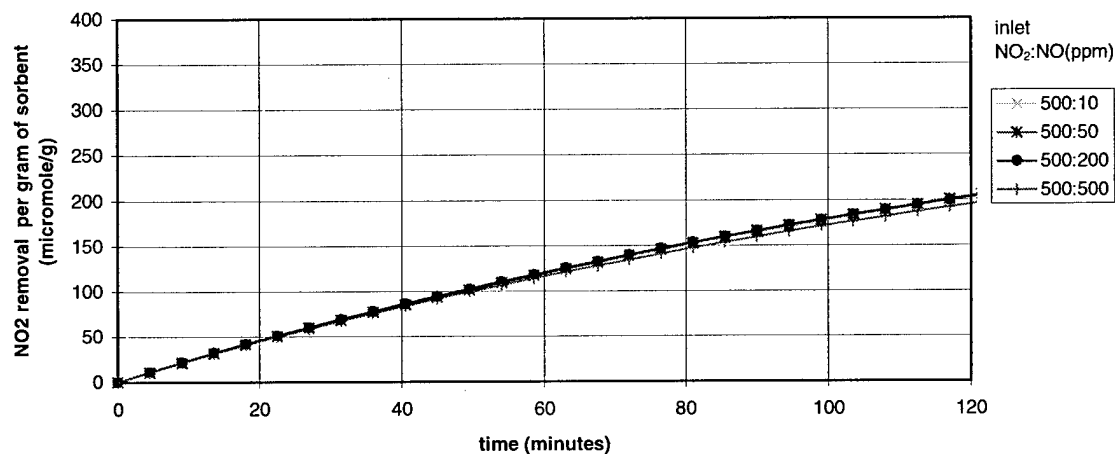
Nox Sorption

untreated Al₂O₃
250 °C

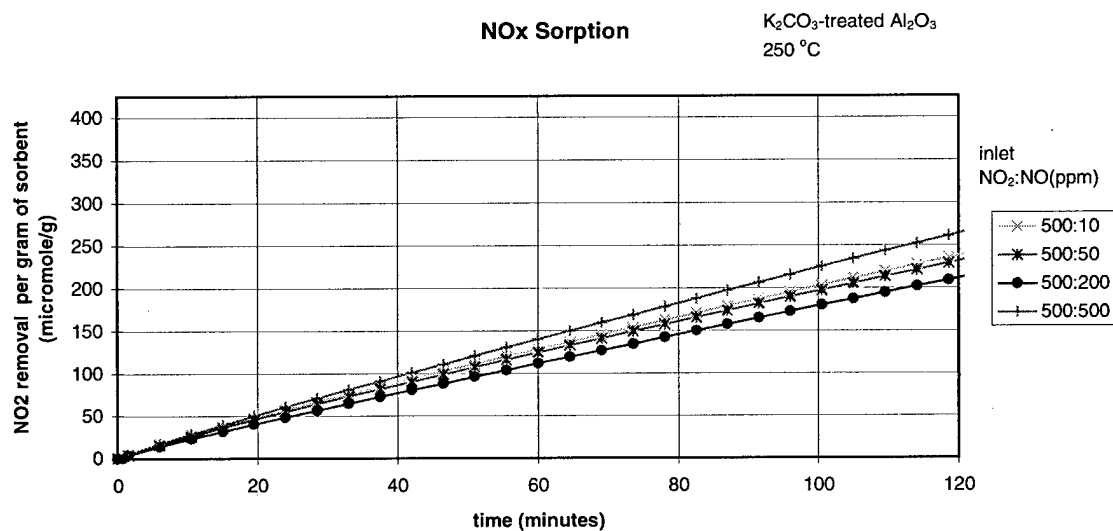
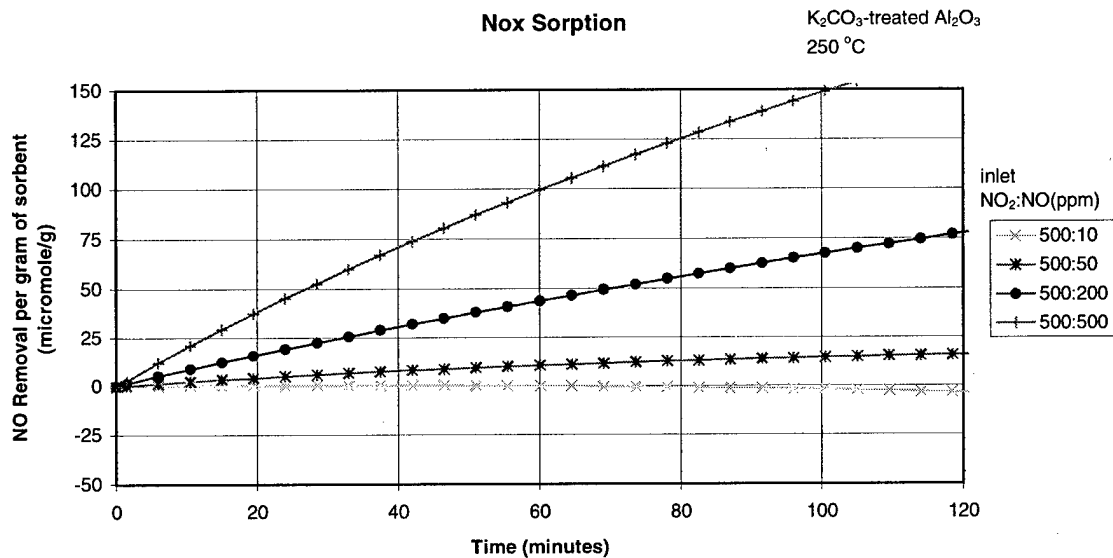


NO₂ Sorption

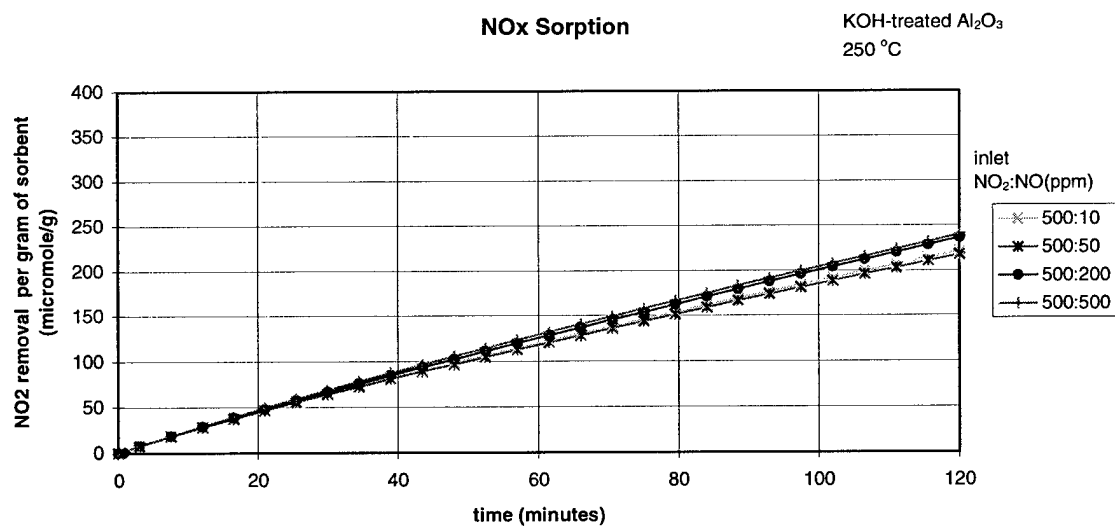
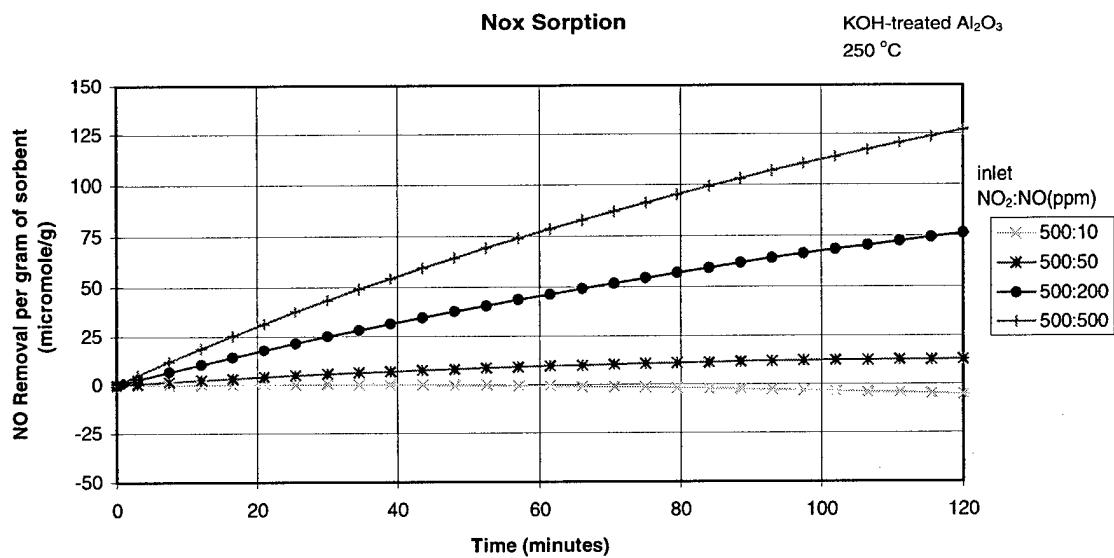
untreated Al₂O₃
250 °C



Untreated alumina, 250 °C.

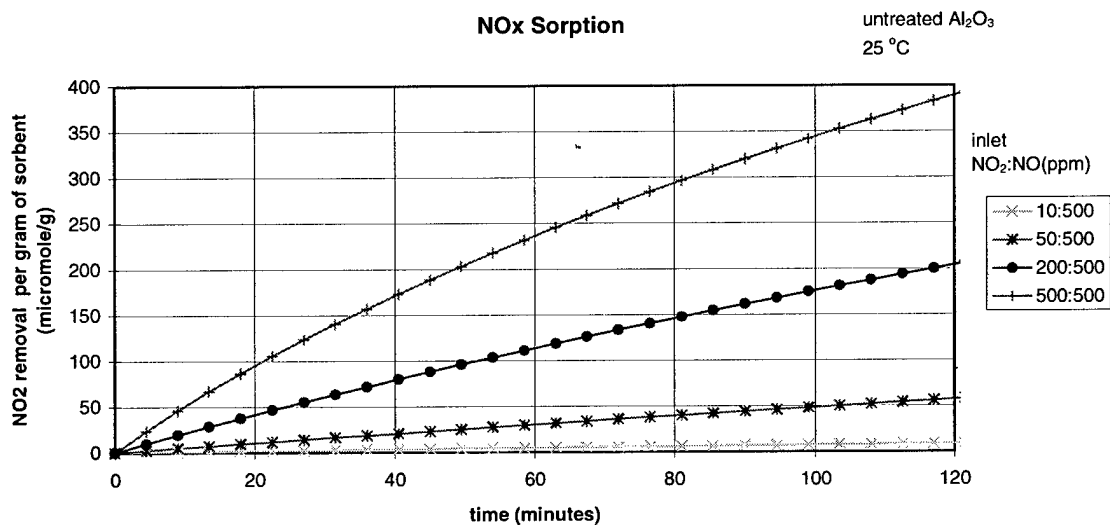
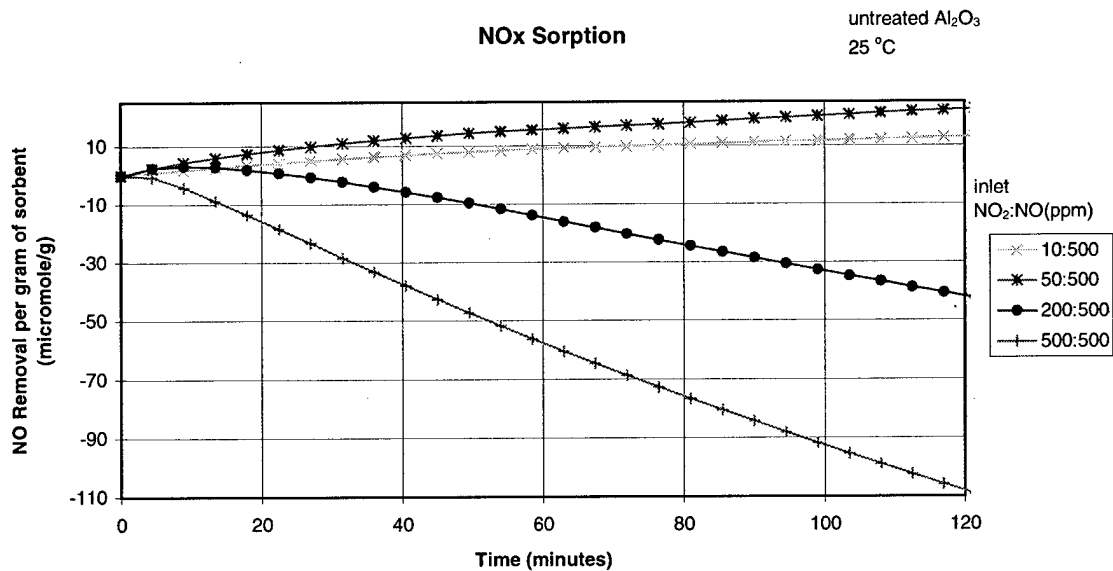


K₂CO₃-treated alumina, 250 °C.



KOH-treated alumina, 250 °C

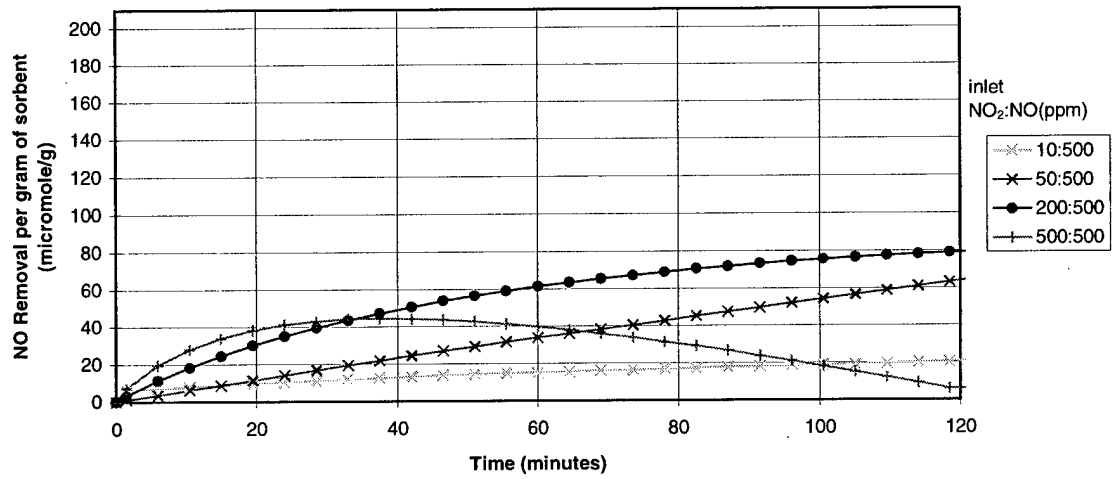
APPENDIX B
NOX SORPTION: CONSTANT NO (500 PPM), VARIED NO₂ CONCENTRATION



Untreated alumina, 25 °C.

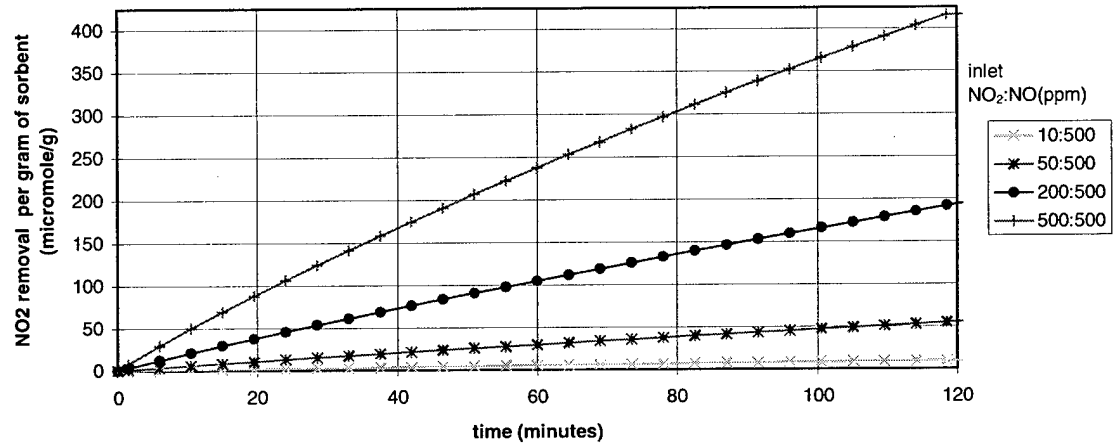
NOx Sorption

K₂CO₃-treated Al₂O₃
25 °C



NOx Sorption

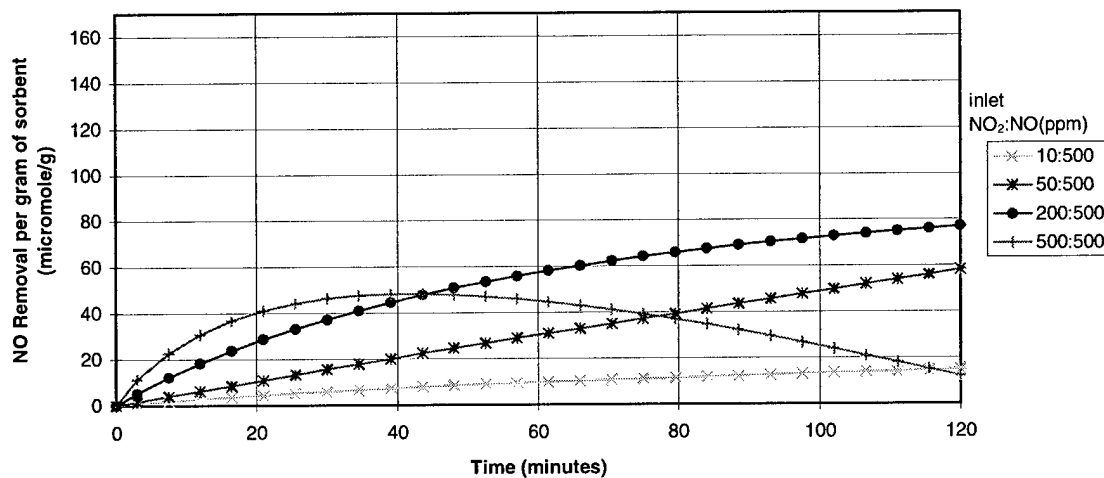
K₂CO₃-treated Al₂O₃
25 °C



. K₂CO₃-treated alumina, 25 °C.

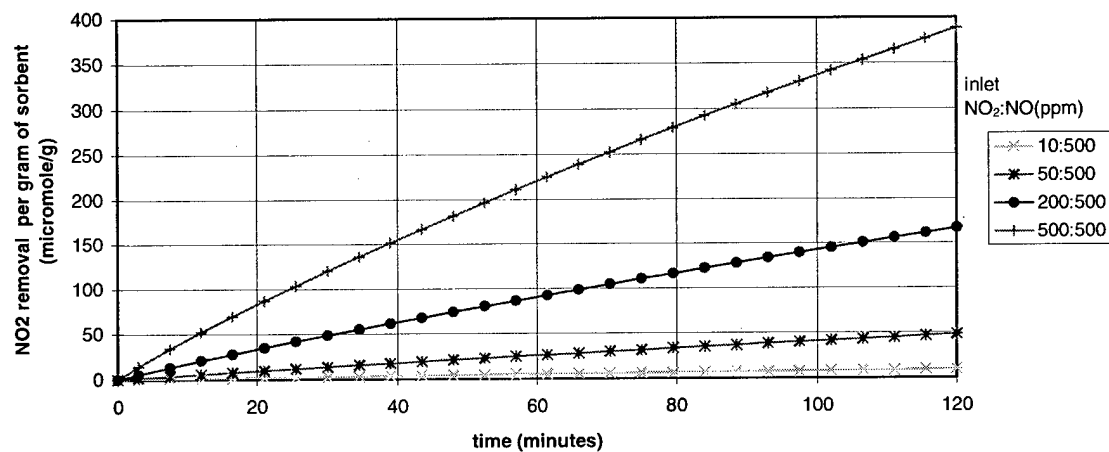
NOx Sorption

KOH-treated Al₂O₃
25 °C

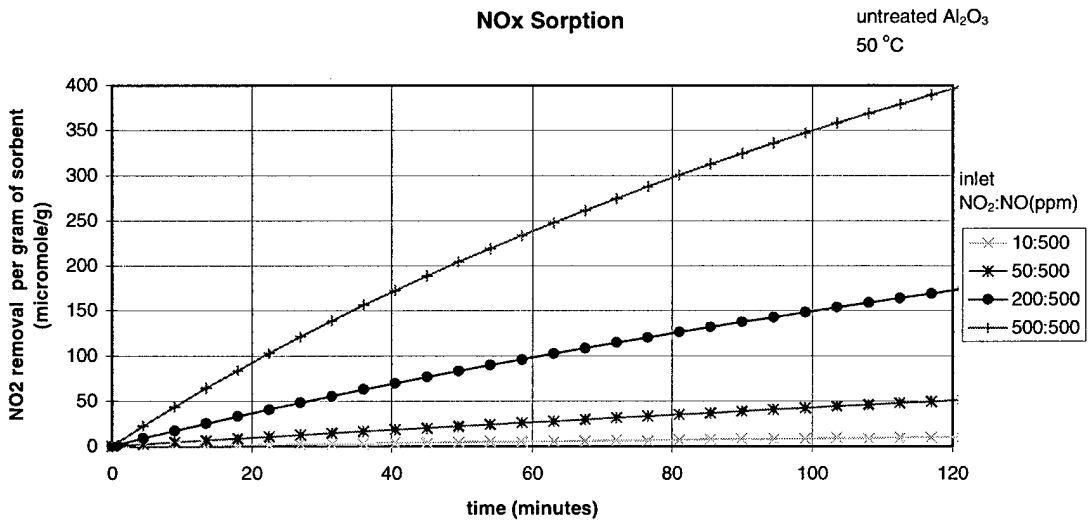
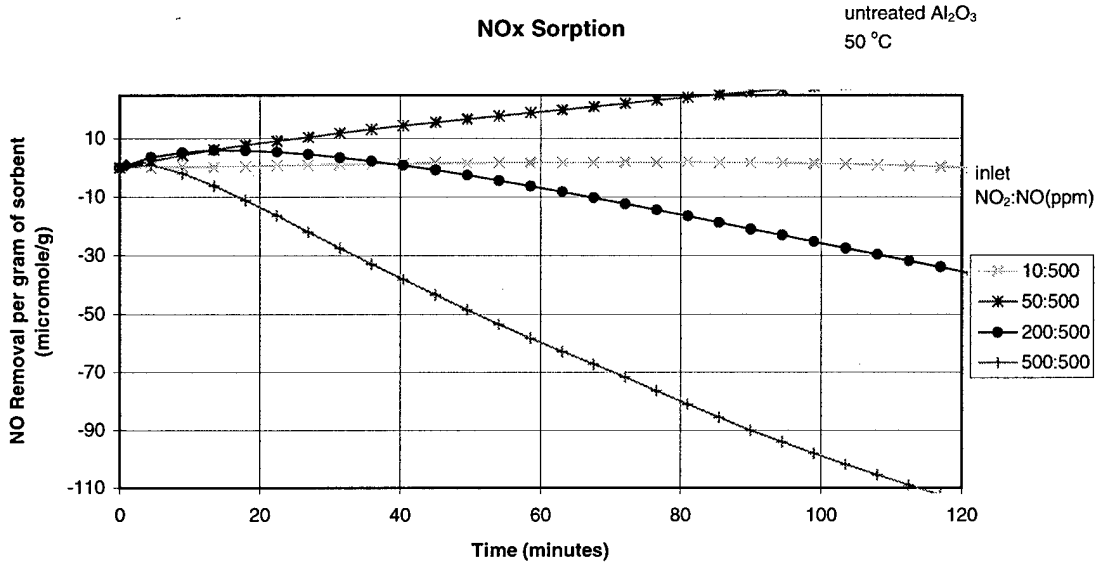


NOx Sorption

KOH-treated Al₂O₃
25 °C



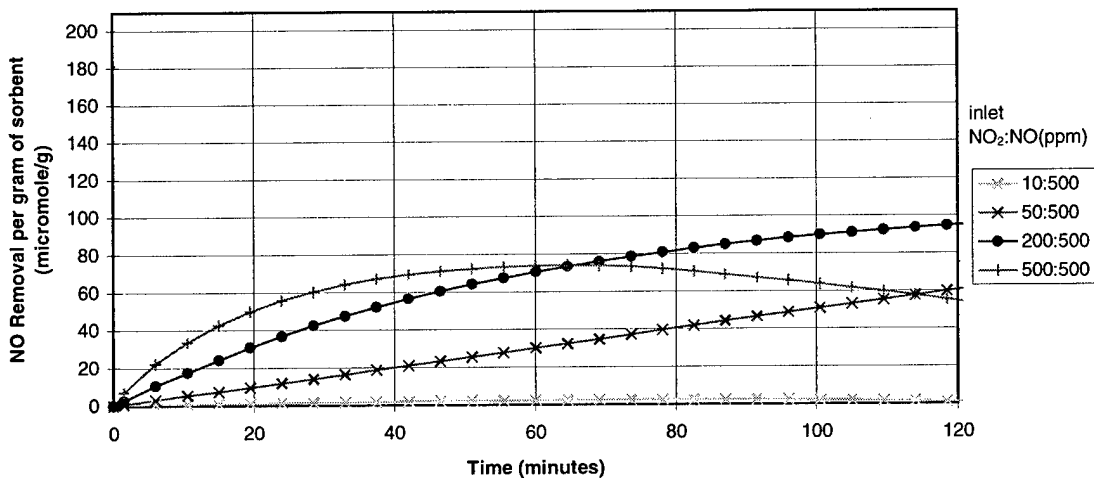
KOH-treated alumina, 25 °C.



untreated alumina, 50 °C.

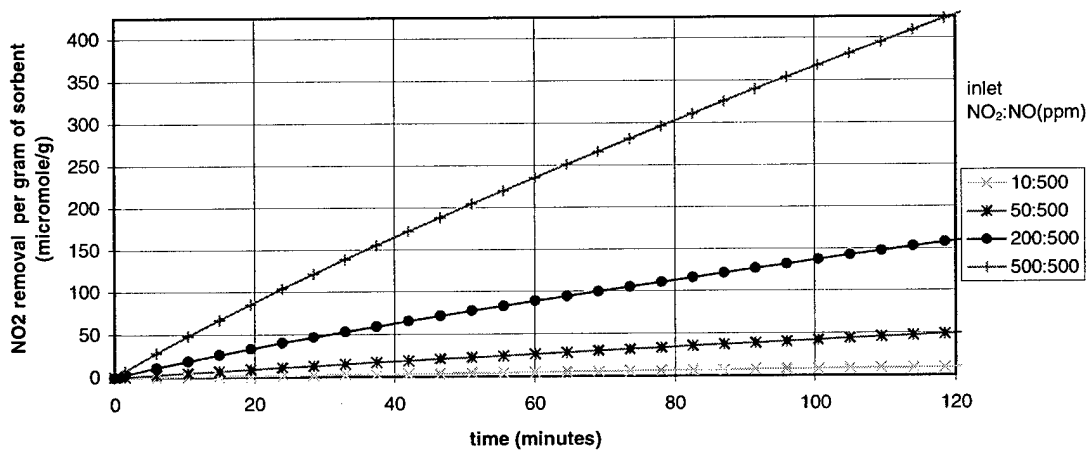
NOx Sorption

K₂CO₃-treated Al₂O₃
50 °C



NOx Sorption

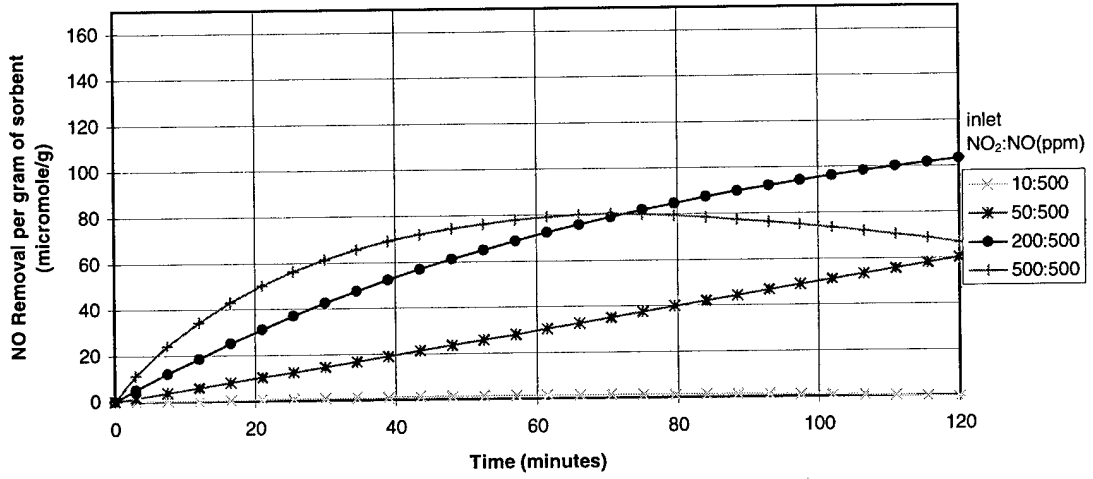
K₂CO₃-treated Al₂O₃
50 °C



K₂CO₃-treated alumina, 50 °C.

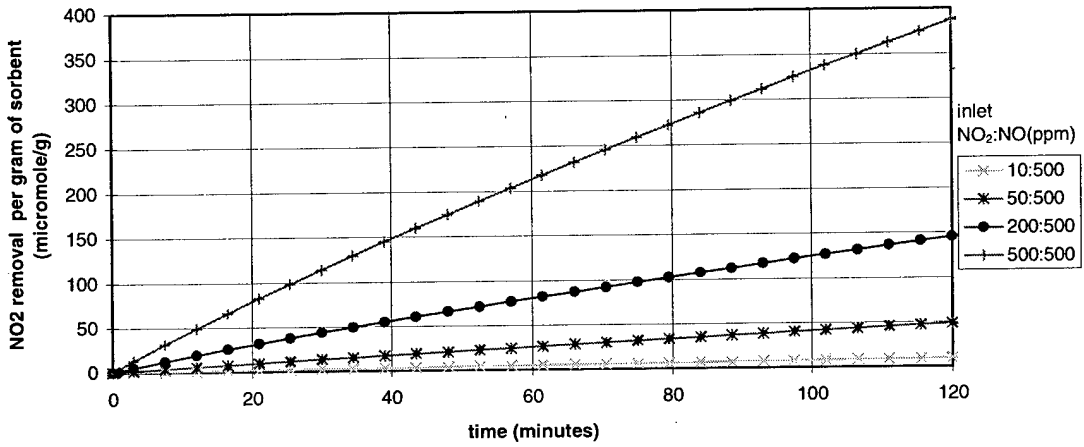
NOx Sorption

KOH-treated Al₂O₃
50 °C



NOx Sorption

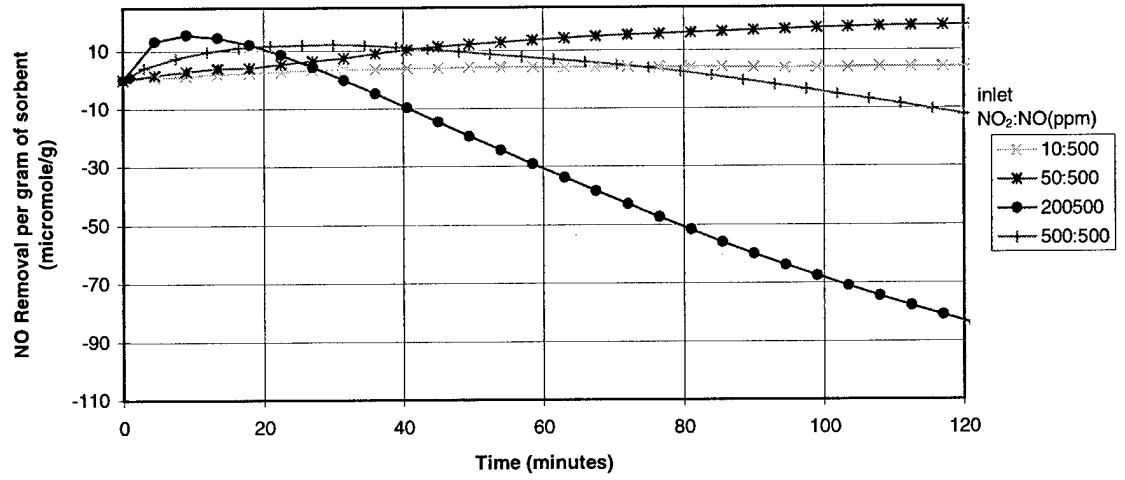
KOH-treated Al₂O₃
50 °C



KOH-treated alumina, 50 °C.

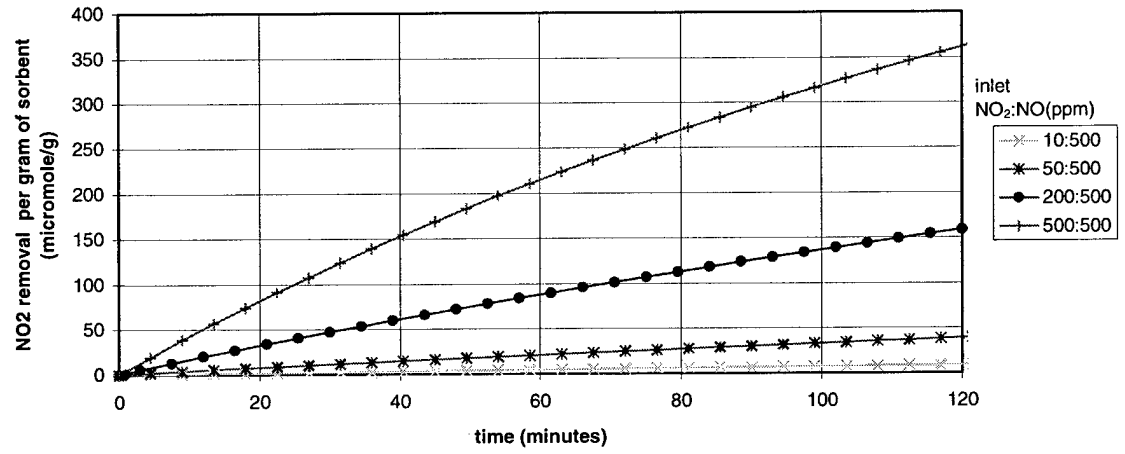
Nox Sorption

untreated Al₂O₃
100 °C



NO₂ Sorption

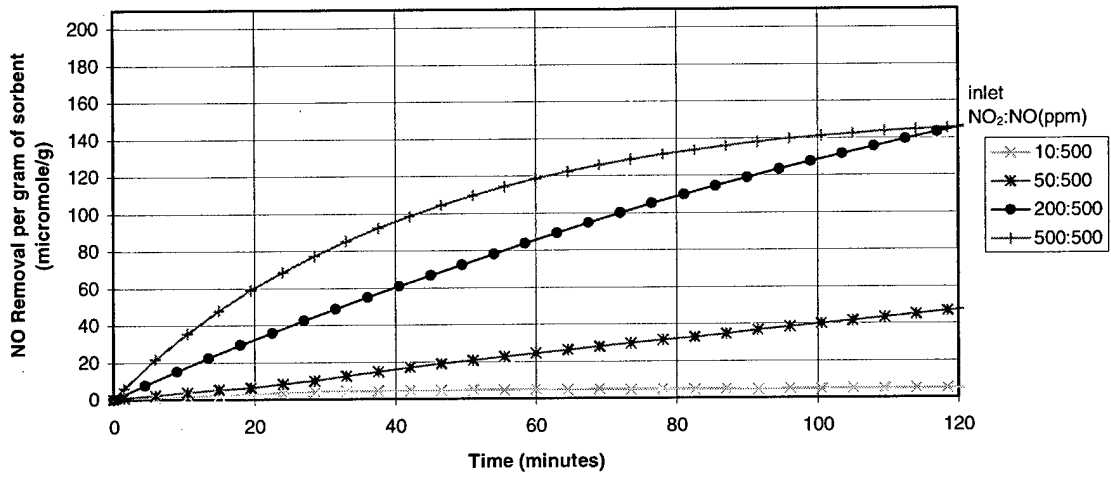
untreated Al₂O₃
100 °C



Untreated alumina, 100 °C.

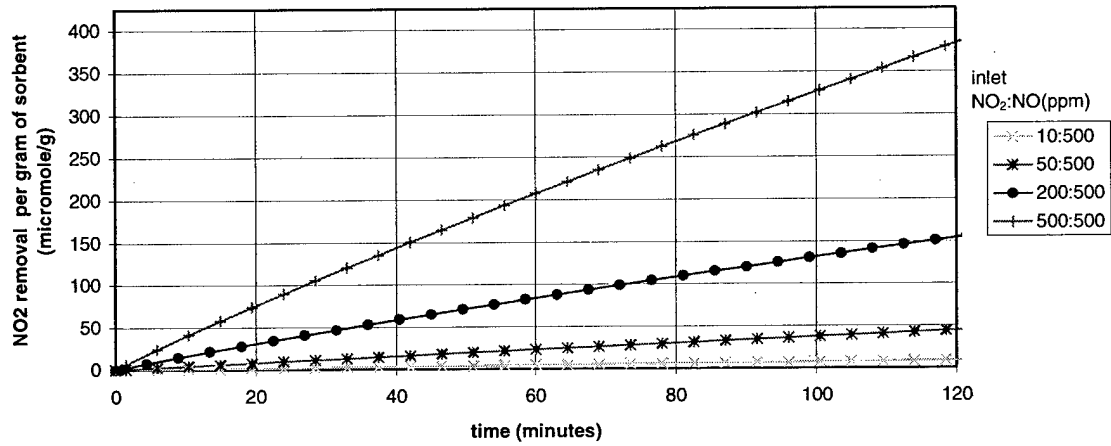
Nox Sorption

K₂CO₃-treated Al₂O₃
100 °C



NO₂ Sorption

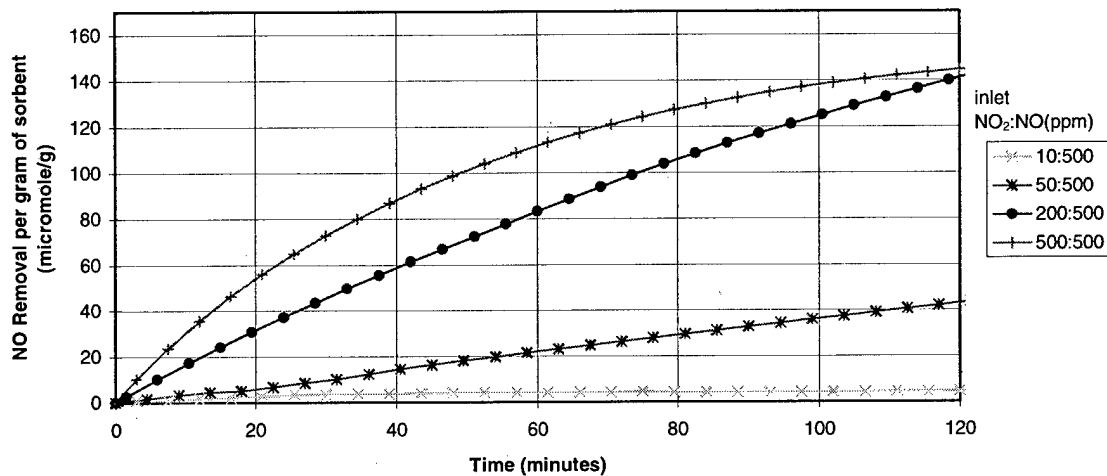
K₂CO₃-treated Al₂O₃
100 °C



K₂CO₃-treated alumina, 100 °C.

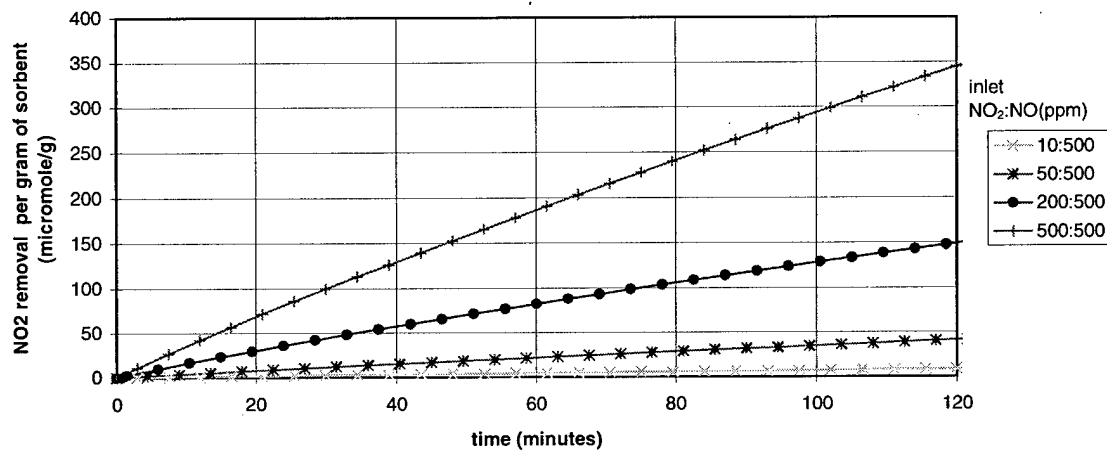
Nox Sorption

KOH-treated Al₂O₃
100 °C

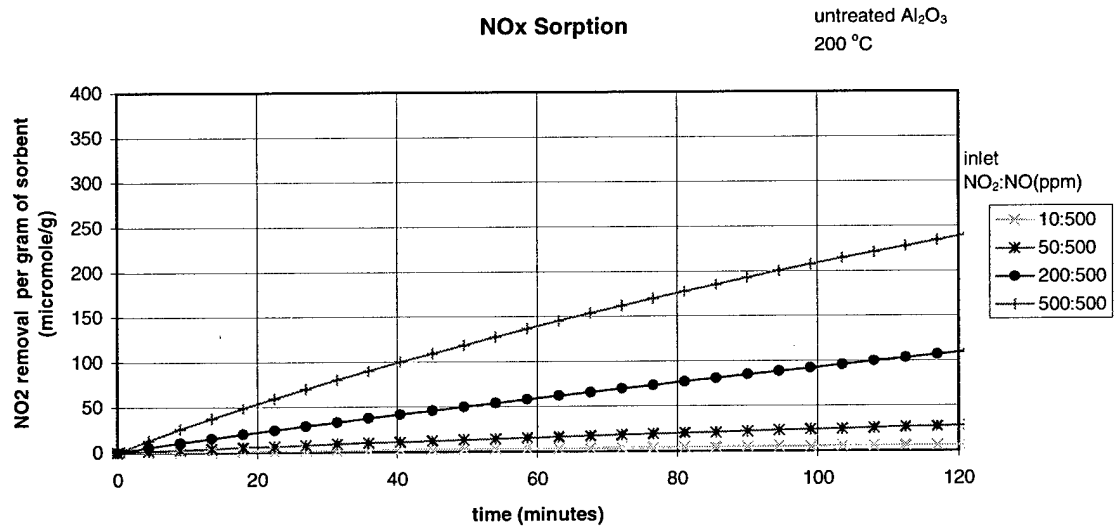
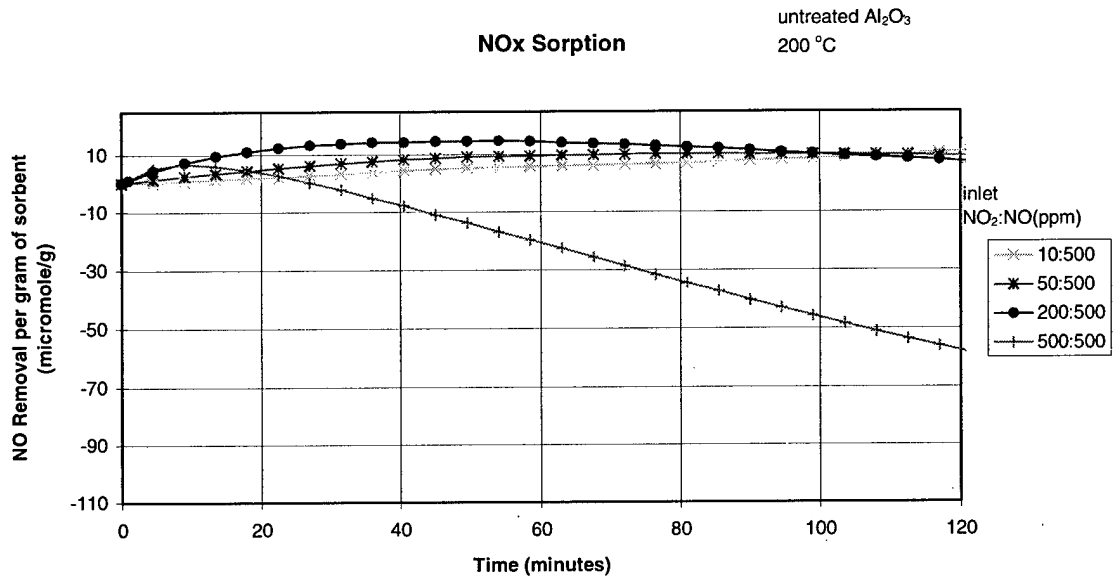


NO_x Sorption

KOH-treated Al₂O₃
100 °C



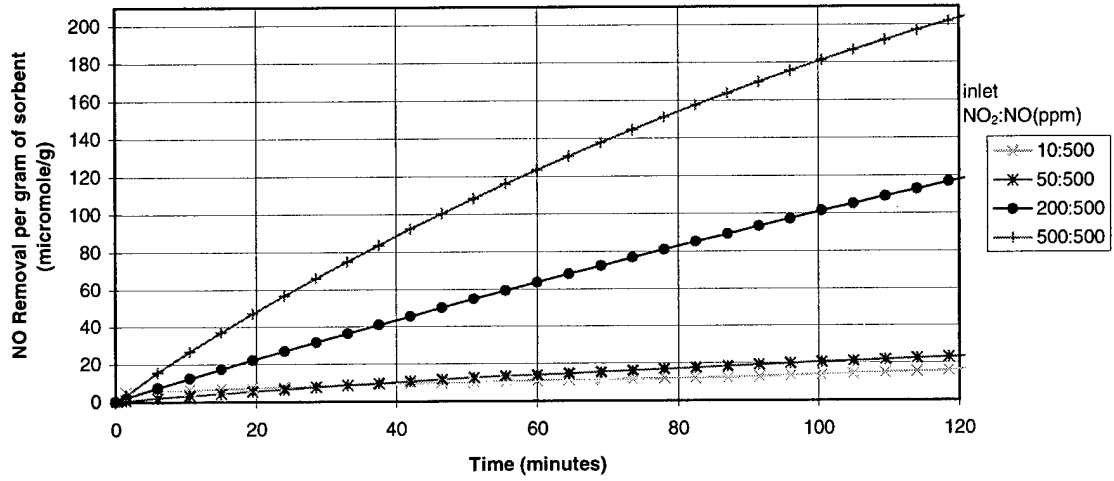
KOH-treated alumina, 100 °C.



Untreated alumina, 200 °C.

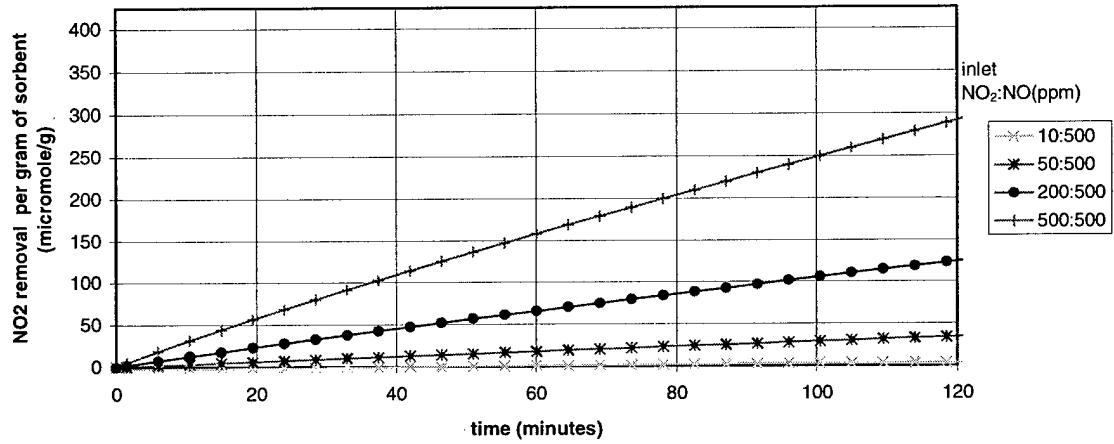
Nox Sorption

K_2CO_3 -treated Al_2O_3
200 °C



NOx Sorption

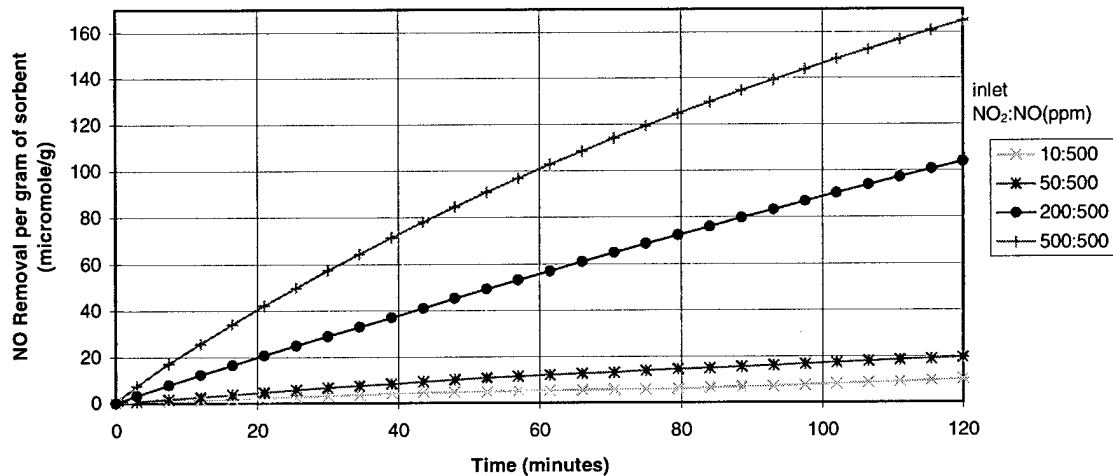
K_2CO_3 -treated Al_2O_3
200 °C



K_2CO_3 -treated alumina, 200 °C.

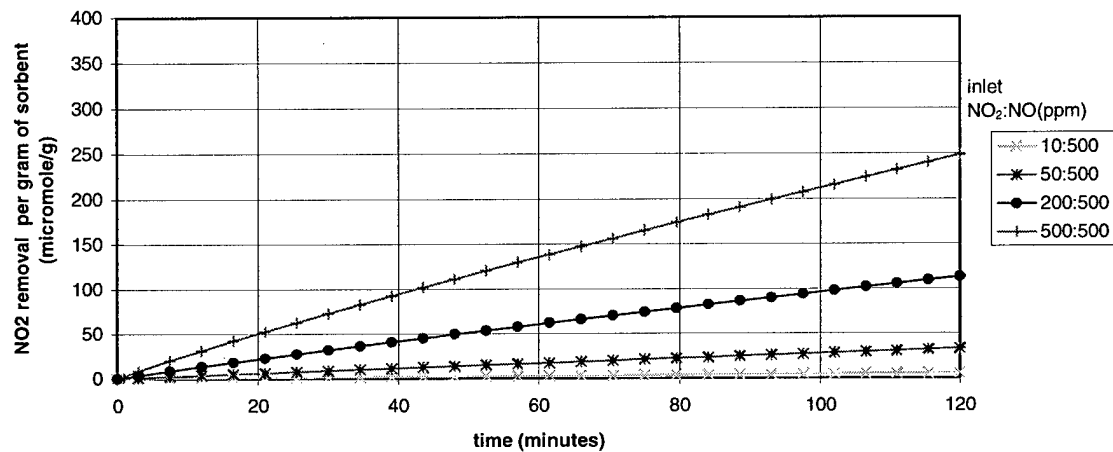
Nox Sorption

KOH-treated Al₂O₃
200 °C

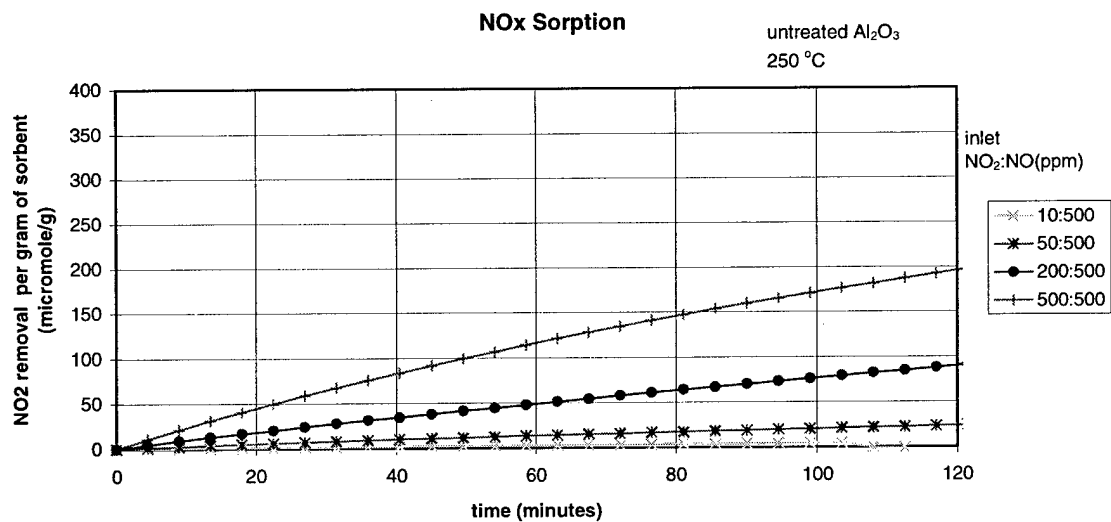
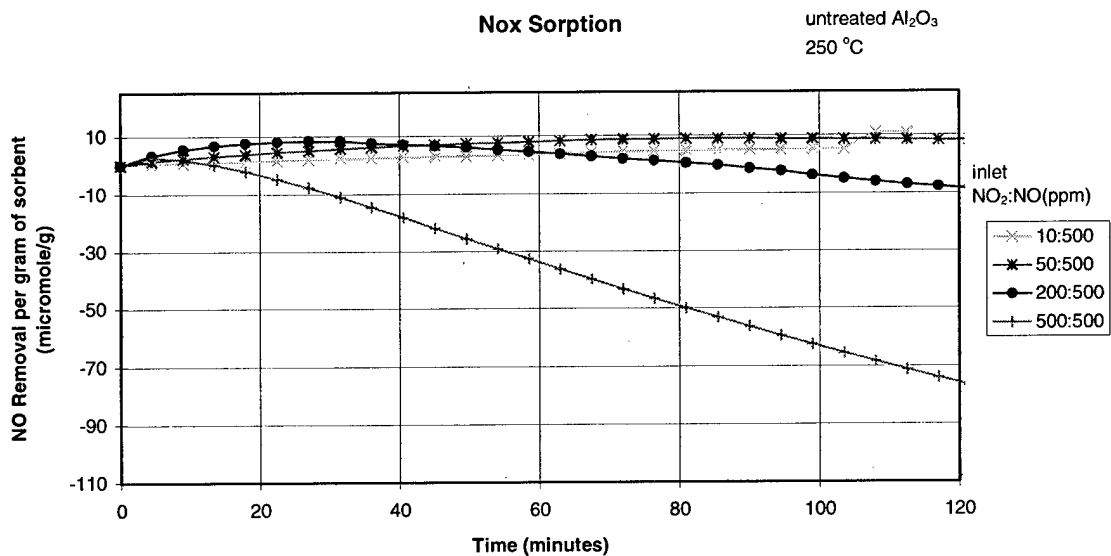


NO₂ Sorption

KOH-treated Al₂O₃
200 °C



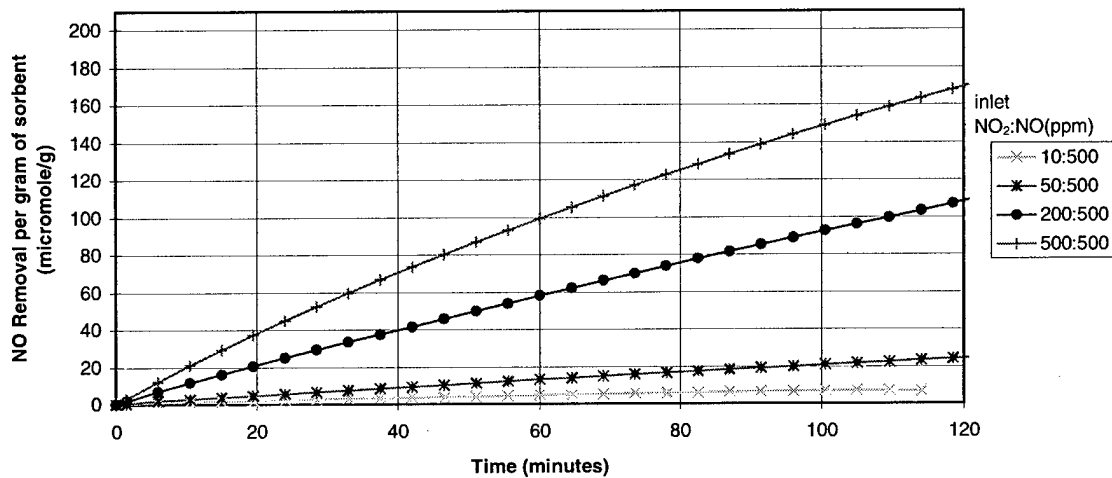
KOH-treated alumina, 200 °C.



Untreated alumina, 250 °C.

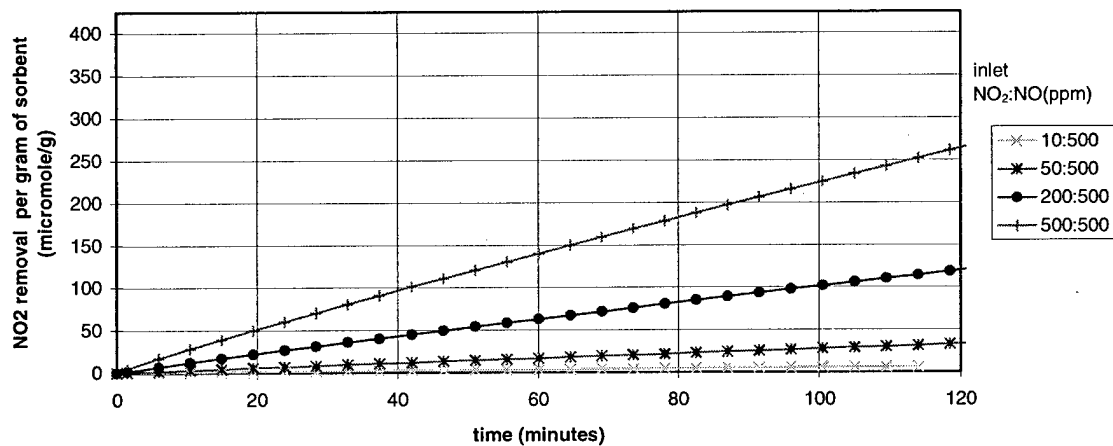
Nox Sorption

K_2CO_3 -treated Al_2O_3
250 °C



NOx Sorption

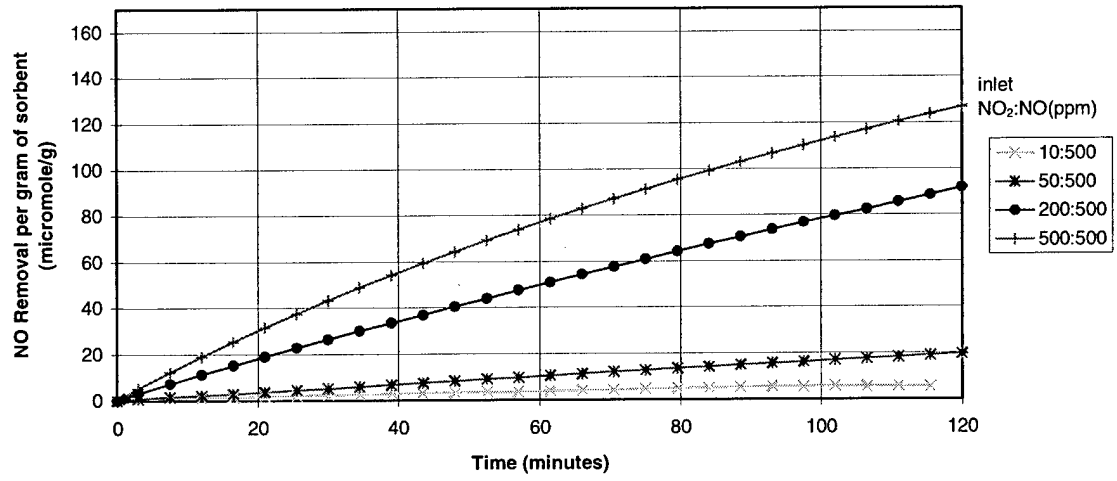
K_2CO_3 -treated Al_2O_3
250 °C



K_2CO_3 -treated alumina, 250 °C.

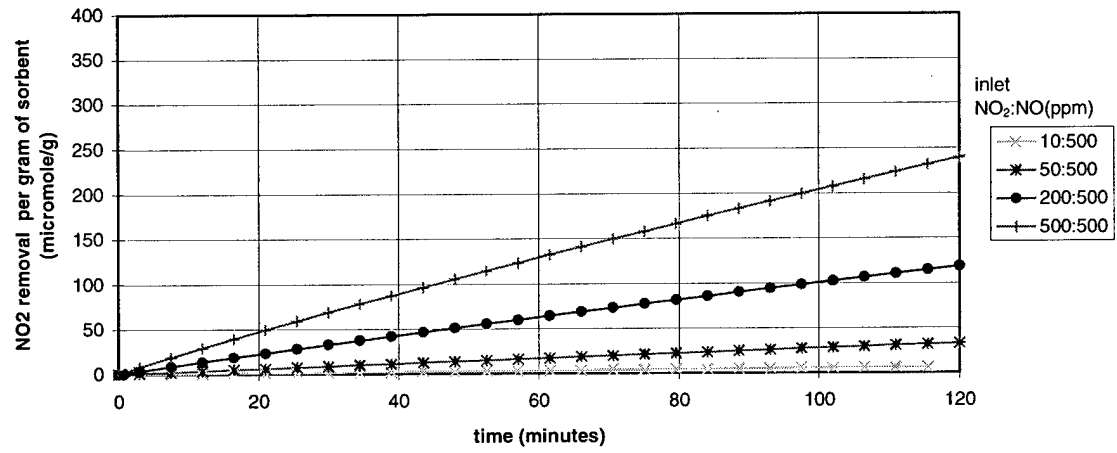
Nox Sorption

KOH-treated Al_2O_3
250 °C



NOx Sorption

KOH-treated Al_2O_3
250 °C

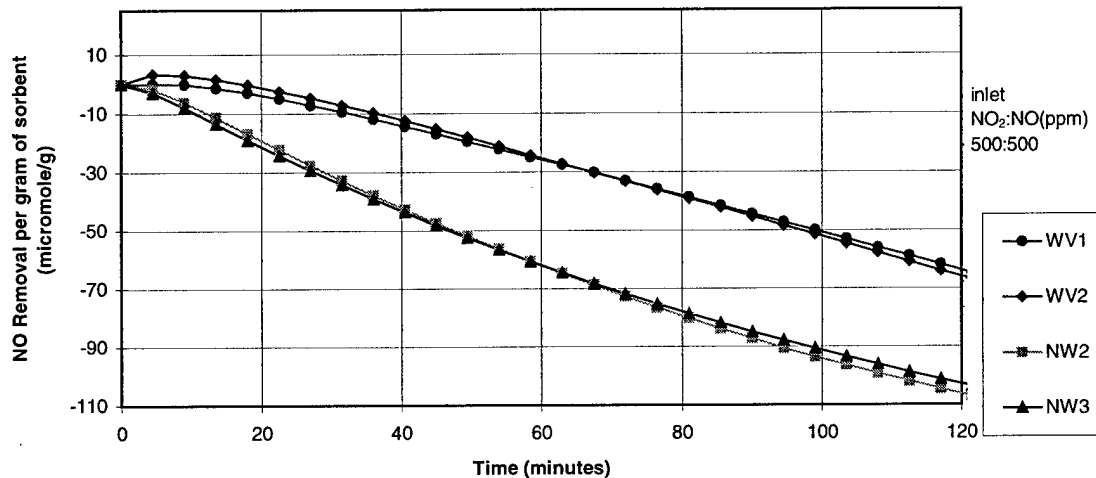


KOH-treated alumina, 250 °C.

APPENDIX C
ADDED GASES, SO₂ AND H₂O

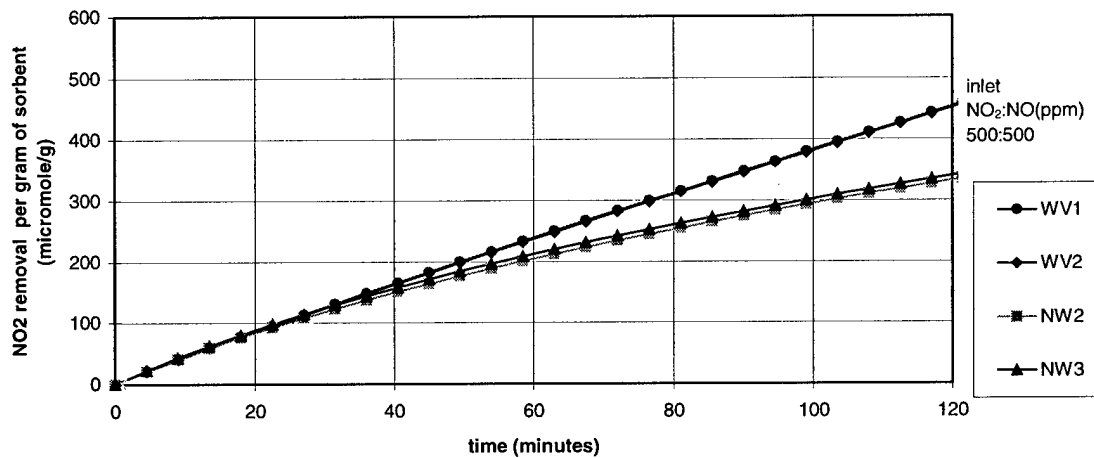
NOx Sorption

untreated Al₂O₃
25 °C

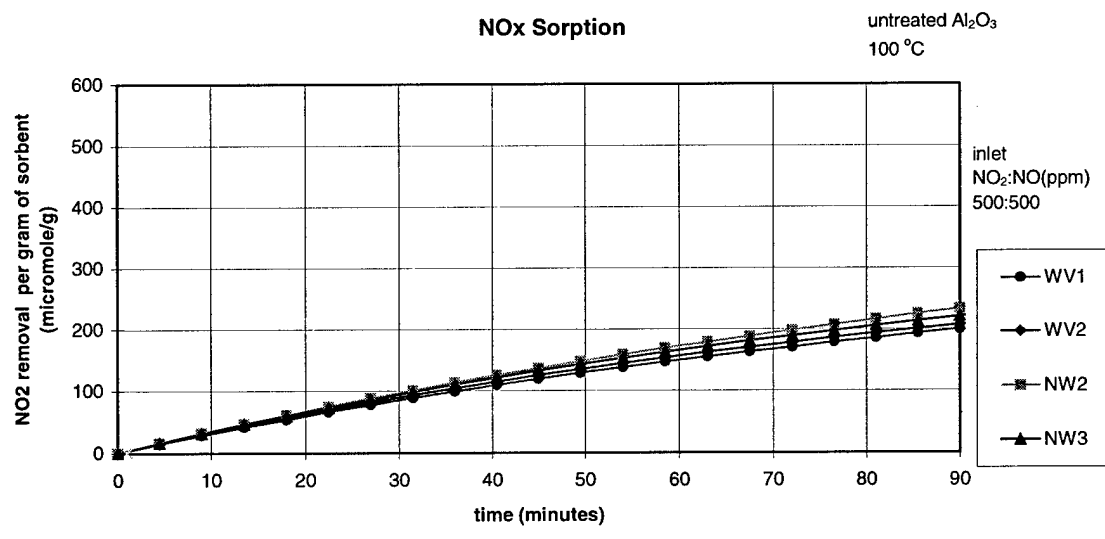
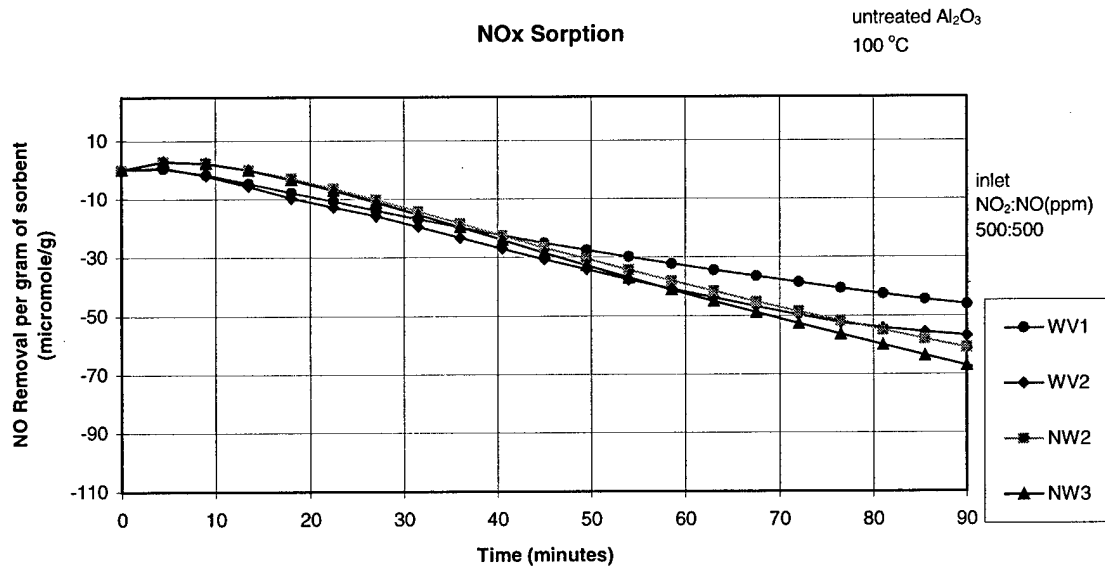


NOx Sorption

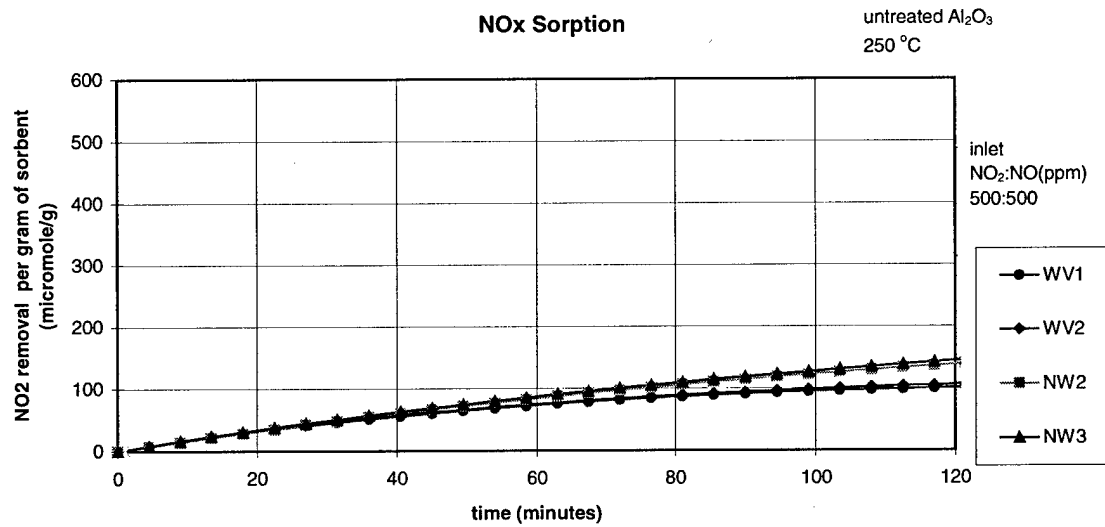
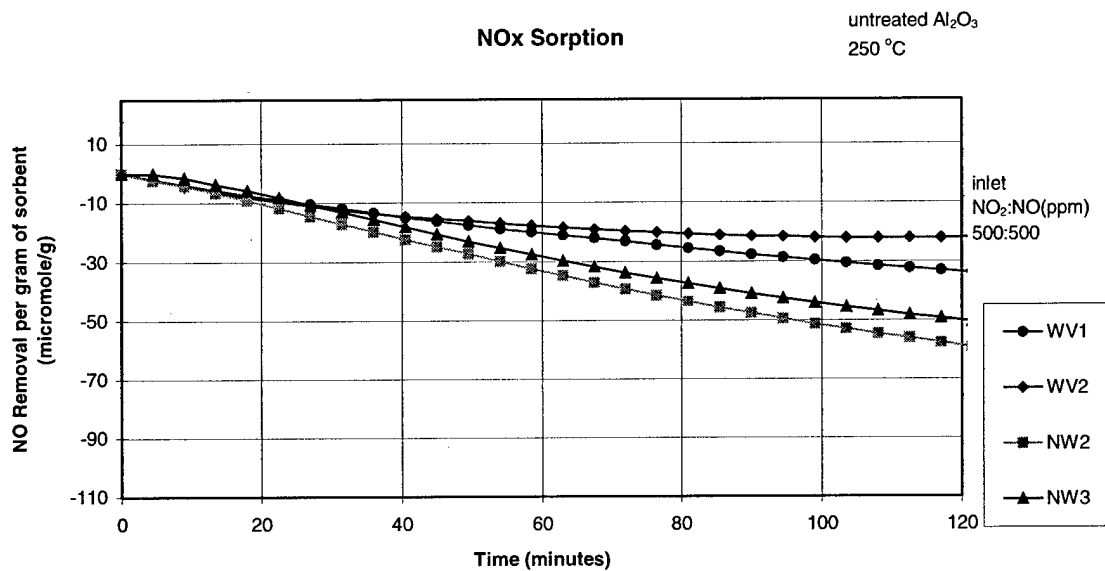
untreated Al₂O₃
25 °C



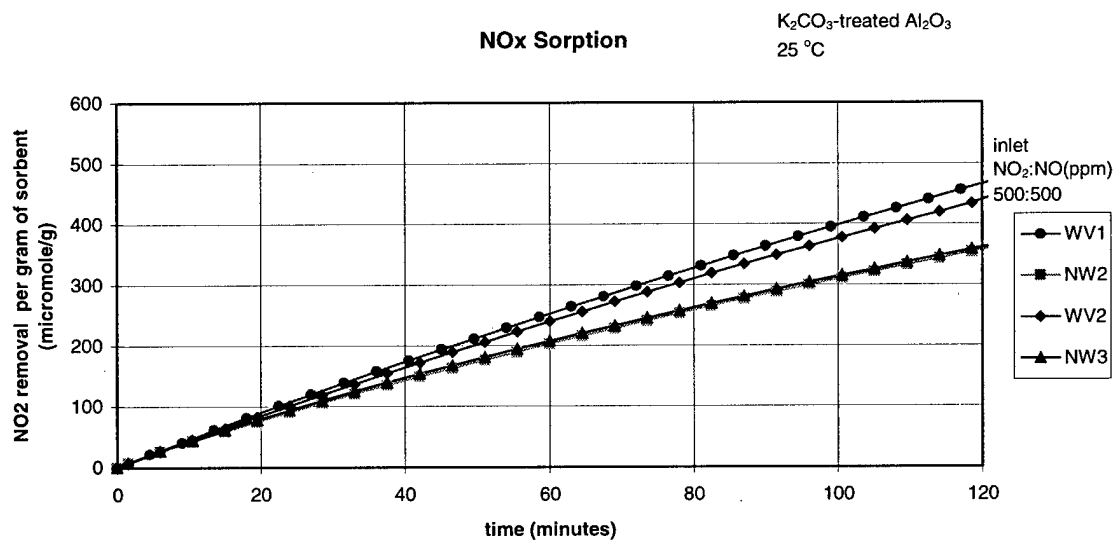
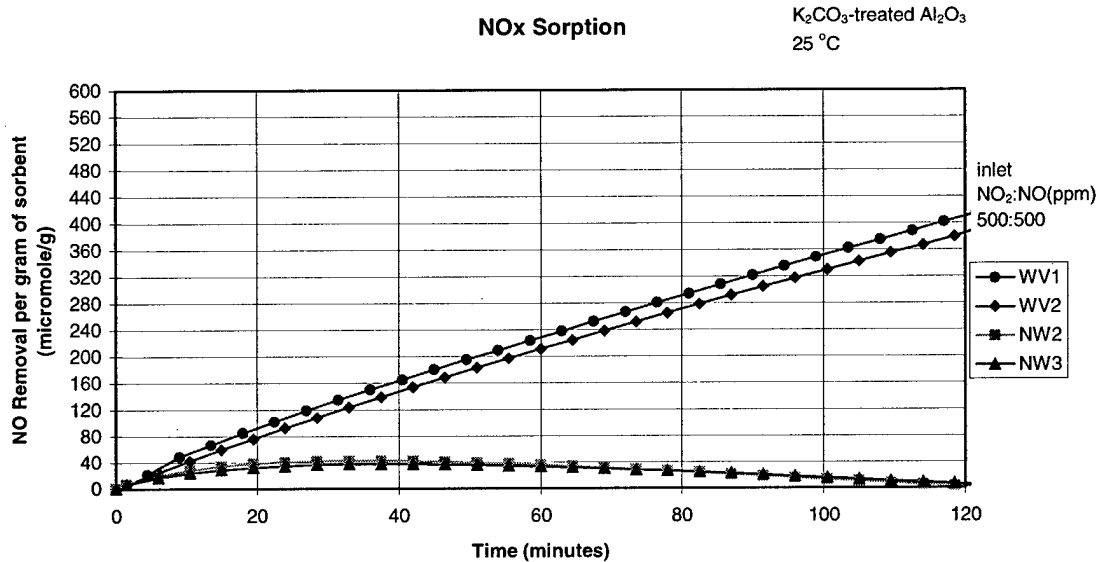
NOx sorption in the presence of water vapor (2.3%) for untreated alumina at 25 °C.



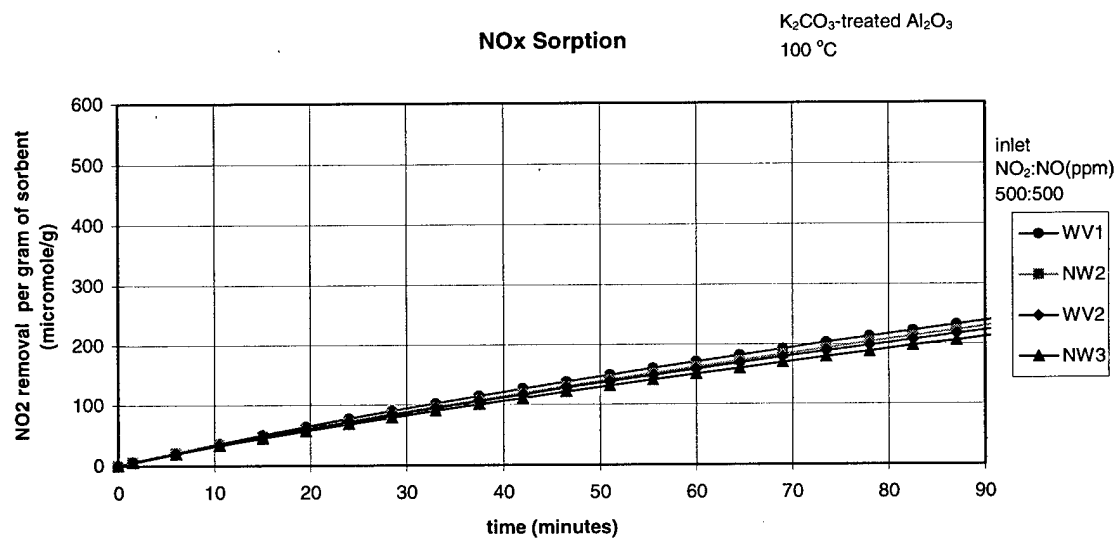
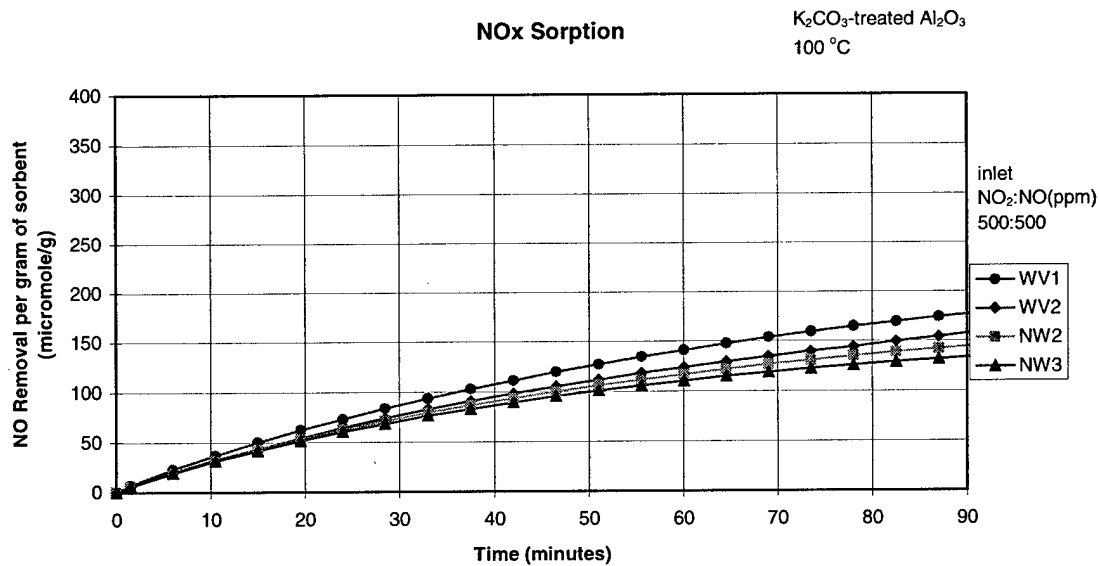
NOx sorption in the presence of water vapor (2.3%) for untreated alumina at 100 °C.



NOx sorption in the presence of water vapor (2.3%) for untreated alumina at 250 °C.



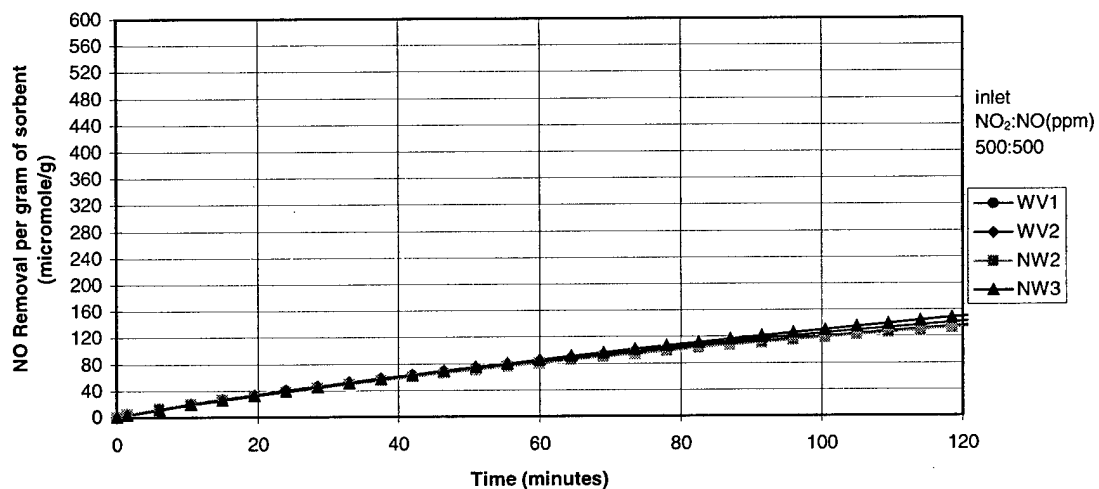
NOx sorption in the presence of water vapor (2.3%) for K₂CO₃-treated alumina at 25 °C.



NOx sorption in the presence of water vapor (2.3%) for K₂CO₃-treated alumina at 100 °C.

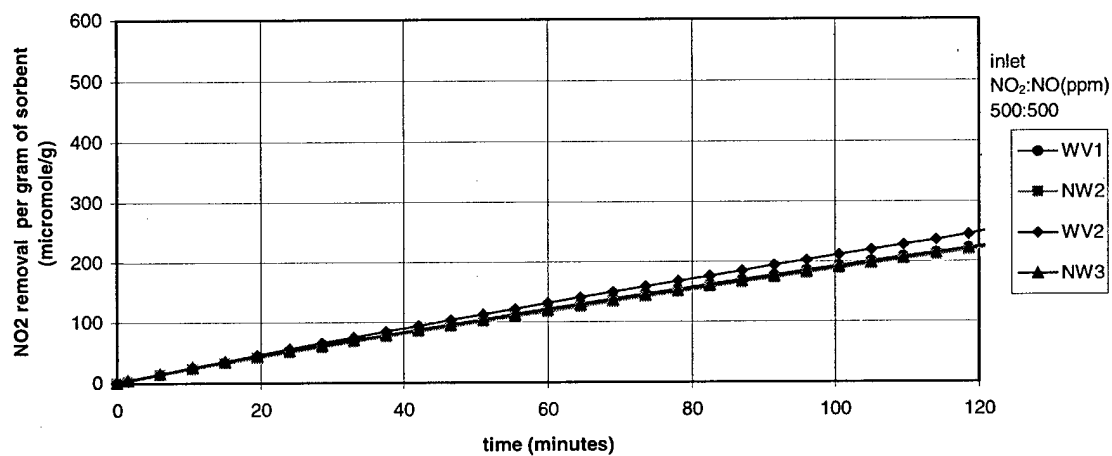
NOx Sorption

K₂CO₃-treated Al₂O₃
250 °C

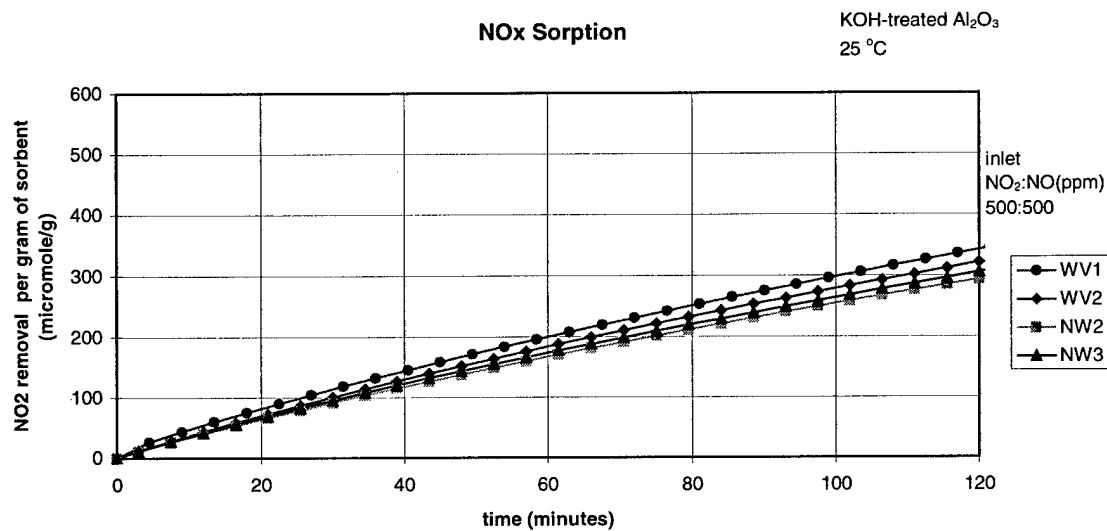
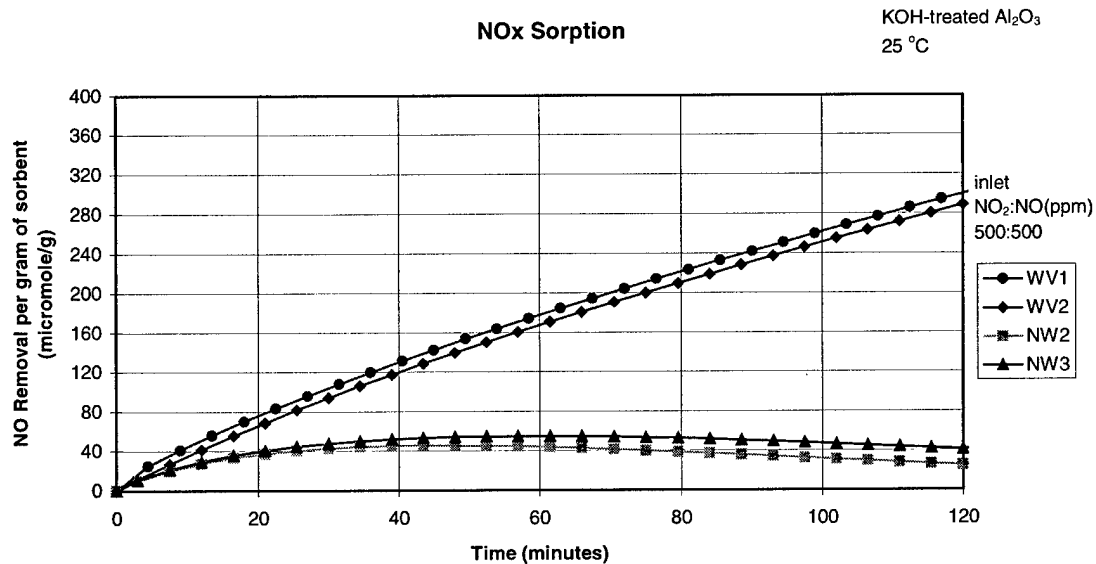


NOx Sorption

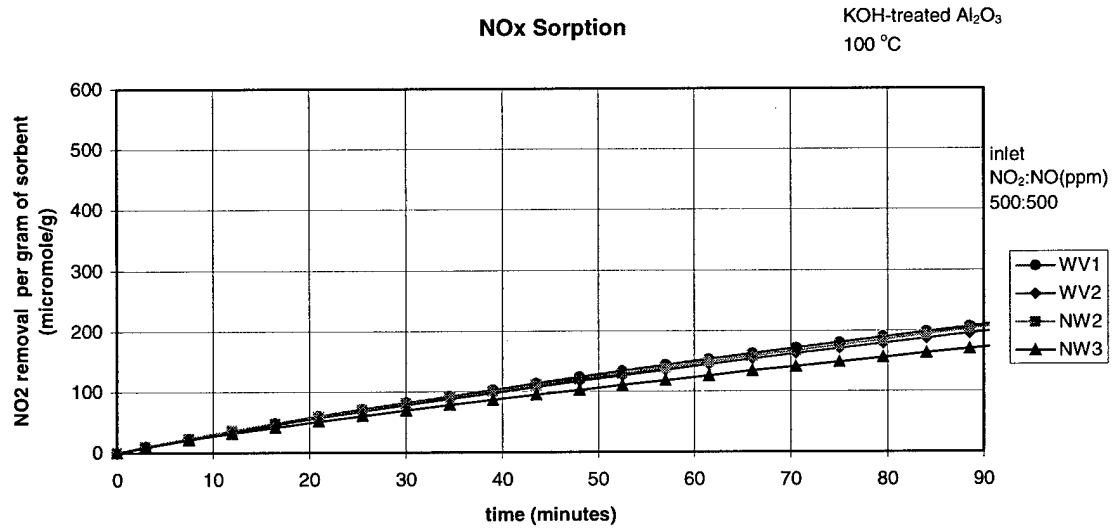
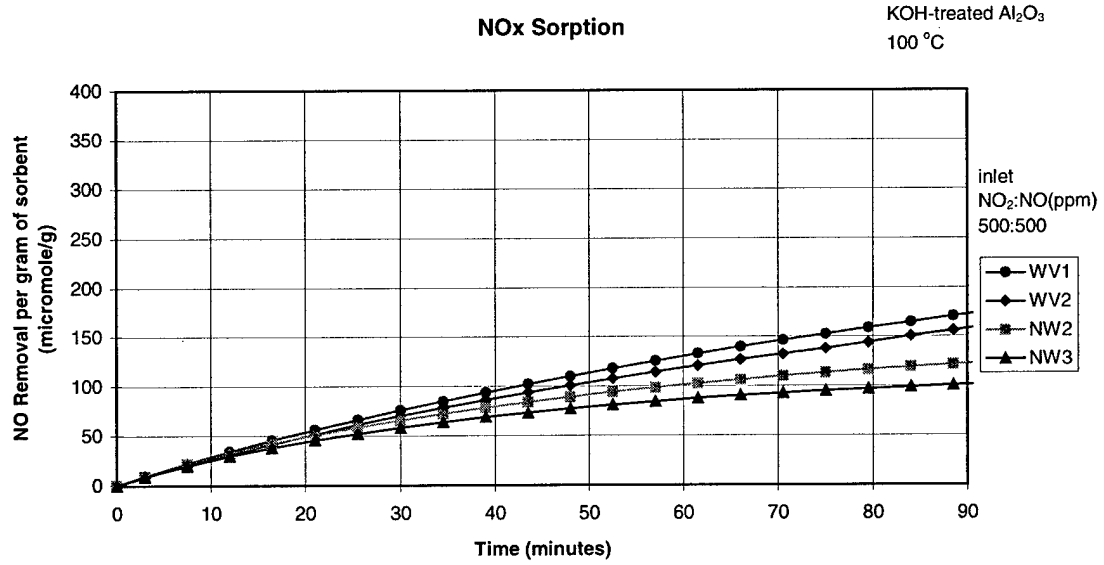
K₂CO₃-treated Al₂O₃
250 °C



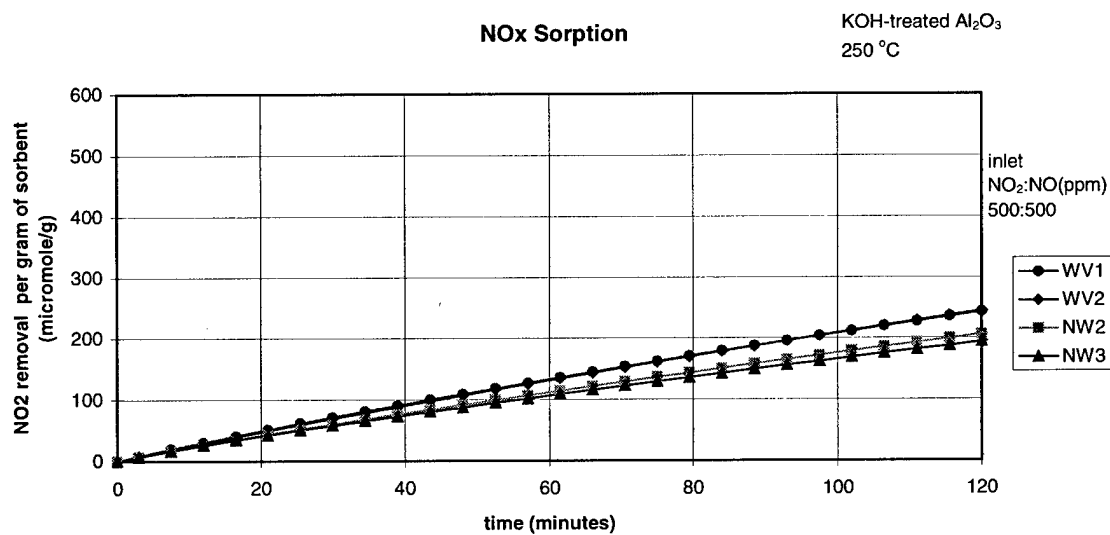
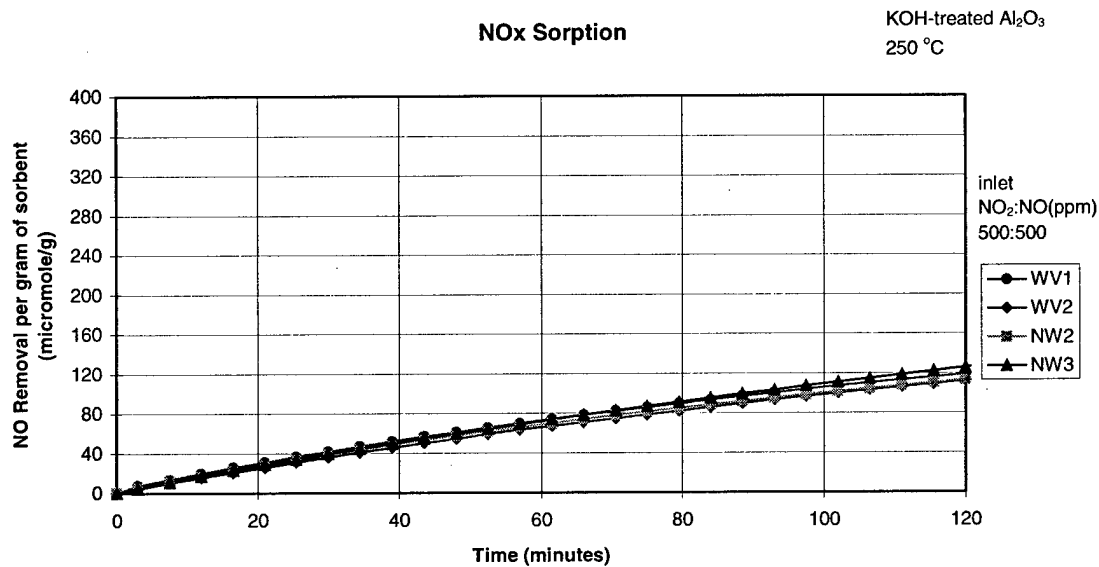
NOx sorption in the presence of water vapor (2.3%) for K₂CO₃-treated alumina at 250 °C.



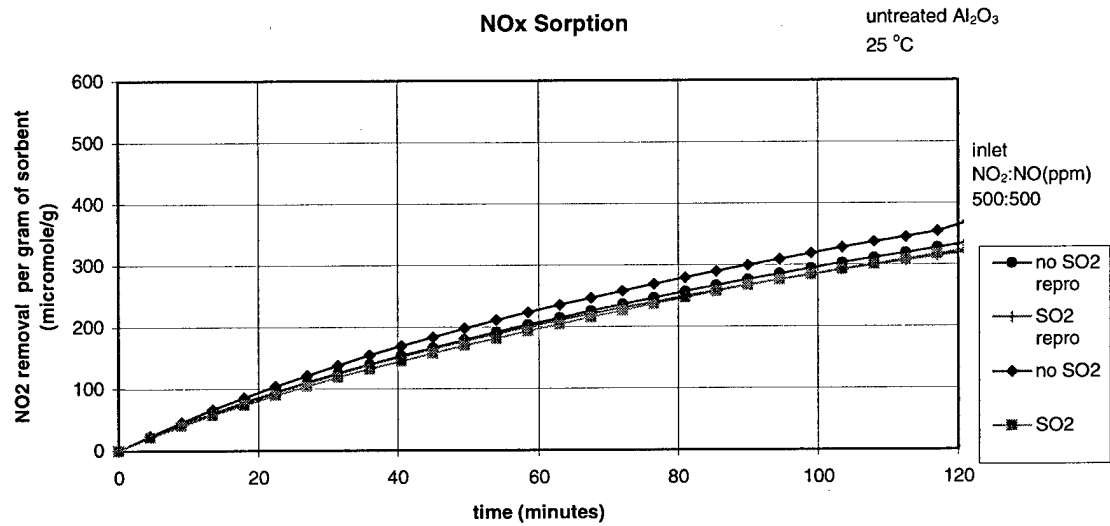
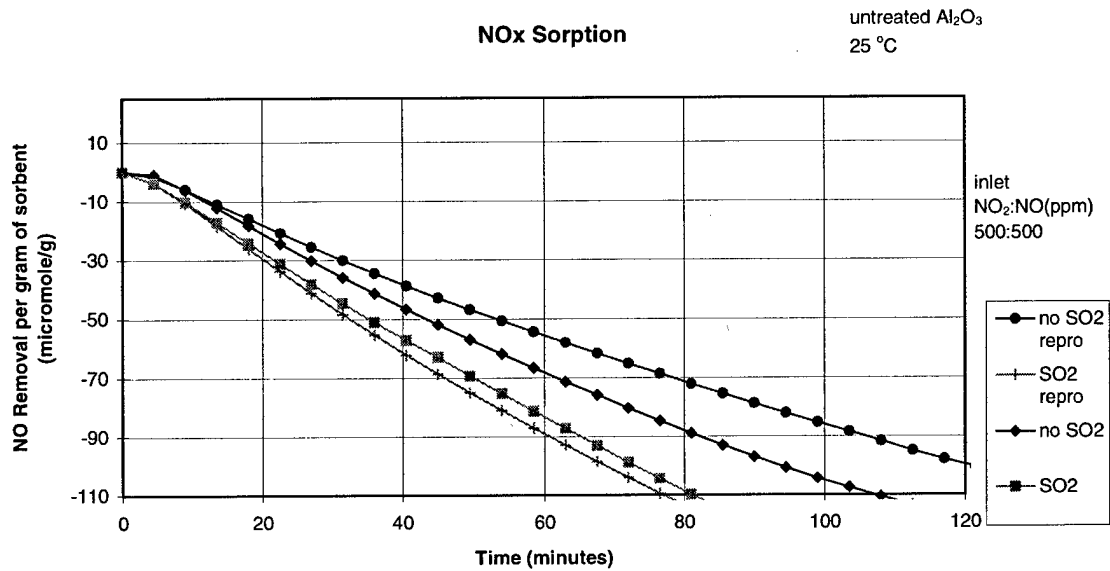
NOx sorption in the presence of water vapor (2.3%) for KOH-treated alumina at 25 °C.



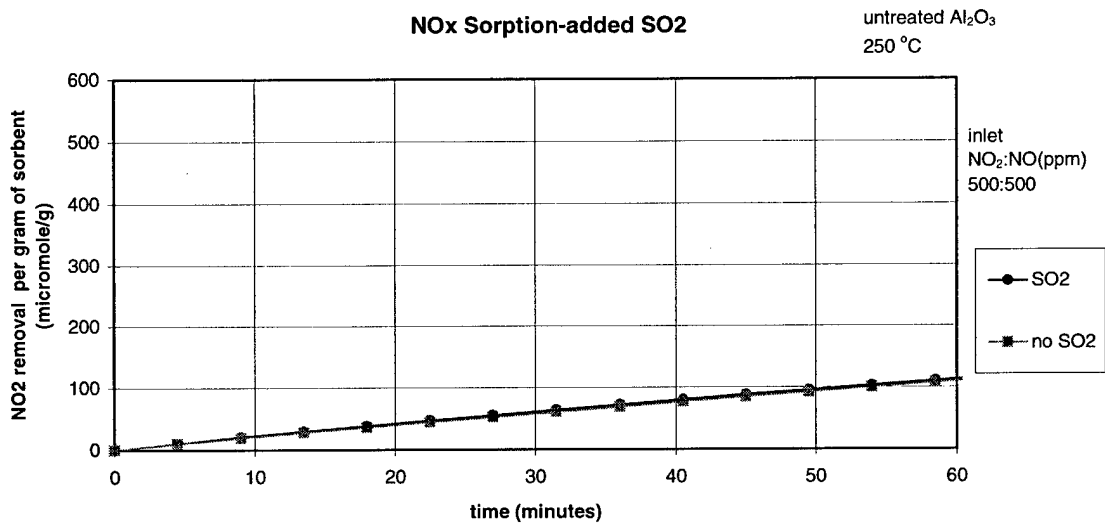
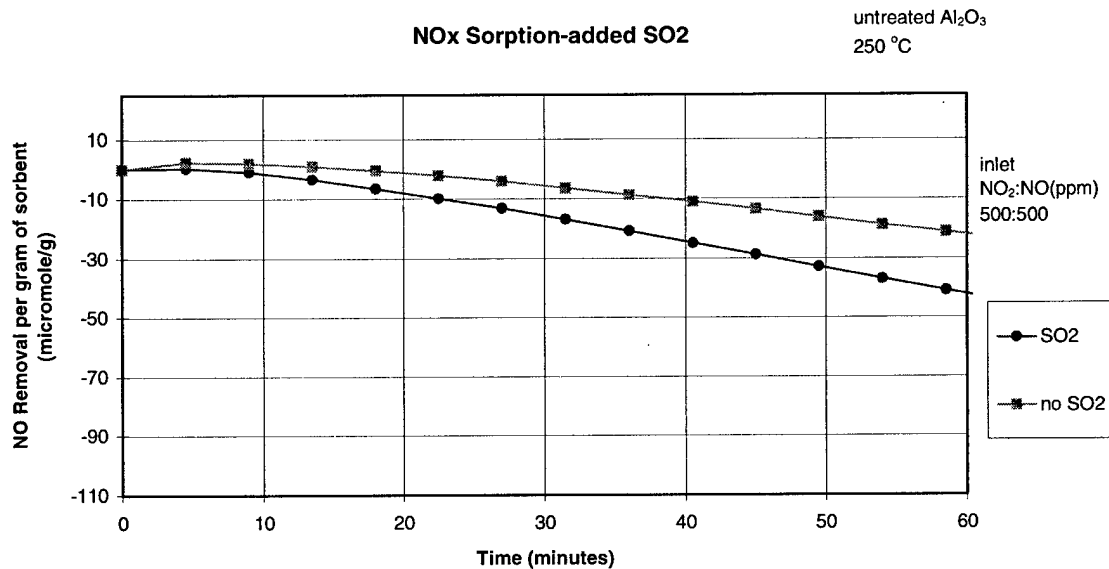
NOx sorption in the presence of water vapor (2.3%) for KOH-treated alumina at 100 °C.



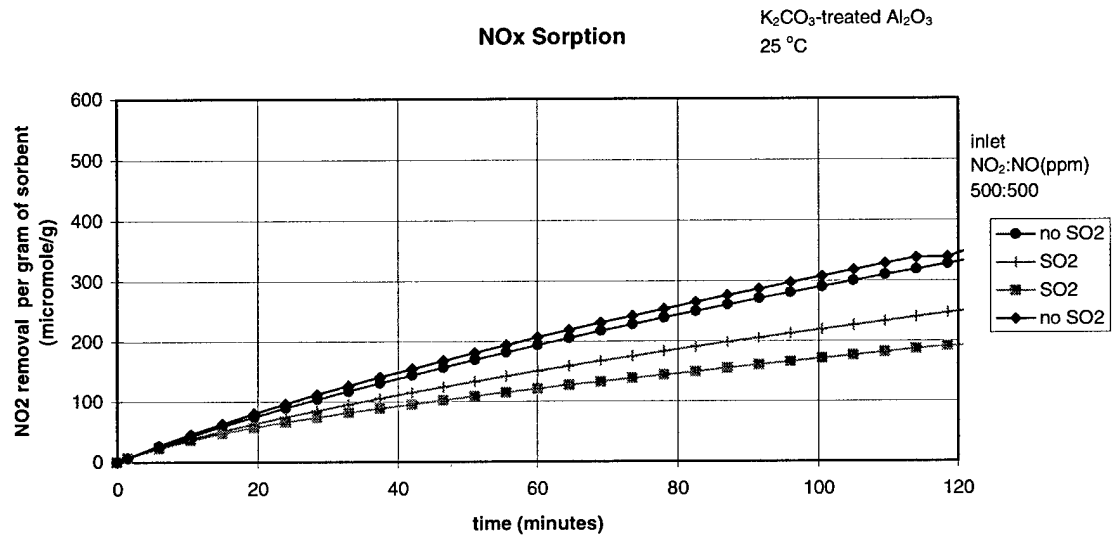
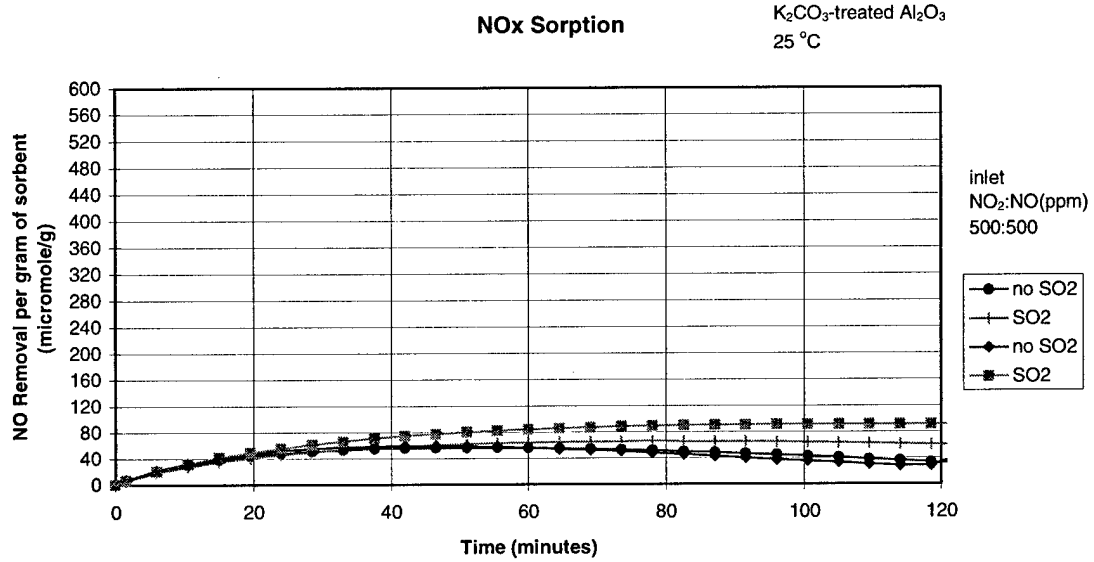
NOx sorption in the presence of water vapor (2.3%) for KOH-treated alumina at 250 °C.



NOx sorption in the presence of SO₂ (83 ppm) for untreated alumina at 25 °C.



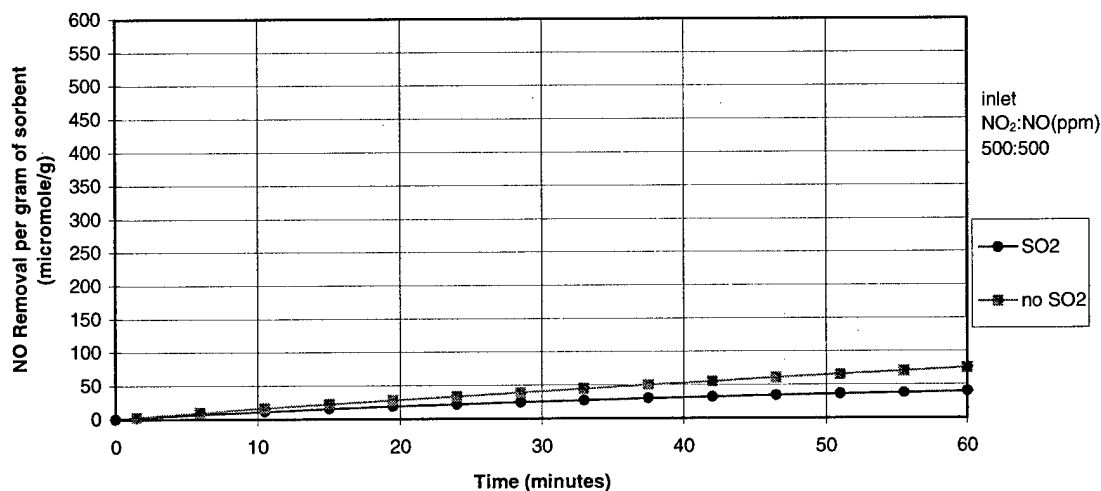
NOx sorption in the presence of SO₂ (83 ppm) for untreated alumina at 250 °C.



NOx sorption in the presence of SO₂ (83 ppm) for K₂CO₃-treated alumina at 25 °C.

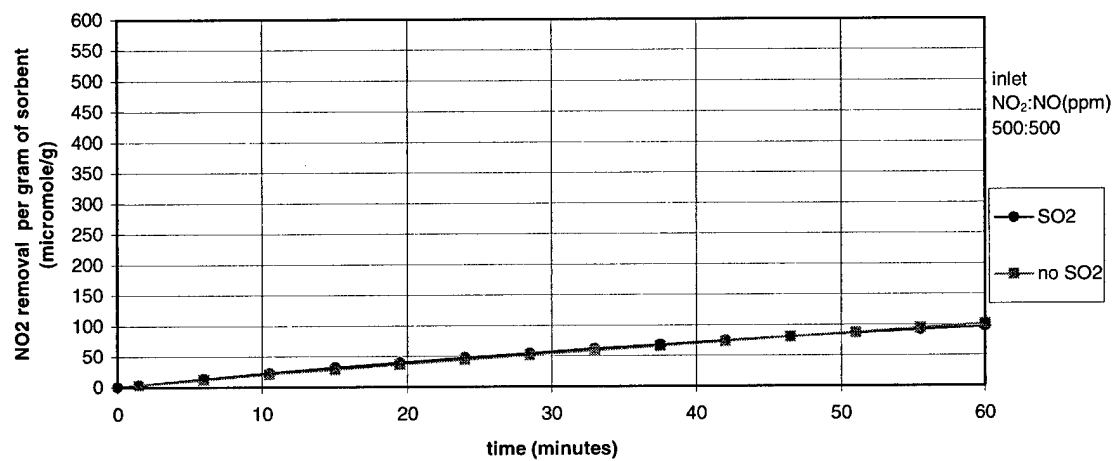
NOx Sorption-added SO2

K₂CO₃-treated Al₂O₃
250 °C

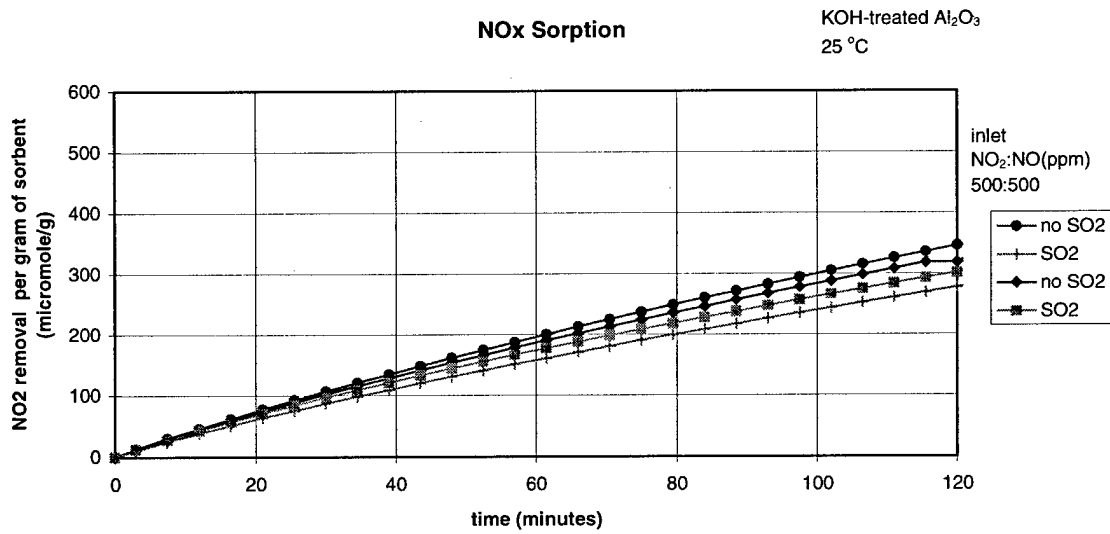
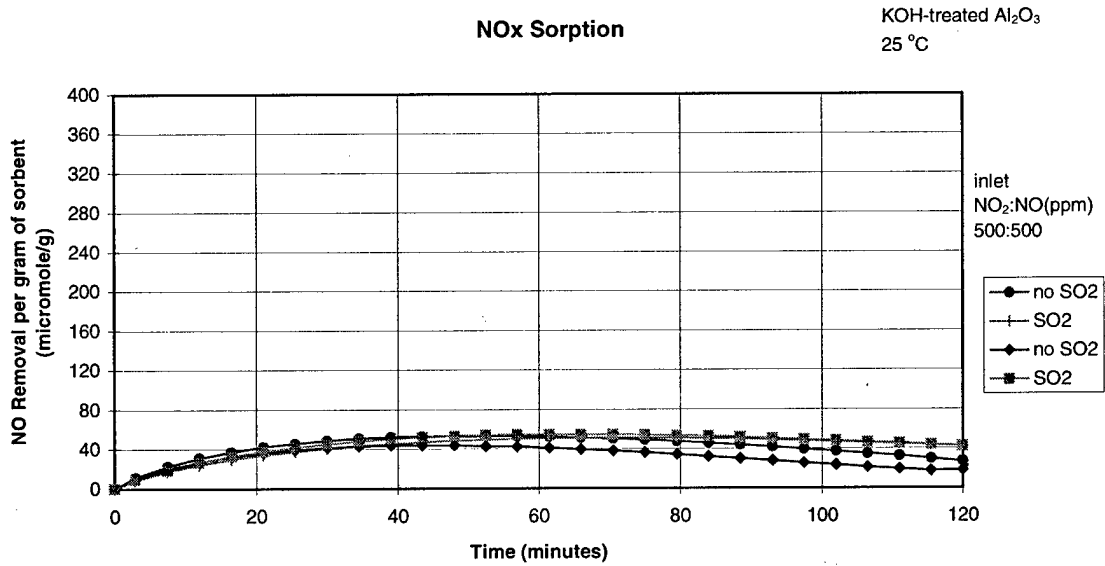


NOx Sorption-added SO2

K₂CO₃-treated Al₂O₃
250 °C



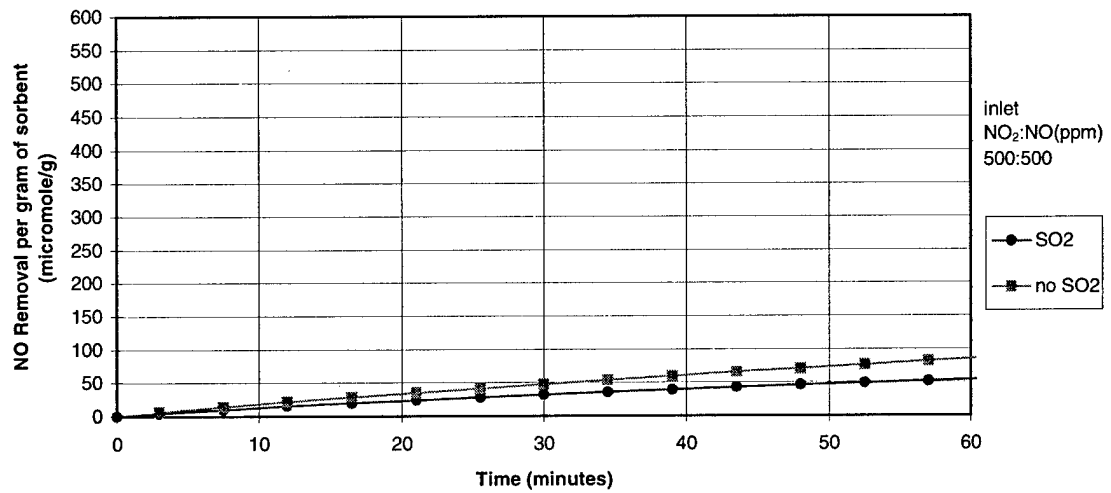
NOx sorption in the presence of SO₂ (83 ppm) for K₂CO₃-treated alumina at 250 °C.



NOx sorption in the presence of SO₂ (83 ppm) for KOH-treated alumina at 25 °C.

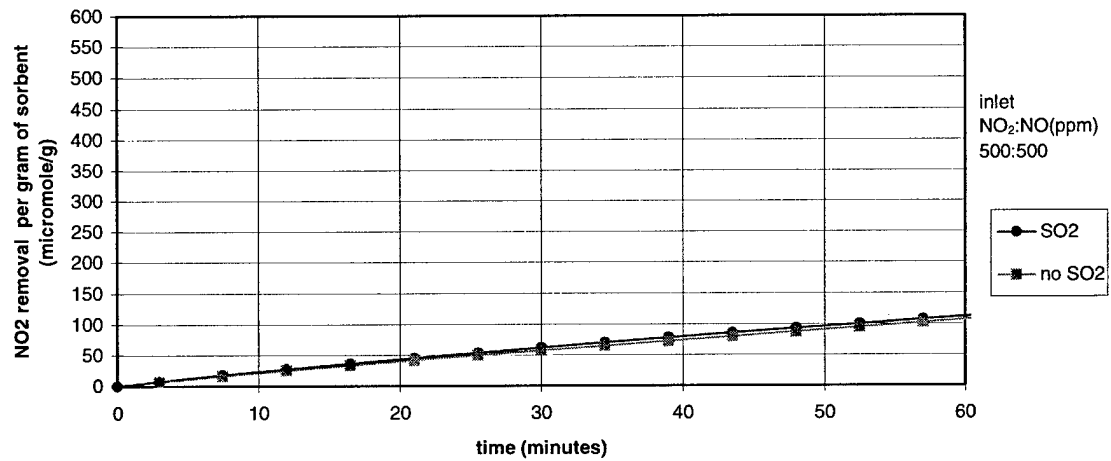
NOx Sorption-added SO2

KOH-treated Al₂O₃
250 °C



NOx Sorption-added SO2

KOH-treated Al₂O₃
250 °C



NOx sorption in the presence of SO₂ (83 ppm) for KOH-treated alumina at 250 °C.

BIOGRAPHICAL SKETCH

Maxwell Lee was born in Atlanta, Georgia on December 12, 1969. After graduation from Northside High School, in Atlanta, Georgia, in 1987 he moved to Tallahassee, Florida and attended Tallahassee Community College. After receiving a 2-year Associate Arts he entered the Civil Engineering program of Florida State University in 1990. In 1992 he transferred to the Environmental Engineering Program at the University of Florida. He received his Bachelor of Science degree with honors from the Environmental Engineering Department in December of 1994. Upon graduation he entered the graduate program of the University of Florida, Environmental Engineering Department. In 1995 he applied for and received direct entrance into the Doctoral Program specializing in Air Pollution with his Principal Advisor, Dr. Eric Allen. He received a National Science Foundation Pre-Doctoral MEDI Fellowship in the Spring of 1996. He began research on the USAF contract (F08637-C-6015) with the University of Florida entitled "Improved Control of Nitrogen Oxides) in 1996 which has been the cornerstone of his dissertation.

I certify that I have read this study and that in my opinion it conforms to acceptable standards of scholarly presentation and is fully adequate, in scope and quality, as a dissertation for the degree of Doctor of Philosophy.

Eric R. Allen, Chair
Professor Emeritus of Environmental
Engineering Sciences

I certify that I have read this study and that in my opinion it conforms to acceptable standards of scholarly presentation and is fully adequate, in scope and quality, as a dissertation for the degree of Doctor of Philosophy.

Dale A. Lundgren
Professor Emeritus of Environmental
Engineering Sciences

I certify that I have read this study and that in my opinion it conforms to acceptable standards of scholarly presentation and is fully adequate, in scope and quality, as a dissertation for the degree of Doctor of Philosophy.

W. Emmett Bolch Jr.
Professor of Environmental
Engineering Sciences

I certify that I have read this study and that in my opinion it conforms to acceptable standards of scholarly presentation and is fully adequate, in scope and quality, as a dissertation for the degree of Doctor of Philosophy.

Gar B. Hoflund
Professor of Chemical Engineering

I certify that I have read this study and that in my opinion it conforms to acceptable standards of scholarly presentation and is fully adequate, in scope and quality, as a dissertation for the degree of Doctor of Philosophy.

Joseph D. Wander
Adjunct Associate Professor of
Environmental Engineering Sciences

This dissertation was submitted to the Graduate Faculty of the College of Engineering and to the Graduate School and was accepted as partial fulfillment of the requirements for the degree of Doctor of Philosophy.

May, 1999

Winfred M. Phillips
Dean, College of Engineering

M. J. Ohanian
Dean, Graduate School

I. 6